UNIVERSITY OF NOTTINGHAM

Department of Civil Engineering

Resilient Behaviour of Granular Materials for Analysis of Highway Pavements

by

Mustafa Karaşahin BSc., MSc.

Thesis submitted to the University of Nottingham for the degree of Doctor of Philosophy

April 1993

ABSTRACT

A research study is described which aims to investigate the behaviour of a wide variety of granular material types under different stress paths using the repeated load triaxial apparatus, to determine the resilient anisotropic characteristics of granular material, to show the applicability of the selected different constitutive models for the prediction of test results and if possible to improve the prediction of the behaviour of granular material under repeated loading and, in particular, to predict the effects of material anisotropy.

Different granular materials of widely varying types and from coarse to fine grain size, were tested under the same stress regime in order to generalize the behaviour of granular material. Resilient anisotropy has been measured on the materials. Attempts have been made to measure the inherent, stress-induced and stress-history-induced anisotropy. Two different constitutive models, one of which incorporates anisotropy, were proposed to predict resilient behaviour of granular material and models are implemented in a finite element program. Prediction of test results was made with selected constitutive models.

Different materials showed different response under the same stress conditions. However, strains are dependent upon the level of deviatoric and cell pressure. Fine materials are less sensitive to the change in anisotropy as opposed to coarse aggregates. Accurate determination of model parameters was found to be important. Some models generally make under-predictions whereas some make over-predictions. Generally speaking the prediction of axial strain is better than radial strain. Finite element analysis showed that isotropic modelling produces larger tensile strains underneath the asphalt layer and smaller vertical strain at the subgrade layer when compared with anisotropic modelling.

CONTENTS

ACKNOWLEDGEMENTS

I wish to thank all those who have helped and given advice during the study. In particular I would like to thank:

Professor S F Brown, Head of Civil Engineering and Dean of Enginering Faculty, for providing all facilities in the department,

Mr A R Dawson and Dr J T Holden, project supervisors, for providing a constant resource when I was faced with unexpected obstacles and for their encouragement which created a pleasant atmosphere in which to work,

Mr J Moody and Mr D Belcher for their help with the repeated load triaxial tests,

Miss L Plaistow for her advice on English,

Dr N H Thom for his valuable comments during the research and reading the draft of the thesis,

Mrs G Fisher for her assistance in formatting this thesis,

Dr M Saidani, Nottingham University, for translating French to English,

Dr A Britto, Cambridge University, for his advice in using CRISP finite element program,

Mr P H Riley for his help in running statistical packages available in the Cripps Computer Centre,

and to all members of the Pavement and Geotechnics Research Group for their friendship and their help during the research.

I would like to thank particularly the Turkish Government for financial support during the research and Akdeniz and S. Demirel Universities for giving permission to study at the University of Nottingham.

I wish also thank my colleques at S.Demirel University-Civil Engineering Department for carrying out my responsibilities in my absence over three years.

Finally I would like to thank my wife Aysen and my daughter Melda for their patience, help and understanding and for being with me during my research.

ABBREVIATIONS

AASHTO	American Association of State Highway and Transportation Officials
A/D	Analogue to digital conventer
ARRB	Australian Road Research Board
ATS	Automated testing system
CCC	Cripps Computing Centre
CRISP	CRItical State Programs
CBR	California bearing ratio
D/A	Digital to analogue converter
ELT	Elastic layered theory
FBA	Furnace bottom ash
FDM	Finite difference method
FEM	Finite element method
FEP	Finite element programs
FS	Fontainebleu sand
FWD	Falling weight deflectometer
GP	Geometry program
GS	Gritstone
GWRS	Graded washed river sand
HCA	Hollow cylinder apparatus
LVDT	Linear variable differential transducers
MP	Main program
RLTA	Repeated load triaxial apparatus
SAG	Sand and gravel
SL	Soft limestone
TRB	Transportation Research Board
TTA	True triaxial apparatus

LIST OF SYMBOLS

A,B,...,Z	Model constants
A_c	Corrected cross-sectional area
A_i	Cross-sectional area normal to the ith coordinate direction
A_o	Initial cross-sectional area
a_{ij}	Direction cosines
[B]	The strain matrix
B_{ij}	Components of initial stress tensor corresponding to the initial strain force state
C_{ijkl}	Tensor of material elastic constants
D	Initial diameter of sample
[D]	D matrix (stress-strain matrix)
D_{ijkl}	Material response moduli
d_o	Diameter of a sample
E	Young's modulus (specifically in the vertical direction)
E_h	Young's modulus in the horizontal direction
e_{ij}	The deviatoric stress tensor
F_j	Component of force F in the direction j
F_{ij}	The elastic response function
G	Shear modulus
G_t	Tangential shear modulus
h_o	Initial height of a sample
Δh	Difference between the initial and final height of sample
I_1	First stress invariant
I_2	Second stress invariant
I_3	Third stress invariant
i,j	indices (i.e. 1,2,3)
J	Coupled modulus
[k]	Stiffness matrix
K	Bulk modulus
K_t	Tangential bulk modulus
l_o	Initial length
l	Final length
M	The extension modulus of the membrane
M_c	Membrane correction
M_r	Resilient modulus

N	Normal force
n	The indicator of anisotropy (axial strain/radial strain (under isotropic stress))
p	Mean normal stress
p_a	Atmospheric pressure (100 kPa)
p_r	Repeated mean normal stress
p_m	Mean value of mean normal stress
p_u	Unit pressure (1 kPa)
p_1	Initial mean normal stress
p_2	Final mean normal stress
q	Deviatoric stress
q_r	Repeated deviatoric stress
q_m	Mean value of deviatoric stress
q_1	Initial deviatoric stress
q_2	Final deviatoric stress
T	Tangential force
t	Subscript indicating condition tangential
u_i, v_j	Vectors (first order tensors)
u, v, w	Displacements in x, y and z directions respectively
u_{kl}	Second order tensor
v_{ij}	Second order tensor (alternative representation)
x, y, z	Cartesian coordinate axis
ε	Strain
ε_a	Axial strain
ε_r	Radial strain
ε_s	Shear strain
ε_v	Volumetric strain
ε_x,ε_y, ε_z	Normal strains in the direction of x, y and z respectively
ε_{ij}	Engineering strain
ε^C	Cauchy's strain
ε^G	Green's strain
ε^H	Henky's strain
ε^A	Almansi's strain
ε^S	Swainger's strain
ε_{oct}	The octahedral normal strain
ε_1, ε_2 ,ε_3	The major, intermediate and minor strains respectively
ε_r, ε_θ ,ε_z	Strains in an axisymmetric solid
σ_{ij}	The stress tensor

σ_x, σ_y, σ_z	Normal stresses in x, y and z directions respectively
σ_n	Principal stresses
σ_a	Axial stress
σ_r	Radial stress
σ_o	Hydrostatic stress
σ_{oct}	Octahedral normal stress
σ_1, σ_2, σ_3	The major, intermediate and minor principal stresses respectively
τ_{xy}, τ_{xz}, τ_{yz}	Shear stresses in the xy, xz and yz planes
τ_{oct}	Octahedral shear stress
δ	"change in"
δ_{ij}	Kronecker delta (if i=j then δ_{ij}=1 otherwise 0)
γ	Tensorial shear strain
γ_{oct}	The octahedral shear strain
υ	Poisson's ratio
υ_1	Effect of horizontal strain in the horizontal strain
υ_2	Effect of horizontal strain on the vertical strain
υ_3	Effect of vertical strain on the horizontal strain
ω	Strain energy density
Ω	Complementary energy function
λ, μ	Lame's constants
t	$\frac{\sigma_1+\sigma_3}{2}$
s	$\frac{\sigma_1-\sigma_3}{2}$

LIST OF TABLES

LIST OF FIGURES

CHAPTER 1

INTRODUCTION

1.1.Pavement structure

A pavement is constructed to carry traffic safely and economically. Safety aspects come from friction between the wheel and the pavement surface. The rougher the surfacing the higher the friction and the greater the skid resistance. The economy is related to the optimum use of available construction material. Layer thicknesses are determined in order that the pavement will meet its structural role of adequate resistance to deformation for a desired period.

A pavement is composed of surfacing layer, base, sub-base, capping (if required) and subgrade layers (Figure 1.1). This composition depends on the design life, traffic volume, availability of materials and subgrade strength. The purpose of the surfacing is to provide a smooth and comfortable riding surface which can be trafficked at minimum operation cost whilst providing the necessary resistance to skidding. The base is the main structural layer which distributes the wheel loads. In the UK it is generally built with an asphaltic mixture, but for secondary roads or roads carrying light traffic where a thin asphalt layer is used, it is often built with granular material. The purpose of the sub-base is to provide a good working platform for the construction of upper layers, to distribute wheel loads so that the subgrade layer will not deform excessively and to prevent the subgrade layer from frost action. Capping, which is

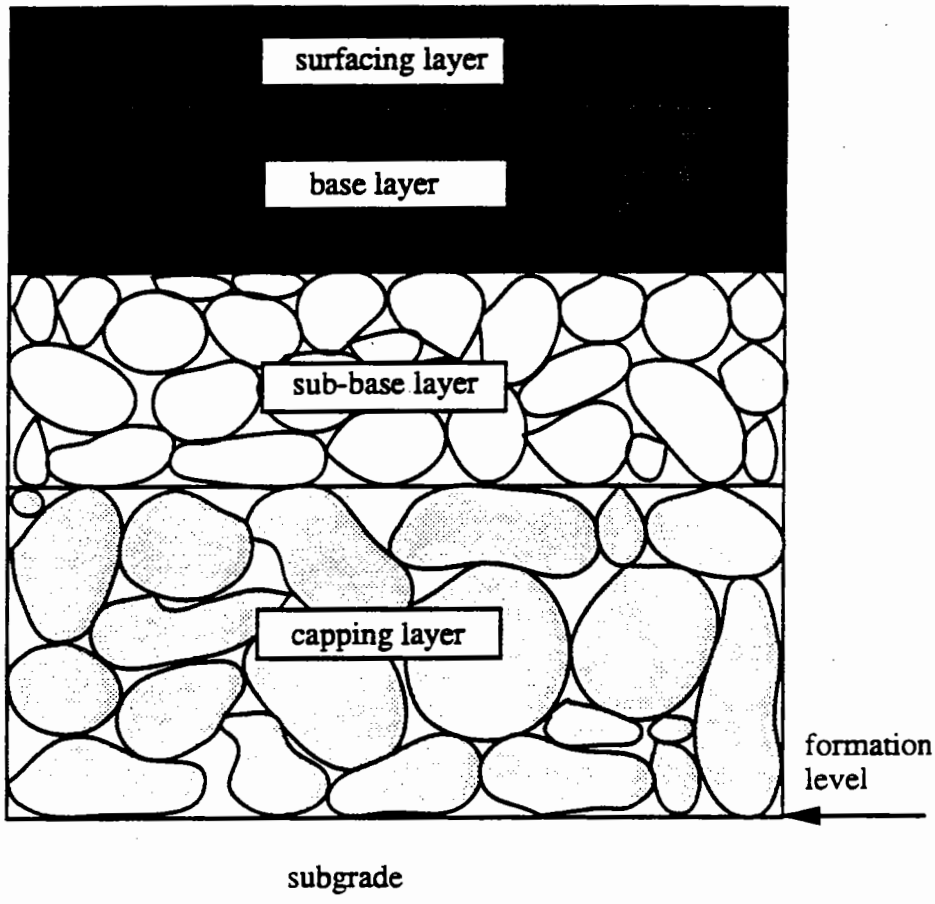

Figure 1.1. A typical flexible pavement

often used when the CBR (California Bearing Ratio) of the soil is low, is a layer of low cost, generally local material and is constructed in order to add stiffness to the subgrade, providing a working platform on which sub-base layer may be constructed safely. Subgrade is the natural or fill material underneath the pavement.

1.2.Pavement design

Design methods for flexible pavements may be classified into two groups: empirical and semi-empirical, and analytical.

The empirical and semi-empirical design methods are related to past experience. They may incorporate laboratory and field tests in order to classify the pavement materials but not to determine their fundamental mechanical properties. One of the best known empirical method is the CBR design method to design the total pavement structure (Department of the Environment, 1970). Some other empirical methods use a "catalogue" (e.g RStO 86 (1986)) in which the thicknesses for each layer are predetermined depending on the soil and traffic classification. These type of design methods are only satisfactory as long as the materials and conditions have not changed from those on which the experience was obtained.

However, due to the increase in traffic, especially of commercial vehicles, and the introduction of new road construction materials the use of analytical methods has become more necessary and more widespread. These methods adopt a structural model of pavement response to loading and use elastic layered theory (ELT) or the finite element method (FEM) to perform the necessary computations to obtain the stresses and strains in the pavement. In the elastic layered theory a pavement is divided into several layers and for each layer a Young's modulus and Poisson's ratio are assigned. The materials comprising each layer are assumed to be linearly elastic. This is not the case for soils and granular materials since they exhibit non-linear behaviour (Hicks and Monismith, 1971). The FEM (Duncan et al, 1968) overcomes this limitation at the expense of more complex analysis and may be used to incorporate the non-linear properties of soil and granular material. The success (or failure) of the FEM comes from the models employed to describe the pavement materials' behaviour. The necessary data required in order to perform an analysis may be obtained from laboratory or field tests for both analytical methods. Calculated strains due to wheel loading are, typically, compared with the allowable tensile strain underneath the bound

layer and the vertical strain in the subgrade at the formation level. If the allowable values are not achieved, thicknesses are changed until the design criteria are satisfied.

The research project described in this thesis has been concerned entirely with determining the behaviour of unbound granular material and modelling that behaviour for pavement analysis purposes.

1.3.Deformation characteristics of granular material

The deformation of a granular layer under traffic loading is composed of two parts- resilient (elastic or recoverable) and permanent (plastic). The stresses observed in a pavement foundation are well below those which might cause conventional shear failure (Brown, 1981). Instead, failure is defined by serviceability limits of which there are two types in pavements. They are

a) fatigue cracking in the bound layers associated with the resilient response of the pavement to transient loading and

b) rutting due to accumulation of permanent strain throughout the pavement structure (Brown and Selig, 1991).

For a pavement foundation, rutting, which is associated with the accumulation of permanent strain, is the only failure criterion since no bound materials (which might suffer resilient fatigue) are involved (Brown and Selig, 1991). However, after constructing the upper layers of a pavement and after a number of traffic loads have been applied, the increment of permanent deformation is much smaller than the

increment of resilient deformation. It is then that the resilient strains, which are of concern to the behaviour of the pavement structure built on the granular layer, gain importance.

A measure of the resilient behaviour of a pavement structure is also required in order to predict the future behaviour of the structure which has important consequences for its maintenance programme (Peattie, 1978).

1.4.Research aims

The main area for study is the non-linear characteristics of granular material which are investigated using the effective stress principle when possible.

In summary the research aims are to:

• Investigate the behaviour of a wide variety of granular materials under different stress paths using a repeated load triaxial apparatus,

• Determine the resilient anisotropic chatacteristics of granular material with the repeated load triaxial apparatus,

• Show the applicability of the selected different constitutive models for the prediction of the test results and in conjuction with this, to propose a new constitutive model to predict the behaviour of granular material under repeated loading,

• Show the applicability of some selected models in pavement analysis using the finite element approach.

1.5.Contents of thesis

Wheel loading causes vertical, horizontal and shear stresses in the pavement. In this research a repeated load triaxial apparatus which can only simulate vertical and horizontal stresses is used. Chan (1990) has shown that shear reversals affect the permanent behaviour of granular material, but their effect on the resilient behaviour is not significant (see Chapter 2). Therefore, the repeated load triaxial apparatus may be used to simulate the resilient behaviour of granular material even though it cannot provide shear reversals in a controlled manner. In Chapter 3 the repeated load triaxial apparatus is introduced.

Different granular materials of widely varying types and from coarse to fine grain size, were tested under the same stress regime in order to generalize the behaviour of granular material. The materials were soft limestone (SL), gritstone (GS), sand and gravel (SAG), furnace bottom ash (FBA), graded washed river sand (GWRS) and Fontainebleu sand (FS). Materials were tested dry except for FBA and FS because they experienced significant permanent deformation after only a few loadings when dry. Detailed knowledge about the materials is given in Chapter 4.

It is well known that traffic loading is repeated and of random magnitude. In order to closely simulate these stresses caused by such loading, a range of different stress paths were applied. These aspects are discussed in Chapter 5.

Anisotropy is defined as the ratio of axial strain to radial strain under isotropic stress conditions (Biarez and Hicher, 1987). Anisotropy is an important characteristic of granular material but has normally been neglected in the design of pavement structures. This may be due to the lack of equipment to measure it. Although early research work studied the anisotropic properties of sand (Arthur et al, 1972), there has been little or no work on the anisotropy of granular materials for pavement construction. This may be due to the difficulty of testing coarse granular material or because of the theoretical problems involved. In this research, resilient anisotropy has been measured on the materials using the repeated load triaxial apparatus. Attempts have been made to measure both the inherent and stress-induced anisotropy and to see these change after the granular material has been subjected to permanent deformation. Results are discussed in detail in Chapter 6.

A further aspect of the research has been the constitutive modelling of the resilient behaviour of the aggregate under repeated loading. Two different mathematical models were proposed to predict the resilient behaviour of granular material. The first one predicts the strains due to repeated deviatoric stress with constant cell pressure. The second model, incorporating inherent anisotropy, is for the prediction of resilient strains due to the repetition of both axial and radial stresses. These aspects are discussed in Chapter 7. Predictions are made with the models and compared with the measured results and with the results of other models (Chapter 8).

The models are then implemented in the CRISP (CRItical State Program) finite element program in order to show its applicability to practical use. This aspect is discussed in Chapter 9.

Chapter 10 gives the conclusions of the research and makes proposals for future work.

CHAPTER 2

LITERATURE REVIEW

2.1.Introduction

The behaviour of granular material is very important in flexible pavements where the wearing course is thin, because it will then provide the main structural element of the pavement. Granular material in the pavement is subjected to repeated loading that can be approximately simulated using a repeated load triaxial apparatus or hollow cylinder apparatus. From the results of tests with these apparatus appropriate constitutive models can be deduced and used for numerical solutions of pavement behaviour. Pavement engineers are principally concerned with sub-failure resilient behaviour of granular materials, therefore, plastic behaviour due to single or repeated loading is excluded from discussion in this chapter.

The literature review is divided into four sections, namely, testing of granular materials, influences on granular material behaviour, modelling of granular material behaviour and anisotropy.

2.2.Testing of granular materials

In order to understand the behaviour of granular material under traffic loading, either site tests or laboratory tests or both should be carried out. Generally speaking, site

testing is more expensive and time consuming when compared with laboratory tests. In order to determine the stress state of a material, a test apparatus is needed which is able to apply six independent stresses to a sample (three normal and three shear stresses). However, this type of equipment has not yet been available even at the research level (Stackel (1991) and O'Reilly (1991)). Therefore, available test equipment in the laboratory able to simulate traffic loading such as the repeated load triaxial, hollow cylinder apparatus or, the cubical triaxial apparatus has to be used.

The hollow cylinder and the cubic triaxial apparatuses are still far away from practical use other than research. These apparatuses are particularly important to study anisotropy in the soils (Arthur et al (1977), Arthur and Menzies (1972), Wong and Arthur (1985), Budiman et al (1992), Symes et al (1982)). The hollow cylinder apparatus can also be used to characterize the granular material behaviour under traffic loading (O'Reilly (1985), Thom (1988), and Chan (1990)). However, the use of triaxial apparatus is widespread all over the world, commercially available, easy to control and cheaper compared with other complicated test equipment.

A triaxial apparatus has a cylindrical sample which is subjected to two independently controlled stress components, vertical load and confining pressure. The confining pressure may be provided by a fluid or air pressure or by an internal partial vacuum. The limitation of the triaxial apparatus is that it only applies two independent stresses out of the six independent stresses developed in a pavement. Horizontal stresses are assumed to be equal to each other and it is impossible to simulate principal stress rotation which occurs when a tyre travels on a pavement. Furthermore the horizontal and vertical stress pulses tend to be of different wave length and may be slightly out of phase with each other. In order to provide a reasonable simulation of pavement loading

with triaxial equipment, it should be able to cycle both the vertical load and cell pressure in-phase. However, many laboratories still use constant confining pressure testing (Sweere, 1990) to determine the resilient behaviour of the material since this type of equipment is more cost effective when compared with the apparatus which can cycle both pressures at the same time. However, Brown and Hyde (1975) have shown that similar resilient behaviour can be obtained from cyclic and constant confining stress when the constant stress is equal to the mean of the cyclic confining stress values.

In conjunction with the repeated loading of granular materials, a triaxial apparatus was developed by Boyce (1976) at Nottingham University which was able to cycle both the deviatoric and confining stresses. Pappin (1979) slightly modified some parts of the apparatus in or order to apply extension stress paths to the granular material. During the research reported here the electronic control system of the apparatus was replaced with a digital control system (Chan and Sausa, 1991). More details about the development of the equipment can be obtained from Boyce (1976), Boyce et al (1976), Pappin (1979) and Brown et al (1989).

The cubic triaxial (true triaxial) has one more degree of freedom than the cylindrical triaxial apparatus in that it allows three independent orthogonal stresses. However, this type of equipment is generally difficult to operate and the sample is surrounded by a mass of mechanical equipment, therefore, the sensitivity is reduced and the apparatus is not suited to measure small strains such as those typical of the pavement layers (Thom, 1988).

The hollow cylinder apparatus (Chan, 1990) applies the confining pressure and the axial deviatoric stress in a similar fashion to the triaxial apparatus, but it also applies a torque to the cylinder which causes shear stresses on cylindrical surfaces. Although it is possible to measure small strains in the sample, there is a non-uniformity in stress which creates some difficulties especially if there is a difference between the external and internal confining stresses. Sample size also limits it to the testing of fine grained granular materials.

Because of these limitations, and because of availability, a repeated load triaxial apparatus was chosen to test granular material in the project described here.

2.3.Influences on granular material behaviour

Stress may be the major effect on granular material behaviour. However there are many other effects which are likely to affect the behaviour of granular material. Of these, particle shape, density, grading and moisture content are considered to be important and are discussed here.

2.3.1.Particle shape

Several methods have been proposed to define particle shape. The parameters classified by Selig and Roner (1987) are useful. They are

a) **Flakiness or flatness** - the ratio of particle thickness to width.

b) **Elongation** - the ratio of length to width

c) **Sphericity** - a measure of how much the shape of a particle deviates from a sphere

d) **Roundness or angularity** - a measure of sharpness of the edges or corners of an individual particle.

Flaky particles which do not lie along the failure line increase the shear strength of granular material, the disadvantage being that an increase in the flakiness may cause problems of breakage, abrasion, increased permanent strain and decreasing stiffness of the material (Selig and Roner, 1987).

Aggregate type may have a significant effect on the resilient modulus when other parameters such as grading, density and applied stress are kept constant. Barksdale and Itani (1989) tested different granular materials with the same grading and they found that angular materials had a higher resilient modulus than rounded gravel, the increase being about 50% at low mean normal stress conditions decreasing to about 25% at high mean normal stress levels.

Thom (1988) and Thom and Brown (1989) carried out repeated load triaxial tests on different granular materials, they found that:

a) The resilient modulus of granular materials at low strain levels may be influenced by particle texture i.e roughness.

b) A correlation exists between elastic stiffness and the surface friction properties of a material.

c) High resilient modulus and good load spreading properties in the pavement may be expected from material with angular to subangular shaped particles and a very rough surface when compared with material with subrounded or rounded particles and a smooth surface.

2.3.2.Grading and Density

Thom and Brown (1988) tested limestone with a maximum size of 10 mm at different gradings and different compaction levels. All tests were carried out using repeated load triaxial equipment. The test results showed that the state of compaction (i.e. density) had little effect on the resilient modulus, (although there was some slight increase for denser material) and uniform gradings gave a stiffness about 1.3 times as large as for broadly graded samples. Brown and Selig (1991) also confirmed that the resilient properties of granular material are not significantly affected by grading or density.

Barksdale and Itani (1989) and Hicks and Monismith (1971) found that as the grading became finer, the resilient modulus decreased dramatically by about 60%. Triaxial tests carried out by Kamal et al (1993) have shown that a material containing more fine material has a lower resilient modulus than the coarse material.

2.3.3. Moisture content

As moisture content increases in granular layer, compaction is facilitated i.e. "workability" increases. But if the moisture content increases above a certain level, the optimum, which can be experimentally found, it will cause a decrease in friction between particles and therefore less strength against shear.

Hicks and Monismith (1971) showed that the resilient modulus steadily decreases as the moisture content increases above optimum.

2.4.Mathematical modelling

The deformation of granular layers under traffic loading is composed of two parts, resilient and permanent. The stresses involved are well below levels which might cause rapid shear failure of a pavement in service (Brown, 1981). Therefore the resilient

rapid shear failure of a pavement in service (Brown, 1981). Therefore the resilient response of the pavement becomes more important during service. However, for a pavement foundation, rutting, which is the accumulation of plastic strain with time is the only failure criteria since no bound materials (which might fail by resilient fatigue) are involved (Brown and Selig, 1991). After constructing the upper layers of the pavement and a number of traffic loads have been applied, the increment of permanent deformation is much smaller than the increment of resilient deformation. Hence the resilient characteristics of the granular layer in the pavement structure gain importance.

Wood (1991) divided models into four groups. First, "children's" models such as linear elasticity and perfect plasticity. Second, "student" models such as a work-hardening plastic model (e.g. Cam clay models). Third, engineering models such as non-linear elasticity, anisotropic elasticity, anisotropic plasticity and those with viscous properties. Fourth, philosopher's models which serve all aspects of soil behaviour even for very complicated structures such as nuclear power stations. According to this classification most of the models developed for pavement analysis are engineering models.

In this section models developed for resilient behaviour of granular material in the pavement will be discussed. Some other elastic models which have not been used for modelling granular material behaviour will also be briefly discussed. Although the models were originally proposed using a variety of terms they are expressed here, wherever possible, in terms of the stress invariants p (mean normal stress) and q (deviatoric stress).

2.4.1.K-θ type models

Granular materials exhibit non-linear, stress dependent behaviour. Early studies (Hicks and Monismith, 1971) showed that the resilient modulus is a function of the maximum mean normal stress or (bulk stress, $\theta=3p$), then the model is written in the form

$$M_r = A\,(3p_{max})^{B} \qquad \text{or} \qquad M_r = A\,p_a\left(\frac{3p_{max}}{p_a}\right)^{B} \tag{2.1}$$

where A, B are material constants

p_{max} is maximum mean normal stress (kPa)

p_a is atmospheric pressure (kPa)

The second formulation is introduced here so as to express the coefficients in a non-dimensional from. The model has been found extremely useful and simple and is still in use for design of new pavements (Thompson, 1992) or pavement evaluation (Brown and Almeida, 1993). However, it has some drawbacks. First, it always assumes that the Poisson's ratio is constant although experimental results have revealed that this is not the case. Second, the resilient modulus varies with the deviatoric stress q as well as the normal stress p (Stackel (1973), Uzan (1985) and May and Witczak (1981)). Therefore it can only be used for low shear stress levels. Clearly such a limitation is unsatisfactory for pavement applications where, in general, shear stresses are relatively large. Third the model has been developed from simple laboratory triaxial test results in which the initial deviatoric stress is always zero and in which the confining pressure is constant.

The second drawback has been considered by Stackel (1973) and Uzan (1985) and they modified the model in order to include the deviatoric stress. The modified form of the model is shown below.

$$M_r = A\,(3p_{max})^{B}\,q^{C} \quad \text{or} \quad M_r = A\,p_a\left(\frac{3p_{max}}{p_a}\right)^{B}\left(\frac{q}{p_a}\right)^{C} \qquad (2.2)$$

where q is the deviatoric stress and
C is a material constant

However, other problems still remain. Uzan et al (1992) proposed a similar expression but solving the dimensional problems. Uzan (1992) derived an expression for the secant Poisson's ratio using path independence of the total work along a closed loading cycle which was adopted from Lade and Nelson (1987) work. He showed that experimental Poisson's ratio are close to the computed results. Uzan et al (1992) showed that the model for Poisson's ratio is also able to predict values larger than 0.5.

2.4.2.G-K type models

From the repeated load triaxial tests it was observed that neither Young's modulus, E, nor the Poisson's ratio, υ, is constant. Therefore, assuming that they are constant may cause serious problems in predicting the behaviour of granular material since it shows non-linear stress-dependent behaviour.

Domashuk and Wade (1969) used bulk modulus, K, and the shear modulus, G, rather than E and υ (to which they are simply related) in order to explain stress-dependent behaviour of sand. They recommended use of a triaxial apparatus to estimate K under isotropic (hydrostatic) test conditions. G ,in theory, is obtained from tests in which only shear but no volumetric strains occur. However, this test condition is difficult to set up in the laboratory, but it can be applied approximately when normal stress is maintained constant and the shear stress is varied.

The approach to divide strains into volumetric and shear instead of axial and radial formulations using K and G was taken by Pappin (1979), Pappin and Brown (1980), Brown and Pappin (1981), Brown and Pappin (1985). They developed a non-linear resilient behaviour model, the so called "contour model" (Figure 2.1) which can directly be applied to non-linear numerical analysis methods. In this thesis this model is called either Pappin (especially for figures) or Pappin and Brown. The model is based on the repeated load triaxial test results. They concluded that the shear strain is path-dependent although the volumetric strain is not. The model is in the form:

$$\varepsilon_v = \delta\left[\left(\frac{p}{A}\right)^B \left(1 - C\left(\frac{q}{p}\right)^2\right]\right] \tag{2.3}$$

$$\varepsilon_s = D\,\delta\left[\frac{q}{p + F}\right]\left[\frac{(p_r^2 + q_r^2)^{0.5}}{p_m}\right]^H \tag{2.4}$$

where δ shows "change in"

A, B, C, D, F and H are material constants, A and F having units of stress

The meaning of other parameters is shown in Figure 2.2

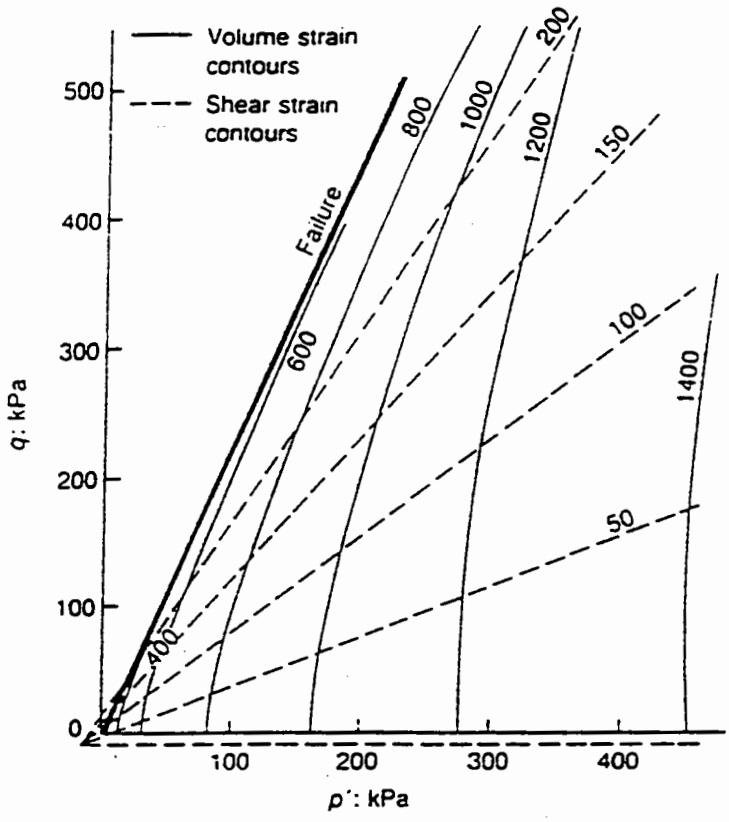

Figure 2.1. Volumetric and shear strain contours (Pappin et al ,1992)

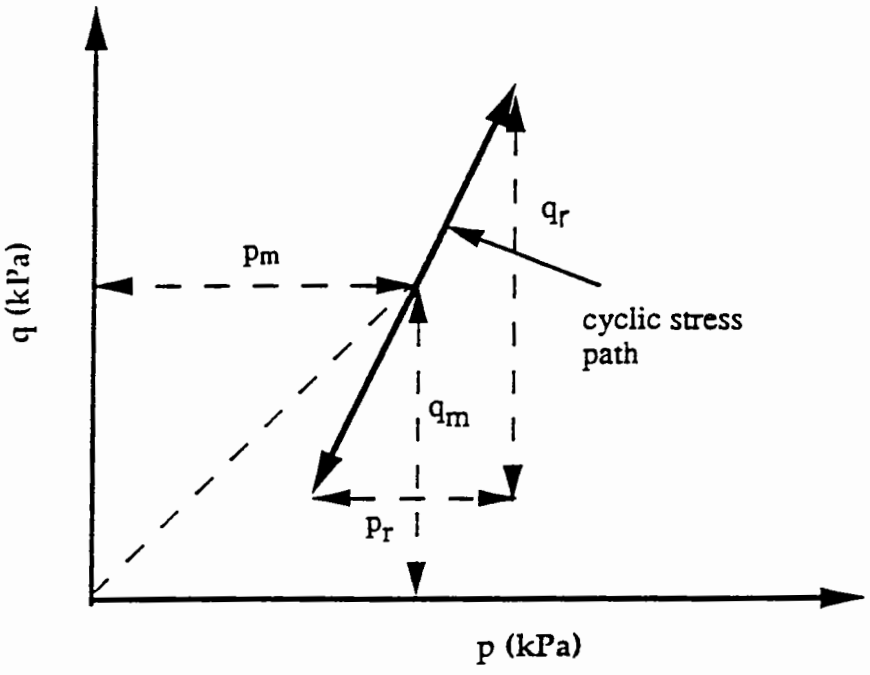

Figure 2.2. Parameters for Pappin and Brown (1985) model

However, Mayhew (1983) found that stress path length, which was included in the model for the shear strain prediction, had no significant effect on the shear strain behaviour. The model was then rewritten by Brown and Selig (1991) in the form of

$$\varepsilon_v = \delta\left[\left(\frac{p}{A}\right)^B \left(1 - C\frac{q^2}{p^2}\right)\right] \tag{2.5}$$

$$\varepsilon_s = \delta\left[\left(\frac{p}{D}\right)^E \frac{q}{p}\right] \tag{2.6}$$

where ε_v and ε_s the volumetric and the shear strain respectively

A, B, C, D and E are material constants, A and D have units of stress

The model predicted the triaxial test results quite well (O'Reilly (1985) and Thom (1988)). Pappin (1979) and Pappin et al (1992) showed that the model is able to predict the behaviour of granular material for both dry and saturated test conditions, in the latter case by treating the stress invariants as effective stresses.

Boyce (1980) developed a non-linear isotropic model with G and K using the theorem of reciprocity (i.e. there is no net loss of strain energy) also expressing it in the volumetric and shear parts. The model is expressed in the form:

$$\varepsilon_v = p^B \left[\frac{1}{A} - \frac{(1 - B)}{6C}\frac{q^2}{p^2}\right] \tag{2.7}$$

$$\varepsilon_s = \frac{p^B}{3C}\frac{q}{p} \tag{2.8}$$

where A, B and C are constants

Mayhew (1983) found that the influence of the mean normal stress on the bulk modulus is different from that on the shear modulus. Therefore, B in the Boyce's model should be different for volumetric and shear strain. This was considered by Sweere et al (1987), Sweere(1990) and Jouve et al (1987) to fit their data into the model. Non-linear analysis performed in this research has revealed that constants B and C should be different for the volumetric and the shear strain. The resulting model is the same as the Pappin and Brown type of model as shown by Brown and Selig (1991). The main drawback of the model is the poor prediction of the volumetric strain although it predicts the shear strain quite well (Allaart,1989). Allaart (1989) modified the model in order to overcome the problem adding another parameter, but results were insufficiently improved.

Elhannani (1991) further introduced anisotropy to the Boyce model. The model then takes the form:

$$\varepsilon_v = p_a^{1-B}\, p^B \left[\frac{1}{A} - \frac{(1 - B)}{6C} \left(\frac{q}{p}\right)^2 - \frac{B}{D}\left(\frac{q}{p}\right)\right] \tag{2.9}$$

$$\varepsilon_s = p_a^{1-B}\, p^B \left[\frac{1}{3C}\frac{q}{p} - \frac{1}{D}\right] \tag{2.10}$$

where p_a is atmospheric pressure (100 kPa)

B and D are the unitless coefficients, A,C and H have the units of stress

The modified Boyce model gave a better prediction between observed and predicted triaxial test results. This model is also able to predict coupling between the volumetric and shear strain.

2.4.3.Hyperbolic models

Hyperbolic stress-strain relations (Kondner (1963), Duncan (1980), Christian and Desai (1977), Ko and Sture (1980)) are also used to predict granular material behaviour. Nataatmadja and Parkin (1989) and Nataatmadja (1992) proposed a hyberbolic type of model to predict granular material behaviour under traffic loading. The model is shown below

$$\frac{M_r}{3p} = B + Aq \qquad (2.11)$$

where A and B are constants

They showed that the model is superior to the K-θ model. However, the model still has the drawback of a constant Poisson's ratio.

2.4.4.Other types of models

Thom (1988) developed a non-linear elastic model for the prediction of results of triaxial and hollow cylinder test results separating the volumetric and the shear strain components in the same manner as Pappin (1979) and Boyce (1980). Major and minor principal stresses are included in the model. Stress path length was considered in the shear strain. The model for the prediction of triaxial test results is in the form of

$$\varepsilon_v = A\,(\delta \ln p)^B \,.\, (\delta p)^C - D\,(\delta((\ln(\sigma_1/\sigma_3))^2))^E \qquad (2.12)$$

$$\varepsilon_s = E\,(\delta(\ln(\sigma_1/\sigma_3)))^F\,(\delta t + \tfrac{1}{3}\,\delta s)^G \qquad (2.13)$$

where σ_1, σ_3 the major and minor principal stresses

$$t = \frac{\sigma_1 + \sigma_3}{2}$$

$$s = \frac{\sigma_1 - \sigma_3}{2}$$

Thom (1988) showed that the model predicts the repeated and hollow cylinder tests quite satisfactorily. However, finding the model constants with the non-linear regression program was found difficult during the research reported in this thesis.

It is possible to develop a new stress-strain relationship using either hyperelastic (Green) or hypoelastic formulations. Hyperelastic formulations are given by Evans and Pister (1966). Ko and Masson (1976) used the hyperelastic formulation to develop a non-linear stress strain relationship. The main drawback of this approach is that it is stress path independent (Chen and Saleeb (1982)).

In order to overcome this difficulty a hypoelastic formulation was first proposed by Truesdell (1955). The formulation was then used by Coon and Evans (1971 and 1972), Darve et al (1976), Hokubec (1968), Collins and Bachus (1987) and Kolymbos (1987). Although the formulation has a theoretical background, the model produced using the formulation has many constants in it , and needs many tests to determine them.

Based on particle contact deformation, models have also been developed consisting of sphere particles in contact and incremental stress strain relationships (Deresiewicz (1958), Mindlin (1949), Duffy and Mindlin (1957)). These models are useful in developing an understanding of the general behaviour of granular assemblies, but use of this type of stress-strain relationship may lead to error in analysis due to oversimplifications (O'Reilly, 1985).

In some certain type of loadings, such as highway loadings, the hysteresis behaviour of granular material may become important-especially where dynamic analyses are carried out. In order to simulate hysteresis behaviour mechanical models consisting of spring/s, block/s and slider/s were used by Iwan (1967), Iwan (1966), Taylor and Larkin (1978), Zytynski et al (1978), Datong and Huicang (1982). However, these models have the same drawbacks as above.

2.5.Anisotropy

In order to better understand the behaviour of granular materials, anisotropy (i.e. directionally varying stiffness) is one of the concepts which should be taken into account. Anisotropy is generally divided into two groups, inherent and stress-induced. However, in this thesis stress-history-induced anisotropy is introduced to differentiate the stress-induced anisotropy from the anisotropy generated after permanent deformation under repeated loading for pavement engineering purposes. Detailed information is given in Sections 6.7.2, 6.7.3 and 6.7.4.

Casagrande and Carillo (1944) may have been the first researchers to differentiate between the inherent and the stress-induced anisotropy. Inherent anisotropy is a physical characteristic inherent in granular material and mainly occurs due to deposition /arrangement of soil particles (Arthur and Menzies (1972), Ochiai and Lade (1983) and Gerrard and Mulholland (1966)). Stress-induced anisotropy occurs during the process of straining of soil particles (Arthur et al (1977), Biarez and Wiendieck (1963)). The reason for the stress-induced anisotropy is mainly permanent strain (Oda and Sudoo (1989)). Oda and Sudoo (1989) found that when a granular material undergoes plastic deformation, new contact points may occur due to compaction but some existing contacts can also disappear and particles may rotate rigidly to take up a new arrangement. They termed this effect stress-induced anisotropy although it is better attributed to stress-history effects to differentiate the change in anisotropy from that occurring during resilient deformation.

In order to measure anisotropy in granular material different apparatus such as the directional shear cell (DSC), true triaxial apparatus (TTA), plane strain apparatus (PSA), hollow cylinder appratus (HCA) and conventional triaxial apparatus (CTA) have been used.

The TTA in which two or three stresses can be applied simultaneously was used by Arthur and Menzies (1972), Haruyama (1981) and Matsuoka and Ishizaki (1981). Figure 2.3 shows the stress condition in a TTA sample. The DSC was used by by Arthur et al (1977), Wong and Arthur (1985) and Budiman et al (1992) in which two normal stresses are applied to the specimen through flexible membranes located within a normal pressure chamber and two shear stresses are transmitted to the specimen by

shear sleeves. Out-of-plane strain is not permitted. Figure 2.4. shows the stresses applied to a DSC sample.

The hollow cylinder apparatus (Hight et al (1983), Hicher and Lade (1987)) is able to apply vertical pressure, torque and confining pressure which can be different inside and outside of the sample. Therefore, it makes possible continous stress rotation. Figure 2.5. shows a hollow cylinder sample and the developed stresses in a cylinder wall.

The conventional triaxial apparatus (Saada and Townsend,1980) is also used to measure anisotropy in a soil. For this purpose, specimens are prepared at various inclinations to the vertical direction (Wesley, 1980) so that principal stress direction will be different for each sample when the vertical load is applied. This method may be easier for clay or fine grained aggregates which have cohesion between the particles, but it may not be practical for road construction materials since they are generally coarser and may not show cohesion between particles. El-Sohby and Andrawes (1973) used a conventional triaxial equipment to measure inherent anisotropy in a sand applying static isotropic pressure incrementally for loading and unloading condition. They also measured the effect of shear stress on stress-induced anisotropy changing the stress ratio σ_1/σ_3 from 1 to 4.5. They concluded that the degree of anisotropy is dependent on the porosity and that a sand mass subjected to hydrostatic pressure is generally anisotropic.

For an anisotropic material, 36 constants would have to be determined-but there is no test equipment yet available which is capable of measuring these (Stackel, 1991). Therefore, some simplifications are necessary when using available test equipment. A

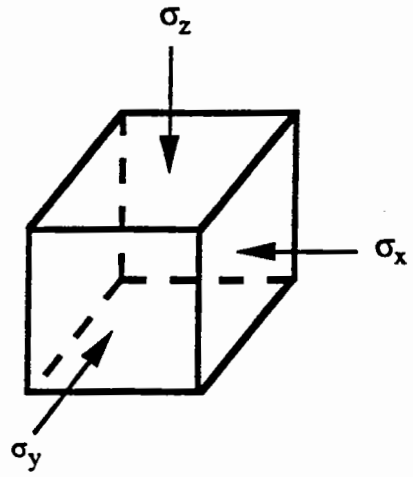

Figure 2.3. Stresses in a TTA sample

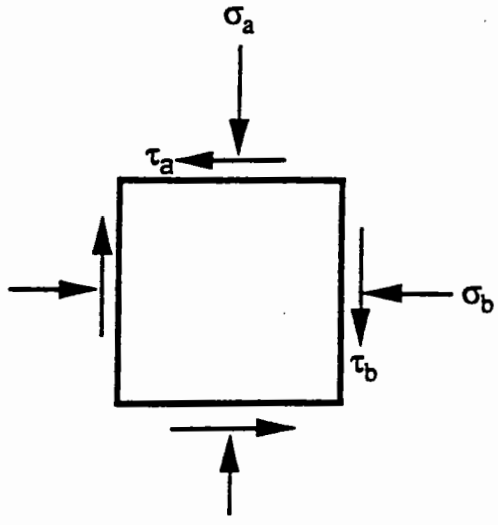

Figure 2.4. Stresses in a DSC sample

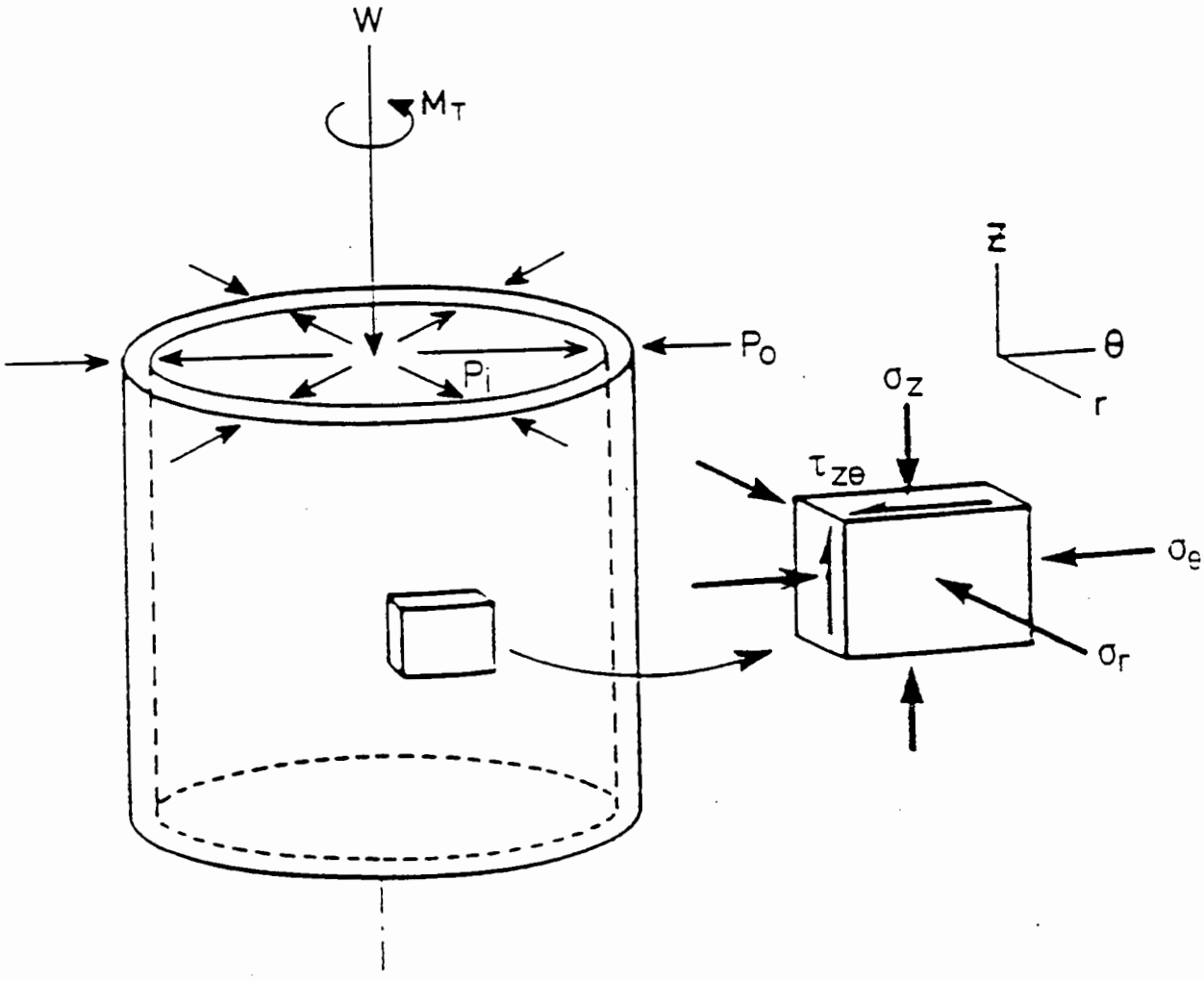

Figure 2.5. Stresses in a HCA sample (Chan, 1990)

first simplification is the symmetry condition in which the material is assumed to show the same properties in one plane. For this purpose soil is generally represented by cross anisotropic (transverse anisotropic) material (Stackel (1991), Chen and Saleeb (1982)) in which the soil behaves isotropically in the horizontal plane whereas it shows a different behaviour in the vertical direction under the same loading conditions. For a linear cross anisotropic material stress-strain relationships were given by Silveria and Souto Silveria (1973), Gazetas (1982), Graham and Houlsby (1983), Pickering (1970), Gerrard (1969), Gerrard and Mulholland (1966) and Barden (1963).

2.5.1.Determination of anisotropy

For a cross-anisotropic material (see Chapter 7), five material constants must be determined from the available test equipment. In order to determine these constants the test apparatus must allow the application of 3 normal and 2 shear stresses which should vary independently. However, this type of equipment is not currently available even for research purposes (Stackel (1991), O'Reilly (1991)). Currently available test equipment which is able to study anisotropy to a certain extent are the cubic triaxial test equipment, the hollow cylinder and cylindrical triaxial test equipment. These test apparatus will be discussed in terms of their ability to make anisotropy measurements.

2.5.1.1.The cubic triaxial test equipment

The cube is an extremely practical shape for varying the principal stresses independently. Stresses can be applied with rigid platens, rubber membranes or a

mixture of both. These cubic test devices can divided into two groups : true triaxial test devices in which stresses in three directions can be independently controlled (Arthur and Menzies (1972), Haruyama (1981) and Matsuoka and Ishizaki (1981)) and plane strain devices e.g. direct shear cells (DSC) in which two normal stresses and shear stresses can be applied and one direction is left free of independent strain application. The DSC has been used by Arthur et al (1977), Wong and Arthur (1985) and Budiman et al (1992). More detailed knowledge about the cubic triaxial apparatus can be obtained from Arthur (1988).

In order to measure the inherent anisotropy due to deposition with TTA cubical samples are prepared at various tilted angles to the direction of pouring. After applying the same stresses to the samples, direct strain results are compared according to the tilting angle (Arthur and Menzies, 1972). Differences between the results show the level of inherent anisotropy. However, isotropic pressure can also be applied to a cubical sample in order to measure the inherent anisotropy (Haruyama, 1981). If a material is isotropic, then the strains obtained from three directions must be equal under hydrostatic test conditions.

In order to measure the stress-induced anisotropy the DSC can be employed for which a sample is prepared in the direction of intermediate principal stress to avoid any influence of inherent anisotropy. Principal stresses are rotated at different angles continously or discontionusly by changing the normal and shear stress. If a material is isotropic, principal stress rotation would have no effect on the stress-strain behaviour of the material. If not, it shows the level of stress-induced anisotropic behaviour.

2.5.5.2.The hollow cylinder apparatus

The hollow cylinder sample is a thick walled cylindrical sample to which four different pressures, namely internal and external pressures, axial load and torque, may be applied (O'Reilly, 1991). Principal stresses can be rotated by changing their relationship to torque.

In order to determine the inherent anisotropy an isotropic pressure is applied to a sample. If the response are the same in the vertical and horizontal direction, the material is isotropic, if not the material is said to be anisotropic.

In order to determine the stress-induced anisotropy the sample is subjected to the rotation of principal stresses by applying normal stress and torque while keeping the confining pressure constant. If the response is the same at various rotation angles, the material has not been affected by stress-induced anisotropy. Otherwise it has stress-induced anisotropy.

2.5.5.3.The repeated load triaxial test apparatus

The repeated load triaxial apparatus (RLTA) does not allow rotation of the principal stresses, unlike the hollow cylinder or cubic triaxial test apparatus, since principal stress directions are fixed due to the equipment design. Chan (1990) monitored the

resilient volumetric and shear strain behaviour of granular material in HCA testing during permanent deformation tests. Peak values of resilient stresses and strains were relatively close to each other both with and without (triaxial condition) shear reversals. Therefore the RLTA has continuing value for the determination of the resilient properties of granular materials and was used in this project. When the cell pressure is cycled the RLTA can be used to measure elastic anisotropy in a sample. For this particular purpose, the material is subjected to different levels of repeated cell pressure which are carefully selected so that they do not cause any plastic strain after each stress path. Radial and axial strains are measured and the ratio of axial strain to radial strain gives an indication of the anisotropy in a sample.

2.5.5.4.Some observations from previous studies

Haruyama (1981) performed isotropic compresion tests by controlling the stresses in each direction independently on cubic specimens consisting of glass beads. The direction of sample deposition was in the direction of gravity. He found that lower compressibility was obtained in the direction of deposition than in the other two perpendicular directions where the horizontal strains were equal to each other.

Ochai and Lade (1983) used sand with a cross-anisotropic fabric in cubic specimens. Samples were prepared in a special mould by pouring and shaking sand grains in several layers. Drained tests were performed under conventional triaxial compression, plane strain and cubic triaxial conditions. After isotropic compression tests they found

that the strains perpendicular to the long axis of grains were only about half of the other two linear strains.

From the above two results it may be concluded that under isotropic stress conditions for a cubic sample, horizontal strains are equal. Assuming the above conclusion to be correct, a conventional cylindrical sample can also be used to study anisotropy in the sample.

σ_x, σ_y, σ_z	Normal stresses in x, y and z directions respectively
σ_n	Principal stresses
σ_a	Axial stress
σ_r	Radial stress
σ_0	Hydrostatic stress
σ_{oct}	Octahedral normal stress
σ_1, σ_2, σ_3	The major, intermediate and minor principal stresses respectively
τ_{xy}, τ_{xz}, τ_{yz}	Shear stresses in the xy, xz and yz planes
τ_{oct}	Octahedral shear stress
δ	"change in"
δ_{ij}	Kronecker delta (if i=j then δ_{ij}=1 otherwise 0)
γ	Tensorial shear strain
γ_{oct}	The octahedral shear strain
υ	Poisson's ratio
υ_1	Effect of horizontal strain in the horizontal strain
υ_2	Effect of horizontal strain on the vertical strain
υ_3	Effect of vertical strain on the horizontal strain
ω	Strain energy density
Ω	Complementary energy function
λ, μ	Lame's constants
t	$\frac{\sigma_1+\sigma_3}{2}$
s	$\frac{\sigma_1-\sigma_3}{2}$

LIST OF TABLES

LIST OF FIGURES

CHAPTER 1

INTRODUCTION

1.1.Pavement structure

A pavement is constructed to carry traffic safely and economically. Safety aspects come from friction between the wheel and the pavement surface. The rougher the surfacing the higher the friction and the greater the skid resistance. The economy is related to the optimum use of available construction material. Layer thicknesses are determined in order that the pavement will meet its structural role of adequate resistance to deformation for a desired period.

A pavement is composed of surfacing layer, base, sub-base, capping (if required) and subgrade layers (Figure 1.1). This composition depends on the design life, traffic volume, availability of materials and subgrade strength. The purpose of the surfacing is to provide a smooth and comfortable riding surface which can be trafficked at minimum operation cost whilst providing the necessary resistance to skidding. The base is the main structural layer which distributes the wheel loads. In the UK it is generally built with an asphaltic mixture, but for secondary roads or roads carrying light traffic where a thin asphalt layer is used, it is often built with granular material. The purpose of the sub-base is to provide a good working platform for the construction of upper layers, to distribute wheel loads so that the subgrade layer will not deform excessively and to prevent the subgrade layer from frost action. Capping, which is

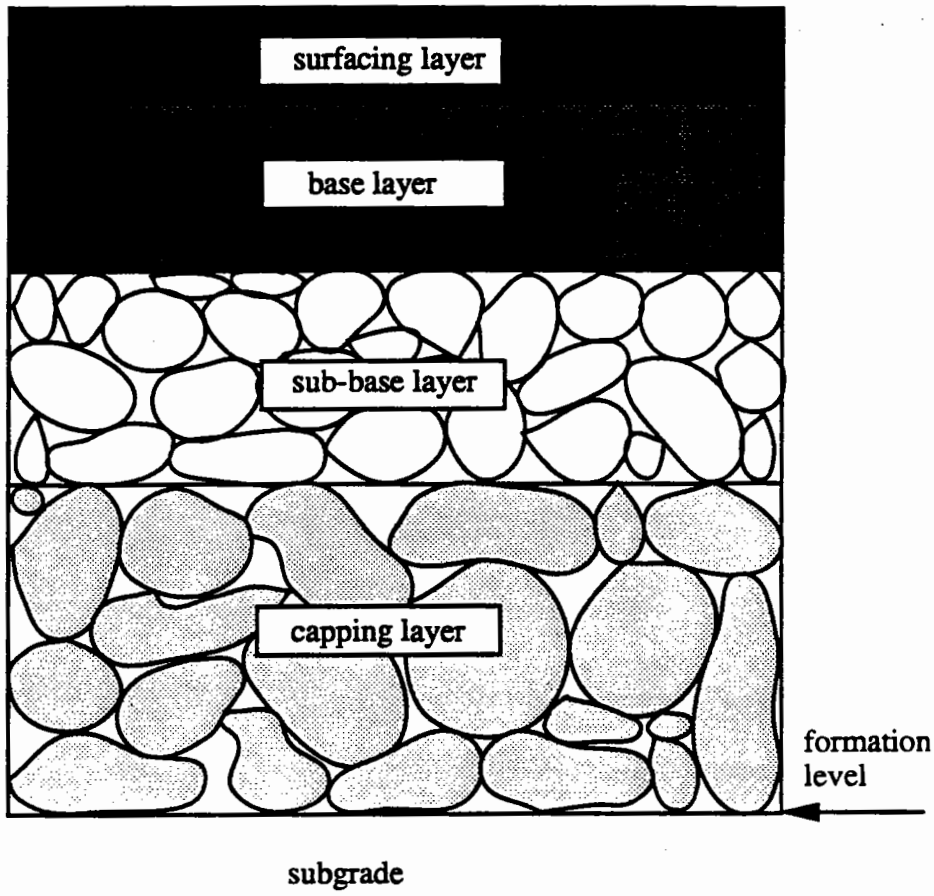

Figure 1.1. A typical flexible pavement

often used when the CBR (California Bearing Ratio) of the soil is low, is a layer of low cost, generally local material and is constructed in order to add stiffness to the subgrade, providing a working platform on which sub-base layer may be constructed safely. Subgrade is the natural or fill material underneath the pavement.

1.2.Pavement design

Design methods for flexible pavements may be classified into two groups: empirical and semi-empirical, and analytical.

The empirical and semi-empirical design methods are related to past experience. They may incorporate laboratory and field tests in order to classify the pavement materials but not to determine their fundamental mechanical properties. One of the best known empirical method is the CBR design method to design the total pavement structure (Department of the Environment, 1970). Some other empirical methods use a "catalogue" (e.g RStO 86 (1986)) in which the thicknesses for each layer are predetermined depending on the soil and traffic classification. These type of design methods are only satisfactory as long as the materials and conditions have not changed from those on which the experience was obtained.

However, due to the increase in traffic, especially of commercial vehicles, and the introduction of new road construction materials the use of analytical methods has become more necessary and more widespread. These methods adopt a structural model of pavement response to loading and use elastic layered theory (ELT) or the finite element method (FEM) to perform the necessary computations to obtain the stresses and strains in the pavement. In the elastic layered theory a pavement is divided into several layers and for each layer a Young's modulus and Poisson's ratio are assigned. The materials comprising each layer are assumed to be linearly elastic. This is not the case for soils and granular materials since they exhibit non-linear behaviour (Hicks and Monismith, 1971). The FEM (Duncan et al, 1968) overcomes this limitation at the expense of more complex analysis and may be used to incorporate the non-linear properties of soil and granular material. The success (or failure) of the FEM comes from the models employed to describe the pavement materials' behaviour. The necessary data required in order to perform an analysis may be obtained from laboratory or field tests for both analytical methods. Calculated strains due to wheel loading are, typically, compared with the allowable tensile strain underneath the bound

layer and the vertical strain in the subgrade at the formation level. If the allowable values are not achieved, thicknesses are changed until the design criteria are satisfied.

The research project described in this thesis has been concerned entirely with determining the behaviour of unbound granular material and modelling that behaviour for pavement analysis purposes.

1.3.Deformation characteristics of granular material

The deformation of a granular layer under traffic loading is composed of two parts- resilient (elastic or recoverable) and permanent (plastic). The stresses observed in a pavement foundation are well below those which might cause conventional shear failure (Brown, 1981). Instead, failure is defined by serviceability limits of which there are two types in pavements. They are

a) fatigue cracking in the bound layers associated with the resilient response of the pavement to transient loading and

b) rutting due to accumulation of permanent strain throughout the pavement structure (Brown and Selig, 1991).

For a pavement foundation, rutting, which is associated with the accumulation of permanent strain, is the only failure criterion since no bound materials (which might suffer resilient fatigue) are involved (Brown and Selig, 1991). However, after constructing the upper layers of a pavement and after a number of traffic loads have been applied, the increment of permanent deformation is much smaller than the

increment of resilient deformation. It is then that the resilient strains, which are of concern to the behaviour of the pavement structure built on the granular layer, gain importance.

A measure of the resilient behaviour of a pavement structure is also required in order to predict the future behaviour of the structure which has important consequences for its maintenance programme (Peattie, 1978).

1.4.Research aims

The main area for study is the non-linear characteristics of granular material which are investigated using the effective stress principle when possible.

In summary the research aims are to:

- Investigate the behaviour of a wide variety of granular materials under different stress paths using a repeated load triaxial apparatus,

- Determine the resilient anisotropic chatacteristics of granular material with the repeated load triaxial apparatus,

- Show the applicability of the selected different constitutive models for the prediction of the test results and in conjuction with this, to propose a new constitutive model to predict the behaviour of granular material under repeated loading,

• Show the applicability of some selected models in pavement analysis using the finite element approach.

1.5.Contents of thesis

Wheel loading causes vertical, horizontal and shear stresses in the pavement. In this research a repeated load triaxial apparatus which can only simulate vertical and horizontal stresses is used. Chan (1990) has shown that shear reversals affect the permanent behaviour of granular material, but their effect on the resilient behaviour is not significant (see Chapter 2). Therefore, the repeated load triaxial apparatus may be used to simulate the resilient behaviour of granular material even though it cannot provide shear reversals in a controlled manner. In Chapter 3 the repeated load triaxial apparatus is introduced.

Different granular materials of widely varying types and from coarse to fine grain size, were tested under the same stress regime in order to generalize the behaviour of granular material. The materials were soft limestone (SL), gritstone (GS), sand and gravel (SAG), furnace bottom ash (FBA), graded washed river sand (GWRS) and Fontainebleu sand (FS). Materials were tested dry except for FBA and FS because they experienced significant permanent deformation after only a few loadings when dry. Detailed knowledge about the materials is given in Chapter 4.

It is well known that traffic loading is repeated and of random magnitude. In order to closely simulate these stresses caused by such loading, a range of different stress paths were applied. These aspects are discussed in Chapter 5.

Anisotropy is defined as the ratio of axial strain to radial strain under isotropic stress conditions (Biarez and Hicher, 1987). Anisotropy is an important characteristic of granular material but has normally been neglected in the design of pavement structures. This may be due to the lack of equipment to measure it. Although early research work studied the anisotropic properties of sand (Arthur et al, 1972), there has been little or no work on the anisotropy of granular materials for pavement construction. This may be due to the difficulty of testing coarse granular material or because of the theoretical problems involved. In this research, resilient anisotropy has been measured on the materials using the repeated load triaxial apparatus. Attempts have been made to measure both the inherent and stress-induced anisotropy and to see these change after the granular material has been subjected to permanent deformation. Results are discussed in detail in Chapter 6.

A further aspect of the research has been the constitutive modelling of the resilient behaviour of the aggregate under repeated loading. Two different mathematical models were proposed to predict the resilient behaviour of granular material. The first one predicts the strains due to repeated deviatoric stress with constant cell pressure. The second model, incorporating inherent anisotropy, is for the prediction of resilient strains due to the repetition of both axial and radial stresses. These aspects are discussed in Chapter 7. Predictions are made with the models and compared with the measured results and with the results of other models (Chapter 8).

The models are then implemented in the CRISP (CRItical State Program) finite element program in order to show its applicability to practical use. This aspect is discussed in Chapter 9.

Chapter 10 gives the conclusions of the research and makes proposals for future work.

CHAPTER 2

LITERATURE REVIEW

2.1.Introduction

The behaviour of granular material is very important in flexible pavements where the wearing course is thin, because it will then provide the main structural element of the pavement. Granular material in the pavement is subjected to repeated loading that can be approximately simulated using a repeated load triaxial apparatus or hollow cylinder apparatus. From the results of tests with these apparatus appropriate constitutive models can be deduced and used for numerical solutions of pavement behaviour. Pavement engineers are principally concerned with sub-failure resilient behaviour of granular materials, therefore, plastic behaviour due to single or repeated loading is excluded from discussion in this chapter.

The literature review is divided into four sections, namely, testing of granular materials, influences on granular material behaviour, modelling of granular material behaviour and anisotropy.

2.2.Testing of granular materials

In order to understand the behaviour of granular material under traffic loading, either site tests or laboratory tests or both should be carried out. Generally speaking, site

testing is more expensive and time consuming when compared with laboratory tests. In order to determine the stress state of a material, a test apparatus is needed which is able to apply six independent stresses to a sample (three normal and three shear stresses). However, this type of equipment has not yet been available even at the research level (Stackel (1991) and O'Reilly (1991)). Therefore, available test equipment in the laboratory able to simulate traffic loading such as the repeated load triaxial, hollow cylinder apparatus or, the cubical triaxial apparatus has to be used.

The hollow cylinder and the cubic triaxial apparatuses are still far away from practical use other than research. These apparatuses are particularly important to study anisotropy in the soils (Arthur et al (1977), Arthur and Menzies (1972), Wong and Arthur (1985), Budiman et al (1992), Symes et al (1982)). The hollow cylinder apparatus can also be used to characterize the granular material behaviour under traffic loading (O'Reilly (1985), Thom (1988), and Chan (1990)). However, the use of triaxial apparatus is widespread all over the world, commercially available, easy to control and cheaper compared with other complicated test equipment.

A triaxial apparatus has a cylindrical sample which is subjected to two independently controlled stress components, vertical load and confining pressure. The confining pressure may be provided by a fluid or air pressure or by an internal partial vacuum. The limitation of the triaxial apparatus is that it only applies two independent stresses out of the six independent stresses developed in a pavement. Horizontal stresses are assumed to be equal to each other and it is impossible to simulate principal stress rotation which occurs when a tyre travels on a pavement. Furthermore the horizontal and vertical stress pulses tend to be of different wave length and may be slightly out of phase with each other. In order to provide a reasonable simulation of pavement loading

with triaxial equipment, it should be able to cycle both the vertical load and cell pressure in-phase. However, many laboratories still use constant confining pressure testing (Sweere, 1990) to determine the resilient behaviour of the material since this type of equipment is more cost effective when compared with the apparatus which can cycle both pressures at the same time. However, Brown and Hyde (1975) have shown that similar resilient behaviour can be obtained from cyclic and constant confining stress when the constant stress is equal to the mean of the cyclic confining stress values.

In conjunction with the repeated loading of granular materials, a triaxial apparatus was developed by Boyce (1976) at Nottingham University which was able to cycle both the deviatoric and confining stresses. Pappin (1979) slightly modified some parts of the apparatus in or order to apply extension stress paths to the granular material. During the research reported here the electronic control system of the apparatus was replaced with a digital control system (Chan and Sausa, 1991). More details about the development of the equipment can be obtained from Boyce (1976), Boyce et al (1976), Pappin (1979) and Brown et al (1989).

The cubic triaxial (true triaxial) has one more degree of freedom than the cylindrical triaxial apparatus in that it allows three independent orthogonal stresses. However, this type of equipment is generally difficult to operate and the sample is surrounded by a mass of mechanical equipment, therefore, the sensitivity is reduced and the apparatus is not suited to measure small strains such as those typical of the pavement layers (Thom, 1988).

The hollow cylinder apparatus (Chan, 1990) applies the confining pressure and the axial deviatoric stress in a similar fashion to the triaxial apparatus, but it also applies a torque to the cylinder which causes shear stresses on cylindrical surfaces. Although it is possible to measure small strains in the sample, there is a non-uniformity in stress which creates some difficulties especially if there is a difference between the external and internal confining stresses. Sample size also limits it to the testing of fine grained granular materials.

Because of these limitations, and because of availability, a repeated load triaxial apparatus was chosen to test granular material in the project described here.

2.3.Influences on granular material behaviour

Stress may be the major effect on granular material behaviour. However there are many other effects which are likely to affect the behaviour of granular material. Of these, particle shape, density, grading and moisture content are considered to be important and are discussed here.

2.3.1.Particle shape

Several methods have been proposed to define particle shape. The parameters classified by Selig and Roner (1987) are useful. They are

a) **Flakiness or flatness** - the ratio of particle thickness to width.

b) **Elongation** - the ratio of length to width

c) **Sphericity** - a measure of how much the shape of a particle deviates from a sphere

d) **Roundness or angularity** - a measure of sharpness of the edges or corners of an individual particle.

Flaky particles which do not lie along the failure line increase the shear strength of granular material, the disadvantage being that an increase in the flakiness may cause problems of breakage, abrasion, increased permanent strain and decreasing stiffness of the material (Selig and Roner, 1987).

Aggregate type may have a significant effect on the resilient modulus when other parameters such as grading, density and applied stress are kept constant. Barksdale and Itani (1989) tested different granular materials with the same grading and they found that angular materials had a higher resilient modulus than rounded gravel, the increase being about 50% at low mean normal stress conditions decreasing to about 25% at high mean normal stress levels.

Thom (1988) and Thom and Brown (1989) carried out repeated load triaxial tests on different granular materials, they found that:

a) The resilient modulus of granular materials at low strain levels may be influenced by particle texture i.e roughness.

b) A correlation exists between elastic stiffness and the surface friction properties of a material.

c) High resilient modulus and good load spreading properties in the pavement may be expected from material with angular to subangular shaped particles and a very rough surface when compared with material with subrounded or rounded particles and a smooth surface.

2.3.2.Grading and Density

Thom and Brown (1988) tested limestone with a maximum size of 10 mm at different gradings and different compaction levels. All tests were carried out using repeated load triaxial equipment. The test results showed that the state of compaction (i.e. density) had little effect on the resilient modulus, (although there was some slight increase for denser material) and uniform gradings gave a stiffness about 1.3 times as large as for broadly graded samples. Brown and Selig (1991) also confirmed that the resilient properties of granular material are not significantly affected by grading or density.

Barksdale and Itani (1989) and Hicks and Monismith (1971) found that as the grading became finer, the resilient modulus decreased dramatically by about 60%. Triaxial tests carried out by Kamal et al (1993) have shown that a material containing more fine material has a lower resilient modulus than the coarse material.

2.3.3. Moisture content

As moisture content increases in granular layer, compaction is facilitated i.e. "workability" increases. But if the moisture content increases above a certain level, the optimum, which can be experimentally found, it will cause a decrease in friction between particles and therefore less strength against shear.

Hicks and Monismith (1971) showed that the resilient modulus steadily decreases as the moisture content increases above optimum.

2.4.Mathematical modelling

The deformation of granular layers under traffic loading is composed of two parts, resilient and permanent. The stresses involved are well below levels which might cause rapid shear failure of a pavement in service (Brown, 1981). Therefore the resilient

rapid shear failure of a pavement in service (Brown, 1981). Therefore the resilient response of the pavement becomes more important during service. However, for a pavement foundation, rutting, which is the accumulation of plastic strain with time is the only failure criteria since no bound materials (which might fail by resilient fatigue) are involved (Brown and Selig, 1991). After constructing the upper layers of the pavement and a number of traffic loads have been applied, the increment of permanent deformation is much smaller than the increment of resilient deformation. Hence the resilient characteristics of the granular layer in the pavement structure gain importance.

Wood (1991) divided models into four groups. First, "children's" models such as linear elasticity and perfect plasticity. Second, "student" models such as a work-hardening plastic model (e.g. Cam clay models). Third, engineering models such as non-linear elasticity, anisotropic elasticity, anisotropic plasticity and those with viscous properties. Fourth, philosopher's models which serve all aspects of soil behaviour even for very complicated structures such as nuclear power stations. According to this classification most of the models developed for pavement analysis are engineering models.

In this section models developed for resilient behaviour of granular material in the pavement will be discussed. Some other elastic models which have not been used for modelling granular material behaviour will also be briefly discussed. Although the models were originally proposed using a variety of terms they are expressed here, wherever possible, in terms of the stress invariants p (mean normal stress) and q (deviatoric stress).

2.4.1.K-θ type models

Granular materials exhibit non-linear, stress dependent behaviour. Early studies (Hicks and Monismith, 1971) showed that the resilient modulus is a function of the maximum mean normal stress or (bulk stress, θ=3p), then the model is written in the form

$$M_r = A\,(3p_{max})^{B} \qquad \text{or} \qquad M_r = A\,p_a\left(\frac{3p_{max}}{p_a}\right)^{B} \tag{2.1}$$

where A, B are material constants

p_{max} is maximum mean normal stress (kPa)

p_a is atmospheric pressure (kPa)

The second formulation is introduced here so as to express the coefficients in a non-dimensional from. The model has been found extremely useful and simple and is still in use for design of new pavements (Thompson, 1992) or pavement evaluation (Brown and Almeida, 1993). However, it has some drawbacks. First, it always assumes that the Poisson's ratio is constant although experimental results have revealed that this is not the case. Second, the resilient modulus varies with the deviatoric stress q as well as the normal stress p (Stackel (1973), Uzan (1985) and May and Witczak (1981)). Therefore it can only be used for low shear stress levels. Clearly such a limitation is unsatisfactory for pavement applications where, in general, shear stresses are relatively large. Third the model has been developed from simple laboratory triaxial test results in which the initial deviatoric stress is always zero and in which the confining pressure is constant.

The second drawback has been considered by Stackel (1973) and Uzan (1985) and they modified the model in order to include the deviatoric stress. The modified form of the model is shown below.

$$M_r = A\,(3p_{max})^{B}\,q^{C} \quad \text{or} \quad M_r = A\,p_a\left(\frac{3p_{max}}{p_a}\right)^{B}\left(\frac{q}{p_a}\right)^{C} \qquad (2.2)$$

where q is the deviatoric stress and
C is a material constant

However, other problems still remain. Uzan et al (1992) proposed a similar expression but solving the dimensional problems. Uzan (1992) derived an expression for the secant Poisson's ratio using path independence of the total work along a closed loading cycle which was adopted from Lade and Nelson (1987) work. He showed that experimental Poisson's ratio are close to the computed results. Uzan et al (1992) showed that the model for Poisson's ratio is also able to predict values larger than 0.5.

2.4.2.G-K type models

From the repeated load triaxial tests it was observed that neither Young's modulus, E, nor the Poisson's ratio, υ, is constant. Therefore, assuming that they are constant may cause serious problems in predicting the behaviour of granular material since it shows non-linear stress-dependent behaviour.

Domashuk and Wade (1969) used bulk modulus, K, and the shear modulus, G, rather than E and υ (to which they are simply related) in order to explain stress-dependent behaviour of sand. They recommended use of a triaxial apparatus to estimate K under isotropic (hydrostatic) test conditions. G ,in theory, is obtained from tests in which only shear but no volumetric strains occur. However, this test condition is difficult to set up in the laboratory, but it can be applied approximately when normal stress is maintained constant and the shear stress is varied.

The approach to divide strains into volumetric and shear instead of axial and radial formulations using K and G was taken by Pappin (1979), Pappin and Brown (1980), Brown and Pappin (1981), Brown and Pappin (1985). They developed a non-linear resilient behaviour model, the so called "contour model" (Figure 2.1) which can directly be applied to non-linear numerical analysis methods. In this thesis this model is called either Pappin (especially for figures) or Pappin and Brown. The model is based on the repeated load triaxial test results. They concluded that the shear strain is path-dependent although the volumetric strain is not. The model is in the form:

$$\varepsilon_v = \delta\left[\left(\frac{p}{A}\right)^B \left(1 - C\left(\frac{q}{p}\right)^2\right]\right. \tag{2.3}$$

$$\varepsilon_s = D\,\delta\left[\frac{q}{p + F}\right]\left[\frac{(p_r^2 + q_r^2)^{0.5}}{p_m}\right]^H \tag{2.4}$$

where δ shows "change in"

A, B, C, D, F and H are material constants, A and F having units of stress

The meaning of other parameters is shown in Figure 2.2

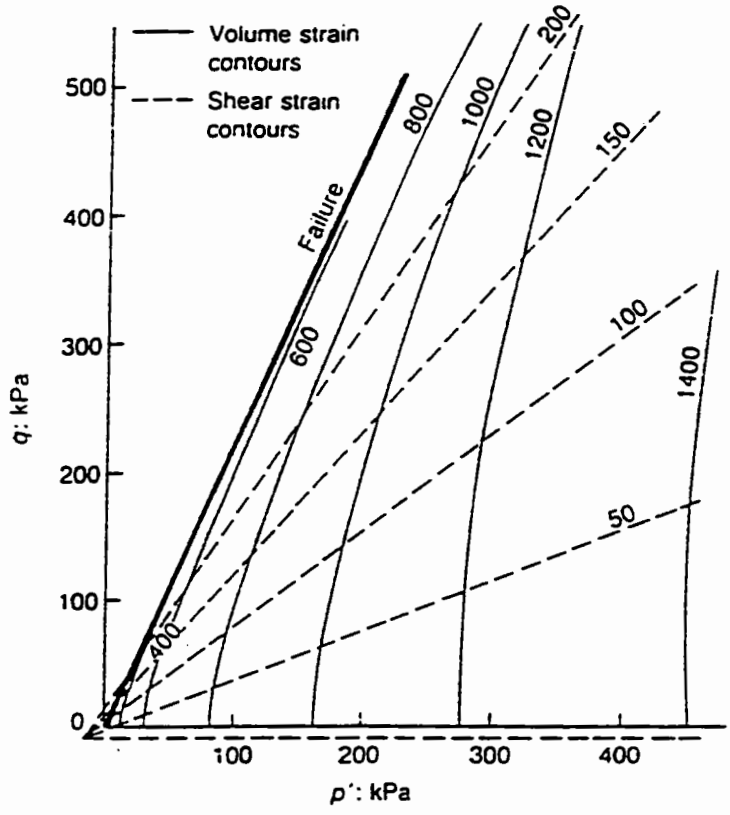

Figure 2.1. Volumetric and shear strain contours (Pappin et al ,1992)

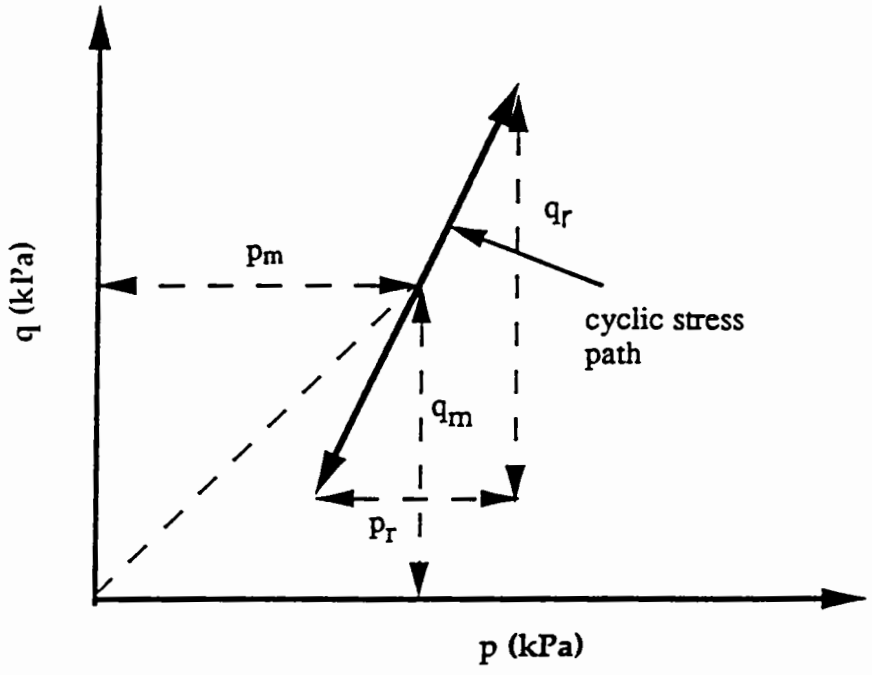

Figure 2.2. Parameters for Pappin and Brown (1985) model

However, Mayhew (1983) found that stress path length, which was included in the model for the shear strain prediction, had no significant effect on the shear strain behaviour. The model was then rewritten by Brown and Selig (1991) in the form of

$$\varepsilon_v = \delta\left[\left(\frac{p}{A}\right)^B \left(1 - C\frac{q^2}{p^2}\right)\right] \tag{2.5}$$

$$\varepsilon_s = \delta\left[\left(\frac{p}{D}\right)^E \frac{q}{p}\right] \tag{2.6}$$

where ε_v and ε_s the volumetric and the shear strain respectively

A, B, C, D and E are material constants, A and D have units of stress

The model predicted the triaxial test results quite well (O'Reilly (1985) and Thom (1988)). Pappin (1979) and Pappin et al (1992) showed that the model is able to predict the behaviour of granular material for both dry and saturated test conditions, in the latter case by treating the stress invariants as effective stresses.

Boyce (1980) developed a non-linear isotropic model with G and K using the theorem of reciprocity (i.e. there is no net loss of strain energy) also expressing it in the volumetric and shear parts. The model is expressed in the form:

$$\varepsilon_v = p^B \left[\frac{1}{A} - \frac{(1 - B)}{6C}\frac{q^2}{p^2}\right] \tag{2.7}$$

$$\varepsilon_s = \frac{p^B}{3C}\frac{q}{p} \tag{2.8}$$

where A, B and C are constants

Mayhew (1983) found that the influence of the mean normal stress on the bulk modulus is different from that on the shear modulus. Therefore, B in the Boyce's model should be different for volumetric and shear strain. This was considered by Sweere et al (1987), Sweere(1990) and Jouve et al (1987) to fit their data into the model. Non-linear analysis performed in this research has revealed that constants B and C should be different for the volumetric and the shear strain. The resulting model is the same as the Pappin and Brown type of model as shown by Brown and Selig (1991). The main drawback of the model is the poor prediction of the volumetric strain although it predicts the shear strain quite well (Allaart,1989). Allaart (1989) modified the model in order to overcome the problem adding another parameter, but results were insufficiently improved.

Elhannani (1991) further introduced anisotropy to the Boyce model. The model then takes the form:

$$\varepsilon_v = p_a^{1-B} p^B \left[\frac{1}{A} - \frac{(1 - B)}{6C} \left(\frac{q}{p}\right)^2 - \frac{B}{D}\left(\frac{q}{p}\right)\right] \tag{2.9}$$

$$\varepsilon_s = p_a^{1-B} p^B \left[\frac{1}{3C}\frac{q}{p} - \frac{1}{D}\right] \tag{2.10}$$

where p_a is atmospheric pressure (100 kPa)

B and D are the unitless coefficients, A,C and H have the units of stress

The modified Boyce model gave a better prediction between observed and predicted triaxial test results. This model is also able to predict coupling between the volumetric and shear strain.

2.4.3.Hyperbolic models

Hyperbolic stress-strain relations (Kondner (1963), Duncan (1980), Christian and Desai (1977), Ko and Sture (1980)) are also used to predict granular material behaviour. Nataatmadja and Parkin (1989) and Nataatmadja (1992) proposed a hyberbolic type of model to predict granular material behaviour under traffic loading. The model is shown below

$$\frac{M_r}{3p} = B + Aq \qquad (2.11)$$

where A and B are constants

They showed that the model is superior to the K-θ model. However, the model still has the drawback of a constant Poisson's ratio.

2.4.4.Other types of models

Thom (1988) developed a non-linear elastic model for the prediction of results of triaxial and hollow cylinder test results separating the volumetric and the shear strain components in the same manner as Pappin (1979) and Boyce (1980). Major and minor principal stresses are included in the model. Stress path length was considered in the shear strain. The model for the prediction of triaxial test results is in the form of

$$\varepsilon_v = A\,(\delta \ln p)^B \,.\, (\delta p)^C - D\,(\delta((\ln(\sigma_1/\sigma_3))^2))^E \qquad (2.12)$$

$$\varepsilon_s = E\,(\delta(\ln(\sigma_1/\sigma_3)))^F\,(\delta t + \tfrac{1}{3}\,\delta s)^G \qquad (2.13)$$

where σ_1, σ_3 the major and minor principal stresses

$$t = \frac{\sigma_1 + \sigma_3}{2}$$

$$s = \frac{\sigma_1 - \sigma_3}{2}$$

Thom (1988) showed that the model predicts the repeated and hollow cylinder tests quite satisfactorily. However, finding the model constants with the non-linear regression program was found difficult during the research reported in this thesis.

It is possible to develop a new stress-strain relationship using either hyperelastic (Green) or hypoelastic formulations. Hyperelastic formulations are given by Evans and Pister (1966). Ko and Masson (1976) used the hyperelastic formulation to develop a non-linear stress strain relationship. The main drawback of this approach is that it is stress path independent (Chen and Saleeb (1982)).

In order to overcome this difficulty a hypoelastic formulation was first proposed by Truesdell (1955). The formulation was then used by Coon and Evans (1971 and 1972), Darve et al (1976), Hokubec (1968), Collins and Bachus (1987) and Kolymbos (1987). Although the formulation has a theoretical background, the model produced using the formulation has many constants in it , and needs many tests to determine them.

Based on particle contact deformation, models have also been developed consisting of sphere particles in contact and incremental stress strain relationships (Deresiewicz (1958), Mindlin (1949), Duffy and Mindlin (1957)). These models are useful in developing an understanding of the general behaviour of granular assemblies, but use of this type of stress-strain relationship may lead to error in analysis due to oversimplifications (O'Reilly, 1985).

In some certain type of loadings, such as highway loadings, the hysteresis behaviour of granular material may become important-especially where dynamic analyses are carried out. In order to simulate hysteresis behaviour mechanical models consisting of spring/s, block/s and slider/s were used by Iwan (1967), Iwan (1966), Taylor and Larkin (1978), Zytynski et al (1978), Datong and Huicang (1982). However, these models have the same drawbacks as above.

2.5.Anisotropy

In order to better understand the behaviour of granular materials, anisotropy (i.e. directionally varying stiffness) is one of the concepts which should be taken into account. Anisotropy is generally divided into two groups, inherent and stress-induced. However, in this thesis stress-history-induced anisotropy is introduced to differentiate the stress-induced anisotropy from the anisotropy generated after permanent deformation under repeated loading for pavement engineering purposes. Detailed information is given in Sections 6.7.2, 6.7.3 and 6.7.4.

Casagrande and Carillo (1944) may have been the first researchers to differentiate between the inherent and the stress-induced anisotropy. Inherent anisotropy is a physical characteristic inherent in granular material and mainly occurs due to deposition /arrangement of soil particles (Arthur and Menzies (1972), Ochiai and Lade (1983) and Gerrard and Mulholland (1966)). Stress-induced anisotropy occurs during the process of straining of soil particles (Arthur et al (1977), Biarez and Wiendieck (1963)). The reason for the stress-induced anisotropy is mainly permanent strain (Oda and Sudoo (1989)). Oda and Sudoo (1989) found that when a granular material undergoes plastic deformation, new contact points may occur due to compaction but some existing contacts can also disappear and particles may rotate rigidly to take up a new arrangement. They termed this effect stress-induced anisotropy although it is better attributed to stress-history effects to differentiate the change in anisotropy from that occurring during resilient deformation.

In order to measure anisotropy in granular material different apparatus such as the directional shear cell (DSC), true triaxial apparatus (TTA), plane strain apparatus (PSA), hollow cylinder appratus (HCA) and conventional triaxial apparatus (CTA) have been used.

The TTA in which two or three stresses can be applied simultaneously was used by Arthur and Menzies (1972), Haruyama (1981) and Matsuoka and Ishizaki (1981). Figure 2.3 shows the stress condition in a TTA sample. The DSC was used by by Arthur et al (1977), Wong and Arthur (1985) and Budiman et al (1992) in which two normal stresses are applied to the specimen through flexible membranes located within a normal pressure chamber and two shear stresses are transmitted to the specimen by

shear sleeves. Out-of-plane strain is not permitted. Figure 2.4. shows the stresses applied to a DSC sample.

The hollow cylinder apparatus (Hight et al (1983), Hicher and Lade (1987)) is able to apply vertical pressure, torque and confining pressure which can be different inside and outside of the sample. Therefore, it makes possible continous stress rotation. Figure 2.5. shows a hollow cylinder sample and the developed stresses in a cylinder wall.

The conventional triaxial apparatus (Saada and Townsend,1980) is also used to measure anisotropy in a soil. For this purpose, specimens are prepared at various inclinations to the vertical direction (Wesley, 1980) so that principal stress direction will be different for each sample when the vertical load is applied. This method may be easier for clay or fine grained aggregates which have cohesion between the particles, but it may not be practical for road construction materials since they are generally coarser and may not show cohesion between particles. El-Sohby and Andrawes (1973) used a conventional triaxial equipment to measure inherent anisotropy in a sand applying static isotropic pressure incrementally for loading and unloading condition. They also measured the effect of shear stress on stress-induced anisotropy changing the stress ratio σ_1/σ_3 from 1 to 4.5. They concluded that the degree of anisotropy is dependent on the porosity and that a sand mass subjected to hydrostatic pressure is generally anisotropic.

For an anisotropic material, 36 constants would have to be determined-but there is no test equipment yet available which is capable of measuring these (Stackel, 1991). Therefore, some simplifications are necessary when using available test equipment. A

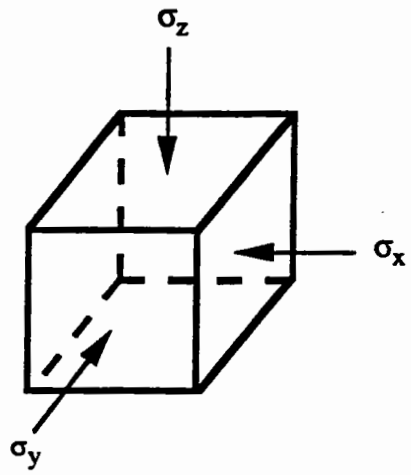

Figure 2.3. Stresses in a TTA sample

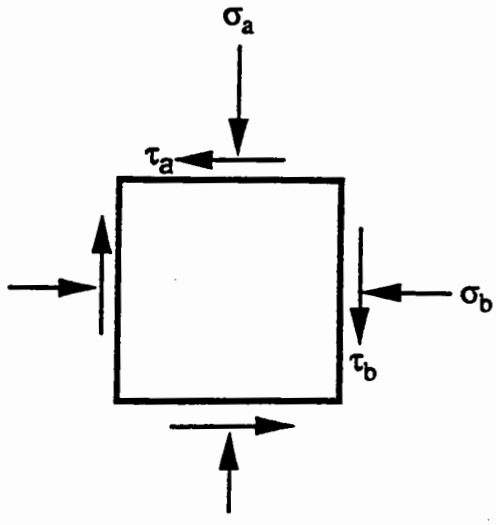

Figure 2.4. Stresses in a DSC sample

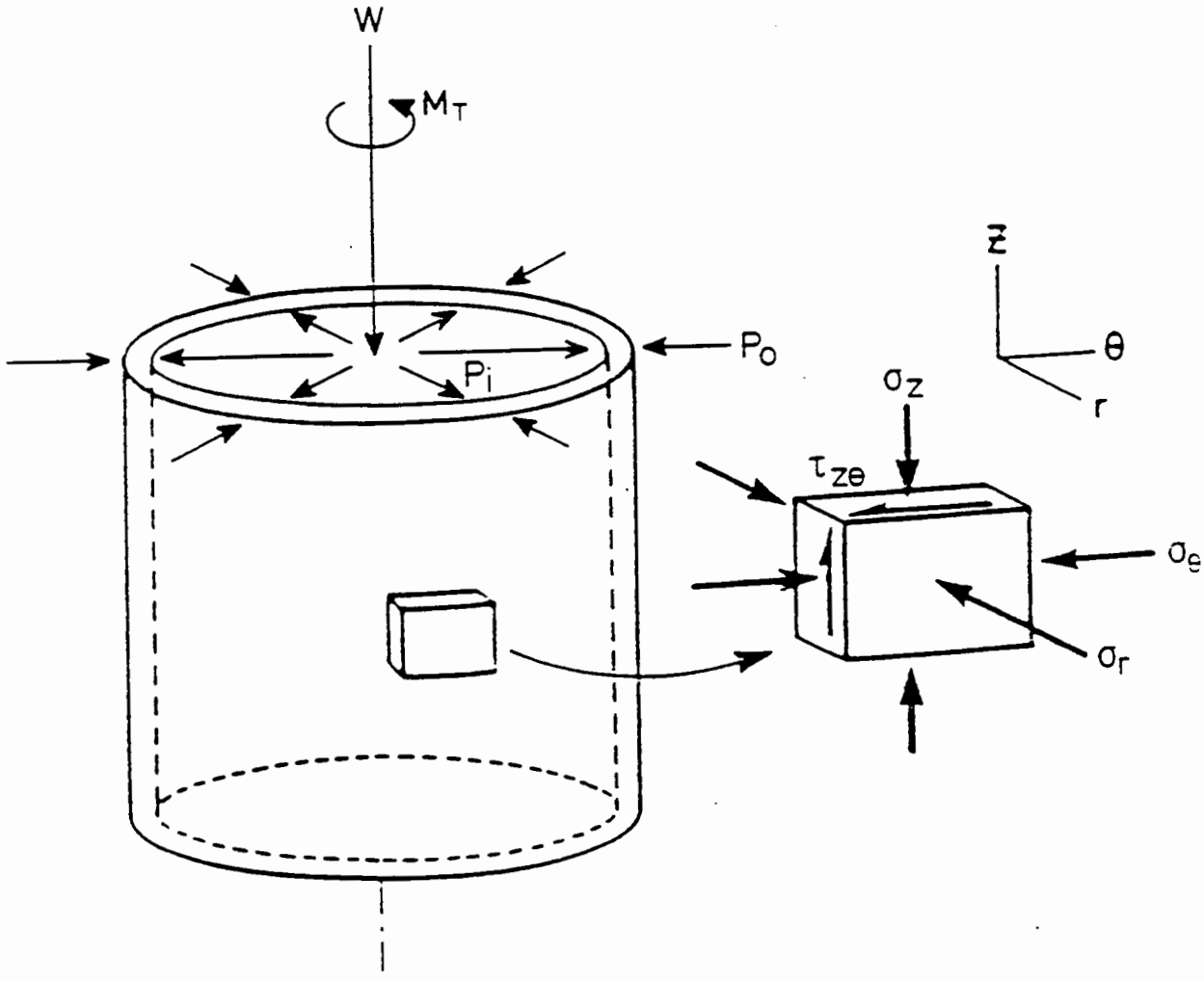

Figure 2.5. Stresses in a HCA sample (Chan, 1990)

first simplification is the symmetry condition in which the material is assumed to show the same properties in one plane. For this purpose soil is generally represented by cross anisotropic (transverse anisotropic) material (Stackel (1991), Chen and Saleeb (1982)) in which the soil behaves isotropically in the horizontal plane whereas it shows a different behaviour in the vertical direction under the same loading conditions. For a linear cross anisotropic material stress-strain relationships were given by Silveria and Souto Silveria (1973), Gazetas (1982), Graham and Houlsby (1983), Pickering (1970), Gerrard (1969), Gerrard and Mulholland (1966) and Barden (1963).

2.5.1.Determination of anisotropy

For a cross-anisotropic material (see Chapter 7), five material constants must be determined from the available test equipment. In order to determine these constants the test apparatus must allow the application of 3 normal and 2 shear stresses which should vary independently. However, this type of equipment is not currently available even for research purposes (Stackel (1991), O'Reilly (1991)). Currently available test equipment which is able to study anisotropy to a certain extent are the cubic triaxial test equipment, the hollow cylinder and cylindrical triaxial test equipment. These test apparatus will be discussed in terms of their ability to make anisotropy measurements.

2.5.1.1.The cubic triaxial test equipment

The cube is an extremely practical shape for varying the principal stresses independently. Stresses can be applied with rigid platens, rubber membranes or a

mixture of both. These cubic test devices can divided into two groups : true triaxial test devices in which stresses in three directions can be independently controlled (Arthur and Menzies (1972), Haruyama (1981) and Matsuoka and Ishizaki (1981)) and plane strain devices e.g. direct shear cells (DSC) in which two normal stresses and shear stresses can be applied and one direction is left free of independent strain application. The DSC has been used by Arthur et al (1977), Wong and Arthur (1985) and Budiman et al (1992). More detailed knowledge about the cubic triaxial apparatus can be obtained from Arthur (1988).

In order to measure the inherent anisotropy due to deposition with TTA cubical samples are prepared at various tilted angles to the direction of pouring. After applying the same stresses to the samples, direct strain results are compared according to the tilting angle (Arthur and Menzies, 1972). Differences between the results show the level of inherent anisotropy. However, isotropic pressure can also be applied to a cubical sample in order to measure the inherent anisotropy (Haruyama, 1981). If a material is isotropic, then the strains obtained from three directions must be equal under hydrostatic test conditions.

In order to measure the stress-induced anisotropy the DSC can be employed for which a sample is prepared in the direction of intermediate principal stress to avoid any influence of inherent anisotropy. Principal stresses are rotated at different angles continously or discontionusly by changing the normal and shear stress. If a material is isotropic, principal stress rotation would have no effect on the stress-strain behaviour of the material. If not, it shows the level of stress-induced anisotropic behaviour.

2.5.5.2.The hollow cylinder apparatus

The hollow cylinder sample is a thick walled cylindrical sample to which four different pressures, namely internal and external pressures, axial load and torque, may be applied (O'Reilly, 1991). Principal stresses can be rotated by changing their relationship to torque.

In order to determine the inherent anisotropy an isotropic pressure is applied to a sample. If the response are the same in the vertical and horizontal direction, the material is isotropic, if not the material is said to be anisotropic.

In order to determine the stress-induced anisotropy the sample is subjected to the rotation of principal stresses by applying normal stress and torque while keeping the confining pressure constant. If the response is the same at various rotation angles, the material has not been affected by stress-induced anisotropy. Otherwise it has stress-induced anisotropy.

2.5.5.3.The repeated load triaxial test apparatus

The repeated load triaxial apparatus (RLTA) does not allow rotation of the principal stresses, unlike the hollow cylinder or cubic triaxial test apparatus, since principal stress directions are fixed due to the equipment design. Chan (1990) monitored the

resilient volumetric and shear strain behaviour of granular material in HCA testing during permanent deformation tests. Peak values of resilient stresses and strains were relatively close to each other both with and without (triaxial condition) shear reversals. Therefore the RLTA has continuing value for the determination of the resilient properties of granular materials and was used in this project. When the cell pressure is cycled the RLTA can be used to measure elastic anisotropy in a sample. For this particular purpose, the material is subjected to different levels of repeated cell pressure which are carefully selected so that they do not cause any plastic strain after each stress path. Radial and axial strains are measured and the ratio of axial strain to radial strain gives an indication of the anisotropy in a sample.

2.5.5.4.Some observations from previous studies

Haruyama (1981) performed isotropic compresion tests by controlling the stresses in each direction independently on cubic specimens consisting of glass beads. The direction of sample deposition was in the direction of gravity. He found that lower compressibility was obtained in the direction of deposition than in the other two perpendicular directions where the horizontal strains were equal to each other.

Ochai and Lade (1983) used sand with a cross-anisotropic fabric in cubic specimens. Samples were prepared in a special mould by pouring and shaking sand grains in several layers. Drained tests were performed under conventional triaxial compression, plane strain and cubic triaxial conditions. After isotropic compression tests they found

that the strains perpendicular to the long axis of grains were only about half of the other two linear strains.

From the above two results it may be concluded that under isotropic stress conditions for a cubic sample, horizontal strains are equal. Assuming the above conclusion to be correct, a conventional cylindrical sample can also be used to study anisotropy in the sample.

CHAPTER 3

THE REPEATED LOAD TRIAXIAL APPARATUS

3.1.Introduction

The triaxial test apparatus has been used for many years to investigate the stress-strain behaviour of granular materials. In connection with the repeated loading of granular materials, a triaxial apparatus was developed by Boyce(1976) at Nottingham University, able to cycle both the deviator and confining stress. Pappin(1979) slightly modified some parts of the apparatus and in 1991 the electronic control system of the apparatus was replaced by a digital control system. More detail about the development of the apparatus can be obtained from Boyce(1976), Boyce et al(1976), Pappin(1979) and Brown et al (1989).

The axial load and confining pressure are applied to the samples in a triaxial cell by hydraulic actuators. The axial load is continuously monitored by a load cell and similarly, the confining pressure is controlled by the output of a pressure sensor in the cell fluid.

A diagramatic representation of the system is given as Figure 3.1.

3.2.Triaxial cell

The internal dimensions were 300 mm diameter and 550 mm high. The cell was made primarily from aluminium alloy to withstand a pressure of 1000 kPa (Boyce,1976).

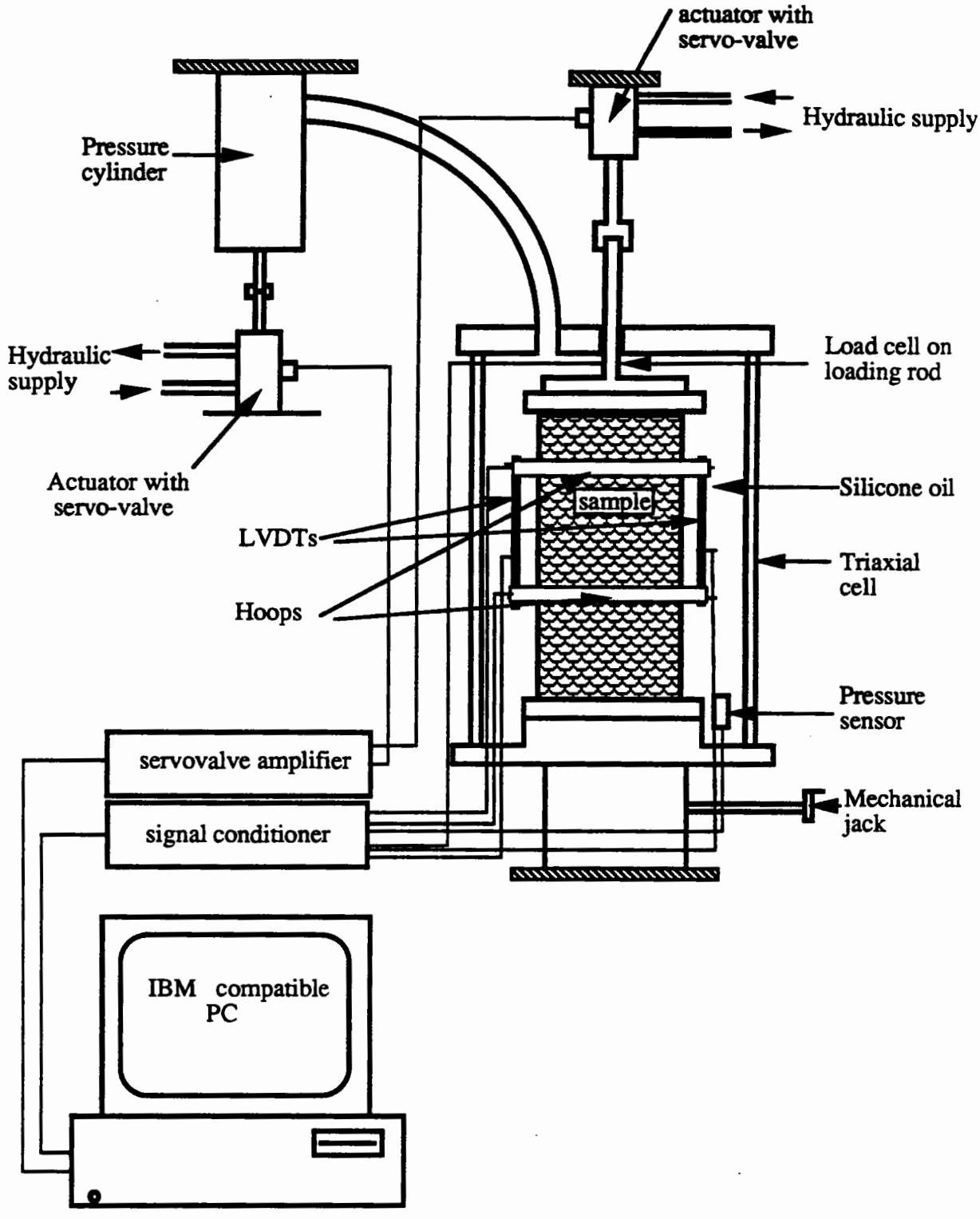

Figure 3.1.Diagram of the repeated load triaxial apparatus

During testing the cell rested on a mechanical jack and at other times it could be lowered onto a trolley and pulled clear of the loading frame.

3.3.Axial load

Axial load was applied by a 50.8 mm diameter hydraulic actuator, which could apply a deviator stress of 1200 kPa on a 150 mm diameter sample at frequencies up to 16 Hz, (Boyce,1976). The load cell, which is very sensitive and linear, is able to measure negative deviator stress.

3.4.Loading platens

The loading platens were made from aluminium alloy with polished steel faces. Two shallow grooves were cut around the circumference to enable the sample membrane to be sealed with 'O' rings.

3.5.Confining stress

Air was used as the confining medium for tests with constant confining stress. Silicone oil was used for tests with the variable confining stress. The reason for choosing this oil is that it has a relatively low density and it is an excellent electrical insulator. It was found that the oil had no effect on latex membranes, strain gauged transducers or LVDTs (Linear Variable Differential Transformers) (Boyce,1976). The pressure of the oil was controlled by a hydraulic actuator, 25.4 mm diameter, operating a pressure

cylinder, 127 mm diameter. Cyclic cell pressures of 400 kPa could be applied at frequencies up to 2 Hz (Boyce,1976).

3.6.Measurement of deformations

Deformation readings are taken from four studs placed in the sides of specimen during preparation and into which threaded rods are then screwed. Axial deformations are measured using linear variable deformation transformers (LVDTs) mounted between the two pairs of threaded rods. Radial deformations are measured by hoops incorporating strain gauges. Two hoops and LVDTs were used to obtain an average strain. Strain instrumentation is fixed to studs compacted into the edge of the specimen at 1/4 and 3/4 height. The range for LVDTs was + and - 2.5 mm and for hoops + and - 1.5 mm. The measurement systems are explained in detail by Boyce and Brown (1976) and Brown et al (1989). Photographs are given in Appendix E.

3.7.New mounting studs

The old instrument mounting studs have been successfully used at Nottingham University for many years (see Figure 3.2) (Brown et al, 1989). However, difficulty associated with the sample preparation using these studs led to the development of another type of stud system. Especially during the compaction, the points where the studs are fixed through the membrane need more attention since these points should be strong enough to hold LVDTs and hoops. Apart from this, around these points, coarse aggregates should not be placed so as to avoid causing weakness at the stud points. Therefore a new system whereby the studs could be fixed to the membrane after normal uninterrupted compaction was designed (see Figure 3.3). The new studs are made of

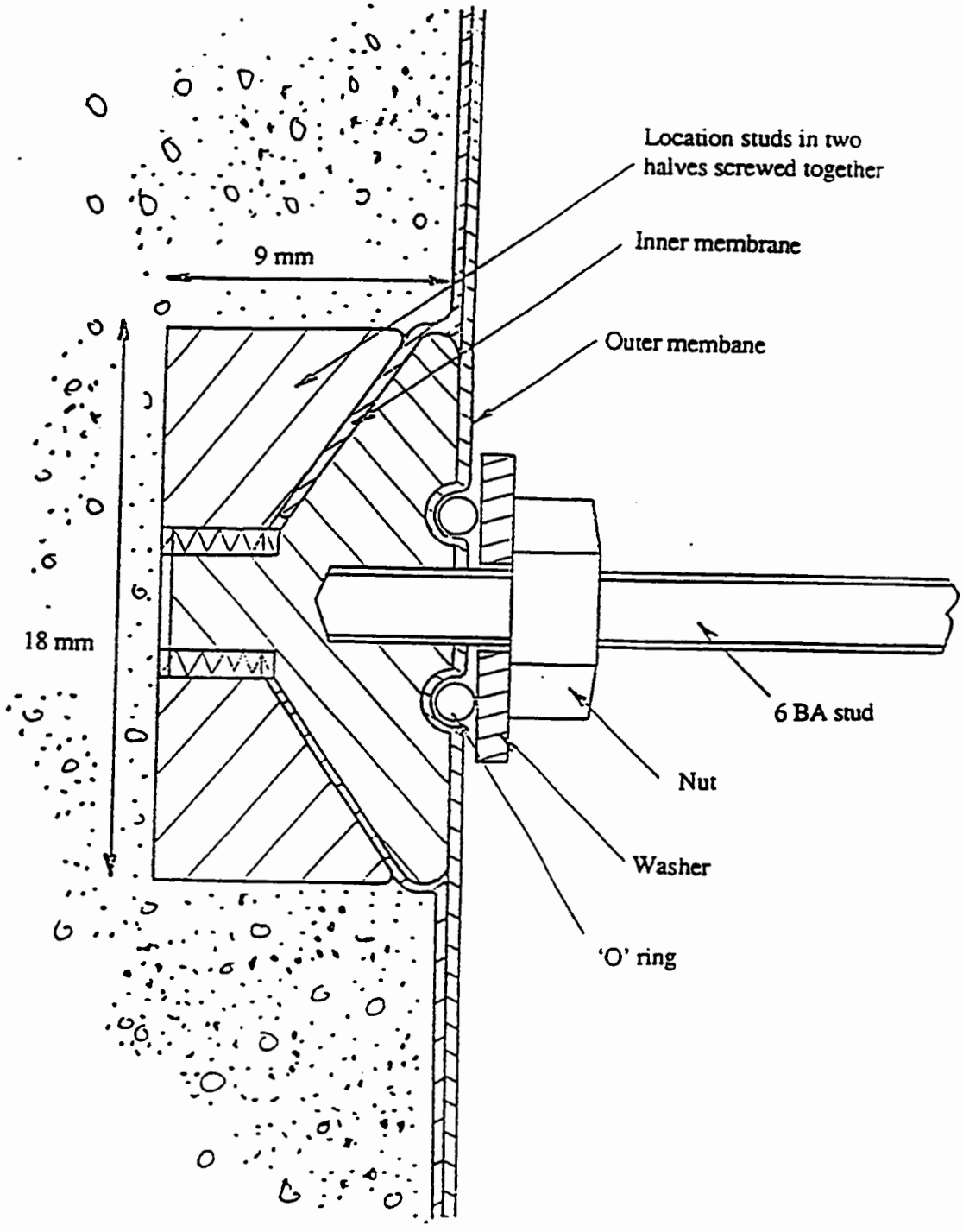

Figure 3.2. The old mounting stud system (Pappin, 1979)

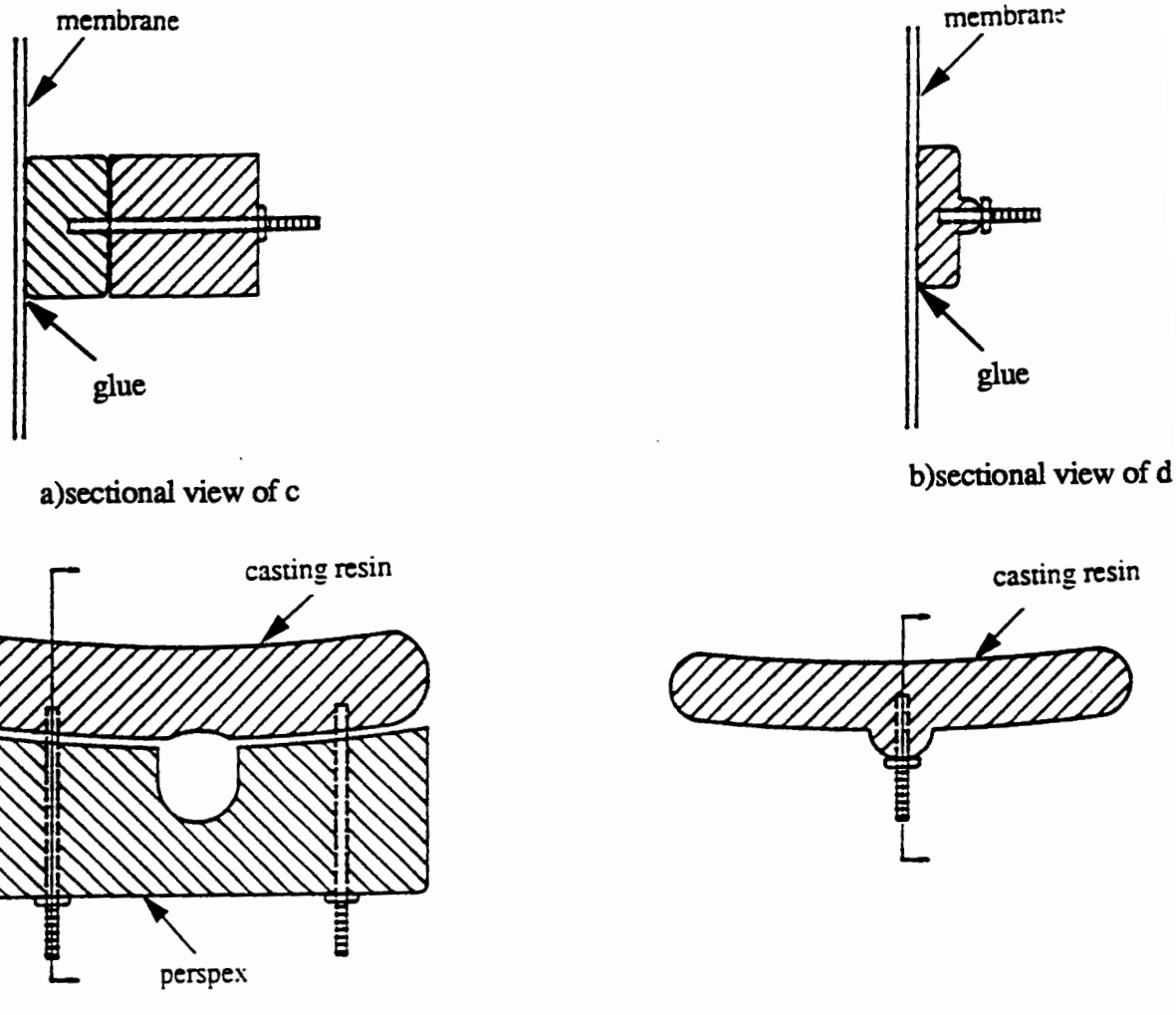

Figure 3.3. The new mounting stud system

casting resin, have a curved shape to suit the sample face and are fitted with perspex clamps. The casting resin faces are fixed to the membrane by an appropriate glue after preparation of the sample.

3.8.Advantages of new studs

With the new studs, LVDTs and hoops could work separately as there is no reasonable limit to the number of fixing positions. Even a small amount of movement of LVDTs or hoops would probably affect each other,and would cause misleading readings. It is evident that there is no positive reason to put LVDTs and hoops onto the same fixings. Therefore, it might be a better idea to separate them from each other.

Using the old system more attention must be given as to where the studs are fixed in relation to their desired position on the completed sample and to the aggregate clasts since studs may not sit properly at particular points and, if so, this causes irremedial problems after compaction. However, with the new system studs are located after the compaction, therefore any smooth surface on the sample can be chosen as an appropriate location.

Under the old system even if careful attention is given it may well be possible to get weak points around the studs after compaction of the aggregate, especially where the coarse aggregate is dominant. This might then cause studs to move independently of aggregate strain, resulting in incorrect readings from the LVDTs and/or the hoops.

In the old system hoops were placed at 1/4 of the sample height from the bottom and 1/4 of the sample height from the top. With the new system any suitable place for the hoops can be chosen to measure radial deformations. In particular radial strain may be measured at the sample centre.

3.9.Disadvantages of the new stud system

The new stud system readings mainly depend on the membrane movement rather than on the particle movement. In some cases, especially when a large cell pressure is applied to the sample, the membrane compresses hence over-measuring the horizontal strain.

In order to prevent the movement of the studs an appropriate glue should be used. Apart from this, the sticking points must be checked carefully in order to ensure good stud adhesion and subsequent performance.

3.10.Choice of glue type

Studs should be stuck firmly on the membrane. The adhesive used had to be instant to save time and strong enough to carry rods on which hoops and LVDTs are mounted. Six types of glue were tested, namely, cow gum rubber solution, Bostik 1 clear

adhesive, Evo-stik impact adhesive, Bostik all purpose, Loctite clear glue and RS instant adhesive.

Six samples, 20 by 20 mm, were cut from the latex rubber membrane used for the triaxial tests. After cleaning up both stud surfaces and rubber surfaces, the studs were roughened by glasspaper. Each adhesive was used according to their directions. Six samples were stuck with the different glue, and they were left at ambient temperature for sixteen hours. All samples were then tested against peeling by applying tension. The hardest to peel off indicating the best adhesive. RS instant glue was chosen as the best performing glue since the adhesion between the stud and membrane was sufficient and it also had a thinner film on the stud and the membrane than other good adhesion glues. Since silicone oil was sometimes used as the cell pressure medium the sample was left in the oil for two hours. Afterwards, it was found that there was still a strong adhesion against peeling off.

3.11.Comparison of stud systems

In order to examine the behaviour of both stud systems a triaxial sample of sand and gravel (150 mm diameter, 300 mm high) was prepared with both types of fixing. Firstly, the old measuring system was tested under different stress paths. Secondly, the new system was tested for the same stress paths. Since the old analogue control system (Boyce, 1976) was used during the test, the magnitude of the applied stresses may have varied, because accurate control was not possible. Data were collected using a x-y plotter. Similar tests were also carried out after the new digital control has been

installed using the same material. Similar results were obtained as before. Results reported here were obtained from digital control system.

When only the cell pressure was cycled it was possible to see the differences between both the axial and the radial strain measurements (see Figure 3.4). In particular the radial strain measurements were about three or four times higher with the new stud system than the old stud system. The explanation for this is that when the cell pressure was applied to the sample the latex membrane tried to penetrate into the sample and also to compress in its own thickness. Therefore, the strain for the membrane and the sample was measured. When the cell pressure was released, the membrane would extend more than the sample since the membrane is more flexible than the granular material. Hence, the radial strain was overestimated by the new stud system. A regression coefficient of 0.99 with the new:old ratio of 1.25 was obtained for the axial strain when the only cell pressure is cycled. Slope values given with the regression coefficient show the deviations in readings.

A good correlation was obtained between the old and the new stud system when only deviatoric stress was only cycled (see Figure 3.5). However it was possible to see some scatter for the radial strain measurement between the old and the new stud system. A regression coefficient of 0.99 with the slope of 0.87 was obtained for the axial strain measurement and the regression coefficient for the radial strain was 0.99 with the slope of 0.74.

As a result, the new stud system should be suitable for triaxial testing where only the deviatoric stress is cycled with constant cell pressure.

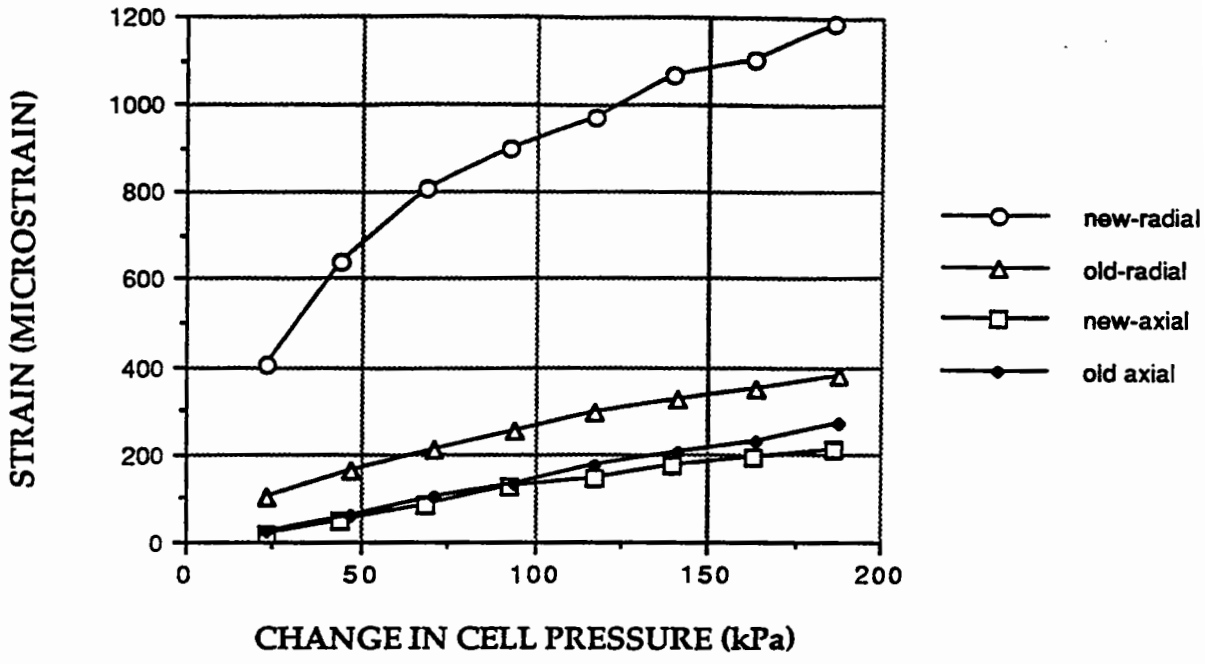

Figure 3.4. Axial and radial strain mesurements under repeated cell pressure

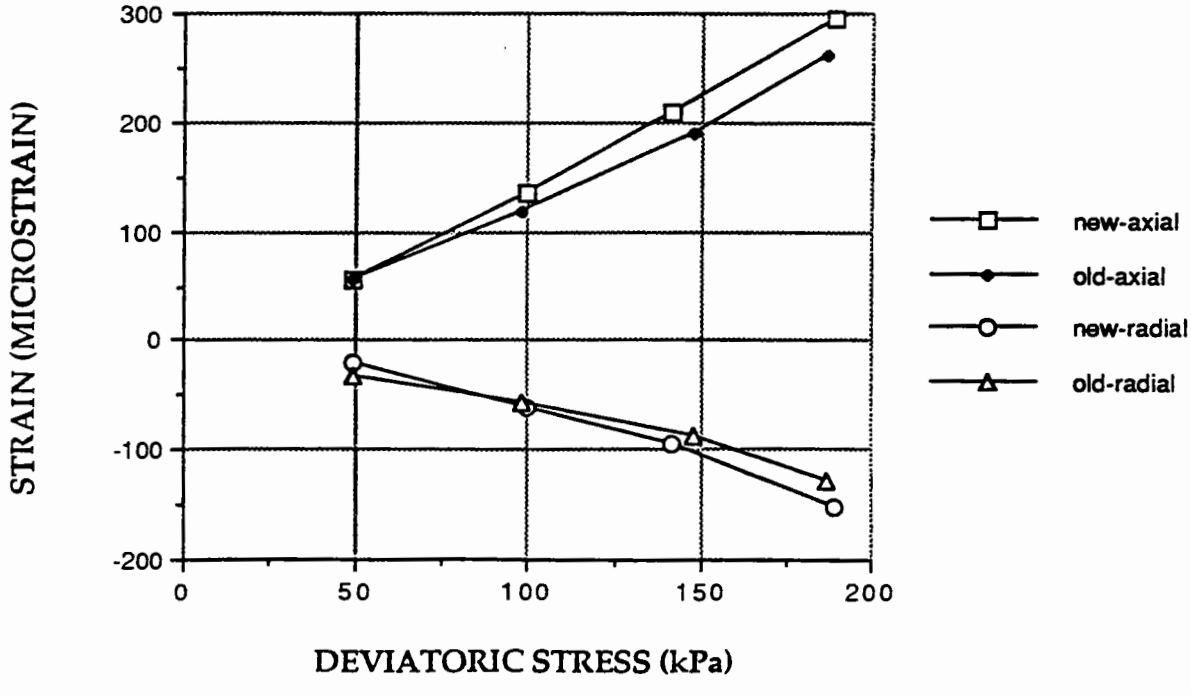

Figure 3.5. Axial and radial strain measurements under repeated deviatoric stress

In this project, there were some stress paths in which only the cell pressure was cycled therefore, the old stud system was used.

3.12.Digital control system

Microcomputer based systems presents some advantages over analogue control systems, these advantages are mainly

- Provides improved (or automated) method of applying the desired loading on a sample (i.e, stress magnitude). That is, it may reduce operator error,
- Reduces the probability of collecting erroneous data,
- Reduces the amount of work required to collect and analyse data, thus improving the productivity,
- Performs decision making, real time sampling and processing and complicated signal generation (Chen et al, 1989).

However, there may be some disadvantages of using the digital control system. These are:

- There are often more than one calibration factor for different output transducers (such as LVDTs and hoops) depending on the sensitivity during the test. Selecting a different calibration factor than intended may lead to wrong results,

- Using software data analysis programs may lead to wrong results because the results also contain noise which, to the software, is indistinguishable from genuine data,
- There is no automated limit of applicability of the instrument calibrations. Therefore, it may be possible to violate the calibration range during the test.

A digital system must comprise hardware and software components. The interface hardware consists of the microcomputer, controllers for the input transducers (such as actuators, servovalves), signal conditioners for the output transducers (such as LVDTs,hoops, load cell), an analogue to digital (A/D) converter and a digital to analogue (D/A) convertor. These convertors are able to communicate between the testing processes, the control and the data acquisition algorithms of the software.

ATS (Automated Testing System) software which runs under Microsoft Windows (Sousa and Chan,1991) was used to acquire data and control the testing apparatus. The software has the capability of setting a desired value for any given control variable and also the capabilities to monitor these variables. The software transmits a signal through the servovalve amplifier to the servovalve to induce a load on the specimen. The applied load is monitored through a signal conditioner and an analogue to digital (A/D) converter back into the control algorithm within the software. Figure 3.6 shows how the repeated triaxial apparatus works with the ATS software.

3.13.Data Collection

Before commencing the test a computer data file was opened for each stress path in which to store the test data. For permanent strain tests, data were collected at certain

specified numbers of cycles. For the resilient tests, data were collected only for the last five repetitions of load. ATS software records the readings as requested by the user. The software is able to analyse the test readings and produces a summary presentation report. A graphical output on the monitor may be displayed which can be plotted on the printer. The use of ATS software is briefly shown in Figure 3.7.

3.14.Sources of errors for the triaxial test results

The apparatus is quite sensitive to noise. When readings are taken by the computer it also picks up some readings of apparent deformation due to noise. Therefore using a spreadsheet program or the ATS Report program the noise in the control system readings should be eliminated. Experience has shown that apparent axial loadings due to noise vary from 2 to 10 kPa.

Friction exists between the top hole in the top of the cell and the piston. Because of this fine control of the axial load, especially when applying a vertical stress less than 20 kPa, is difficult. Because of the friction a control tolerance of plus and minus 7 % error was allowed so that the required stress could be applied approximately on the sample without excessive control instability resulting. Therefore, it is difficult to precisely apply a specified stress level with the system. The actual applied stress readings are recorded and should be checked by using either the ATS Report program or any spreadsheet program. These will be accurately collected and thus interpretation can be based on the applied rather than the desired stresses.

Before the test, all instrument calibrations should be checked so that any misleading results are not obtained. The calibration of LVDTs should be checked especially

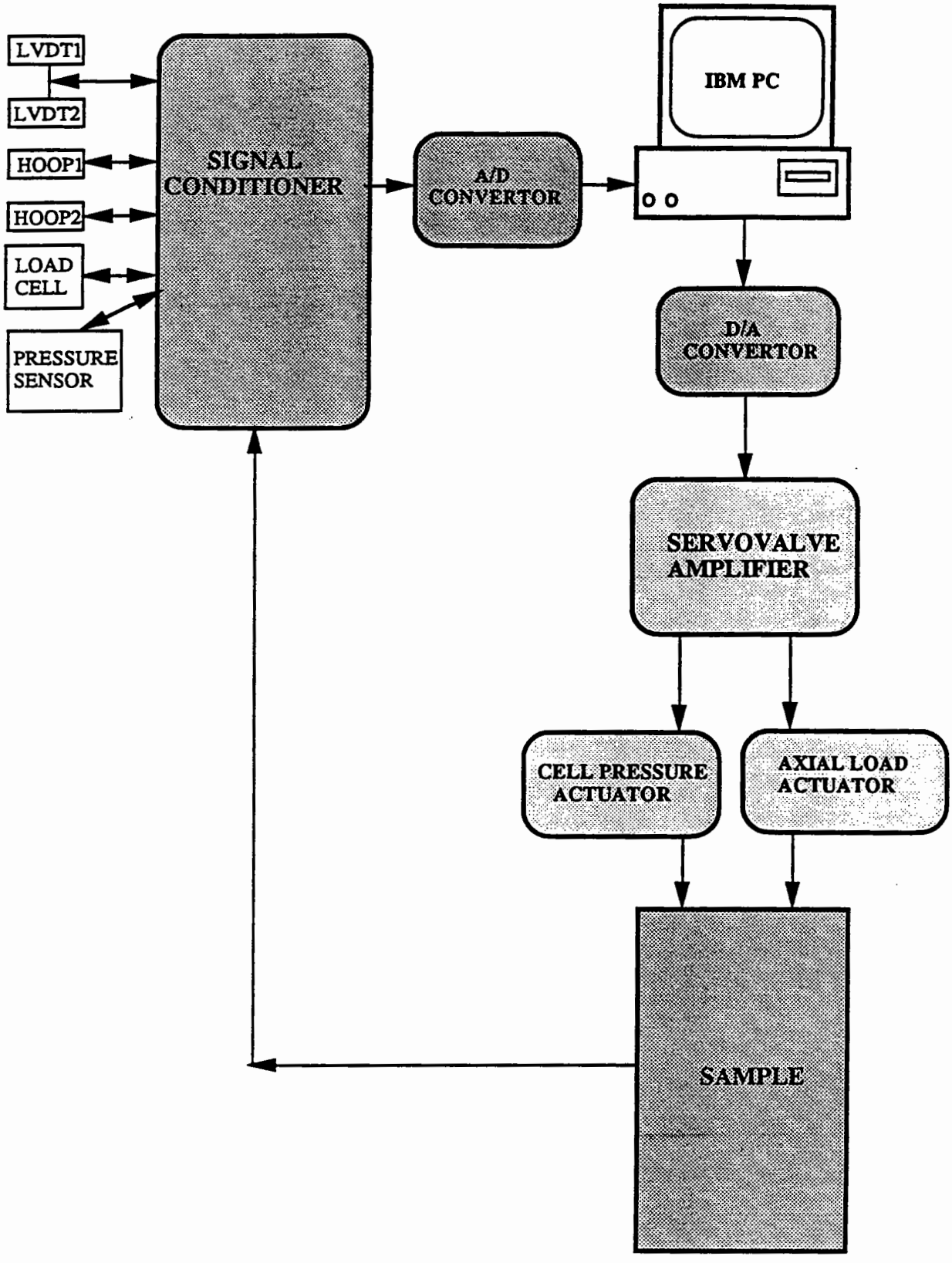

Figure 3.6. Repeated load triaxial apparatus with digital control system

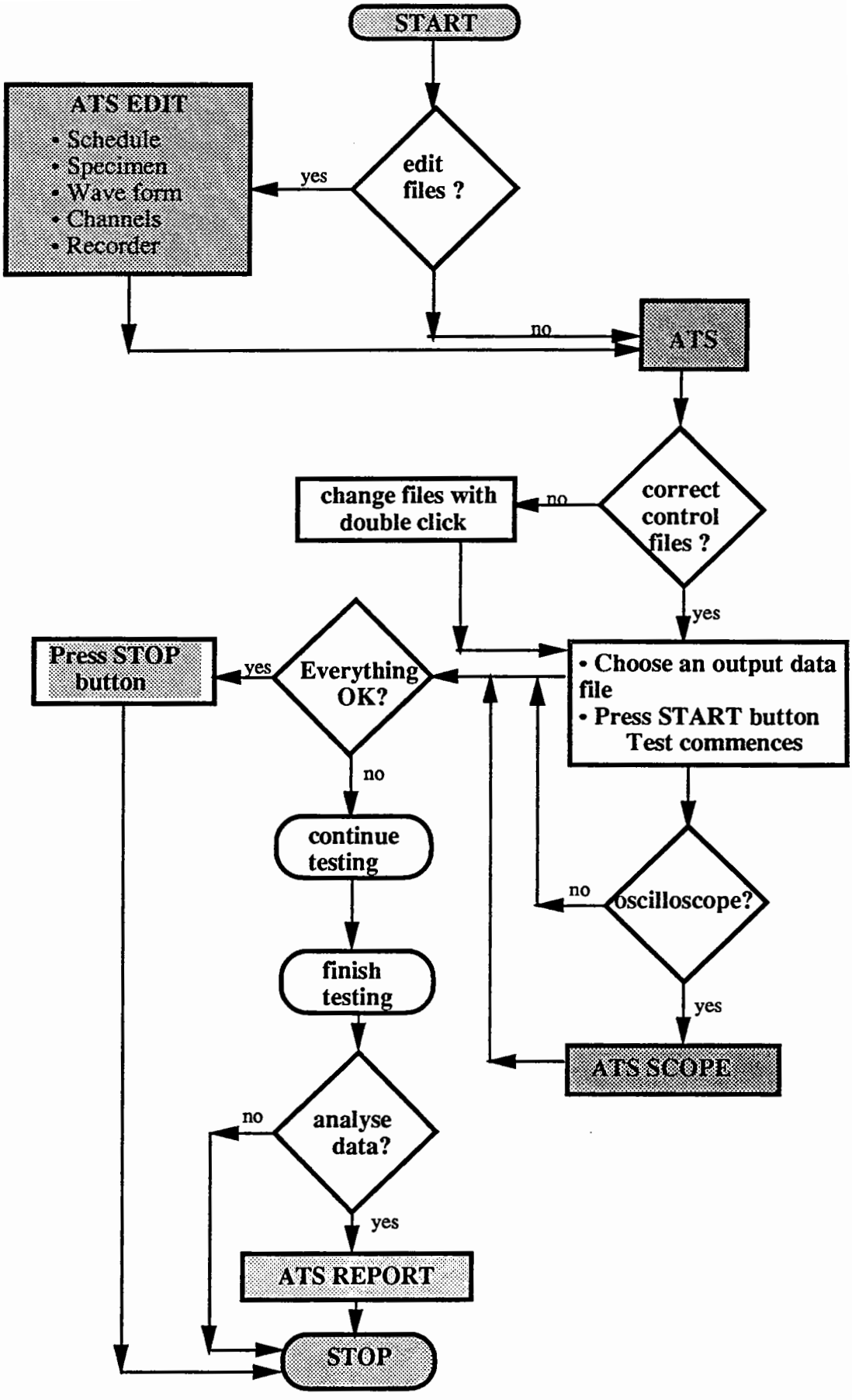

FIGURE 3.7. Procedure for the ATS software

carefully. With the current system both LVDTs are calibrated together as they use the same record channel and one overall calibration is obtained for both.

CHAPTER 4

THE MATERIALS AND SAMPLE PREPARATION

4.1.Introduction

In order to understand the general behaviour of granular material under traffic loading, six materials from different origins were tested. The materials chosen are representative of the likely range of granular materials used for the construction of road base, sub-base and capping layers. These are soft limestone (SL), gritstone (GS), sand and gravel (SAG), graded washed river sand (GWRS), Fontainebleau sand (FS) and furnace bottom ash (FBA).

Granular material is a two-phase continuum which consists of particles and a pore fluid at a pressure (due to air and/or water). The behaviour of the material is affected to some extent by pore pressure and which can be modelled using the concept of effective stress (Terzaghi, 1943). This project's concern is principally the stress-strain behaviour of the particle phase. Therefore, although usually used in a moist condition in pavement construction, dry material was generally used so that the applied stress measured would be the same as effective stress. However, in preliminary tests (not reported here) the weaker materials (FBA and FS) were found to have inadequate resistance to permanent deformation under repeated loading and this made resilient testing unworkable. Therefore these materials were tested moist. This generated a

considerable, but unmeasured, suction which avoided further problem. The disadvantage is that only a total stress analysis is available for those materials. However, the moisture contents are far from saturation (degree of saturation of 8% and 12% for FBA and FS respectively) and thus changes in suction level are unlikely to occur during repeated loading thus change in effective stress changes and change in total stress changes should be sensibly equal.

Materials were tested as-delivered without changing the grading. Grading curves are shown in Figure 4.1.

4.2.Materials tested

In this section the six aggregates are briefly described. Their basic properties are given in Appendix A.

4.2.1.Furnace Bottom Ash

In recent years environmental concerns have gained importance all over the world as waste products have increased dramatically as a result of more energy use and an increasing population. One of the waste products of a coal-fired power station is furnace bottom ash (FBA). Dawson et al(1989) have shown that the performance of FBA in moist conditions is adequate for pavement sub-bases, with little deterioration of

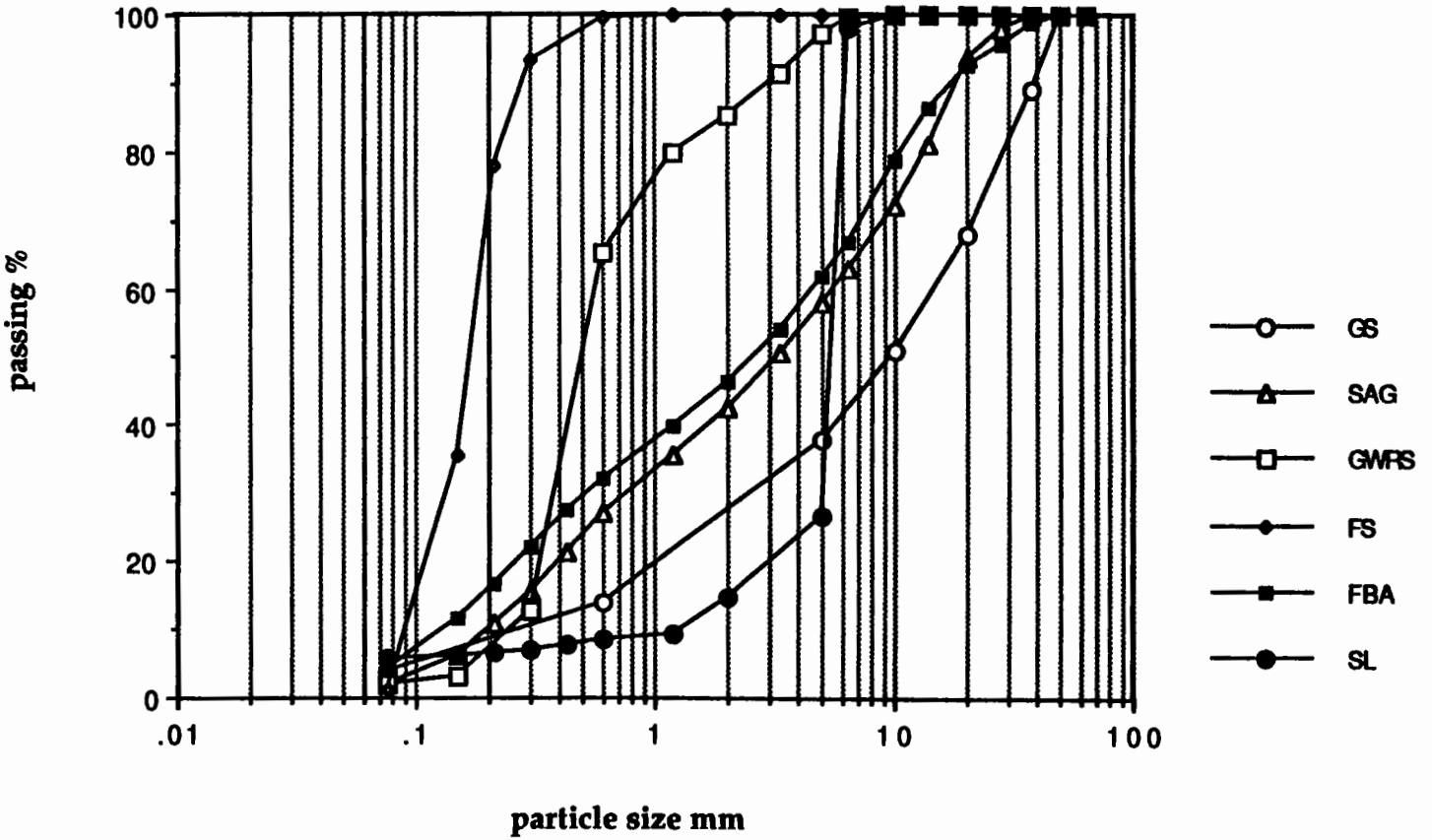

Figure 4.1. Grading curves

stiffness, and that FBA has a relatively low susceptibility to the development of permanent deformation. Dawson and Bullen (1991) have shown that FBA-

- has good permeability,
- was difficult to compact to high densities,
- had a reasonable CBR (California Bearing Ratio) and
- had a fairly good elastic stiffness.

They also recommended using FBA in lightly trafficked roads as a sub-base layer.

The FBA material used in the test was delivered from the Ferrybridge B power station in the UK. The material was oven dried at 110°C for 24 hours. Its grading is finer than some crushed rock aggregates but is still fairly broad. During the first three resilient strain test stages (see Chapter 5) the sample underwent rapid permanent deformation. As a result the LVDTs and hoops were close to the limit of their calibrated range (Section 3.6). The sample was thus removed from the triaxial test apparatus and, in order to give the material some strength, 3% water (by mass) was added and the material was recompacted on the vibrating table. The addition of water had almost no effect on the ease of compaction the same density being obtained as that given for the moist sample in Table 4.1.

4.2.2.Sand and gravel

Sand and gravel (SAG) is a road construction material mostly limited to use as a capping layer in the UK. It contains mainly rounded coarse aggregates as well as fine grains. The material was obtained from a pavement trial at Bothkennar, Scotland

(Little, 1993) and was tested dry. The grading is that of a conventional sub-base aggregate.

4.2.3.Soft limestone

Crushed limestone is an important road construction material in the UK. It is generally used for sub-base or capping layers in pavement structures. Many researchers at Nottingham University (Boyce, (1976), Pappin, (1979), Thom, (1988) and Chan (1990)) have studied crushed limestone to determine its stress-strain characteristics. A softer limestone (SL) was tested as part of this project. The material used was a dolomitic limestone supplied from Whitwell Quarry in Derbyshire. It has a time-dependent self-cementing ability when it is partially saturated and, therefore, may give a higher and varying stiffness at optimum moisture content than when in a dry condition. For this reason it was compacted and tested in a dry condition. The grading chosen was not typical of a crushed rock aggregate as used in pavements being largely single sized but with some fines. This grading was chosen so as to broaden the variety of material types tested.

4.2.4.Gritstone

Gritstone (GS) manufactured from sound clean rock, is an important road construction material in Northern Ireland, where it is mainly used for sub-base and capping layers.

The material used in this project was supplied from a Colas quarry in Belfast. It was compacted and tested in a dry condition.

The physical properties of the material, obtained from the records of the Materials Testing Station at Castlenavan, are shown in Appendix A. Its grading is typical of crushed rock sub-base materials.

4.2.5.Sands

Sand is an important road construction material in the western part of Netherlands where clayey subgrades exist (Sweere, 1990). Sand is used there as a sub-base material, for the working platform, and as a drainage layer in pavement structures. Sand is also used in the northern part of Yugoslavia (Stojadinovic, 1989) as a road construction material since local natural sand is one of the few suitable materials available in the area.

Two kinds of sand were investigated. These were the well-graded washed river sand (GWRS) supplied by Tarmac Roadstone from Hoveringham and Fontainebleau sand(FS), comprising single-sized very fine grains, from Melun, South of Paris in France. The GWRS was tested dry, whereas the FS had an as-supplied water content of 2.76%. The FS was used in a partially saturated condition for the same reason as described in Section 4.2.1.

4.3.Compaction method

In road construction, granular material is first laid over the subgrade by a grader, then a roller compacts the granular material in several layers to a desired density.

Density depends on the particle shape, fines content, gradation and compaction method used. Thom and Brown (1988) showed that the degree of compaction had almost no effect on elastic stiffness, although denser material was seen as being slightly stiffer. However, they also showed that density (degree of compaction) was important in limiting the plastic strain.

There are several compaction methods which are available in order to obtain an appropriate sample density. The more important methods are the falling hammer, the vibrating hammer, vibrating table and gyratory compaction methods (Boyce(1976)). At the University of Nottingham, the falling hammer and the vibrating table were available during the period of test. The falling hammer method was not found to be a good compaction method for granular materials because

a) Larger particles are likely to break under the extremely high impact stresses applied during the sample preparation, therefore the material grading would change, in an uncontrolled manner, from the initial state.

b) The top of the sample is left in a rough condition, and must then be smoothed by another method.

c) The instrument fixing studs are easily displaced and/or the membrane damaged by the hammer.

A more satisfactory method of compacting dry material is by using a vibrating table (Boyce(1976)). Boyce(1976), Pappin(1979) and Thom(1988) used the vibrating table for compaction. In this project the vibrating table (Figure 4.2) was chosen instead of vibrating hammer because the material could be vibrated around the instrument fixing studs so that sound location points could be obtained. The vibrating table was 300 mm square and could produce accelerations of 4g on a mass of 30 kg. It was driven by an electro-magnetic drive which allowed the amplitude of vibration to be continuously varied. The principal disadvantage of the vibrating table is that high densities are difficult to achieve but as this project's aim was particularly to study elastic (resilient) behaviour, therefore the degree of compaction achieved was of not over-riding importance.

4.4.Sample preparation

The bottom platen of the triaxial apparatus was placed on a smooth table and an inner membrane was stretched to fit around it. An 'O' ring was then placed over the inner membrane to form an air tight seal. The mould was then placed on top of the bottom platen while the inner membrane was held inside. The membrane was stretched upwards and folded over the top of the mould upon which an extension ring was placed, locking the membrane in place. A vacuum was applied through the mould to hold the membrane against its sides.

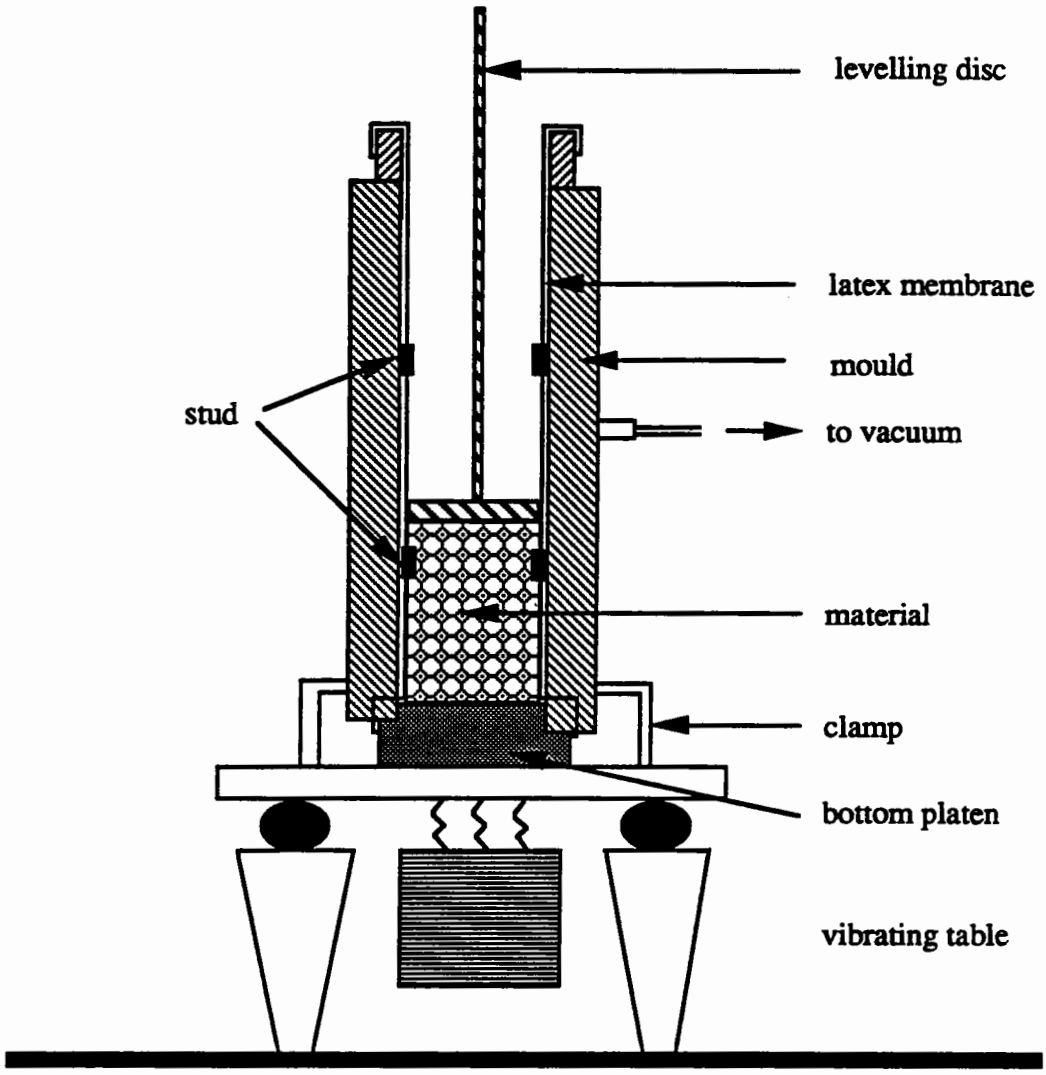

Figure 4.2.Sample preparation mould on vibrating table

It was seen from the first specimen preparation that fine particles tended to migrate downwards whereas coarse aggregates moved upwards during the vibration. In order to prevent this migration of fine material, in well graded materials the coarse fraction of the aggregates were laid by hand before vibration so that the voids available for fines migration was reduced. This was done for each layer to obtain a uniform sample. During compaction a full-face 150 mm diameter circular shaped surcharge load (applying 30 N), made of brass, was placed on the layer. Each layer was subjected to vibration for 15 seconds (Hicks and Monismith, (1971), Boyce, (1976), Pappin, (1979)). The densities achieved are given in Table 4.1. The lower densities of the FBA and the SL in Table 4.1 are attributable to their low specific gravity and grading respectively.

Table 4.1.Sample densities

Material	Density kg/m3
FBA	1240
GWRS	1813
FS	1701
SAG	2163
SL	1641
GS	2106

Having compacted the sixth layer, the extension ring was removed from the mould and the surface of the sample was tamped manually, by the surcharge load, until a smooth surface was obtained. The inner membrane was again stretched over the side of the mould by one person allowing another person to put the top platen on top of the sample. The membrane was then released and an 'O' ring was placed over the membrane to seal the sample to the platen.

The sample and its platens, surrounded by the mould, was then put into the triaxial test apparatus. A vacuum was applied through the top and bottom platen in order to support the sample after the mould was removed. Once the mould was removed, the presence of any punctures in the membrane was determined by comparing the magnitude of the vacuum applied at the base of the sample to that measured at the top of the sample. These were almost the same if a good seal existed, if not, a second membrane was added to cover the punctures so that the sample is protected from the silicone oil in the cell during the tests.

CHAPTER 5

REPEATED LOAD TRIAXIAL TEST PROCEDURE

5.1.Introduction

It is important to determine the basic mechanical properties of a granular material in order to design a new flexible pavement or to maintain an existing pavement. Most of this basic information about granular materials may be obtained from repeated load triaxial tests on laboratory prepared specimens.

There are two components of resulting deformation under traffic loading, resilient (elastic or recoverable) and plastic (permanent or irrecoverable). After certain applications of wheel loading, the increment of irrecoverable deformation is much smaller than the increment of resilient deformation. Therefore, the resilient characteristics of a pavement come to play an increasingly important role under wheel loading.

Six resilient strain tests were carried out in the repeated load triaxial apparatus by the application of a wide range of stress paths. Results of each stress paths were saved onto the hard disk of the microcomputer and analysed by a spreadsheet program.

5.2. Importance of resilient behaviour in pavement engineering

The deformation of a granular layer under traffic loading is composed of two parts, resilient and permanent (see Figure 5.1). The stresses involved are well below those which might cause failure (Brown, 1981). For a pavement foundation, rutting which is associated with the accumulation of plastic strain is the only failure mode since no bound materials are involved (Brown and Selig, 1991). However, after constructing the upper pavement layers and a number of traffic loads have been applied, the increment of permanent deformation is much smaller than the increment of resilient deformation. Therefore, the resilient characteristics of the granular layer in the pavement structure gain importance.

There are generally two types of failure in pavements due to traffic loading. They are fatigue cracking of the bound (asphalt) layers and vertical permanent deformation throughout the structure which causes wheel track rutting (Figure 5.2). Fatigue cracking is a result of the resilient response of the pavement to transient loading (Hveem, 1955).

Figure 5.3a and 5.3b illustrate the improvement in load spreading capability which occurs when increasing the elastic stiffness of a pavement, thus reducing the peak stress transmitted to the subgrade (Brown, 1990). This causes a decrease in shear stress in the subgrade, but creates higher tensile stresses at the bottom of the bound layer which will lead to the more rapid development of cracking (Figure 5.4). Hence,

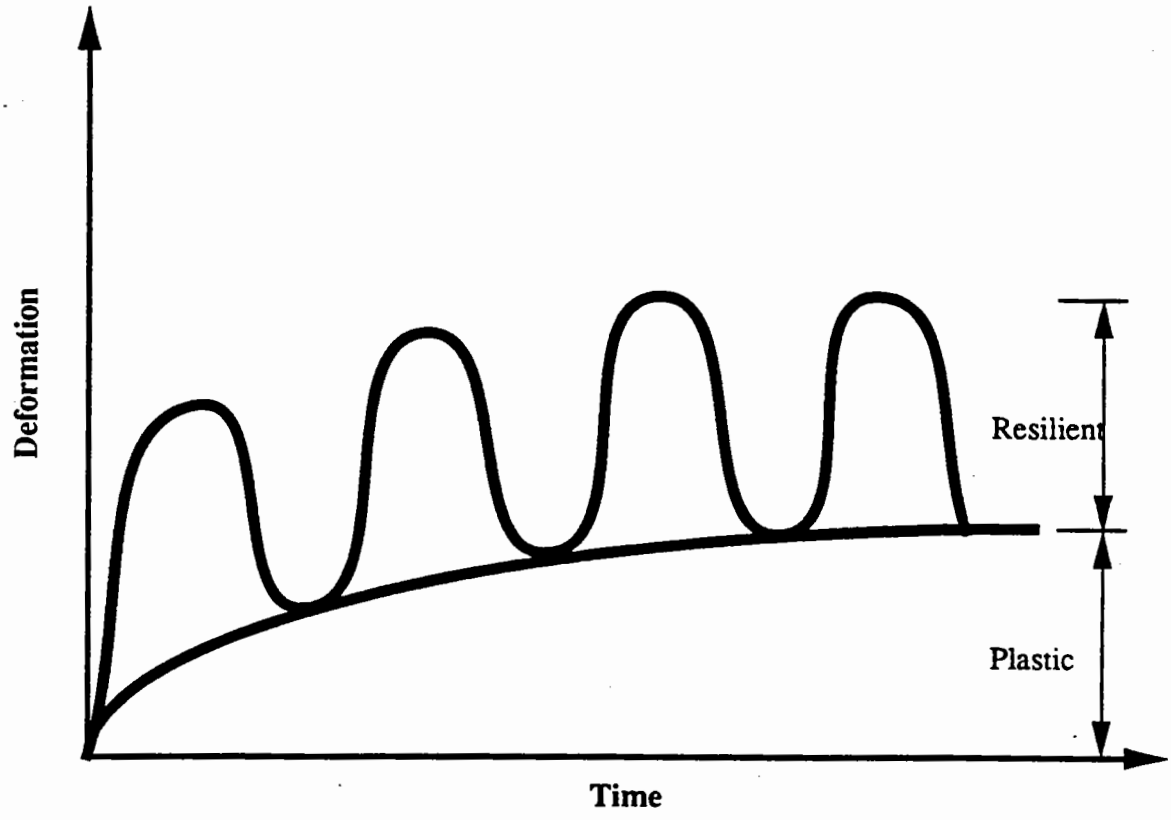

Figure 5.1. Resilient and plastic deformation against time (Brown, 1990)

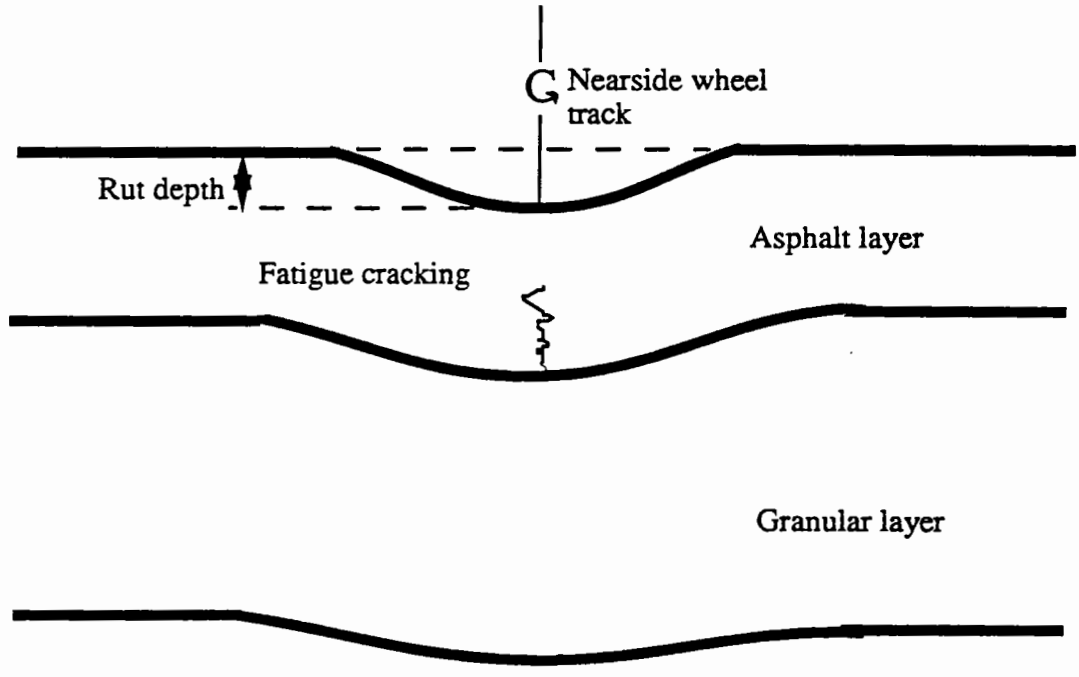

Figure 5.2. Typical failure of flexible pavement (Brown, 1990)

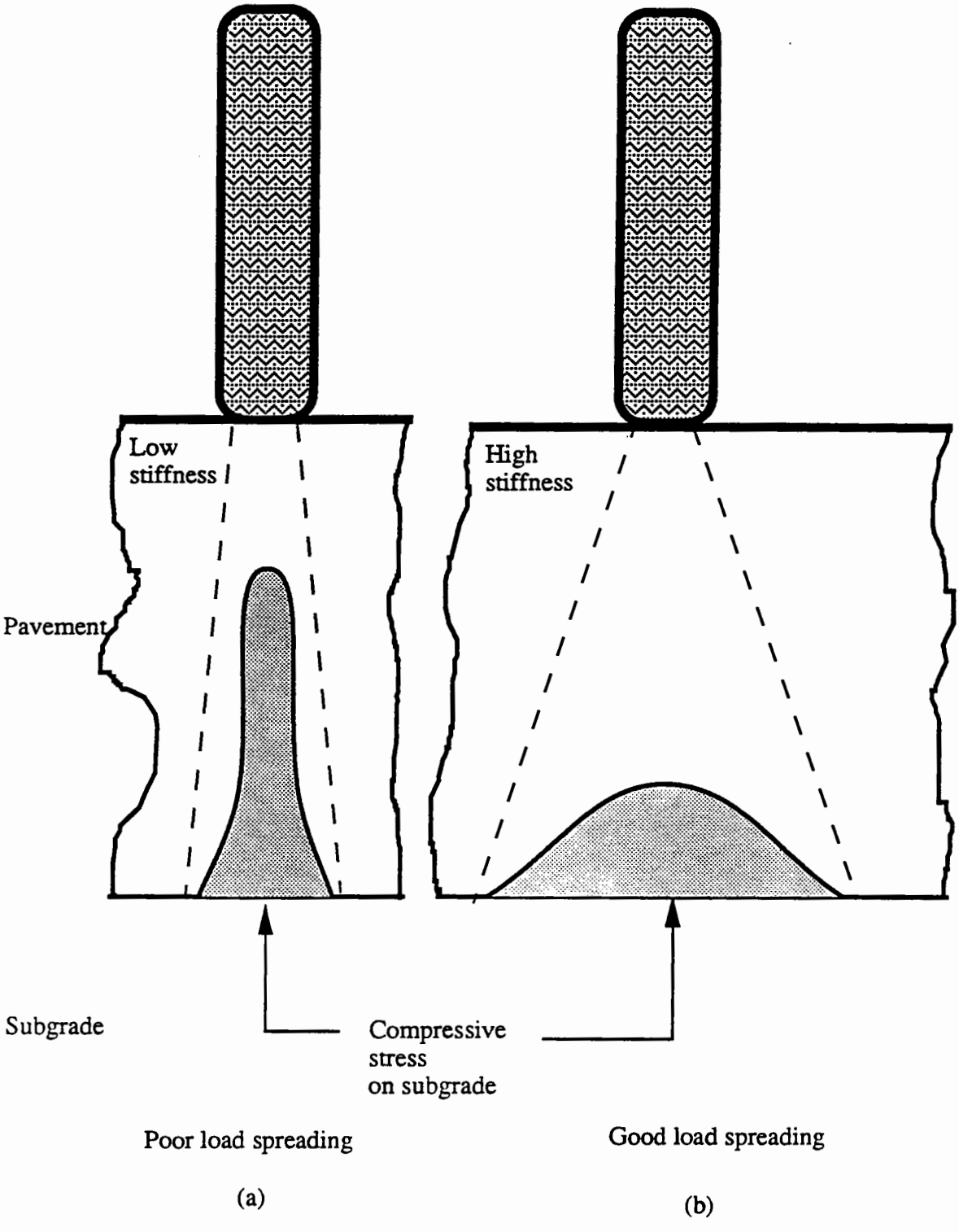

Figure 5.3. Load spreading properties of a pavement (Brown, 1990)

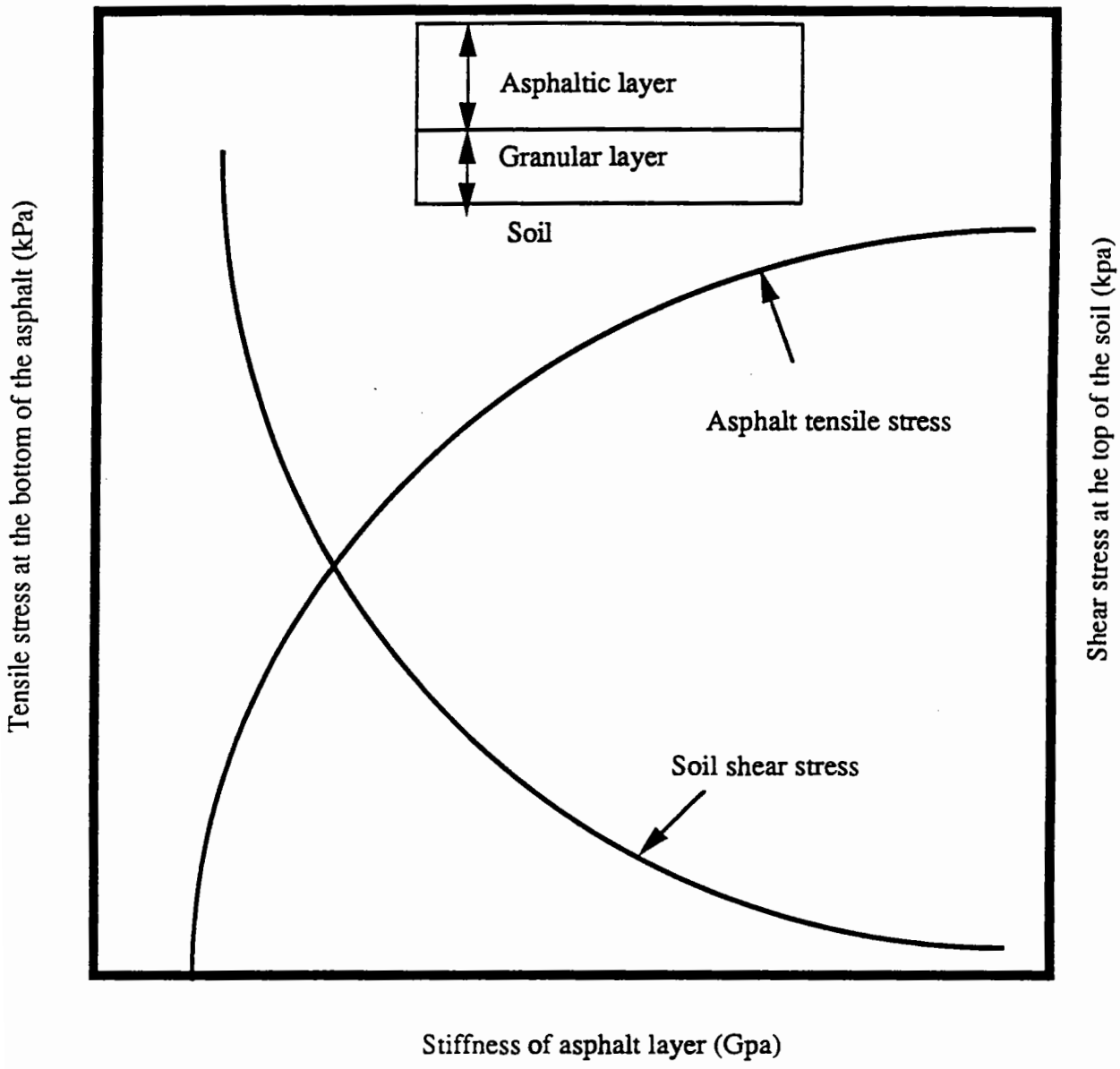

Figure 5.4. Balance in stiffness (Brown, 1990)

for a given pavement thickness, a balance in elastic stiffness is required in a pavement design so that cracking and subgrade rutting do not occur. For these reasons it is very important to make an accurate assessment of the stiffness of the component layers-including that of the aggregate layers.

5.3.Stress paths

Stresses applied to a sample were chosen so as to be well below the failure line so that the possibility of getting permanent strain after a stress path would be eliminated or much reduced. This case is quite similar to the behaviour of granular material under either concrete or flexible pavements which has a low overburden pressure and very low live (traffic) load when compared with the wearing course or base course materials.

In order to simulate traffic loading, which is random and repeated, stress paths of different amplitudes were applied in several directions in stress space (Figure 5.5). The applied stress paths can be divided into three groups:

• The first group (Type 1) comprises cyclic deviatoric (axial) stress paths under a constant cell (confining) pressure which have a gradient of 3 in p-q space.

• The second group (Type 2) involves the cycling of only the cell pressure (isotropic stress) whilst the deviatoric stress is constant or zero. Zero deviatoric stress paths are particularly important in determining anisotropy in the granular material for which the load ram was removed.

• The third group (Type 3) comprises paths in which both cell pressure and deviatoric stress are cycled in-phase. Of these, two types were applied:

a) Constant mean normal stress (dashed vertical lines in Figure 5.5, Type 3a)

b) Changing mean normal and deviatoric stress at the same time (dashed inclined lines in Figure 5.5, Type 3b)

Stress paths in which the mean normal stress increases independently of the deviatoric stress are likely to be more representative of a real pavement loading. However, many laboratories still use a constant confining pressure testing procedure to determine the resilient behaviour of the material since this type of equipment is more economic when compared with the apparatus which can cycle both both pressures at the same time. Australian Road Research Board (ARRB (1991)), AASHTO (1986) and TRB (1975) have all recommended the use of a constant cell pressure for routine resilient modulus determination, although, ARRB (1991) suggested using a cyclic deviatoric and cell pressures to determine the permanent strain behaviour and Poisson's ratio.

Some stress paths (Type 3a above) were selected with the intention of reducing the proportion of volumetric strain. However, the error caused by the software, as explained in Section 3.14, prevented the exact stresses from being applied as intended. Small amounts of volumetric strains were obtained from these particular stress paths. This may be partly be because of the control problem and partly because the material does not behave in an ideal elastic manner.

The sequence of testing is set out in detail in Appendix F.

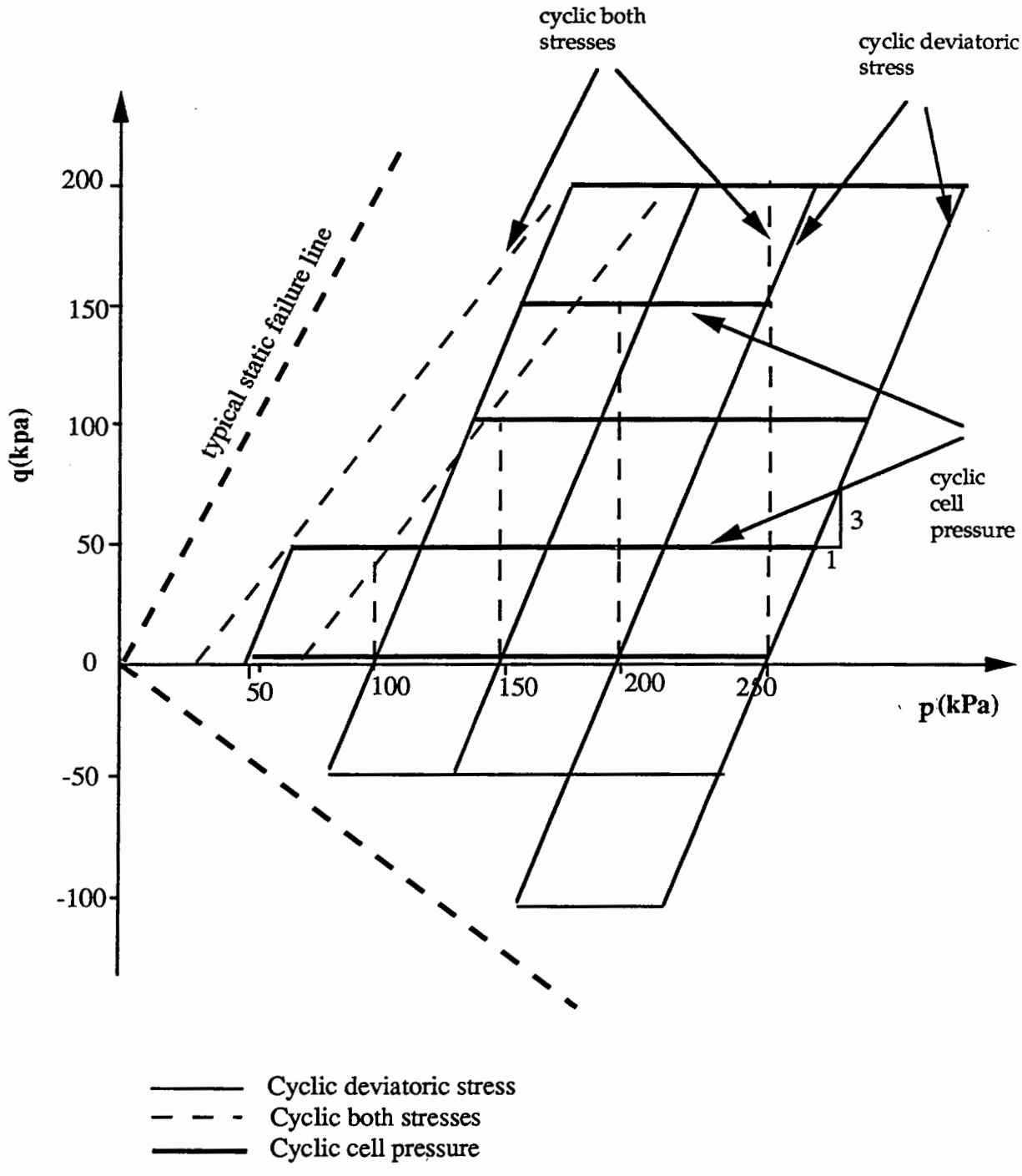

Lines indicate position of stress paths. Actual stress paths listed in Appnedix B

Figure 5.5. Stress paths

As a special case of the above stress paths (types 1 and 2), material was also subjected to extension as the test apparatus allows tensile deviatoric stress to be applied to a sample. Some stress paths were chosen either entirely in the extension zone or partly in both the compression and extension zones. The aim of testing in this area was to make comparison between extension and compression behaviour of granular material.

5.4.Resilient strain tests

Six resilient strain tests were carried out by the application of a wide range of stress paths (Figure 5.5). Consecutive applications of different stress paths at levels well beneath failure have almost no effect on the resilient behaviour of granular material (Kalcheft and Hicks, 1973; Allen and Thompson, 1974; Boyce, 1976 and Pappin, 1979). Hence, it is possible to apply a wide range of stress paths to a sample if the stress ratio is well below the failure line. However, the stress history of the sample is a very important factor for the permanent strain test (Chan, 1990; Brown and Hyde, 1975). In order to avoid confusing the two types of strain when taking measurements Hicks and Monismith (1971) suggested that the resilient properties of granular material should be determined after 50 to 100 cycles of loading although Allen and Thompson (1974) recommended that readings should be taken after 25 to 100 cycles and Brown and Selig (1991) recommended data gathering after 10 to 20 cycles. Sweere (1990) collected the resilient deformation readings after 100 cyclic deviatoric stress applications. Resilient modulus test procedures developed by AASHTO (1986) and TRB(1975) recommended applying 200 cycles for each deviatoric stress path before taking the resilient deformation readings. In this project, 50 cycles were applied to each

sample for each stress path and the last 5 cycles were recorded as being representative of the resilient behaviour of the material.

Researchers (Boyce, 1976; Kalcheft and Hicks, 1973 and Allen and Thompson, 1974) have tested granular material under different frequencies from 0.1 to 25 Hz. Brown (1974) tested crushed granite under different frequencies from 0.01 Hz to 10Hz. However, the general conclusion for materials a long way from saturation is that the effect of frequency on the resilient behaviour of granular material is negligible. In this project, a loading frequency of 1 Hz (Brown (1974), Sweere (1990)) was chosen as recommended by Brown and Selig (1991).

Stresses were applied in a half sine wave form (see Figure 5.6) in the project since the actual stress pulse caused by a moving wheel load is similar to a half sine in shape (TRB, 1975). A rest period of one second was used between pulses.

50 cycles of loading were applied to the sample on each stress path. When the difference between the top and bottom stress levels became high, it took some time for the control system to reliably obtain the desired stress level. Because of the limitation of the ATS software, the computer hardware and/or the physical apparatus (or all of these) it was difficult to obtain the precise stress path, therefore a 7% tolerance was introduced in the control unit. Data were collected for each stress path for the last five cycles of each series of stress applications

5.4.1.Measurement of anisotropy

In order to measure the inherent anisotropy, a sample which had been prepared as discussed in Chapter 4, was first subjected to a repeated cell pressure application with a haversine waveform from a lower stress of 25 kPa to an upper stress, increased in 25 kPa increments, ranging from 50 kPa to 225 kPa.

Afterwards the other resilient tests were performed on the sample and the sample was then allowed to experience permanent strain of approximately 1% in order to see the change in inherent anisotropy. Subsequently the same test procedure was again applied to the sample. The anisotropy in the sample was estimated using the ratio between the axial and radial strains as suggested by Biarez and Hicher (1988).

5.5.Analysing test results

The ATS software can be used to analyse test results. However, some noise was observed in the results due to the test system. The ATS reporting software hunts for the maximum and minimum readings in each cycle so, should ATS be used for data analysis, the results would be overestimates of the genuine values (see Figure 5.6, 5.7 and 5.8). Subsequently it was decided to manually filter the results by means of inspection of the graphical plot of the results from stress path. For this reason, all ATS files were imported to LOTUS 123 spreadsheet files. The ASEASYAS spreadsheet

program was then used with all stresses and strains plotted against each other using a macro program. Possible noise in the results was inspected by eye. Examples are shown in Figures 5.6, 5.7 and 5.8. Hence, the results given in the appendix B are unlikely to have incorporated noise effects. Figures 5.7 and 5.8 also illustrate the digitisation of the original signal. At small strain levels the signal becomes a series of steps and estimation of the noise-free maxima and minima becomes more unreliable when considered as a proportion of the genuine peak-to-peak strain reading.

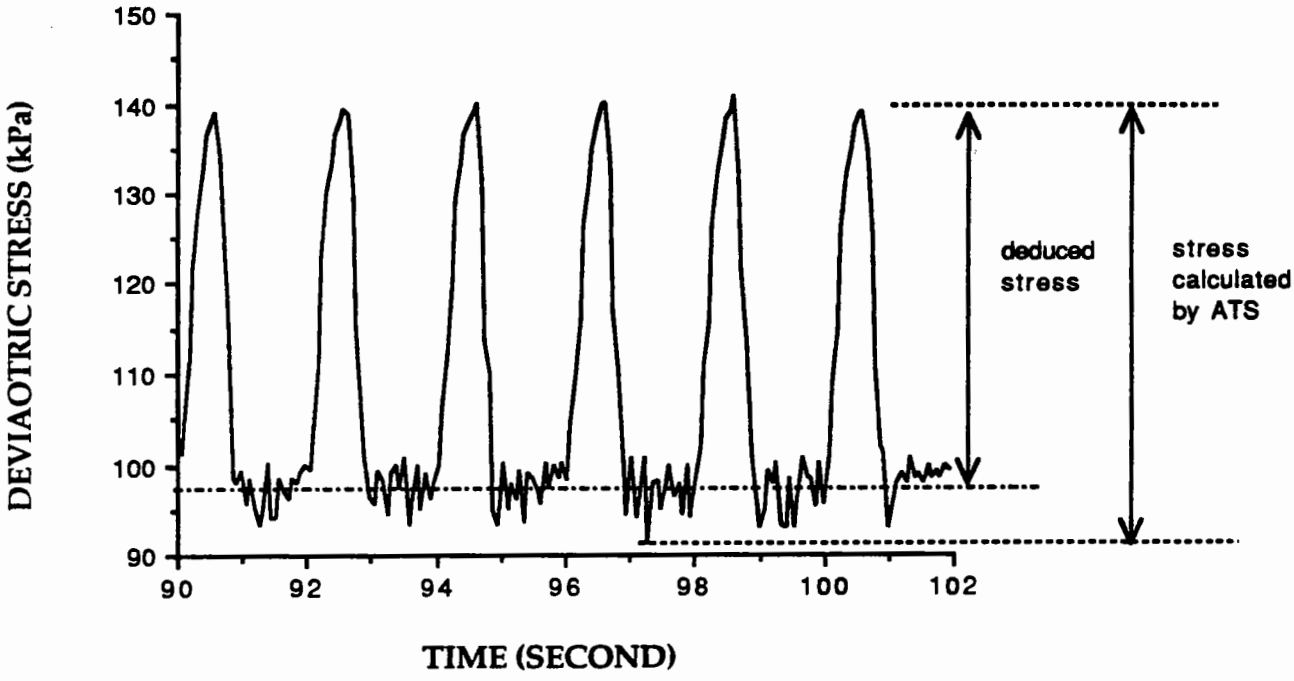

Figure 5.6. Noise in the deviatoric stress (FBA)

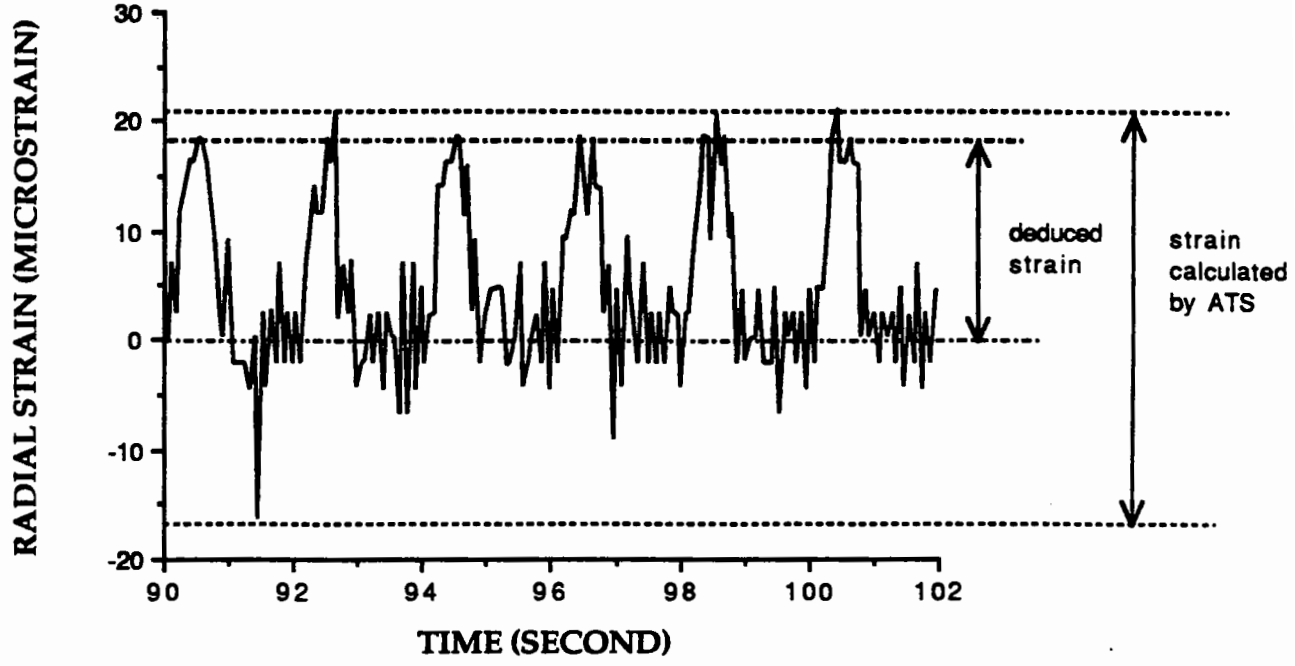

Figure 5.7. Noise in radial strain results (FBA)

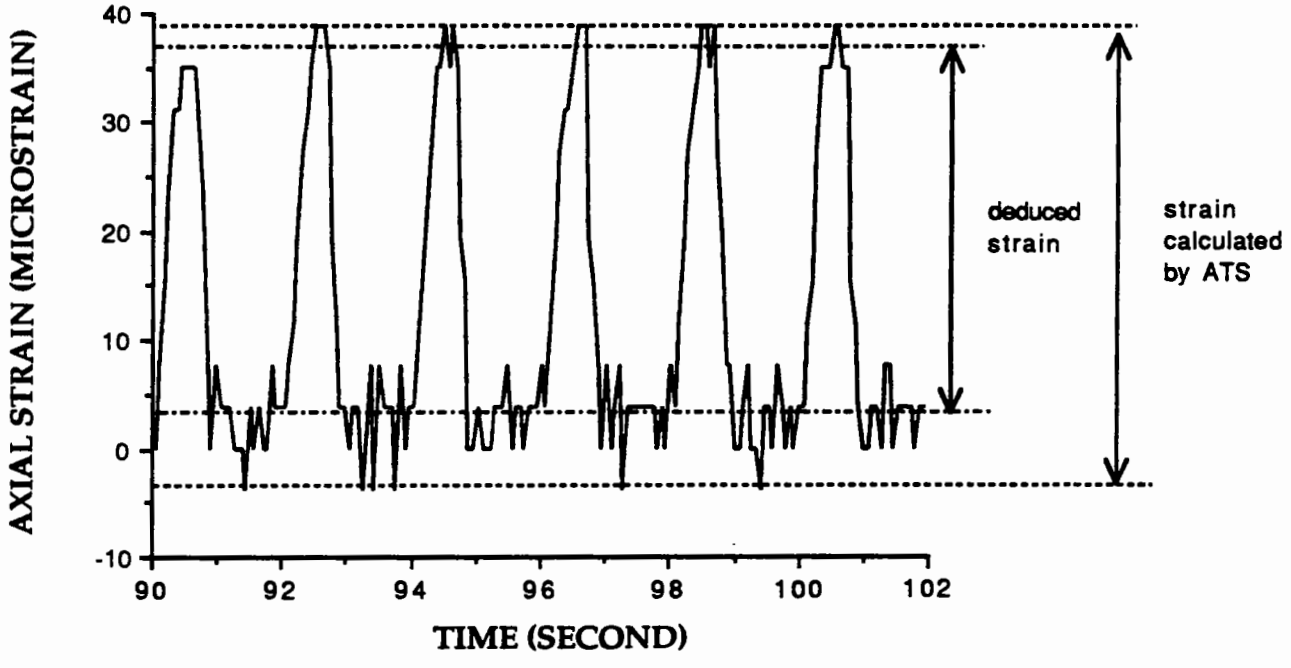

Figure 5.8. Noise in axial strain results (FBA)

CHAPTER 6

DISCUSSION OF TEST RESULTS

6.1.Introduction

Six resilient repeated load triaxial tests were carried out on granular materials from different origins. Certain equipment effects which could influence the test results are discussed: leakage, cross-sectional area correction and membrane effects . The effects of the mean normal stress and the deviatoric stress on strains is shown since they provide the basis for the development of a constitutive model. Inherent anisotropy and its change with number of load applications is also discussed.

6.2.Equipment factors affecting the test results

There may be some influences of the equipment which is likely to affect the triaxial test results, even if only by a small amount. These may be the leakage of cell fluid into the sample through the membrane during the test, area change after each successive cycle and membrane contribution to the applied stress. Therefore, it is necessary to correct the results if these effects are significant. Each factor will be discussed in turn regarding its influence and mitigation.

6.2.1.Leakage

Silicone oil was used as a cell fluid when the confining pressure was cycled. If there is a hole in the membrane, even a small one, it is likely that the cell fluid will disturb the behaviour of the sample to some extent. Therefore, the sample will no longer have the same properties as intended at the beginning of the test. In order to determine whether there was a hole in the membrane, a vacuum was applied through the top platen before the cell and the silicone cell fluid was in place and a reasonable time was allowed for the establishment of equilibrium in the sample. Vacuum readings were taken at the bottom and top platens. If these vacuum readings were not the same it was likely that the loss of vacuum in the sample was due to a membrane puncture. However, it is still possible for a hole to develop in the membrane during a test due to the penetration of particles into the membrane. For this reason, the material was poured into a tray after each test and inspected for the presence of silicone oil to determine whether there was a leakage problem during the test. No such problem was observed with all the dry material samples tested. Inspection of the moist samples did not show any serious sign of oil ingress, but it is recognized that some oil might have been visually undetectable.

6.2.2.Cross-sectional area correction

The cross section of a triaxial sample changes during a test due to the radial plastic strain which the sample experiences. Therefore it is necessary to correct the cross-sectional area to find out the real stresses applied to a sample.

Granular materials generally experience a bulging (barrelling) mode of failure with no apparent shear plane, unlike clay samples. The maximum permanent radial strain, ε_{rp}, measured in any test was 1.5%. This gives rise to a percentage change in cross sectional area of

$$\Delta A = \frac{2 \pi r^2 \varepsilon_{rp}}{A_o} \tag{6.1}$$

where A_o = initial cross-sectional area at the beginning of the test
ε_{rp} = permanent radial strain (%)
ΔA = change in cross-sectional area (%)

Use of this formula assumes that the specimen deforms as a cylinder with a constant diameter throughout its height (Figure 6.1) and is therefore an approximation. Using this approach the greatest correction required was by a factor of 1.0011 which is insignificant compared to the errors due to insrumentation and control. Hence no correction for area change was subsequently applied.

6.2.3.Membrane correction

The membranes enclosing a triaxial sample may slightly reduce deviatoric stress-induced deformations by restraining the sample. For a barrelling type of failure, which is the case for granular material, the membrane correction depends upon the axial strain of the specimen, the extension modulus of membrane material and initial diameter of the specimen. Henkel and Gilbert (1952) recommended use of the formula given below:

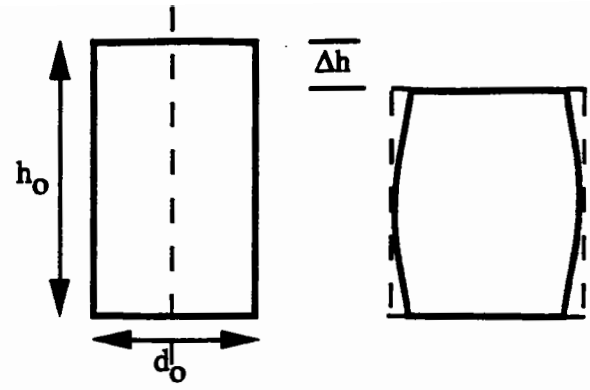

Figure 6.1.Barreling type of failure

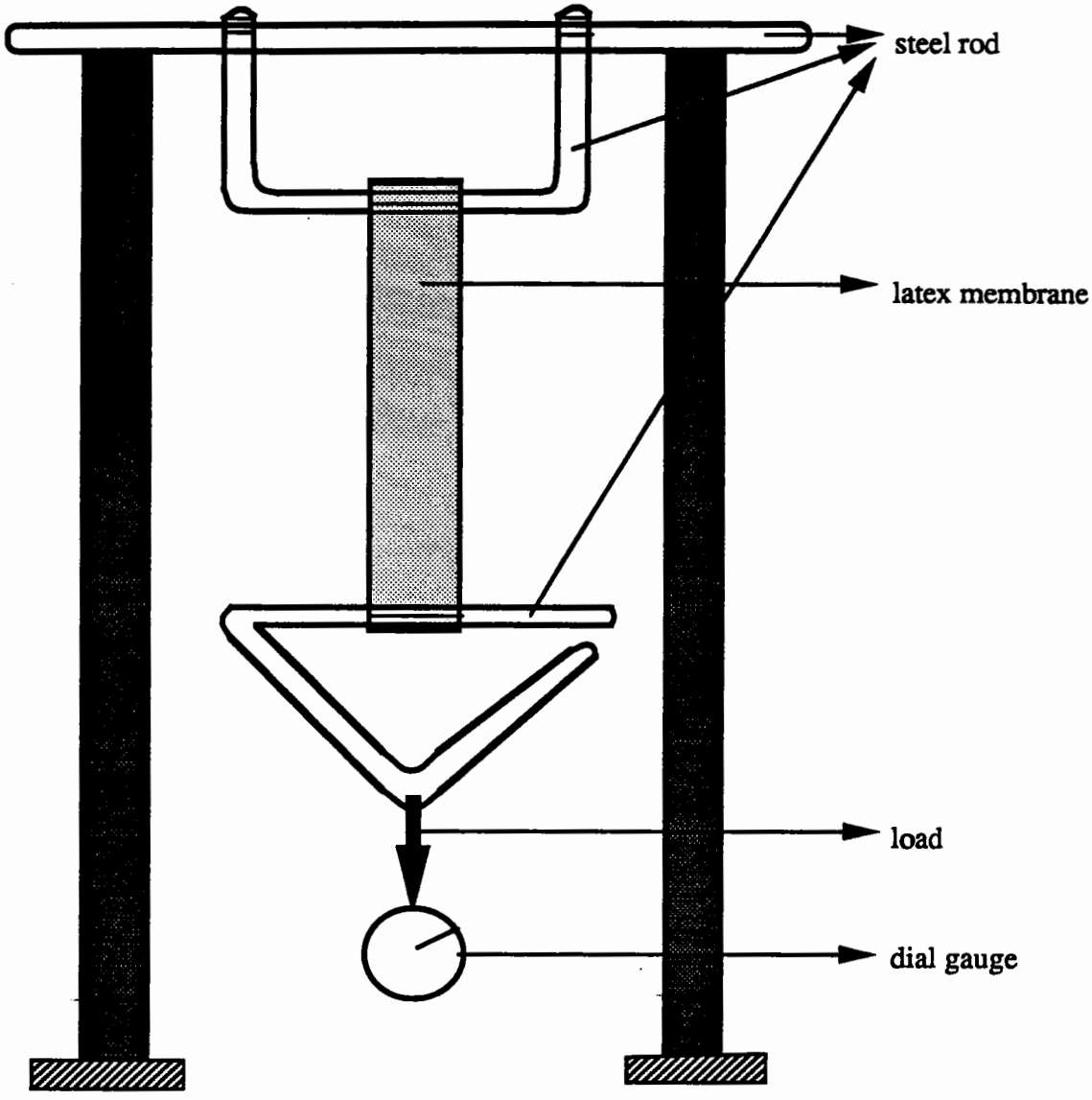

Figure 6.2.Apparatus to measure the compressive modulus of the membrane

$$M_c = \frac{0.4\ M\ \varepsilon_a\ (100 - \varepsilon_a)}{D} \qquad (6.2)$$

where M_c = membrane correction (kN/m^2)
M = the extension modulus of the membrane (kN/m)
ε_a = axial strain in the specimen (in %)
D = the initial diameter of the specimen (m)

The compression modulus M of the membrane material is taken as being the same as its extension modulus (Henkel and Gilbert (1952), Bishop and Henkel (1962) and Head (1981)).

In order to determine the extension modulus of the rubber of which the latex membrane is comprised, a 25 mm wide strip of membrane, with a thickness of 0.5 mm, was cut. An apparatus was set up as shown in Figure 6.2 and weights were added from 50 to 350 grams in increments of 50 grams. The relationship between the applied load and the axial strain was plotted and a membrane correction curve was obtained. Granular materials tested in the laboratory generally experienced a maximum resilient strain of 1.5 %, therefore the maximum value for membrane correction is $6x10^{-5}$ kPa. Even allowing for initial stretching to place the membrane on the sample the maximum stress applied would be $2x10^{-5}$ kPa. As a result, the membrane correction on the resilient results was found to be insignificant even for double membranes.

Before using the apparatus described above, an attempt was made to use an artificial (polymeric) triaxial sample which had the same diameter and height as the original triaxial sample (150 mm diameter and 300 mm height). The sample was tested without a membrane and with two membranes under a static compressive load with no confining pressure. Each static load was applied for three minutes. When the results were compared, no significant effect of the membrane was found. Initially, it was

thought that genuine differences might be masked by control system errors. However, the observations described above have proved that using a membrane has negligible effects on the results.

6.3. Effect of deviatoric stress on resilient behaviour

The resilient test procedures of AASHTO(1986) and TRB(1975) require granular materials to be tested under a range of confining and deviatoric stresses. According to these test procedures, to determine the resilient characteristics of granular material, the confining stress is kept constant whilst the deviatoric stress is cycled. In this section the effect of deviatoric stress on axial strain, radial strain, volumetric strain, shear strain and Poisson's ratio will be discussed with the results obtained from the repeated load triaxial tests. The results discussed in following sub-sections are those measured under stress paths in which q/p=1/3, i.e. the positive paths (Type 1) in Figure 5.5. Except where otherwise noted secant measurements (i.e. at maximum stress conditions in a cycle) are given.

6.3.1.Axial strain

As the deviatoric stress is increased, the axial strain increases substantially. The relationship between the deviatoric stress and the axial strain is non-linear. Non-linearity increases as the confining pressure decreases (Figure 6.3, 6.4, 6.5, 6.6). In almost all cases the stiffness is highest at the commencement of loading.

As the confining pressure decreases, the axial strain under the same deviatoric stress increases (e.g. Figure 6.3, 6.4, 6.5 and 6.6). At low levels of deviatoric stress the axial strains at different confining pressures are similar, but as the deviatoric stress increases they differ significantly.

6.3.2.Radial strain

At high levels of deviatoric stress, a disproportionate increase in radial stain was often observed. As the confining pressure increased, the radial strain due to deviatoric stress repeating tended to decrease. It appears that there is some stress hardening behaviour for the washed graded river sand and for the furnace bottom ash at the two largest confining pressure in each case (Figure 6.7 and 6.8). Inconsistent results were obtained for a confining pressure of 150 kPa for Fountaineblau sand, gritstone and single size limestone (e.g. Figure 6.9 and 6.10)- the radial strains being little different from those measured at a cell pressure of 200 kPa. Part of this may be due to the relatively poor discrimination of the insrumentation at low radial strain levels.

6.3.3.Shear strain

Shear strain behaviour computed from the axial and radial strain measurements of the materials was generally consistent with that of axial strain (e.g. see Figure 6.4 and

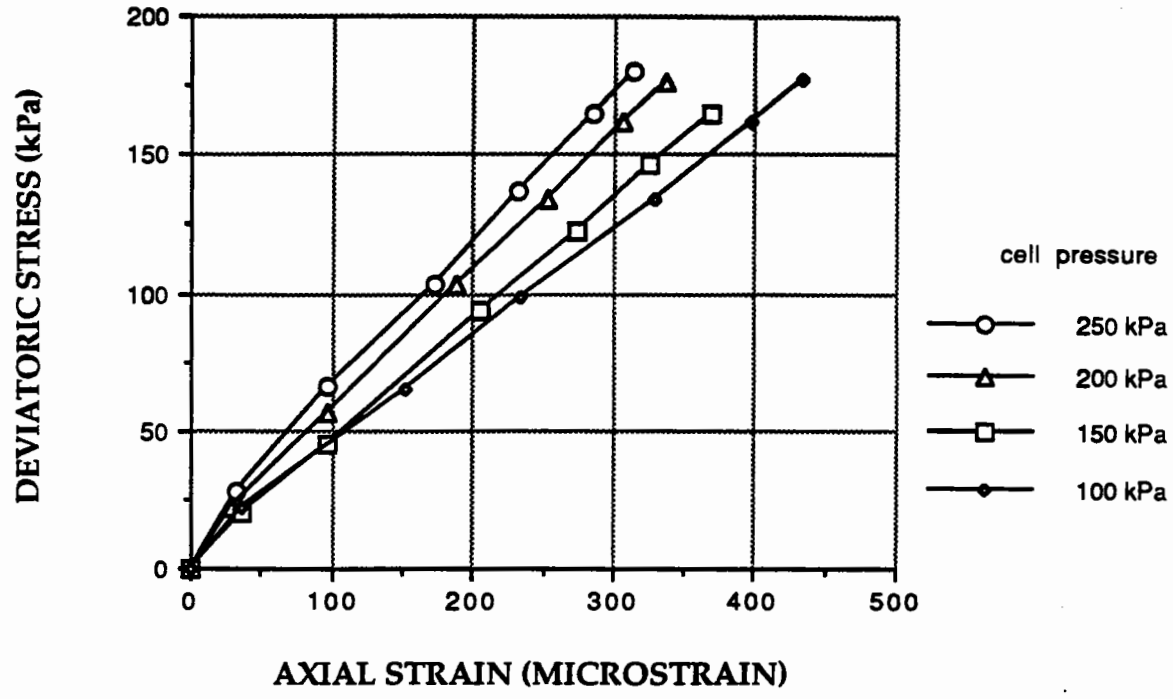

Figure 6.3. Secant axial strain during one loading cycle (FS)

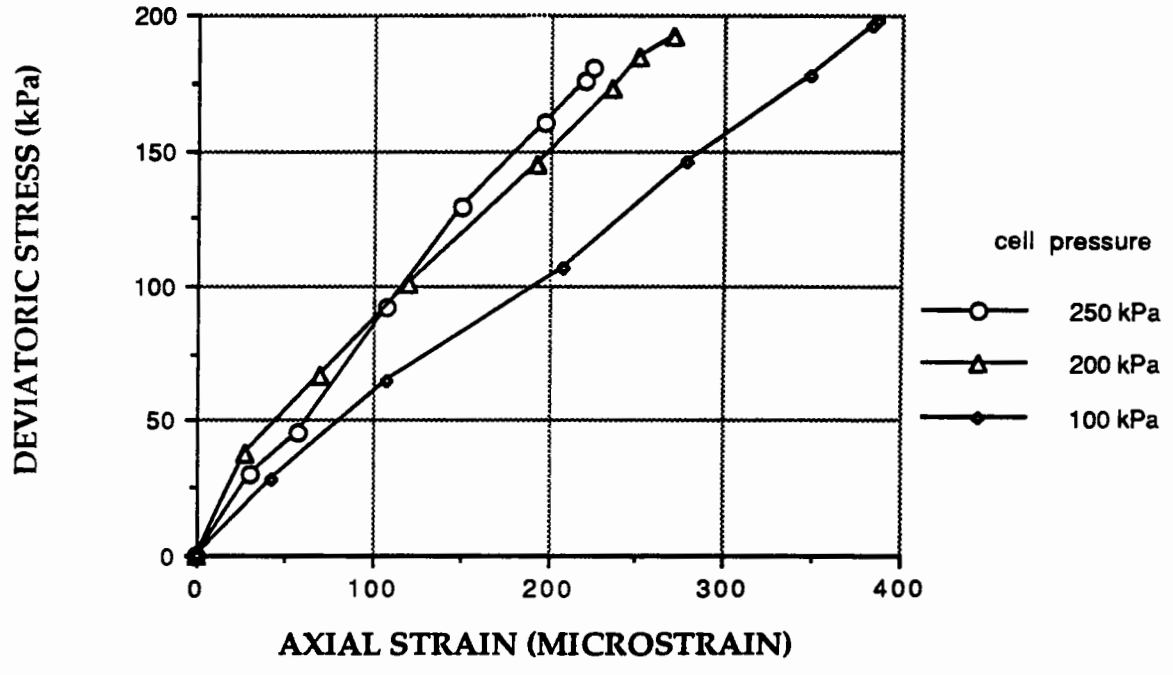

Figure 6.4. Secant axial strain during one loading cycle (FBA)

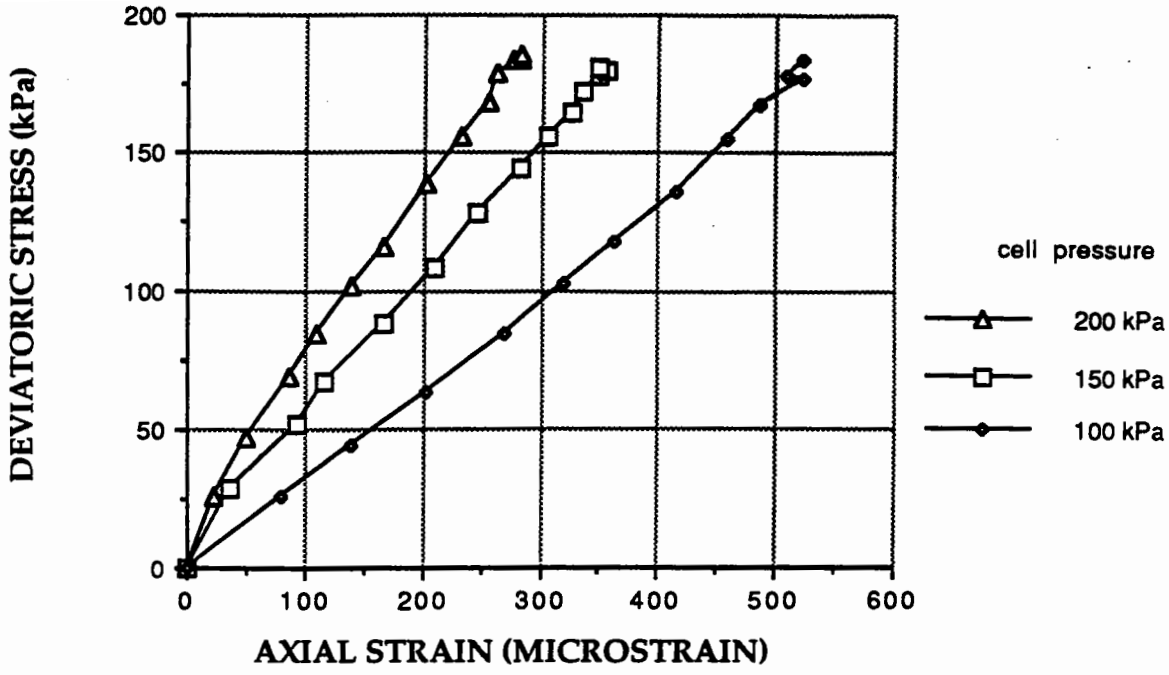

Figure 6.5. Secant axial strain during one loading cycle (SL)

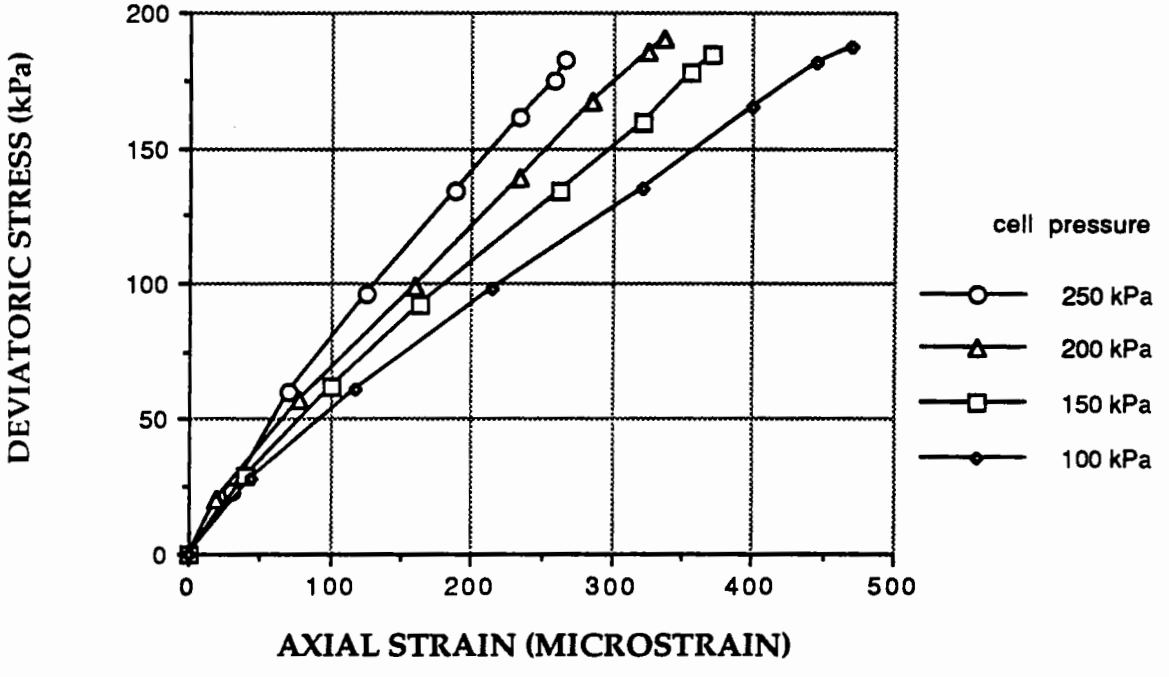

Figure 6.6. Secant axial strain during one loading cycle (SAG)

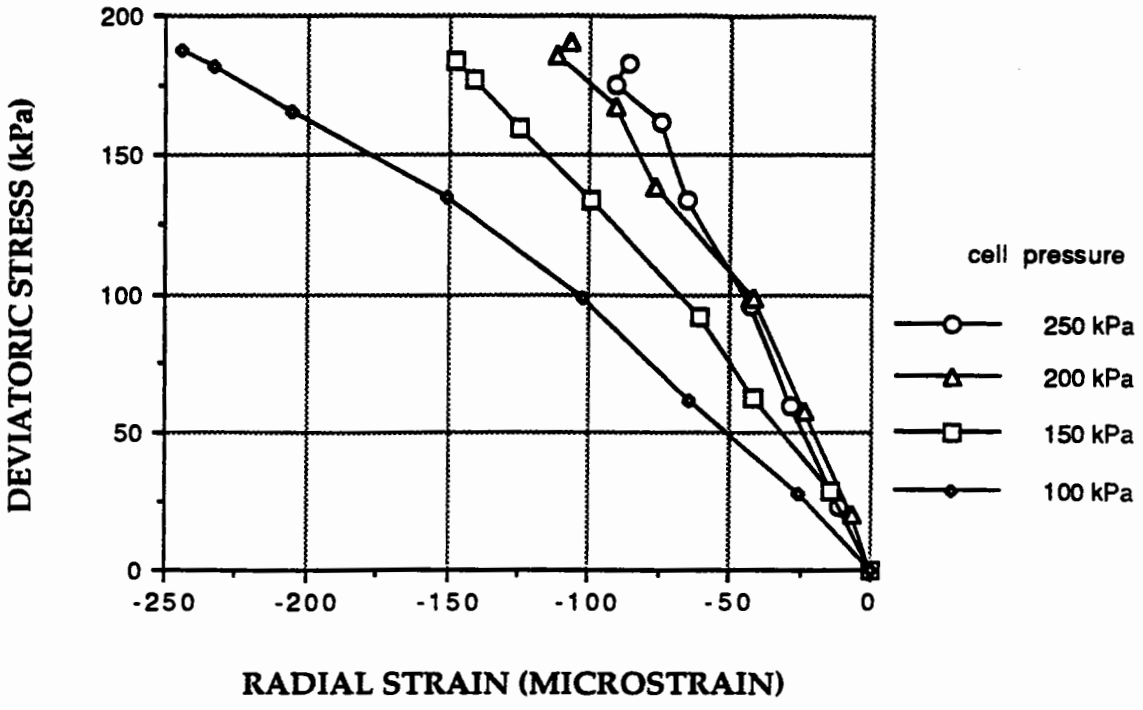

Figure 6.7. Secant radial strain during one loading cycle (GWRS)

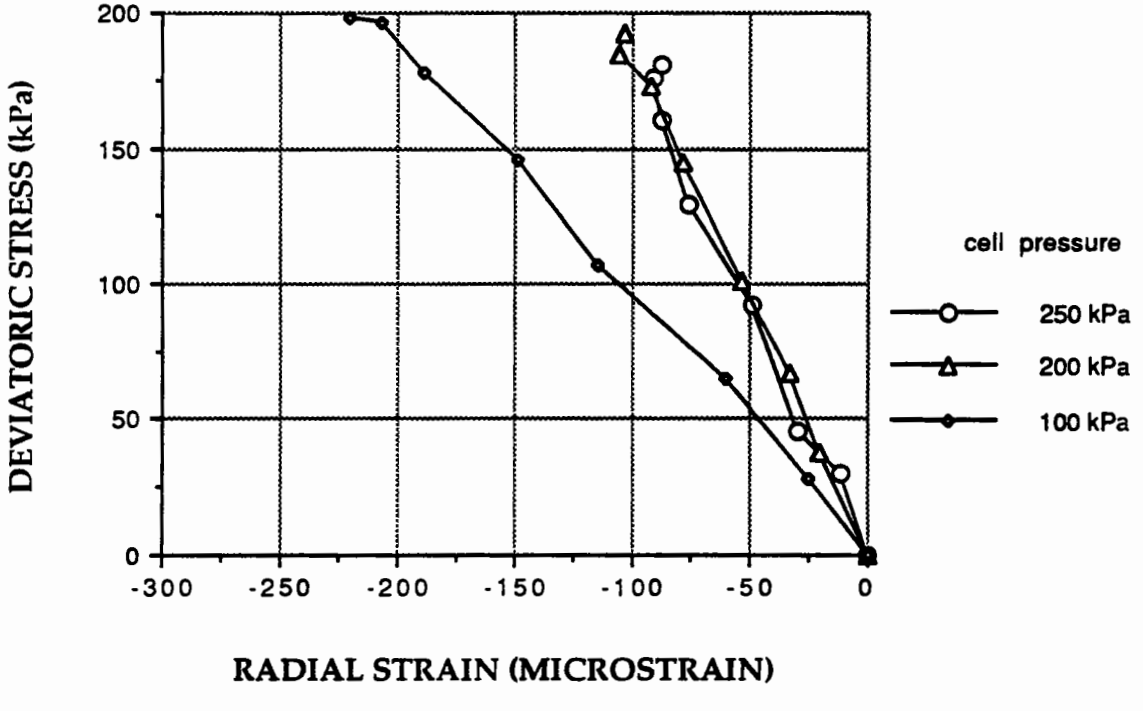

Figure 6.8. Secant radial strain during one loading cycle (FBA)

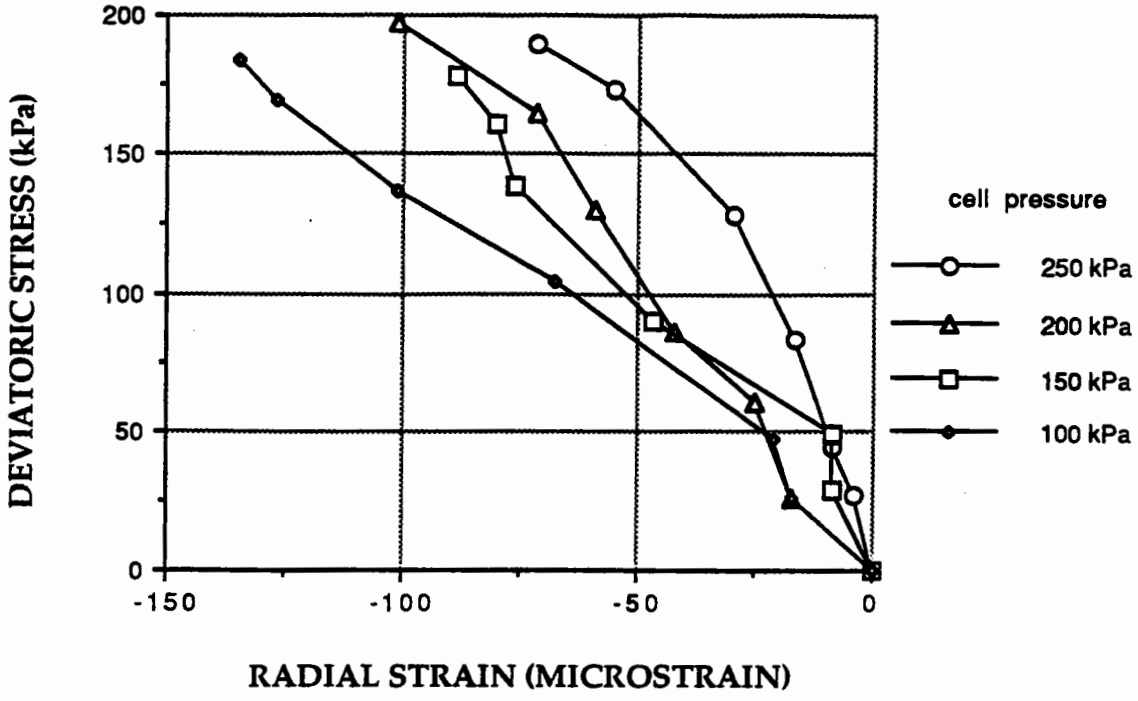

Figure 6.9. Secant radial strain during one loading cycle (GS)

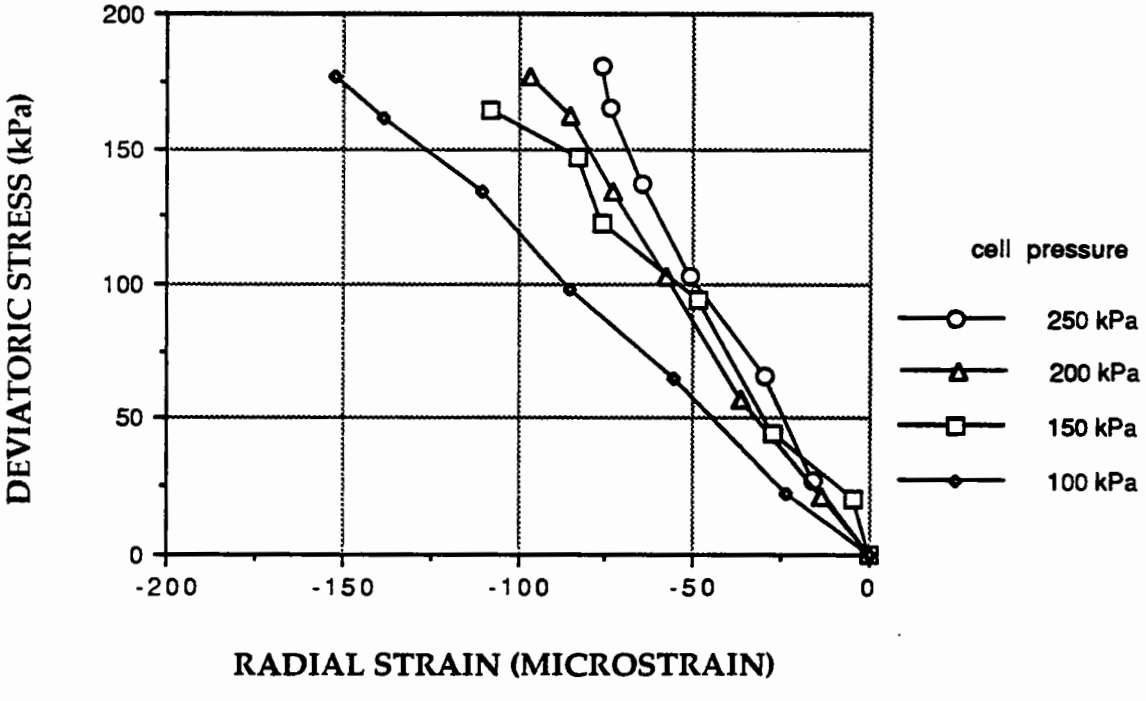

Figure 6.10. Secant radial strain during one loading cycle (FS)

6.13). As the the confining pressure increased at the same level of deviatoric stress, the shear strain tended to decrease (Figure 6.11, 6.12, 6.13 and 6.14). At low levels of deviatoric stress for different confining pressures, the shear strains are similar to each other.

6.3.4.Volumetric strain

No clear pattern in behaviour was observed for the volumetric strain results, perhaps partly because of the radial strain discrimination problem. However, as the deviatoric stress increased the volumetric strain also generally increased (Figure 6.15, 6.17, 6.18). This behaviour is only valid at high levels of confining pressure except for gritstone (Figure 6.16) which showed no trend in its behaviour. Resilient dilation (increase in volume) was observed at 100 kPa confining pressure for washed dry sand, furnace bottom ash and sand and gravel (Figure 6.15, 6.17 and 6.18). For furnace bottom ash at 100 kPa confining pressure the material experienced dilation at all levels of deviatoric stress whereas, for washed river sand and sand and gravel, dilation was only significant at higher deviatoric stress.

6.3.5.Poisson's ratio

The measured secant values of Poisson's ratio are generally larger at low levels of deviatoric stress and at low levels of confining pressure. This may be due, partly, to the decreased accuracy of strain measurements at the low strain values used to calculate

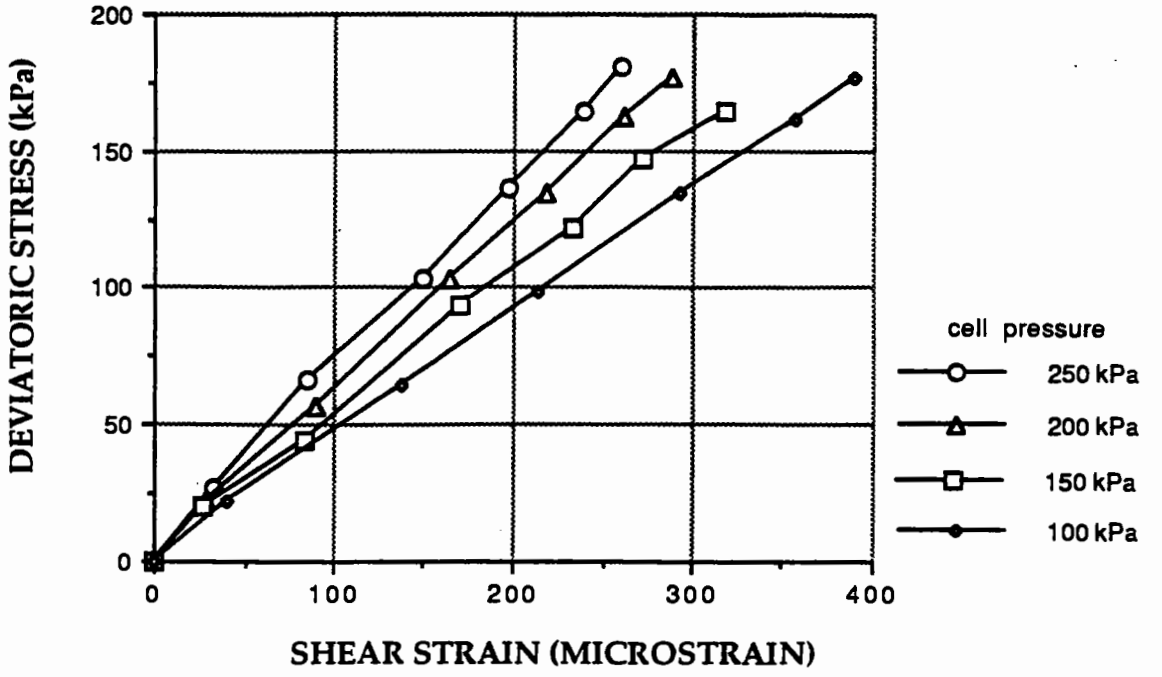

Figure 6.11. Secant shear strain during one loading cycle (FS)

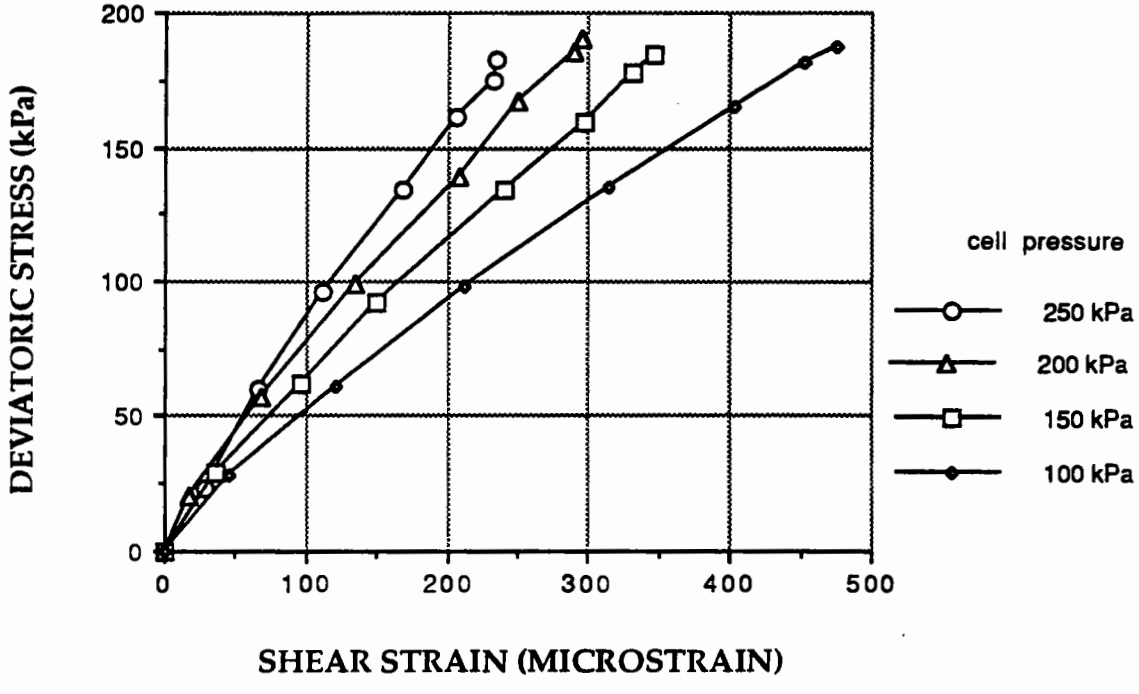

Figure 6.12. Secant shear strain during one loading cycle (SAG)

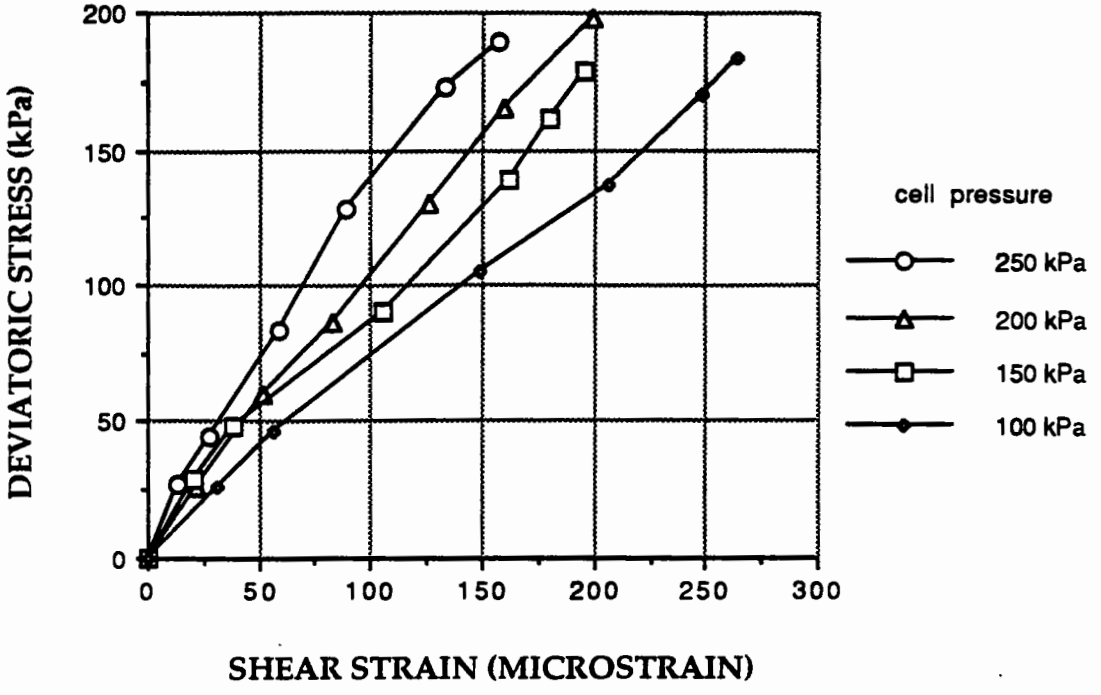

Figure 6.13. Secant shear strain during one loading cycle (GS)

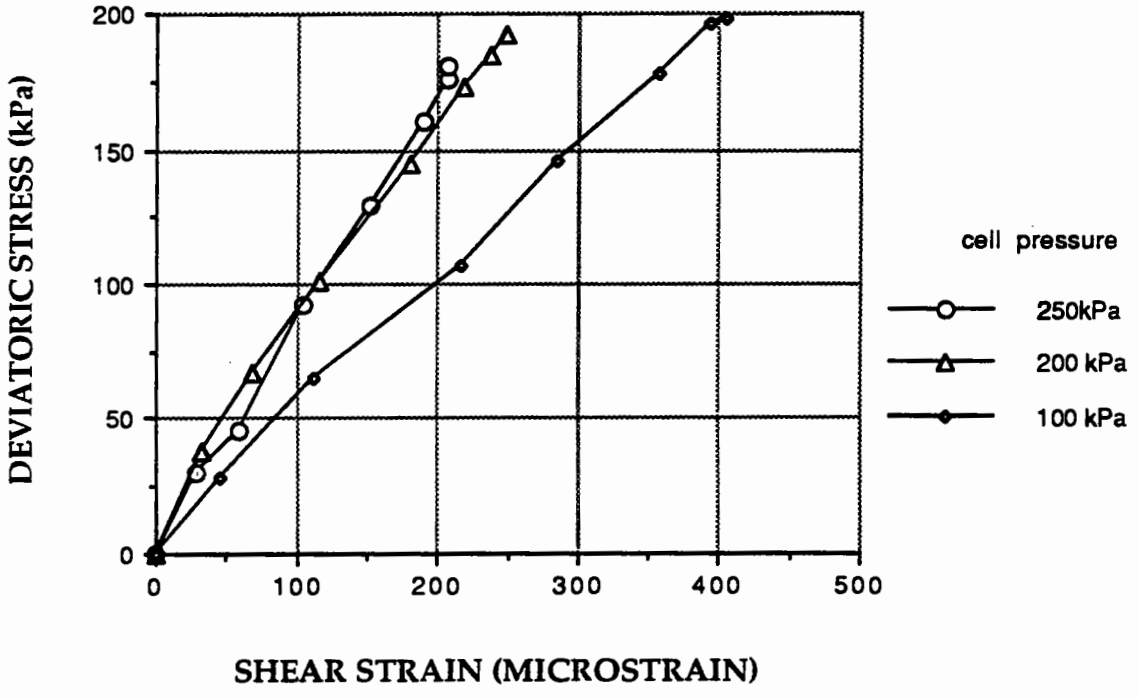

Figure 6.14. Secant shear strain during one loading cycle (FBA)

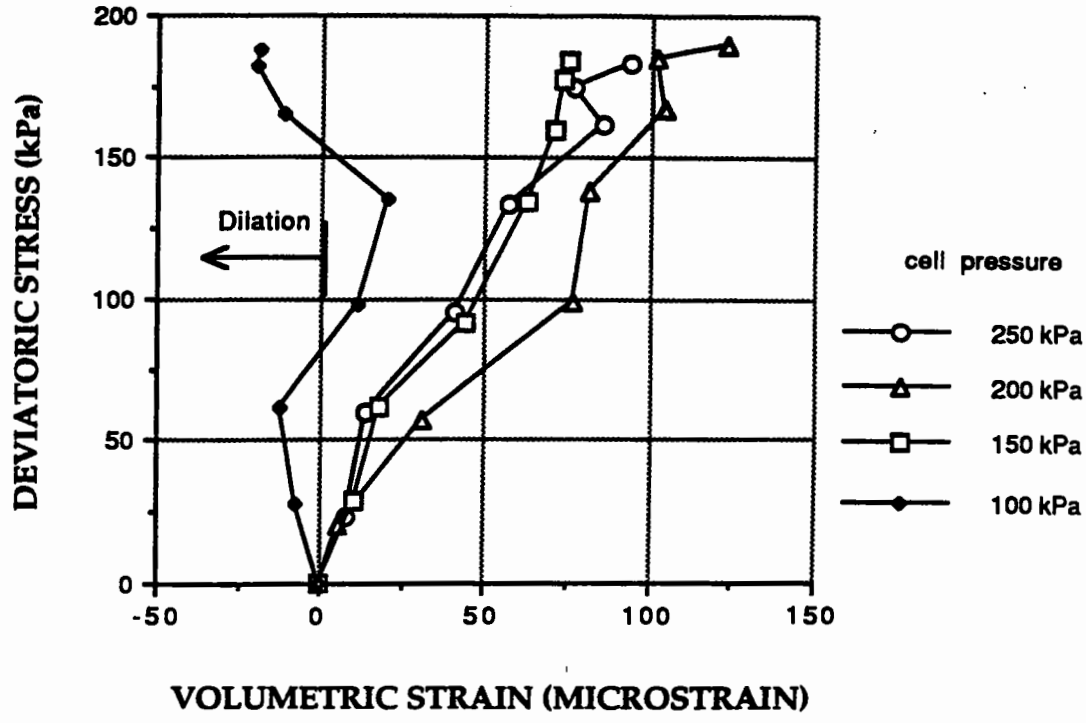

Figure 6.15. Secant volumetric strain during one loading cycle (GWRS)

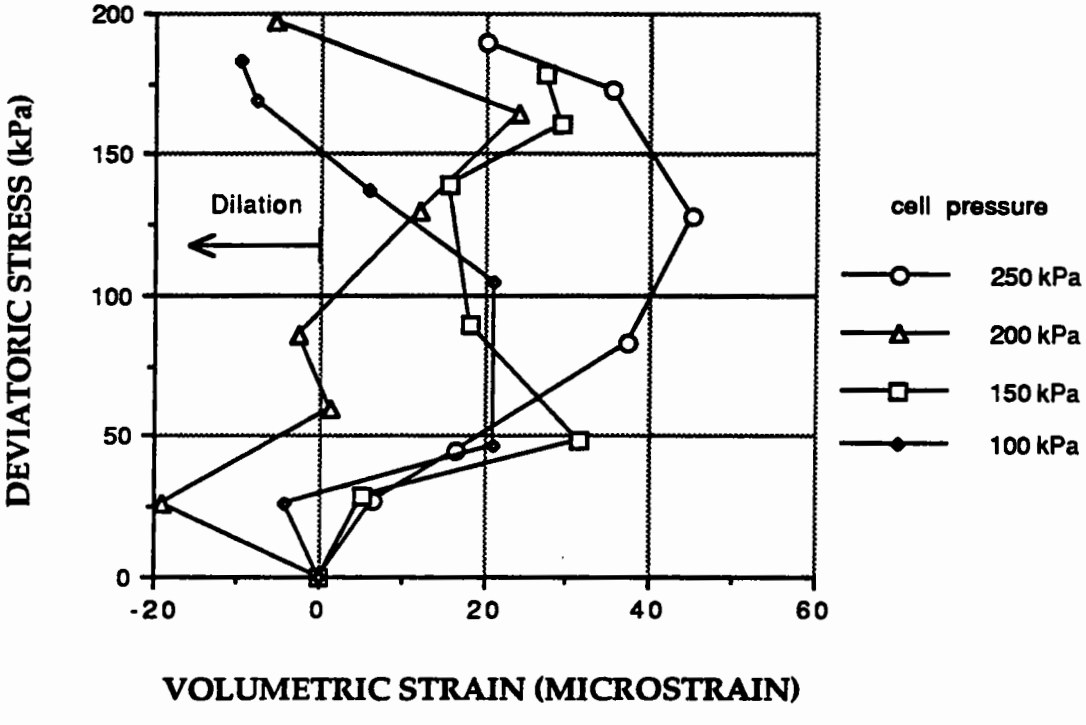

Figure 6.16. Secant volumetric strain during one loading cycle (GS)

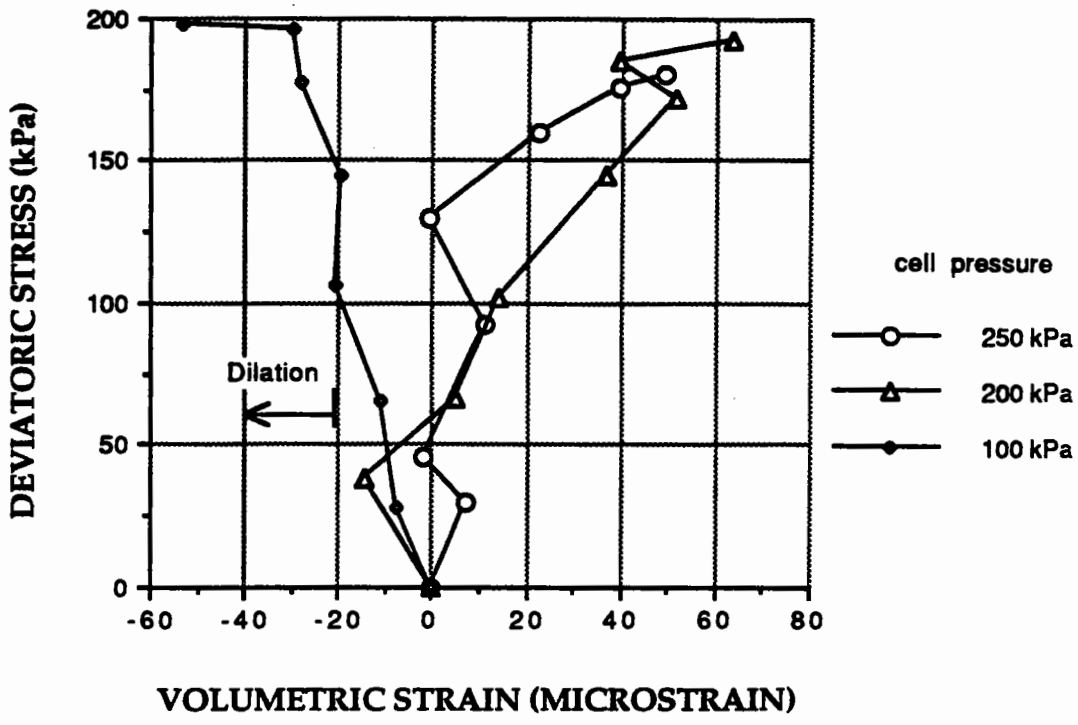

Figure 6.17. Secant volumetric strain during one loading cycle (FBA)

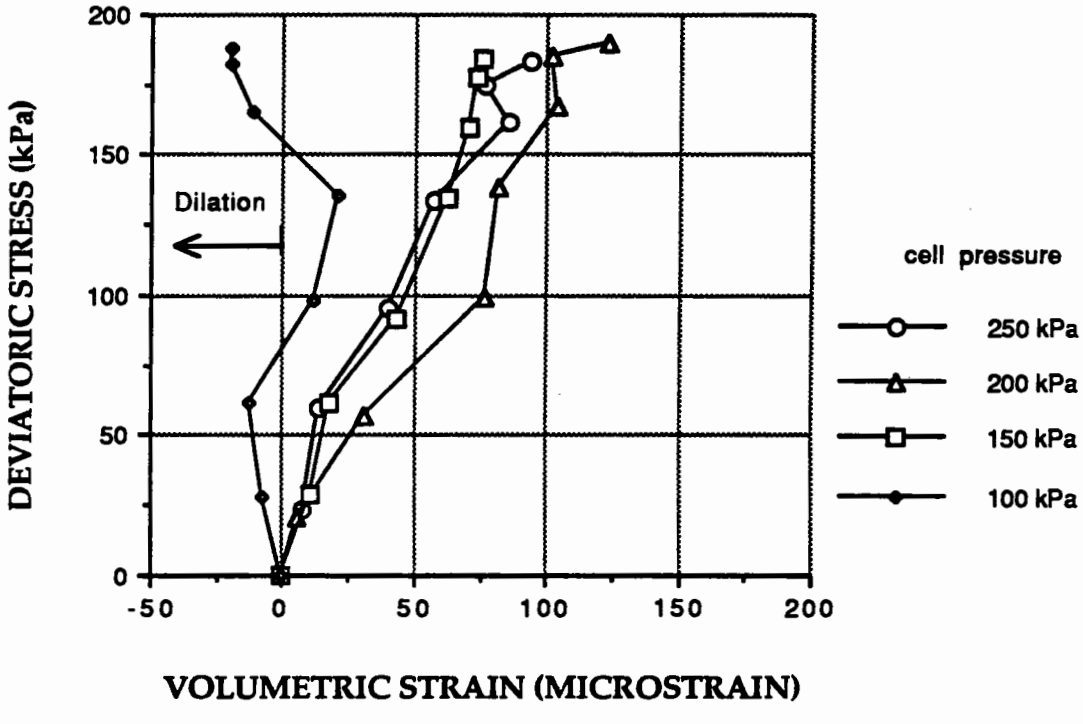

Figure 6.18. Secant volumetric strain during one loading cycle (SAG)

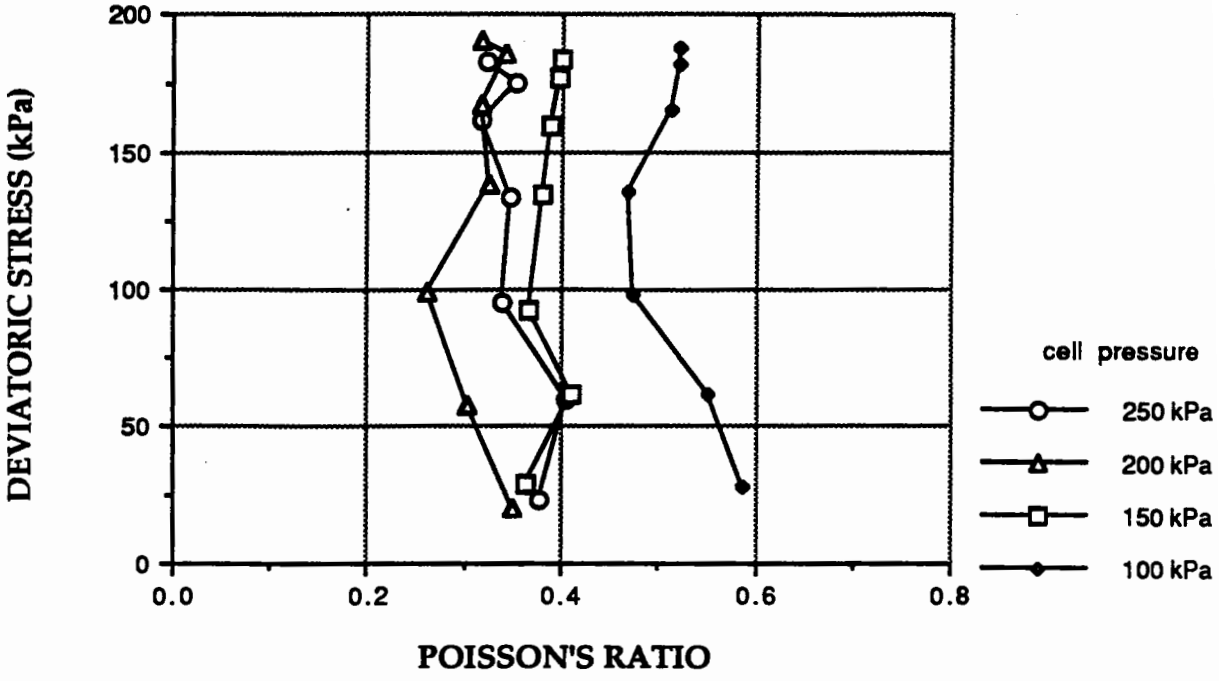

Figure 6.19. Secant Poisson's ratio during one loading cycle (GWRS)

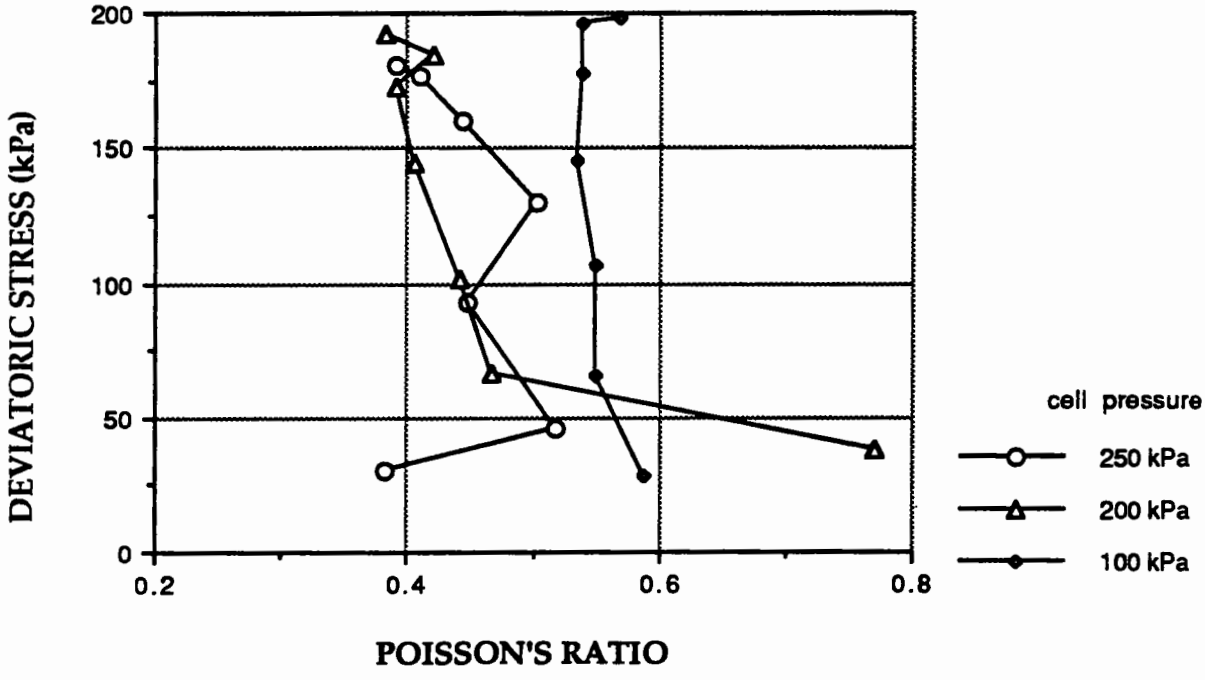

Figure 6.20. Secant Poisson's ratio during one loading cycle (FBA)

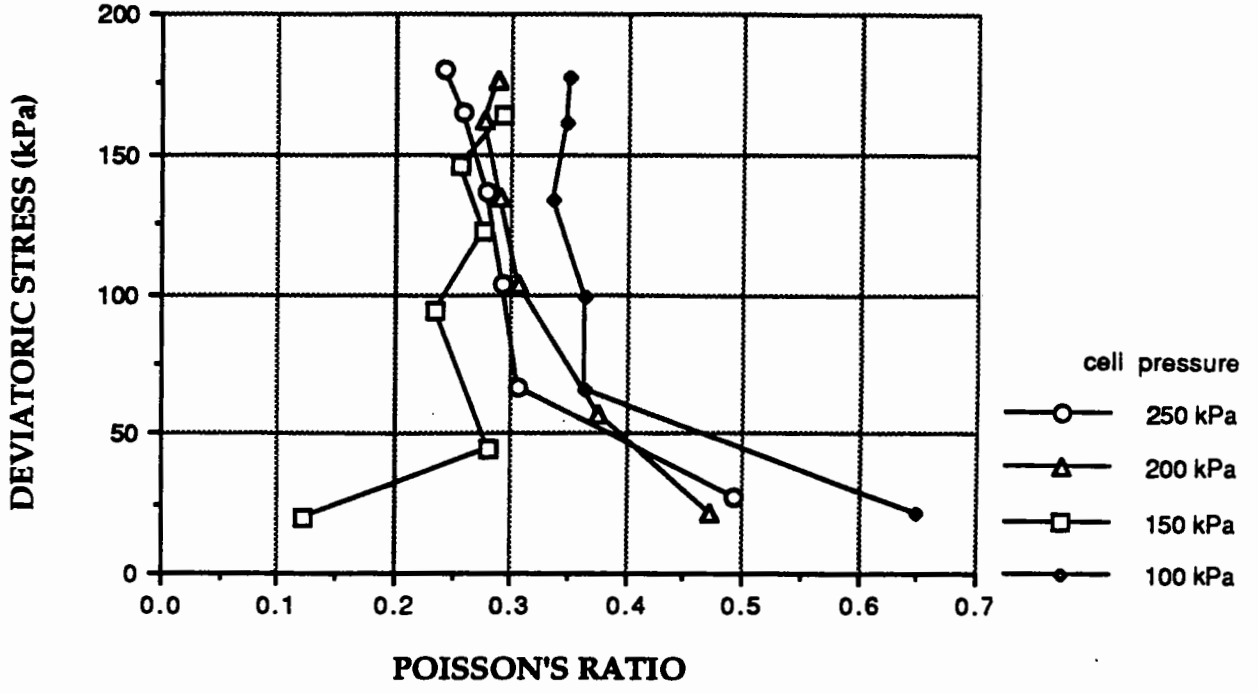

Figure 6.21. Secant Poisson's ratio during one loading cycle (FS)

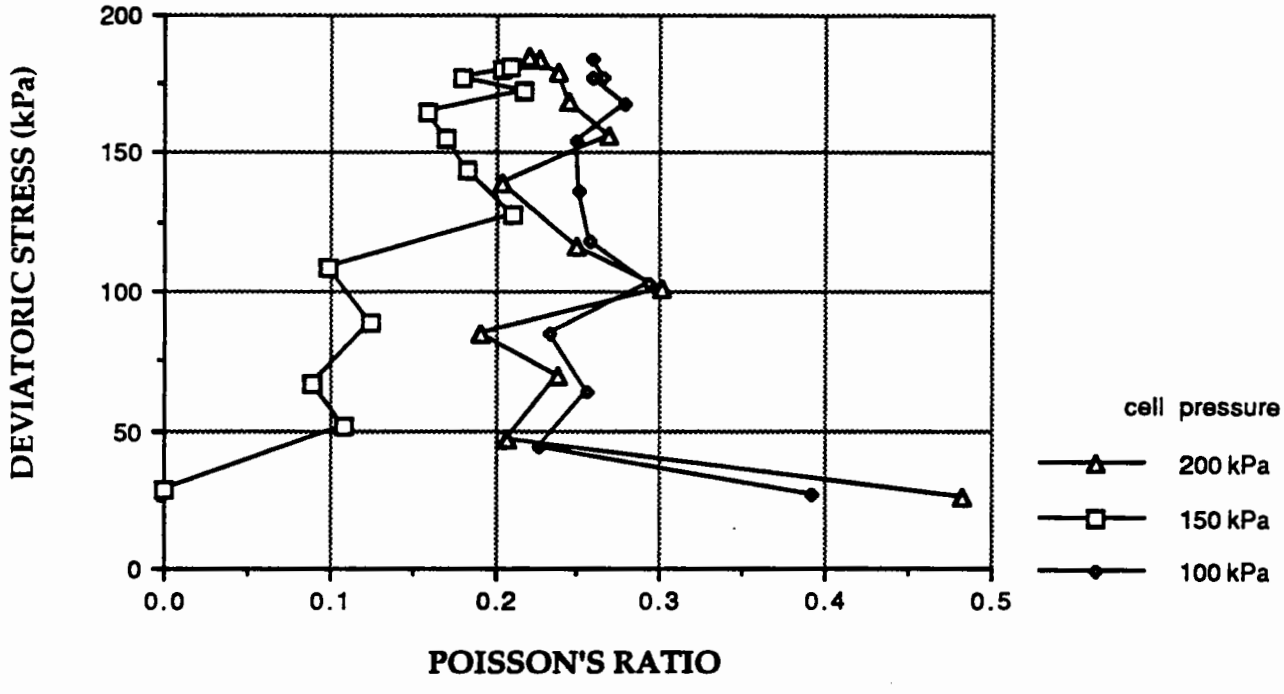

Figure 6.22. Secant Poisson's ratio during one loading cycle (SL)

the Poisson's ratio. The observed Poisson's ratio for six different materials ranges between 0.1 and 0.8 (Figure 6.19, 6.20, 6.21 and 6.22). When the Poisson's ratio is larger than 0.5 the material is said to be resiliently dilative. Materials containing more fine materials in their gradings such as washed dry sand and furnace bottom ash generally have a high value of Poisson's ratio when compared with the coarse materials. However, the Poisson's ratio during repeated loading changes throughout the cycle. In Figure 6.23, which shows the hysteresis in secant Poisson's ratio over one load-unload, cycle for the FBA, it can be seen that the computed value of Poisson's ratio is sometimes close to unity where the effects of noise in the system are significant.

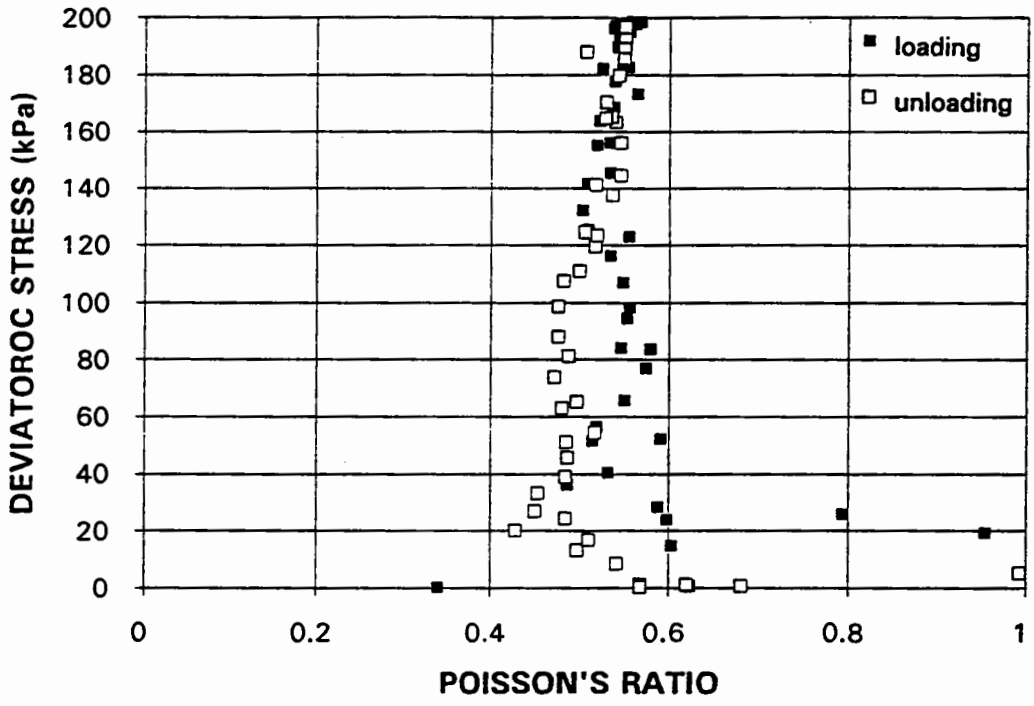

Figure 6.23. Secant values of Poisson's ratio during one cycle (FBA)

6.4.Effect of confining pressure on resilient behaviour

As well as causing deviatoric stress changes, a moving wheel load over the pavement causes a change in confining pressure within the pavement.

However, triaxial test apparatus currently used in many laboratories are unable to cycle cell pressure although the apparatus described in Chapter 3 is able to apply repeated applications of cell pressure. The effect of such repetitions on resilient properties will now be discussed. The results presented in Figures 6.24-6.27 are for the horizontal stress paths (Type 2) in Figure 5.5 which lie along the q=0 axis. Results given here are the peak values obtained from different stress applications for a certain material.

In theory, all the curves in Figures 6.24-6.27 should pass through the graphs' origins as the absence of a repeated cell pressure must be accompanied by zero strain. However, it is recognized that initial behaviour under tiny loadings may be atypical and that, in the lowest readings obtained, the errors in measurements will be more significant.

6.4.1. Axial strain

The axial strain increases as the cell pressure increases (Figure 6.24). The materials do not clearly show non-linear behaviour for the repeated cell pressure tests. The FBA may be slightly non-linear in its behaviour. It is interesting to note that the single-sized

FS obeyed Hooke's law whereas other materials diverge, even by a small amount, from a straight line response. It is interesting to note that the secant stiffnesses are all similar.

6.4.2. Radial strain

The radial strain also increases as the cell pressure increases (Figure 6.25) but this time the material clearly shows a non-linear behaviour, except for the FS. FS shows again a linearly elastic behaviour as did its axial strain response. Some other materials also show a linearly elastic behaviour but only at a low level of cell pressure. By comparing Figures 6.24 and 6.25 it can be seen that, for the same change in cell pressure, much larger radial strains were recorded than axial strain.

6.4.3. Shear strain

The shear strain increases (becomes more negative) as the repeated cell pressure increases but in a highly non-linear manner (Figure 6.26). Sand and gravel shows a fairly constant behaviour after passing 90 kPa change in cell pressure, gritstone shows a decrease in shear strain after the same stress level has been reached. SAG and SL show a similar reversal in shear stress development but at higher cell pressure levels. FS still continues to show a linearly elastic behaviour.

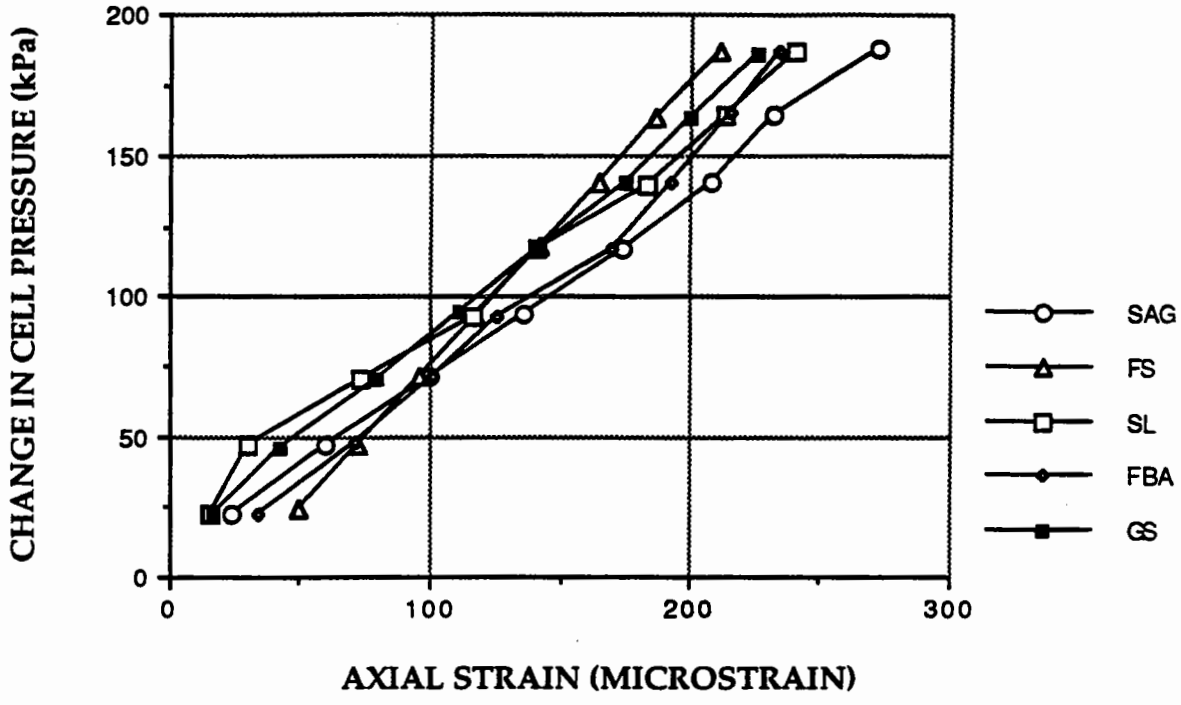

Figure 6.24. Peak values of axial strain at different cell pressure levels

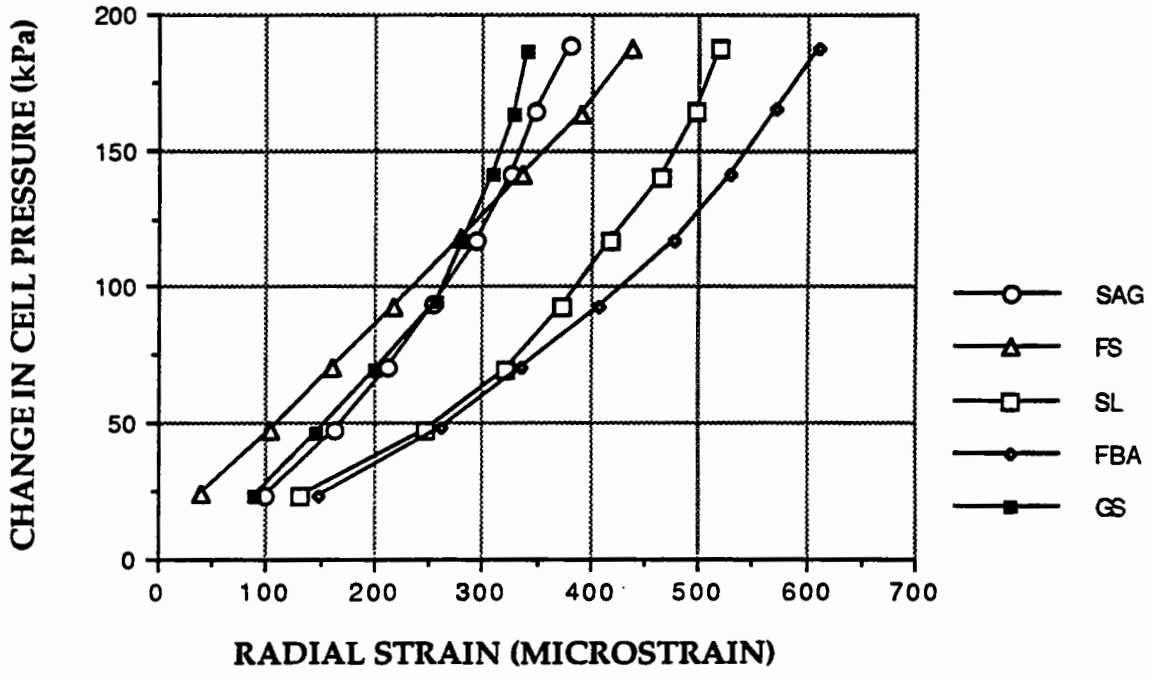

Figure 6.25. Peak values of radial strain at different cell pressure levels

When only the cell pressure is cycled, no shear strain should be observed if a material is isotropic. However, the results show that a considerable amount of shear strain resulted under the repeated cell pressure.

6.4.4. Volumetric strain

The volumetric strain also increases as the cell pressure increases (Figure 6.27). All materials showed a similar pattern to the strain measurements. The behaviour of materials is clearly non-linear except for the FS.

6.4.5.Behaviour under stress paths with constant non-zero deviatoric stress

In this section the results of the horizontal stress paths (q=constant), shown in Figure 5.5, are discussed. From this type of stress path, zero axial strain was observed at all levels of deviatoric stress. This must be due to a negative change in deviatoric stress while the cell pressure is cycled (Figure 6.28) although the intention was to keep the deviatoric stress constant. Hence no results are presented for the axial strain. It is thought that the load cell was, effectively, stretched by the cell pressure cycles due to "stiction" between the load cell shaft and the bushing in the cell thus causing a small unloading and no strain. As no intentional cyclic command signal was being provided

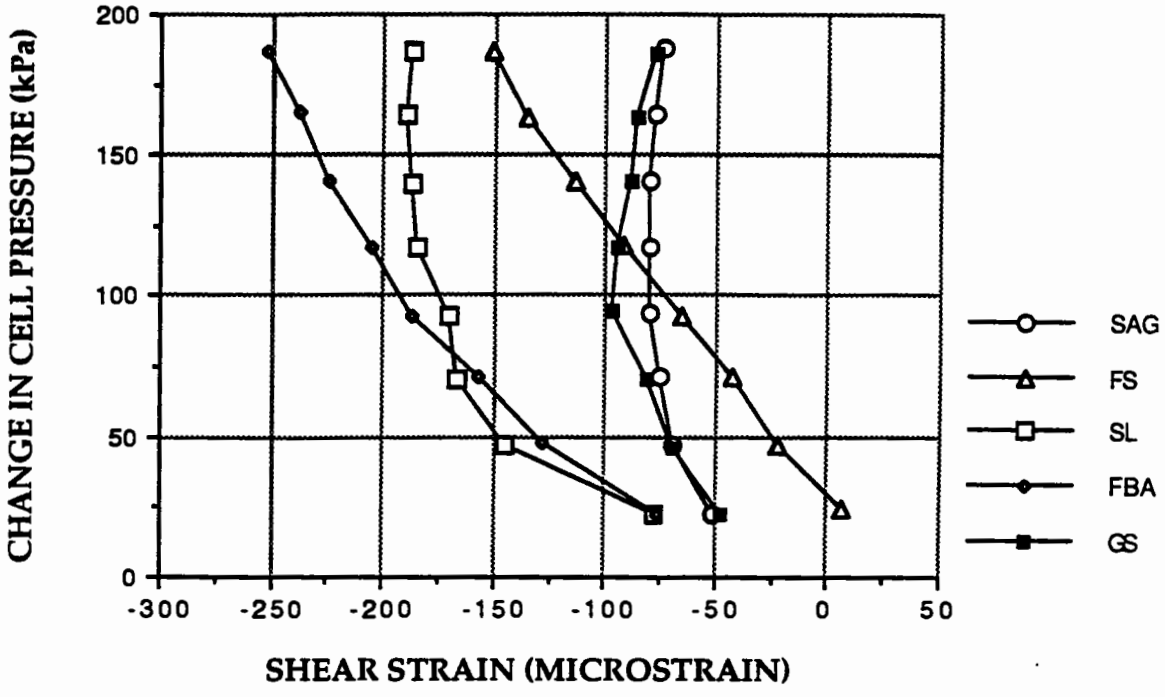

Figure 6.26. Peak values of shear strain at different cell pressure levels

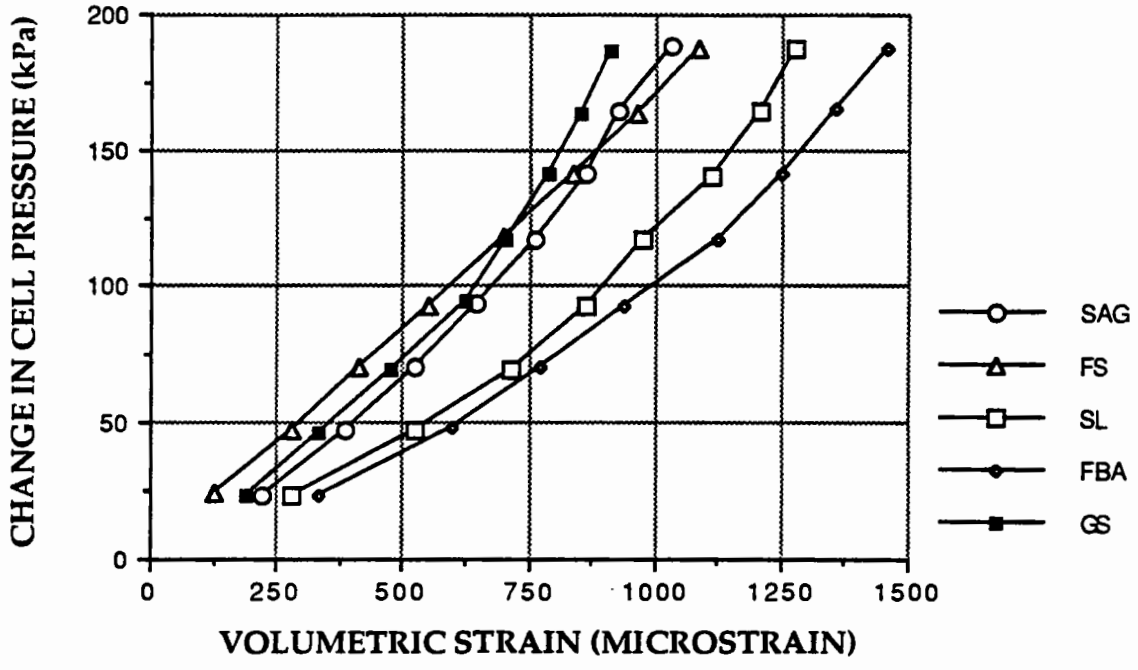

Figure 6.27. Peak values of volumetric strain at different cell pressure levels

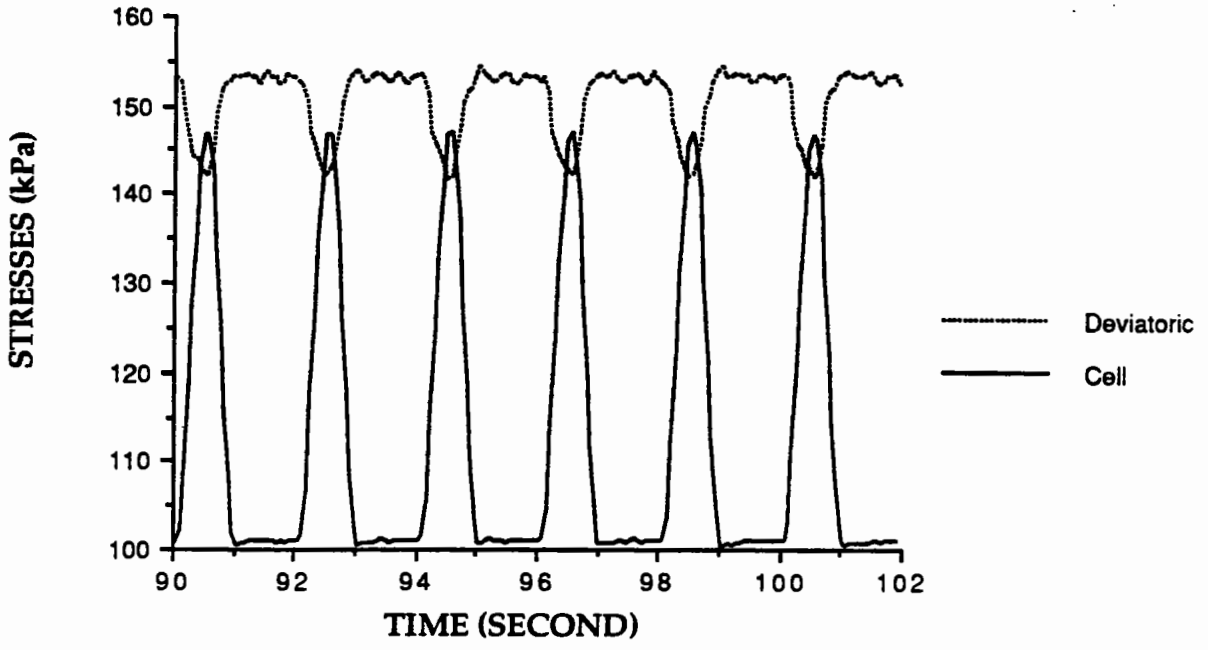

Figure 6.28. A typical stress application when attempting to provide constant deviatoric stress (SAG)

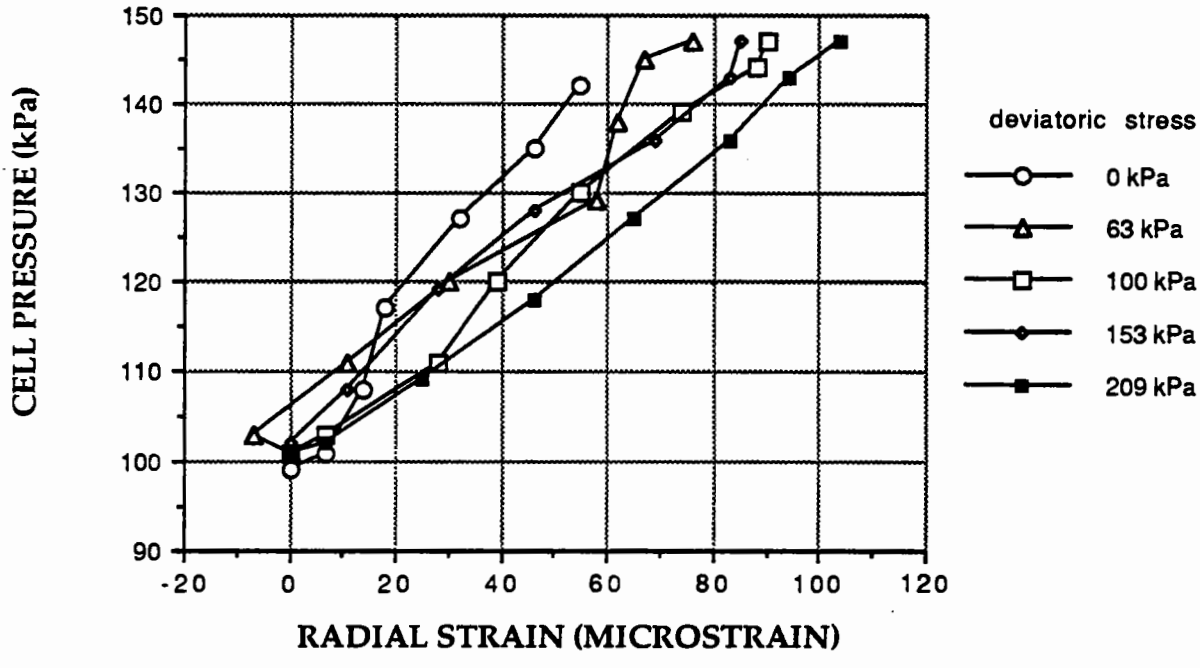

Figure 6.29. Secant radial strain during one loading cycle (SAG)

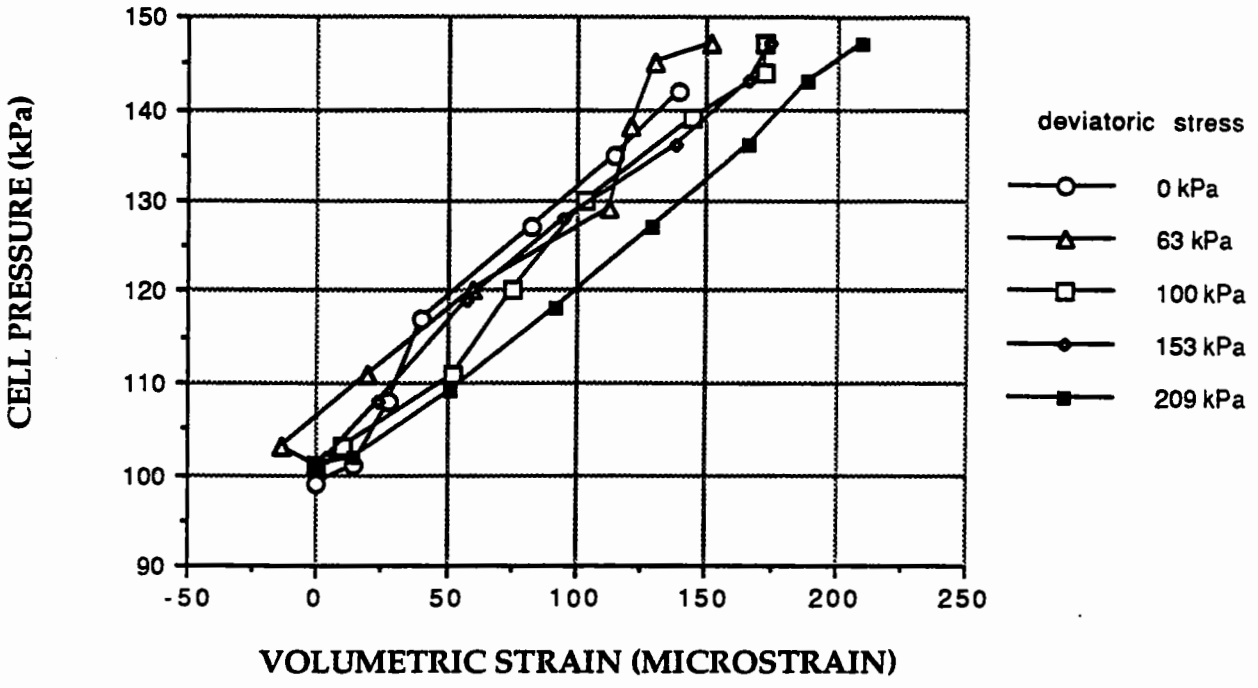

Figure 6.30. Secant volumetric strain during one loading cycle (SAG)

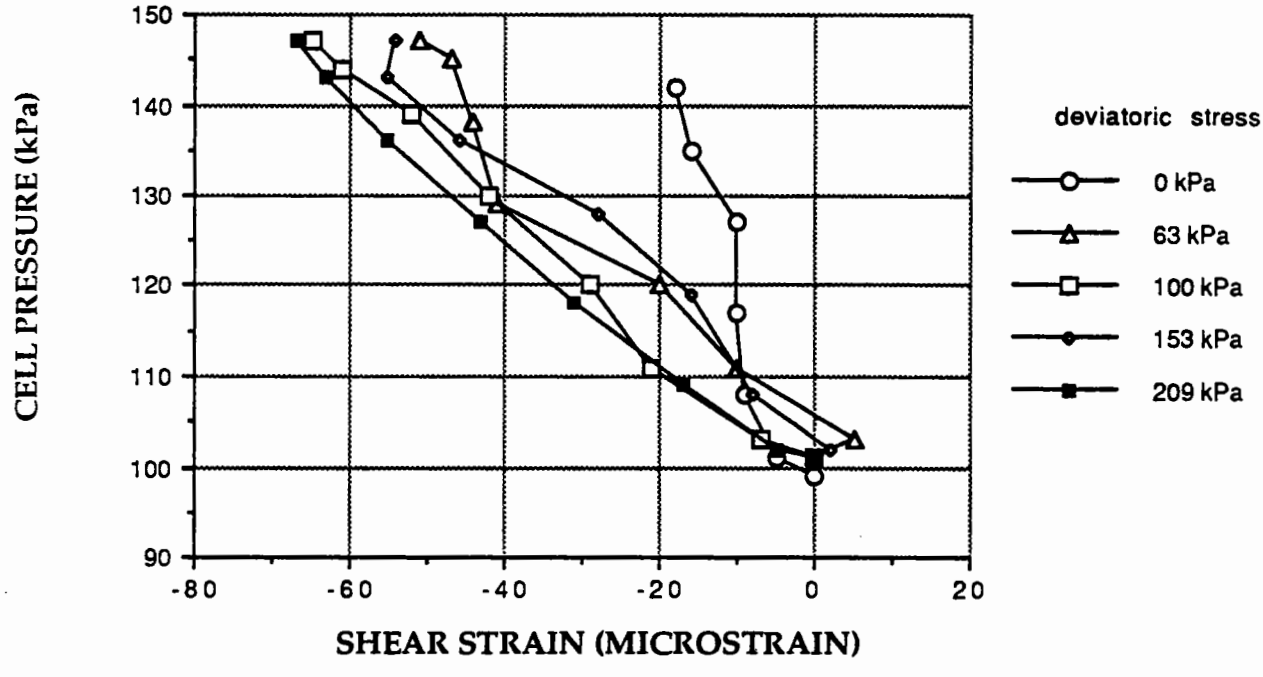

Figure 6.31. Secant shear strain during one loading cycle (SAG)

to the axial actuator the normal feedback loop was not available for the actuator to correct this unloading.

The results show that, as the cell pressure increases from 100 approximately 100 kPa the radial, volumetric and shear strains also increases at all levels of deviatoric stress (Figures 6.29, 6.30 and 6.31). It is interesting to note that, generally,

a) Strain response is linear with respect to magnitude of the cell pressure cycle,

b) The increase in strain due to increasing cell pressure is not affected by the level of deviatoric stress,

c) The highest strains are recorded for the highest deviatoric stress levels.

Observations b) and c) together suggest that non-linearity of response is limited to "bedding" or similar effects during the initial application of cell pressure only. Clearly these observations have to be made in the light of the inaccuracies in deviatoric stress applied and may not, therefore, be generally applicable.

6.5.Hysteresis behaviour of granular material under repeated loading

When granular material is subjected to repeated loading it does not follow the same path for loading and unloading cycles even when no (or negligible) plastic strain is

developed at the end of the stress application. Therefore, it creates an area between loading and unloading cycles which is called the hysteresis loop. This shows a measure of the energy dissipation within granular particles which may be due to destruction of edges, sound or heat energy. However, energy dissipation is mainly due to the non-linear characteristics of stress-strain relationships of granular material (Tatsuoka et al, 1978). In pavement engineering the term called "resilient" is used to mean that the stress-strain relationship produces a closed loop response rather than a loop with zero area (elastic) (O'Reilly and Brown, 1992).

As the load increases, the hysteresis loop becomes larger due to more energy consumption (e.g. Figure 6.32 and 6.33). The strong non-linearity of radial strain response during a repeated cell pressure cycle is particularly evident in Figure 6.33. Hysteresis loops obtained at low levels of strain have not got a smooth shape as compared with those at higher levels of strain (Figure 6.32). This may be due to the lower sensitivity of the measurement system at low values of measured strain.

The area of loop depends on the stiffness of the material in different directions and on the direction and the level of applied load. For instance, if an isotropic stress is applied to a sample of granular material, the largest hysteresis loop occurs in the volumetric strain direction as expected (Figure 6.34). Another example is that if deviatoric load is applied the largest hysteresis loop would occur in the axial and the shear strain directions (Figure 6.35).

Under vertical repeated loading granular material shows more non-linearity during unloading than the loading cycle (Figure 6.32). However, under isotropic stress the

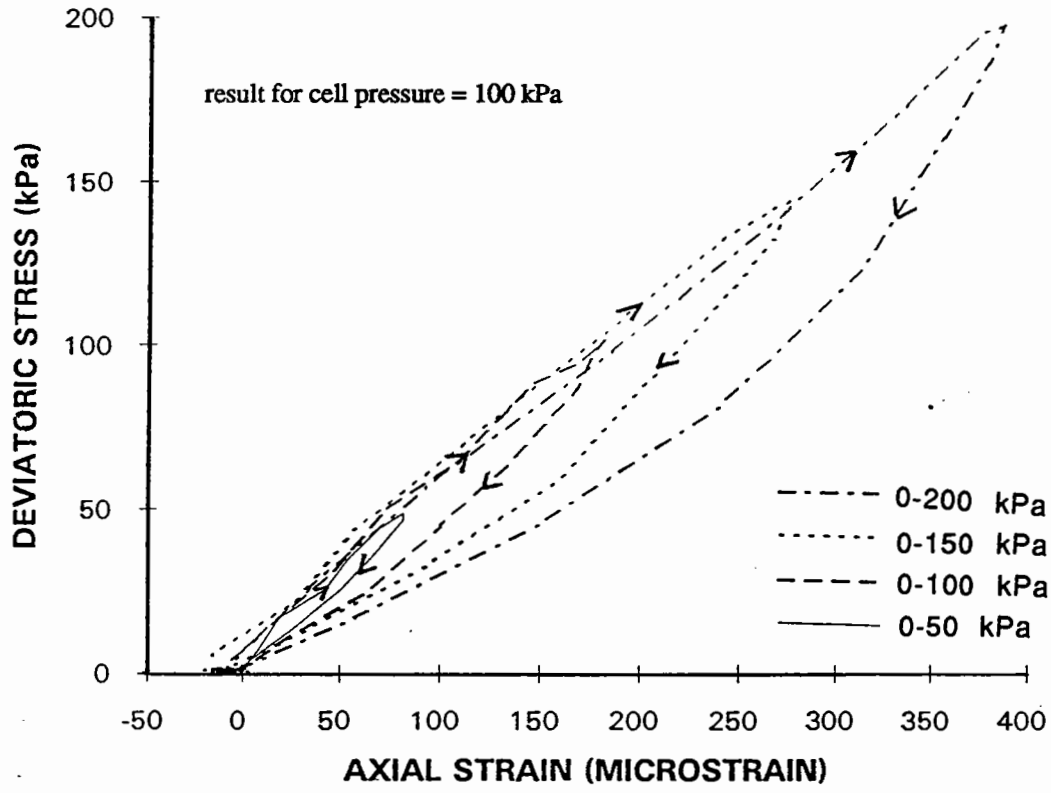

Figure 6.32. Axial strain hysteresis loops at different repeated deviatoric stress levels (FBA)

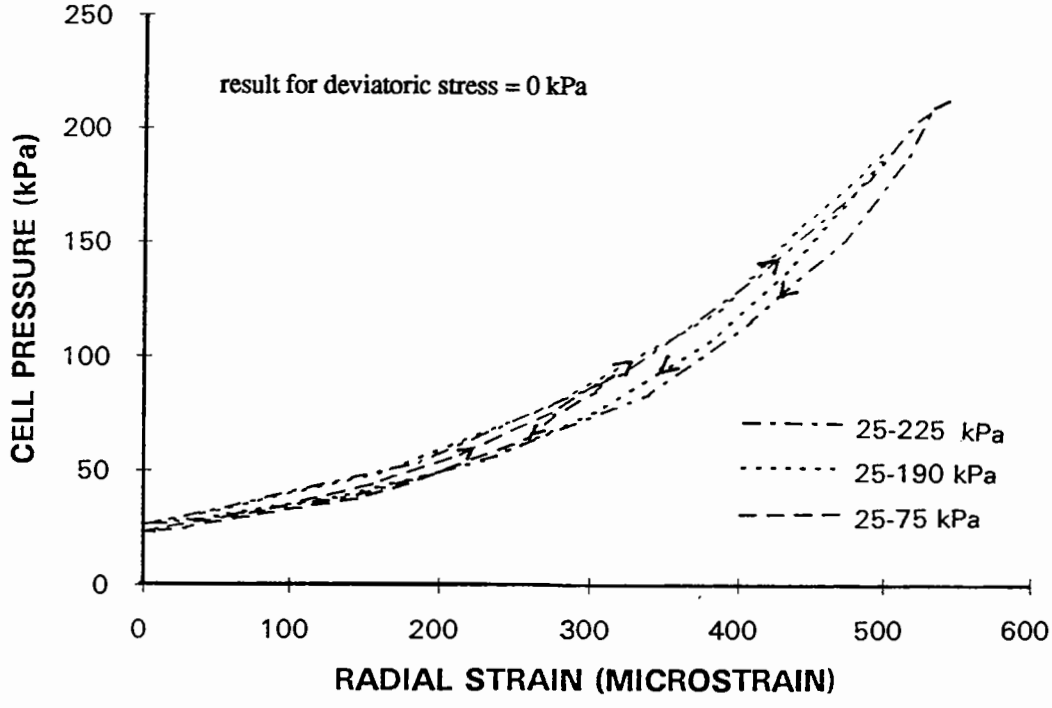

Figure 6.33. Radial strain hystresis loops at different repeated confining stress levels (FBA)

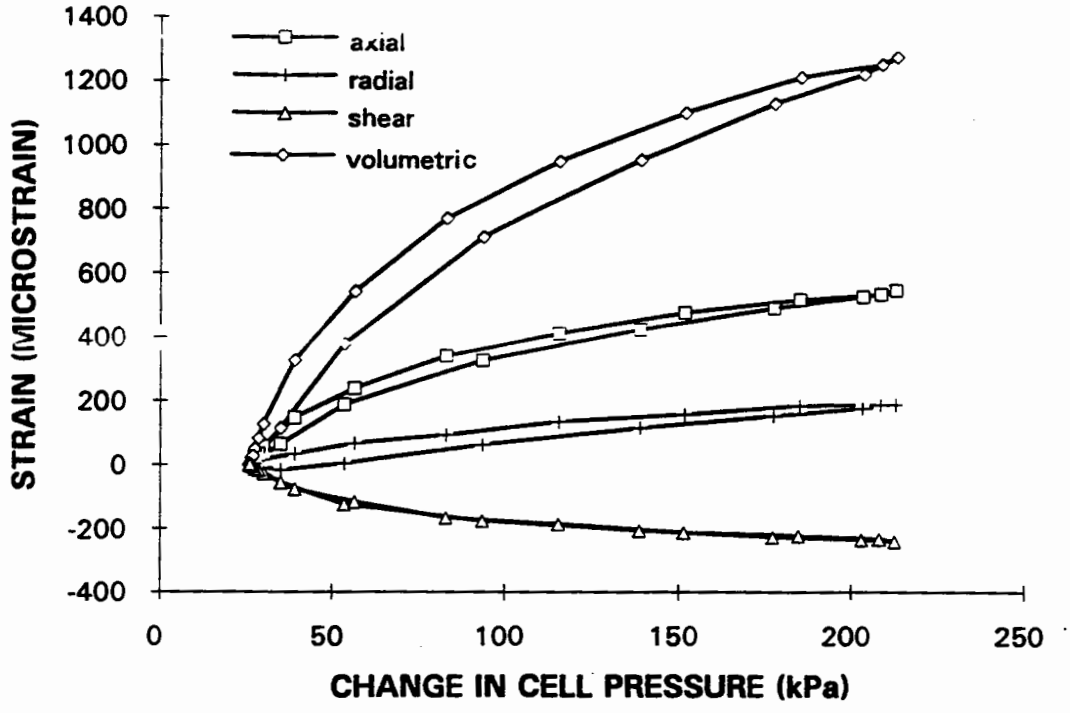

Figure 6.34. Hysteresis loops due to repeated cell pressure (FS)

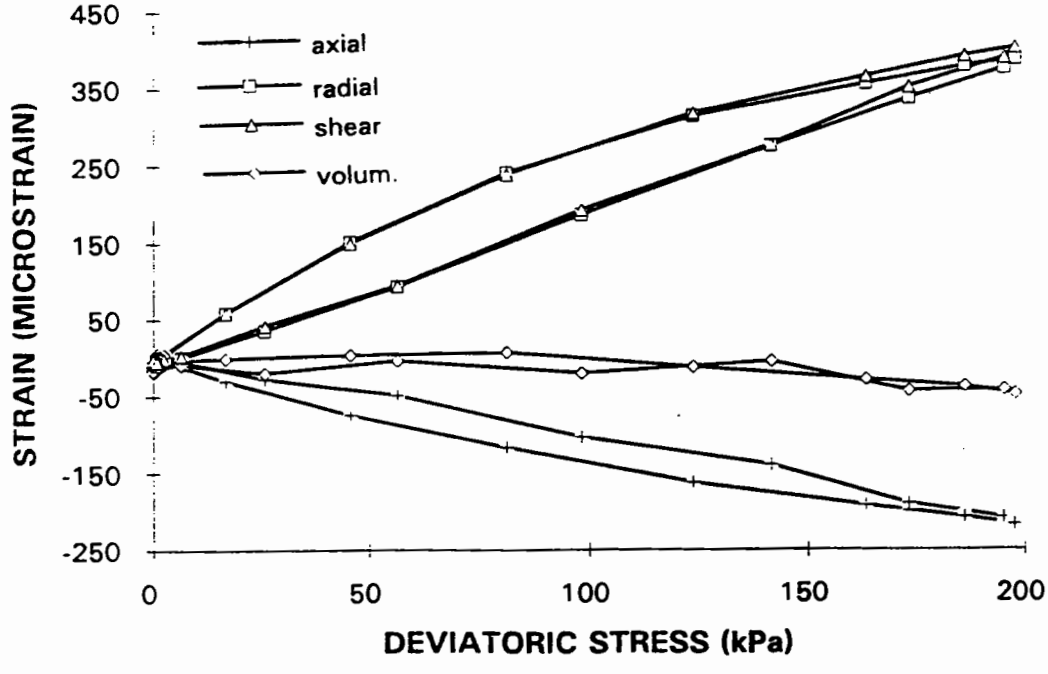

Figure 6.35. Hysteresis loops due to repeated deviatoric stress (FS)

material shows similar non-linear behaviour for both loading and unloading (Figure 6.33).

6.6. Behaviour of granular material under extension stress paths

To examine the behaviour of granular material in the extension stress zone (paths below the q=0 axis in Figure 5.5) a few stress paths were chosen entirely in the extension region as well as some partly in the extension and partly in the compression region. The granular materials behaved in the same way as under simple compression paths but showed slightly higher axial and radial strains.

Figure 6.36 and 6.37 shows a comparison of typical absolute values of strains obtained from compression and extension tests. In each case the fully compressive path yields the stiffest material and in most cases the fully extension path gives rise to the softest material. These figures are only typical examples to show that granular material has some strength in extension at low stress levels. However, the test results do not give information at high extension levels where very low stiffnesses are expected. Nevertheless the results illustrate the reduction in stiffness associated with stress paths in Figure 5.5 which went closest to failure.

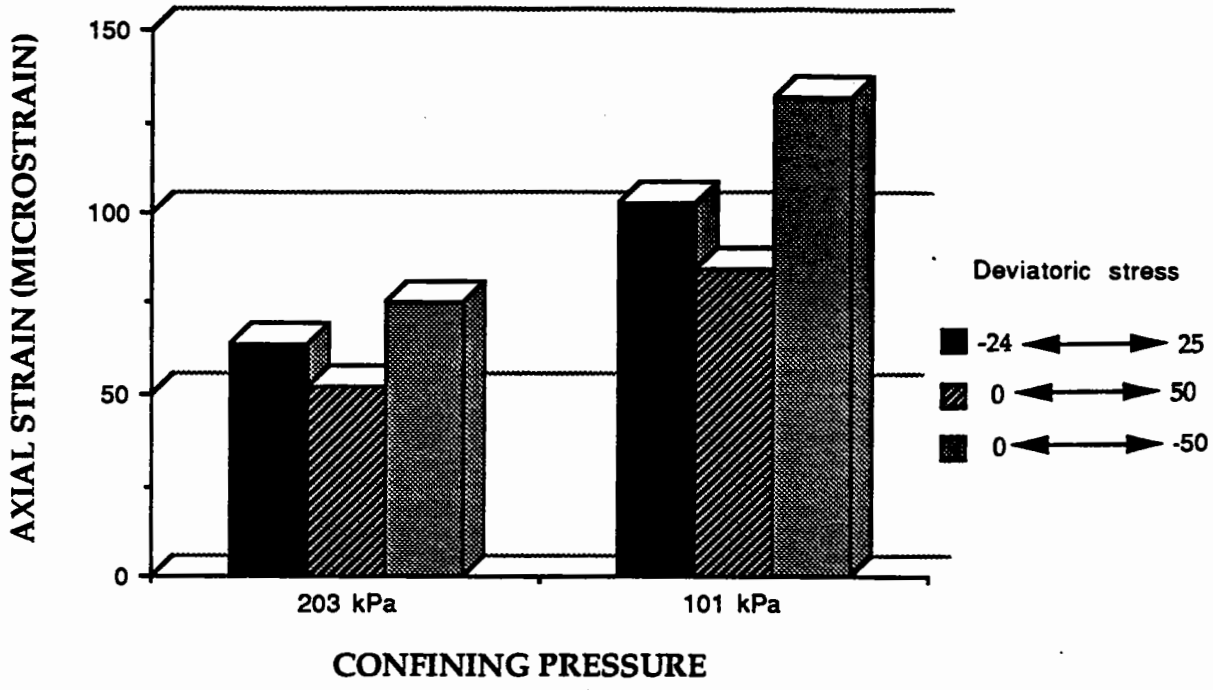

Figure 6.36. Axial strain comparisons (FBA)

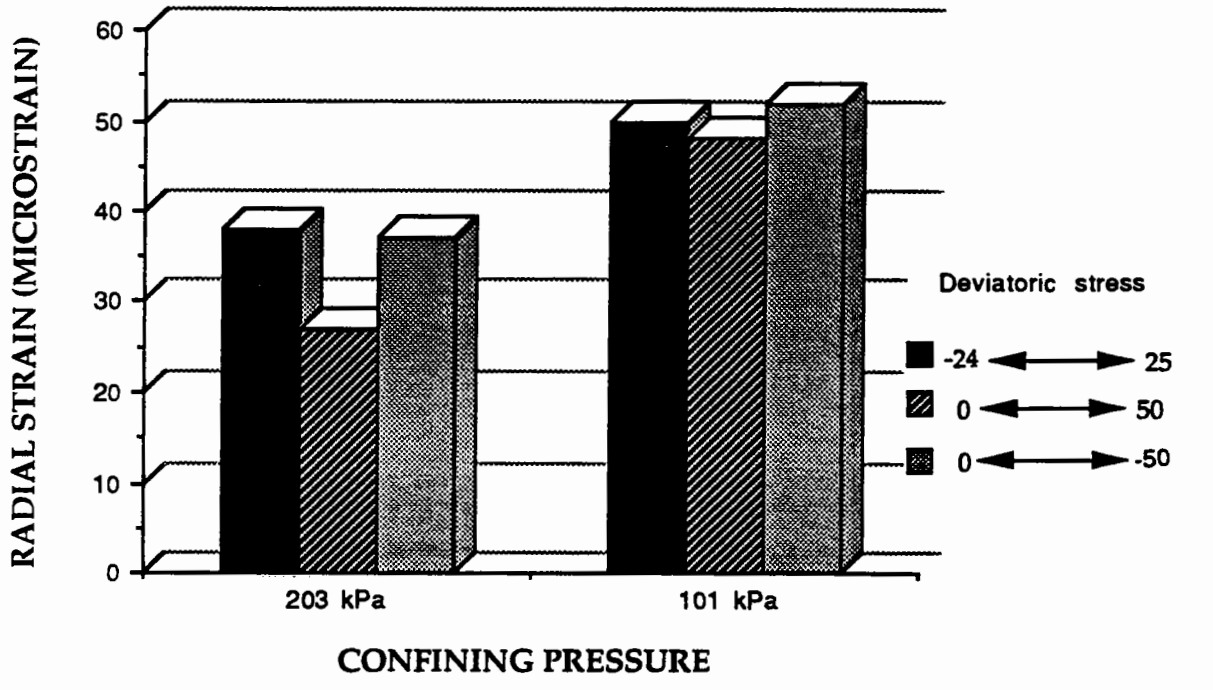

Figure 6.37. Radial strain comparisons (FBA)

In these figures linear extrapolation has been used to normalize the results which were obtained at slightly different repeated stress magnitudes.

6.7.Anisotropy

Anisotropy in granular layers has often been thought to be unimportant and thus neglected, perhaps because the equipment necessary to investigate anisotropy has not usually been available. In the last twenty years studies of anisotropy have been made (Saada, 1988) using traditional triaxial equipment with tilted samples, cubic triaxial samples and the hollow cylinder apparatus.

In the following sections anisotropy is plotted as the ratio $\varepsilon_a/\varepsilon_r$ (Biarez and Hicher, 1988). An isotropic materal therefore has an anisotropy value of unity. Thus a highly anisotropic material has a low anisotropy value.

6.7.1.Occurrence of anisotropy in a granular layer

In naturally occurring soil deposits, grains are sedimented under a gravitional force in such a way that nonspherical grains are situated with their long sides perpendicular to the direction of the gravitional force. As a result of this orientation the soil usually has

a higher stiffness in the vertical direction than in the horizontal direction. However, in the granular layer of a pavement construction the situation is slightly different. Granular layers in the pavement (either base or sub-base) are compacted to achieve a maximum density so that they can provide adequate support and reduced surface deflection. During the compaction process the layer will almost certainly become anisotropic due to the vertical compactive load applied to it. The layer will then be expected to be stiffer vertically than horizontally. Three different forms of anisotropy in a granular layer (particularly for highway construction) will be discussed in the following sections. They are inherent, stress-induced and stress-history-induced anisotropy.

6.7.2.Inherent Anisotropy

In highway construction, granular material is generally obtained from a local quarry such that it satisfies a specification and is brought to site and spread over the subgrade layer. Subsequently a suitable vibrating roller compacts the granular layers in order to achieve an appropriate density. It is implicitly assumed that a material with an adequate density and which meets the specification will have an acceptable stiffness. This will then permit the layer to spread traffic loading which is applied at a much higher stress level than the subgrade layer could support. The roller compacts a layer in the vertical direction. As a consequence the layer is expected to be stiffer in this direction than in the horizontal direction. Put another way, under the same stress conditions the layer will deform more in the horizontal direction than in the vertical direction under the same imposed stress in the given direction.

A definition of inherent anisotropy has been proposed as follows: "The inherent anisotropy is defined as a physical characteristic inherent in the material because of the formation of its original structure under the gravitional field" (El-Sohby and Andrawes, 1972). For pavement engineering purposes the same definition of inherent anisotropy can be adopted for a compacted layer except that the imposed compaction must be added to the gravitational cause.

6.7.3.Stress-induced anisotropy

Stress-induced anisotropy is defined as a physical characteristic of a soil due to only the strain associated with an applied stress (Arthur et al, 1977). Alternatively, the change of moduli with applied stress may be considered as a measure of stress-induced anisotropy (Chang et al, 1992). Consider an isotropic material which shows isotropic behaviour under isotropic test conditions. However, when the stress is anisotropic, in other words it is no longer the same in all directions, the material will no longer strain isotropically. Therefore, contact points move apart and new contact points occur. However, when the stress is removed the contacts will return to the original structure as long as the strain is resilient. As the contact points change it is likely that the material's stiffness will also change.

If a granular layer in a pavement structure is considered, stress-induced anisotropy is experienced as a resilient change in granular layer structure due to the passage of a vehicle.

6.7.4.Stress-history induced anisotropy

Once compacted, the granular layer supports the construction of the upper layers of the pavements. The construction traffic mainly consists of heavy vehicles which cause large amounts of recoverable (elastic) and some irrecoverable (plastic) deformation. During plastic deformation some contacts between grains disappear, some particles could break, some particles slide relative to one another and some new contact points may develop. Whilst undergoing plastic strain, the fabric of the layer changes. As a result the inherent anisotropy which existed before trafficking has changed. Therefore, the deformation characteristics of the granular layer before repeated trafficking and afterwards will not be the same.

Stress-history-induced anisotropy for pavement engineering can thus be defined as the change in inherent anisotropy caused by the repeated application of traffic loading in a granular layer. It is a similar definition to that given by Oda and Sudoo (1989) although they gave it an inappropriate term (see Chapter 2). Clearly other forms of stress-history-induced anisotropy also exist (for example, change in inherent anisotropy after anisotropic consolidation of clay soils) but these are beyond the scope of this thesis. The stress-induced anistropy may also change, of course, and thus needs to be redefined after permanent deformation has taken place.

6.7.5.Discussion of anisotropy test results

Inherent, stress-induced and stress-history-induced anisotropy will be discussed separately. For the discussion, the results obtained for a wide range of repeated cell pressures starting from 25 kPa and rising to 225 kPa was chosen. However, for the comparison of inherent and stress-history-induced anisotropy the results obtained from all materials are presented. But limited test results are given for the stress-induced anisotropy since, for various reasons, incomplete data was avalable from the tests. Anisotropy testing was not carried out succesfully on GWRS so no results are presented for this material in the following sections.

6.7.5.1.Inherent anisotropy

When granular material is loaded it shows more inherent anisotropy than when it is unloaded (for example Figure 6.38). At low levels of isotropic stress significant anisotropy was observed (low values of $\varepsilon_a/\varepsilon_r$ in Figure 6.38). The anisotropy decreases as the isotropic pressure increases. For unloading the material initially behaves more isotropically, however it reverts to its highly anisotropic characteristics on subsequent reloading. Peak values of anisotropy for different materials are shown in Figures 6.39, 6.40, 6.41, 6.42 and 6.43- values calculated from the measured resilient strains over the full stress cycle. SAG, GS and FBA shows an asymptotic value as the change in cell pressure increases. SL and FS become more close to isotropic behaviour as the change in cell pressure increases. The most anisotropic material was FBA whereas the least one was FS. GS, SAG and FBA show a non-

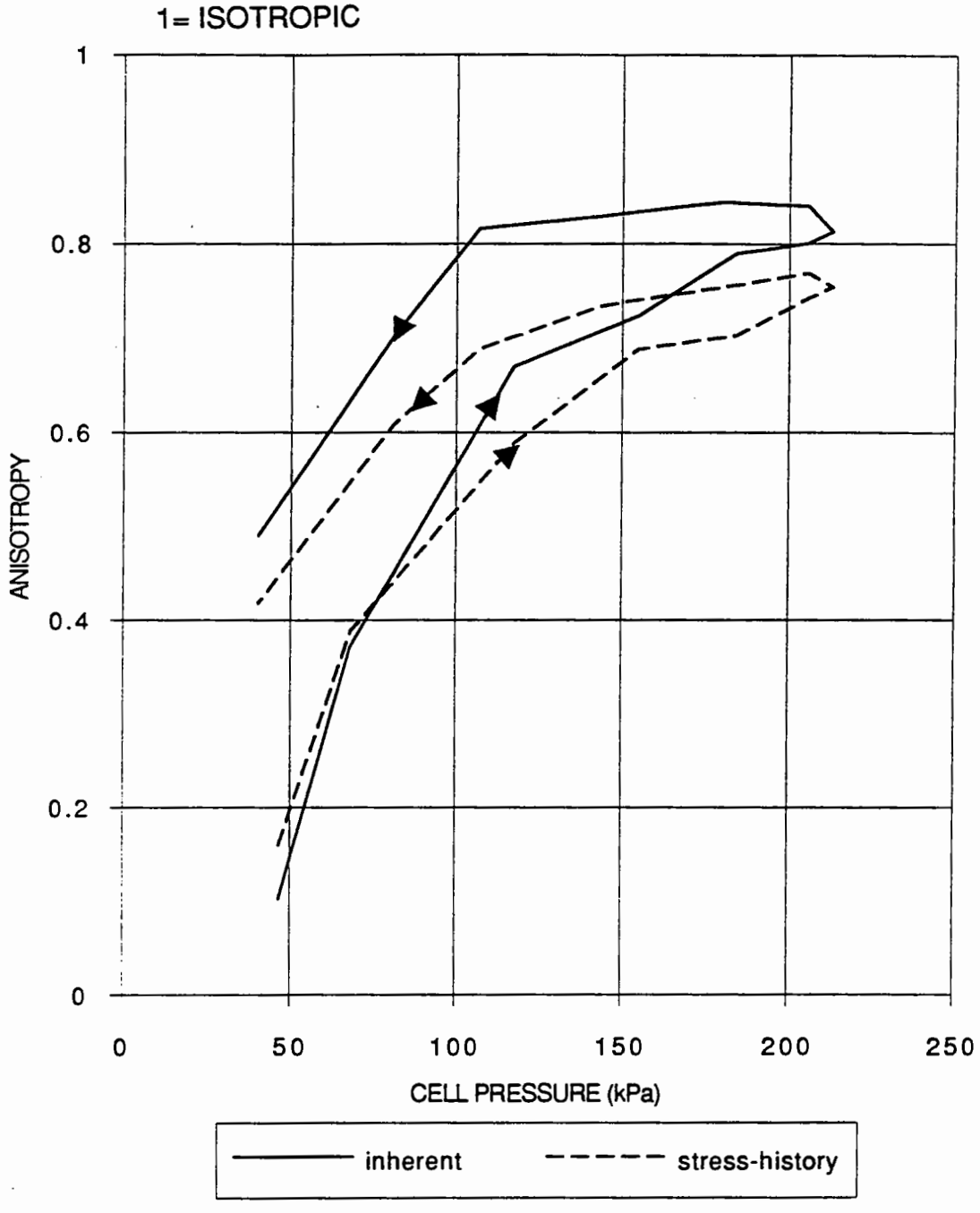

Figure 6.38.Change in anisotropy during a cycle (FS)

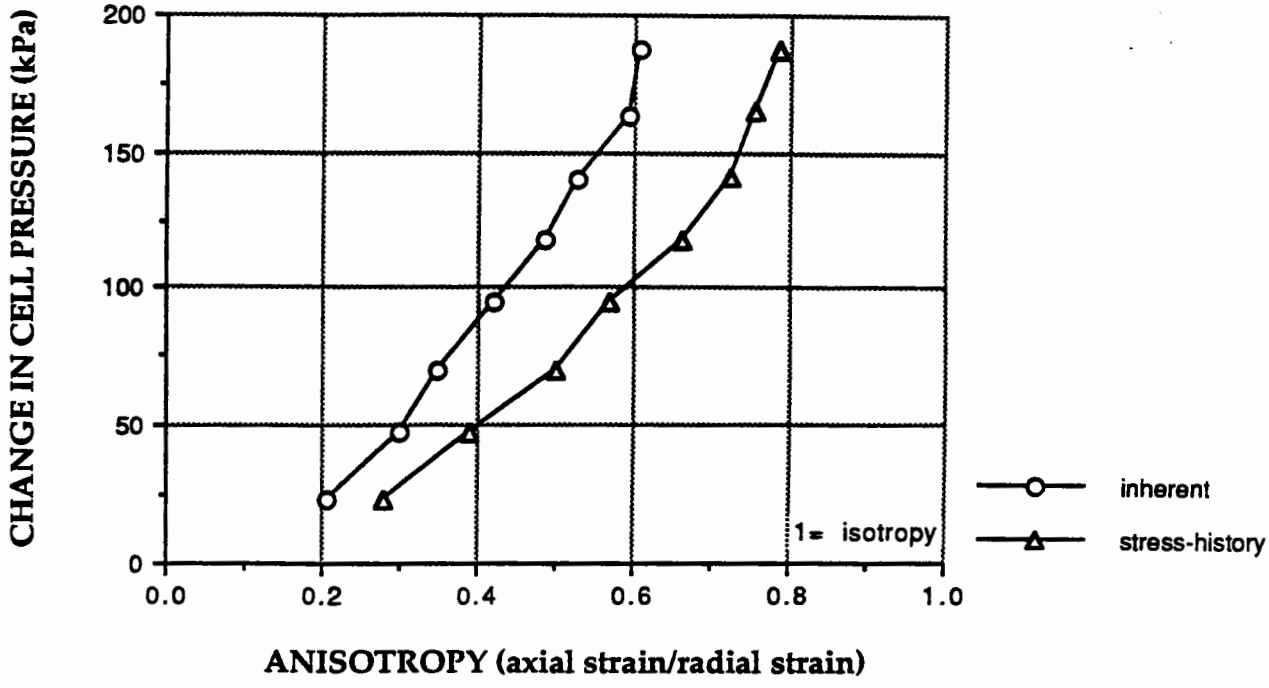

Figure 6.39. Peak values of anisotropy at different cell pressure levels (GS)

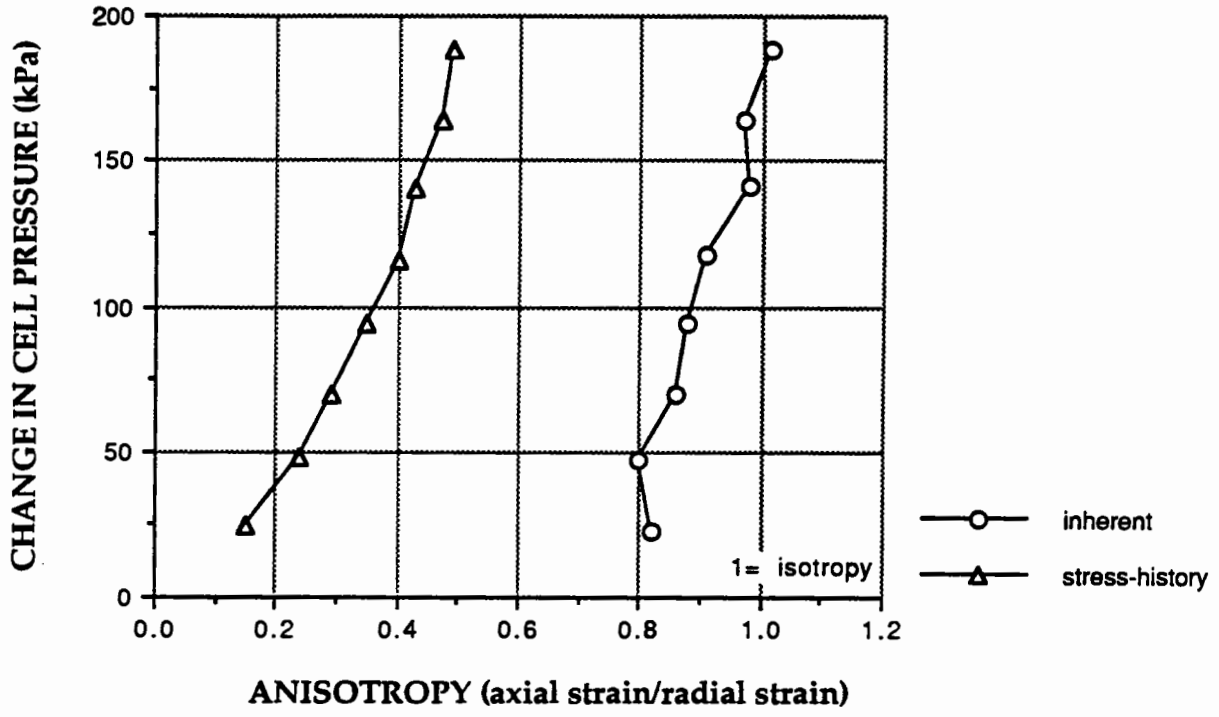

Figure 6.40. Peak values of anisotropy at different cell pressure levels (SAG)

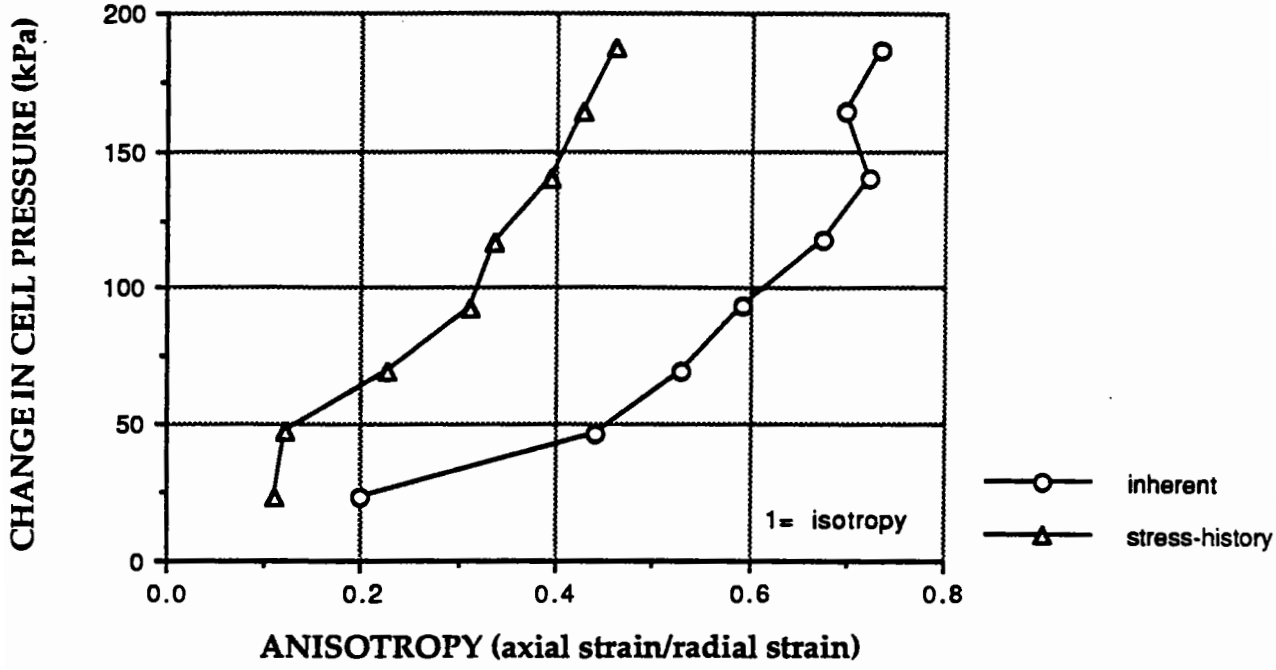

Figure 6.41. Peak values of anisotropy at different cell pressure levels (SL)

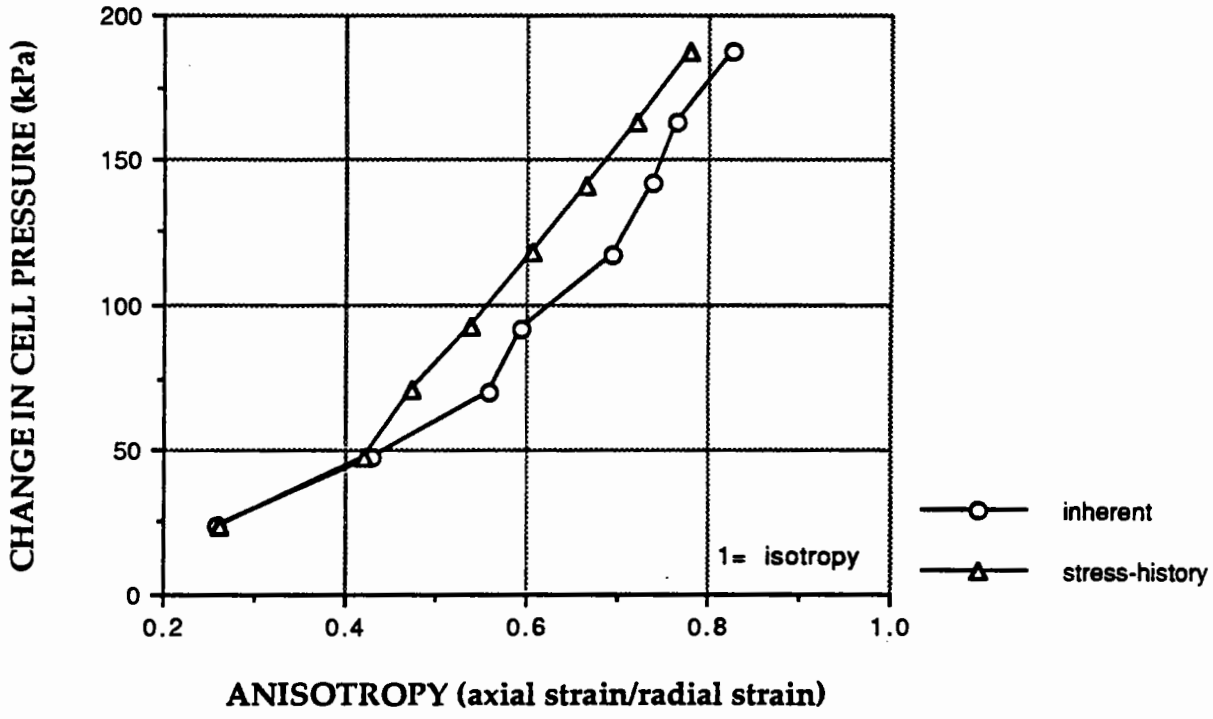

Figure 6.42. Peak values of anisotropy at different cell pressure levels (FS)

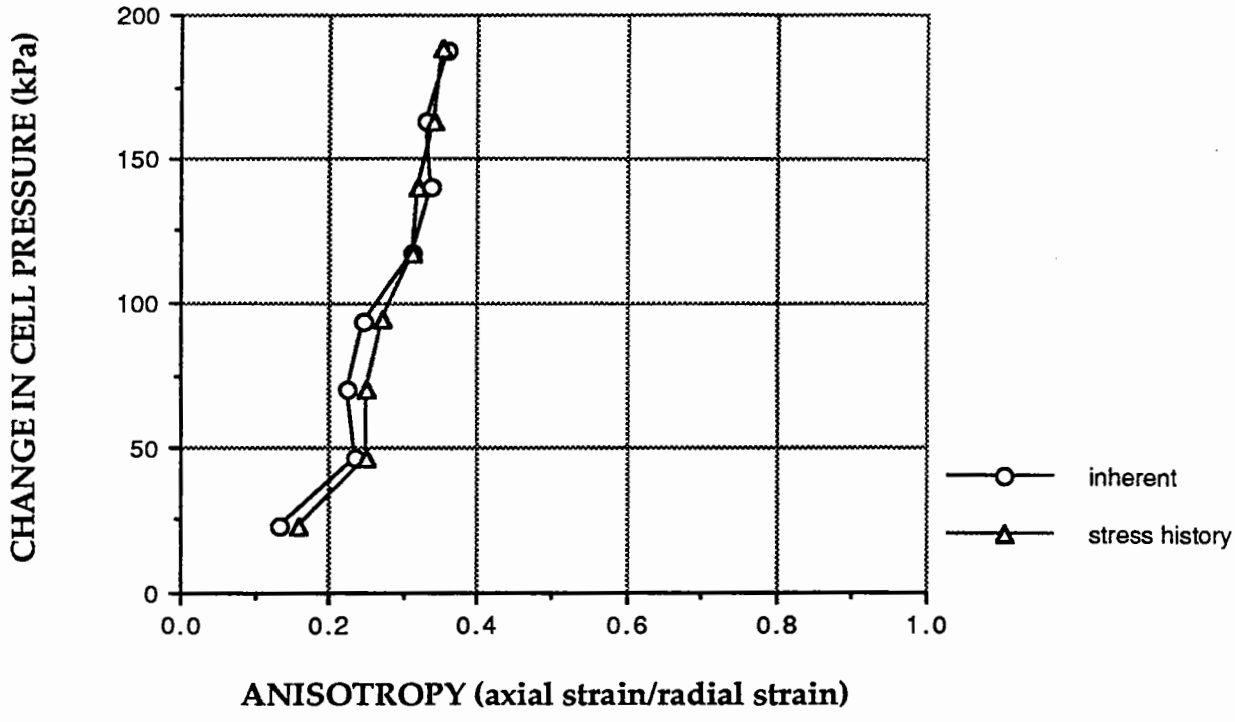

Figure 6.43. Peak values of anisotropy at different cell pressure levels (FBA)

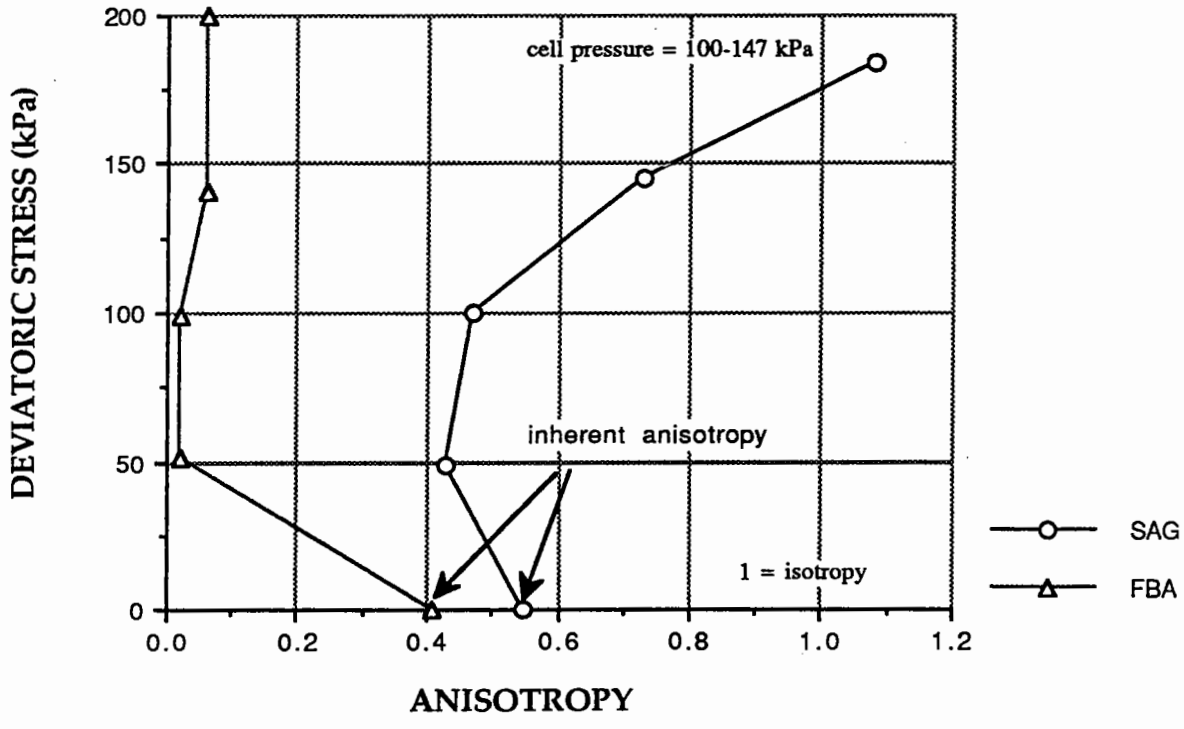

Figure 6.44. Stress induced anisotropy

linear relationship between the change in cell pressure and anisotropy. However, SL and FS tend to show a linear relationship although it is not smooth.

In summary, at low levels of stress similar to those experienced by the granular layer in a pavement under traffic loading, inherent anisotropy is not negligible and should be considered in modelling.

6.7.5.2.Stress-induced anisotropy

In order to see the effect of anisotropic stress, in this case deviatoric stress, on inherent anisotropy in granular material, a limited number of tests were carried out. First only the cell pressure was cycled from 100 to 147 kPa without deviatoric stress to measure the inherent anisotropy. Subsequently both the deviatoric stress (starting from 0 and rising to 200 kPa in increments of 50) kPa and the cell pressure (which was unchanged) were cycled at a frequency of 1Hz.

During the application of a deviatoric stress cycle the inherent anisotropy will change (Figure 6.44). It was observed that the FBA became more anisotropic as the deviatoric stress increases. However, the anisotropy in SAG increased as the deviatoric stress level increased to 50 kPa, but as the deviatoric stress increased still further it became more isotropic. In order to construct Figure 6.44, a number of assumptions were required since two Young's moduli and two Poisson's ratios are needed to interpret the test results. It is possible to determine Young's modulus and Poisson's ratio due to

vertical load using repeated deviatoric test results with constant cell pressure. After determining these two constants, Young's modulus and Poisson's ratio due to horizontal load can then be found from Equation (7.60) using data obtained from testing under repeated both stresses.

6.7.5.3.Stress-history-induced anisotropy

After a permanent strain test, the structure of the granular layer is probably altered, the density of the layer is increased (i.e. the voids in the structure have decreased), so particles comes closer to each other.

At low stress levels a high inherent anisotropy, now termed the stress-history-induced anisotropy to distinguish from the original values, was again obtained (Figure 6.39, 6.40, 6.41, 6.42 and 6.43). However, for loading and unloading conditions, the anisotropy is closer when compared with the original anisotropy. To illustrate the change in anisotropy only one cycle was chosen (Figure 6.38). It shows again that the anisotropy decreases with increasing isotropic stress. Anisotropy in the sample when being unloaded, although still high (a small number), was less than that under loading.

The granular material behaviour generally becomes more anisotropic after many stress applications (Figure 6.39, 6.40, 6.41, 6.42 and 6.43). Clearly, plastic strain in the pavement caused by traffic loading alters the inherent anisotropy.

Fontainebleau sand also experienced only a small change in anisotropy after the permanent strain compared with other coarser materials (Figure 6.42). It was this material which showed the least non-linearity in its stress-strain behaviour (see Section

6.4). Coarse materials such as gritstone, sand and gravel and soft limestone showed larger changes in anisotropy after the permanent strain test (Figure 6.39, 6.40 and 6.41). Sand and gravel, in particular, was, initially, an almost isotropic material (Figure 6.40). However, after the permanent strain test it showed the highest change in anisotropy. Furnace bottom ash did not show a considerable change in anisotropy after permanent strain test although it had the highest inherent anisotropy among the materials tested.

6.7.5.4.Summary of anisotropy test results

In summary, different materials showed different anisotropic characteristics under the same testing procedure. This indicates that anisotropy is probably affected by many factors such as mineral type, particle shape, density and grading. The results reveal that it is quite difficult to establish a pattern for change in anisotropy. Nevertheless, it would appear that materials containing more fine material do not seem to be less sensitive to change in anisotropy than the coarse materials.

6.8.Behaviour under stress paths with cyclic axial and radial stresses

In this section the results of stress paths which are dashed vertical and inclined lines in Figure 5.5 are discussed.

6.8.1.Behaviour when stresses give constant mean normal stress

The results discussed in this subsection are those measured under stress paths in which the deviatoric stress compresses the sample while the cell pressure decreases (dashed vertical lines (Type 3a) in Figure 5.5). Thus these stress paths may be used to assess the effects of resilient dilation. Volumetric strain is a direct measure of shear effects at constant mean normal stress.

The main intention of this type stress path was to detect inelasticity. A perfectly elastic soil will have zero volumetric strain when there is no change in mean normal stress. The shear strain took the highest magnitude followed in turn by axial, radial and volumetric strain (Figure.6.45 and 6.46). Although the magnitude of the volumetric strain is the smallest, its magnitude increases as the deviatoric stress is increased with constant mean normal stress.

The ratio of radial to axial strain takes higher values at low level of deviatoric stress and decreases as the deviatoric stress increases (Figure 6.47). However, the trend is not smooth. This may be due to instrumentation error. For different levels of p the same observation was also observed (Figure 6.48). It is interesting to note that the strain ratio took similar values at different values of p when the deviatoric stress is high (Figure 6.48). This may show that after a certain level of the deviatoric stress the importance of the mean normal stress on this ratio is not significant.

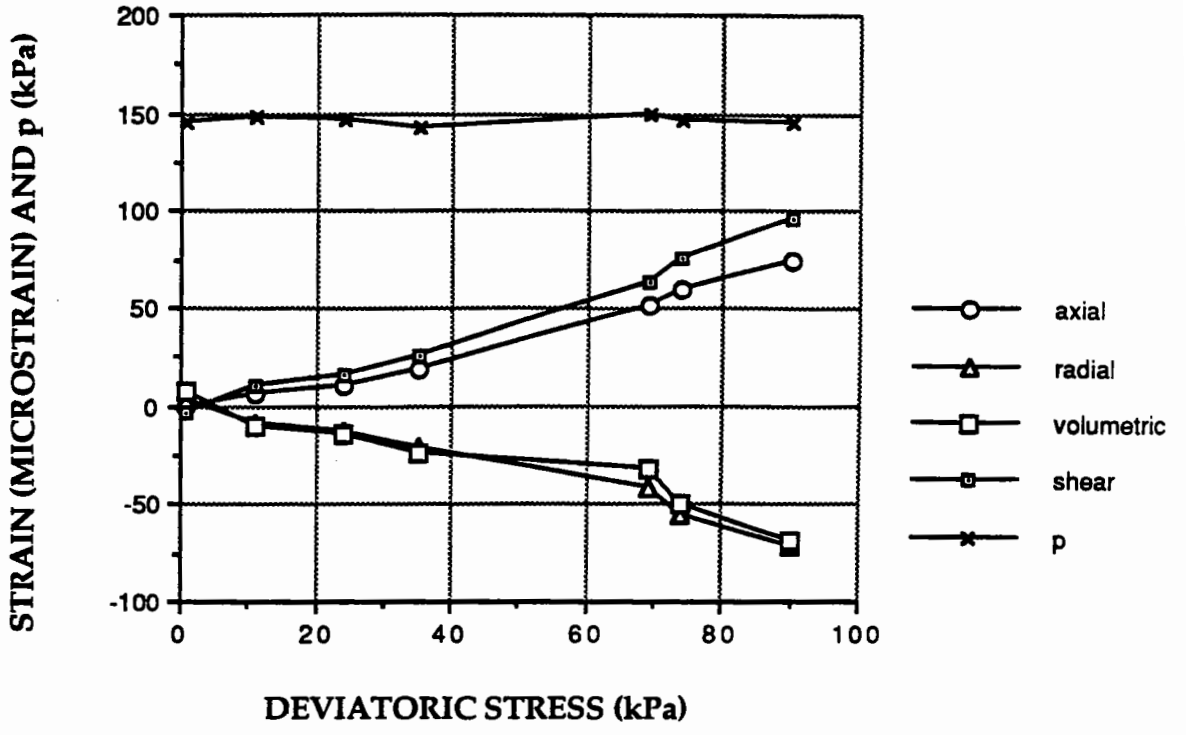

Figure 6.45. Cyclic both stresses with constant p (GS)

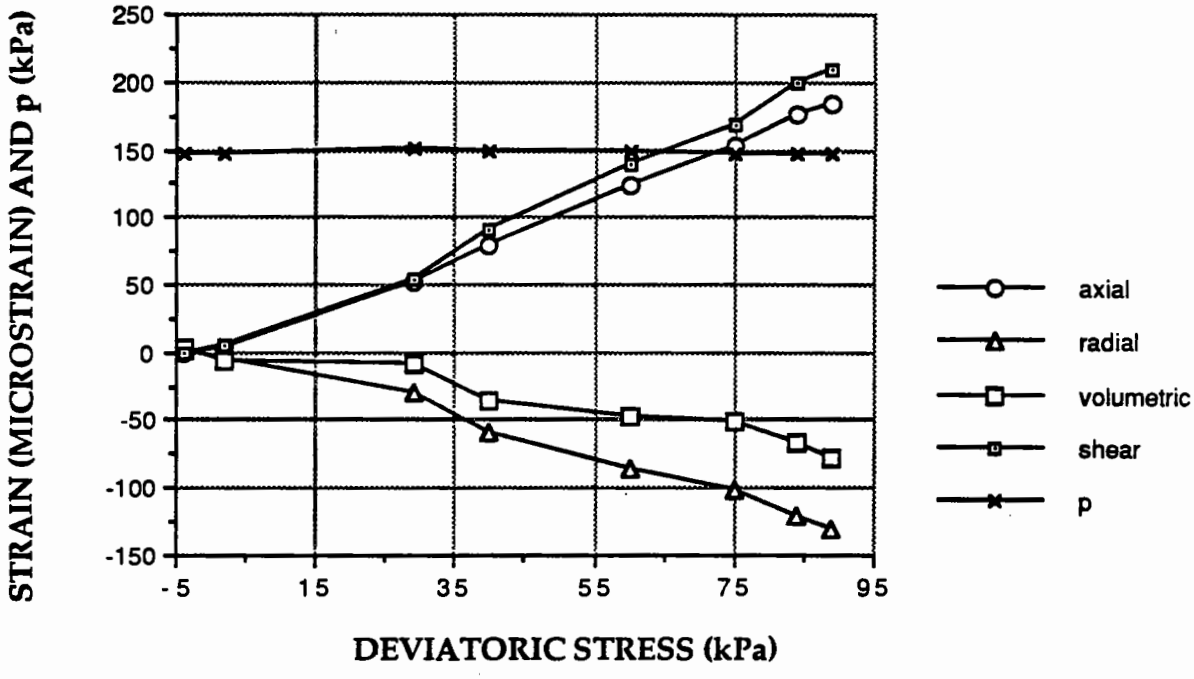

Figure 6.46. Cyclic both stresses with constant p (FS)

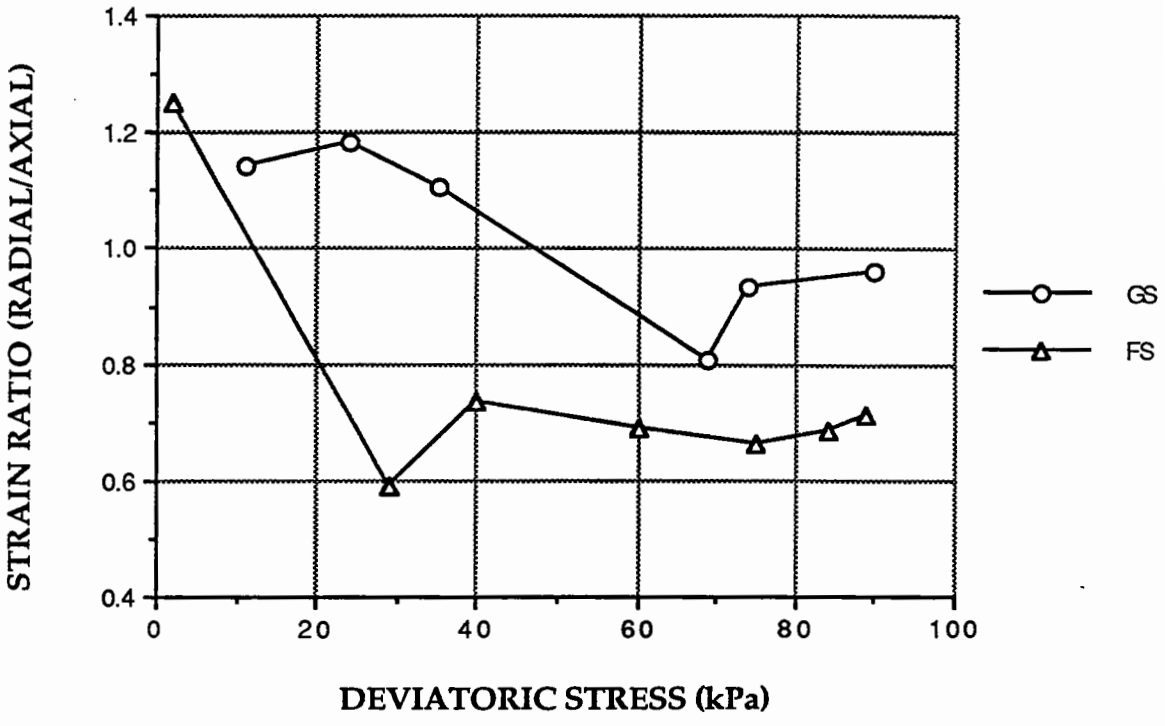

Figure 6.47. Secant strain ratio when both stresses cycled with constant p

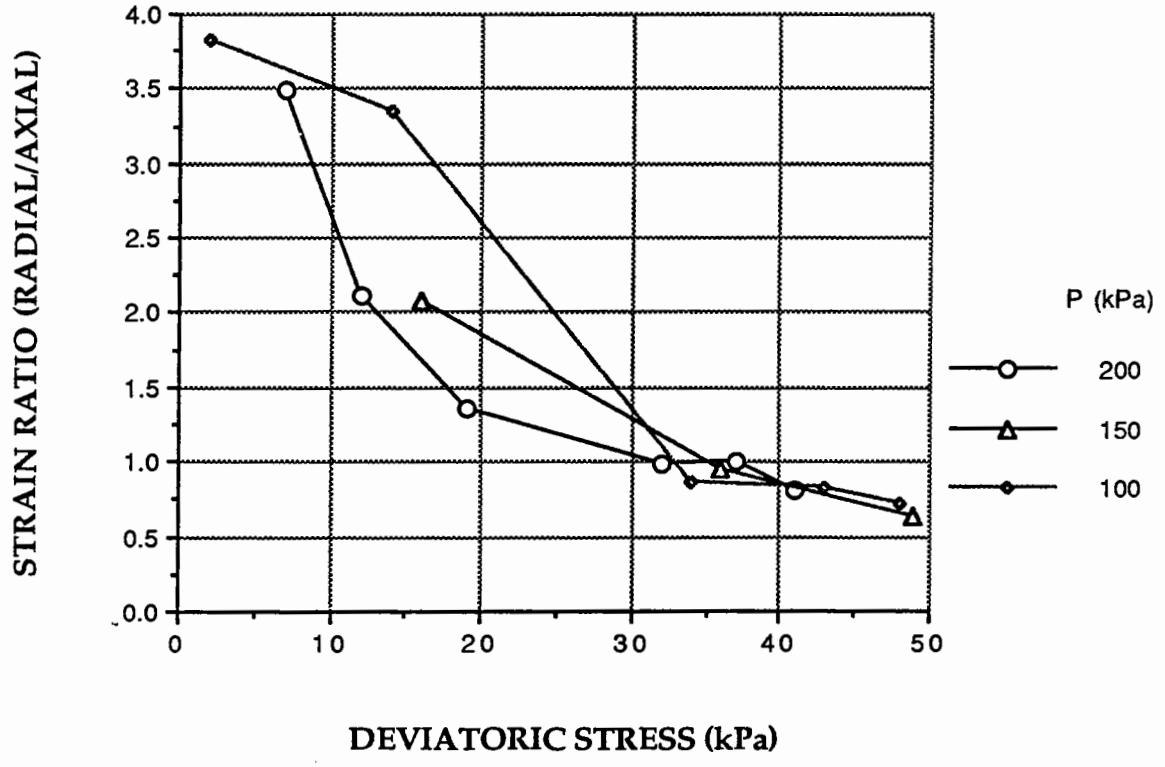

Figure 6.48. Secant strain ratio with constant p (FS)

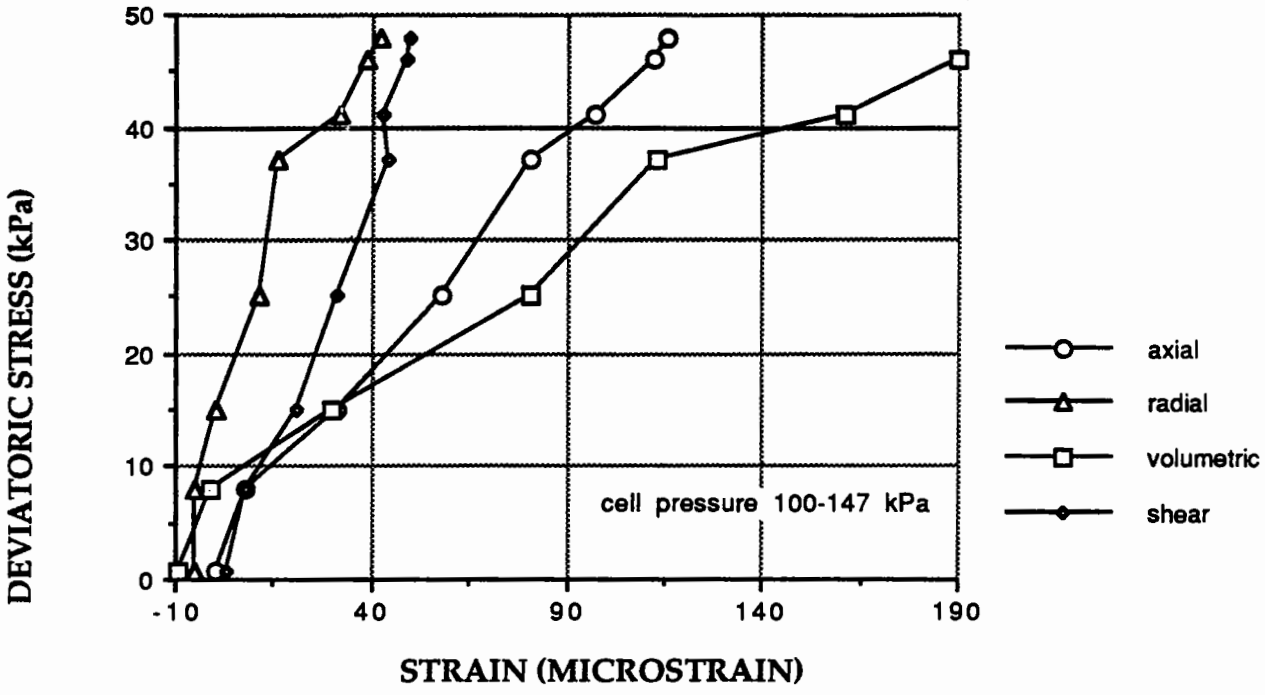

Figure 6.49. Strains due to repeated both stresses in compression (FBA)

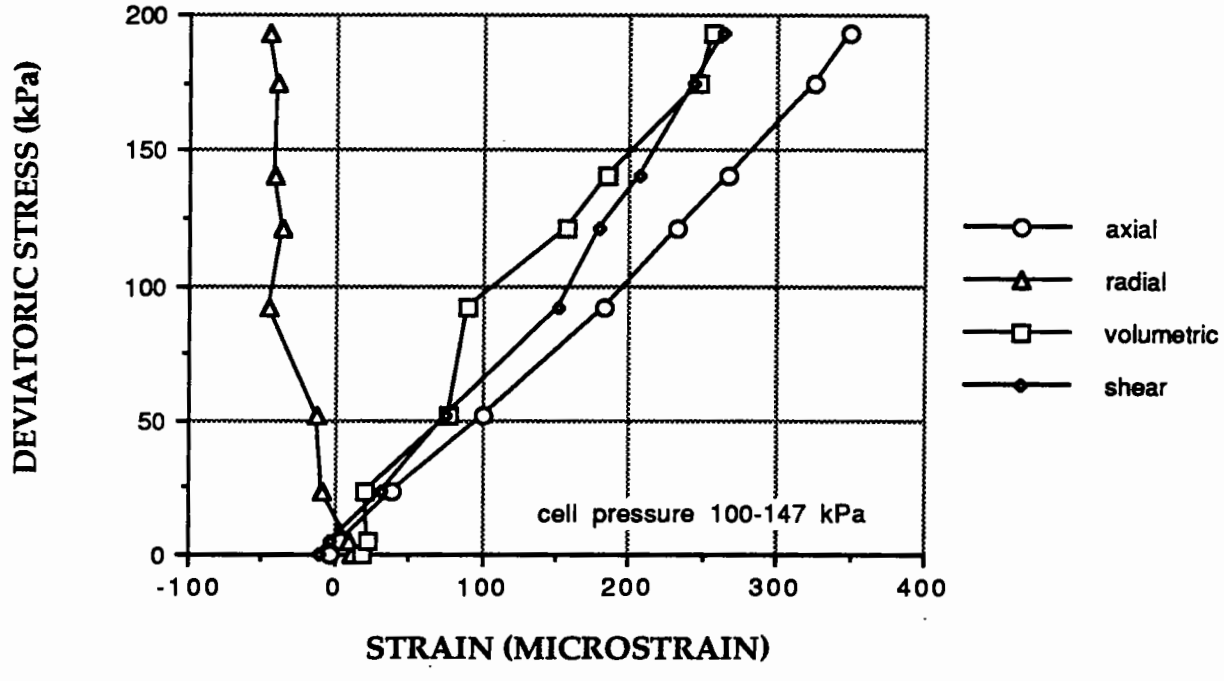

Figure 6.50. Strains due to repeated both stresses in compression (FBA)

6.8.2.Behaviour when both stresses in compression

The results discussed in this subsection are those measured under stress paths where both the deviatoric and the cell pressure are cycled in compression (dashed inclined lines in Figure 5.5).

As both stresses are increased strains also increase. For example the strains measured during two different deviatoric stress excursions each with a cyclic cell pressure between 100 and 147 kPa are chosen. If the level of the deviatoric stress is low, the volumetric strain takes the highest (compressive) value (Figure 6.49) as expected. However, if the deviatoric stress level is increased the axial and shear strain takes higher values (Figure 6.50). The radial strain also increases as the deviatoric stress increases but it may change sign depending on the deviatoric stress level (compare Figures 6.49and 6.50). Thus deviatoric stress becomes a more significant influence on the material behaviour at high q/p values.

CHAPTER 7

STRESS-STRAIN RELATIONSHIPS

7.1.Introduction

A granular material layer is composed of discrete particles which have negligible bonding forces. As a result, such layers have different mechanical properties to those of bound materials such as asphalt layers or concrete pavements. Since there is no bonding between the particles, deformation is mainly caused by sliding, elastic deformation of individual particles, breakage and rearrangement of particles during deformation.

In this chapter, the definitions of stress, strain and the invariants of stress and strain are explained. The basic variables for the development of a model such as bulk modulus and shear modulus are mentioned briefly.

7.2.The particulate nature of granular material

If a granular layer in the pavement is examined by the naked eye, it is evident that the granular layer is composed of discrete particles. The same can be said for all soils, although many individual particles are too small to be seen by the naked eye. The discrete particles do not bond to each other strongly in the way that they do in asphalt or

portland cement concrete. Hence, the granular particles have more freedom to move with respect to each other. However, granular particles are solid and cannot move relative to each other as easily as in a fluid. Thus, a granular material is inherently a particulate system.

7.3.Granular material deformation

Figure 7.1 shows a cross section through a box filled with granular material and a vertical load is being applied by a piston to the composite. The applied force is transmitted through the granular material, hence contact forces develop between adjacent particles. These contact forces can be grouped into normal (N) and tangential (T) forces. The individual particles deform as a result of these contact forces, and this deformation can be separated into elastic (resilient) and plastic (permanent) deformation (see Chapter 6 for details). Particle crushing may be important at high stress levels especially during the construction of sub-base and base layers in a pavement. This leads to an enlargement of the contact area, and results in the particles moving closer together. The overall strain of a granular material will partly be due to relative sliding between particles. However, experience has shown that interparticle sliding, with the resulting rearrangement of the particles, generally makes the most important contribution to overall strain (Lambe and Whitman, 1979). The deformations discussed above cause mainly permanent deformation in the granular layer. However, elastic deformation occurs in the granular material is also due to elastic deformation of particles and only partly due to rebound of sliding when the load is removed. As a

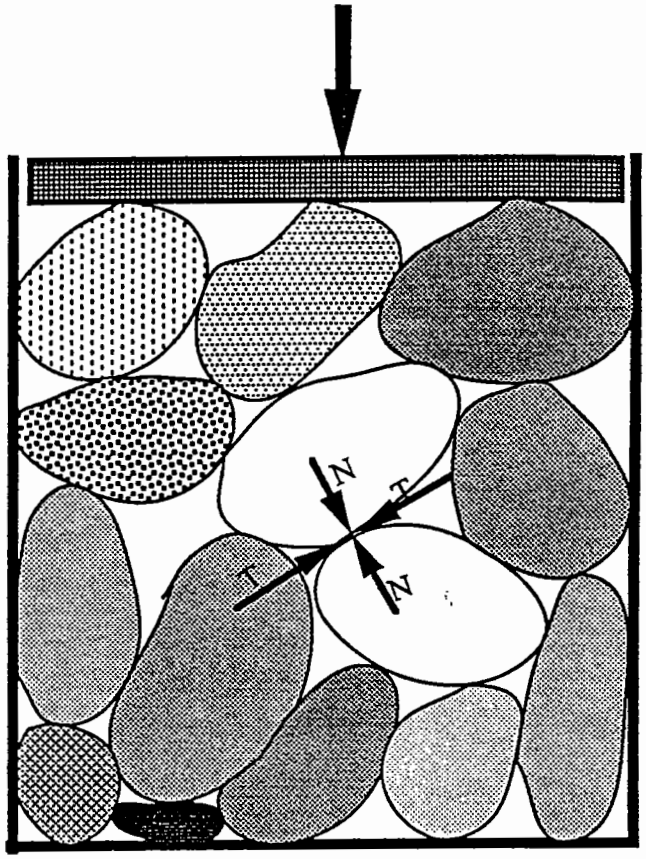

Figure 7.1. Contact forces

result, the deformation of a granular material is controlled by interactions between particles.

Moreover, the study of contact points may be fundamental to the behaviour of granular material. Large numbers of individual contact points exist within a granular layer. For example, there will be 5 million contact points within just 1000 mm^3 of a fine sand (Lambe and Whitman, 1979). It is therefore very difficult, if not impossible, to build up a stress-strain relationship by considering each individual particular contact in turn. However, the study of the behaviour of contact points (Rowe, 1971) gives a guide to the understanding and interpretation of the experimental measurements. In this project,

continuum mechanics rules were applied to establish a stress-strain relationship. Hence stress and strain definitions based on continuum mechanics will be introduced.

7.4.Introduction to tensors

Stress-strain relationships are usually written using tensor notation because this ensures that the components of both stress and strain are related by the same equations in any coordinate system. It also enables these equations to be written in a compact form. Summation is indicated where a suffix, say j, is repeated twice implying the expression is a sum from j=1 to j=3.

A vector which has a magnitude and direction is completely determined by a knowledge of its three components. If the components of a vector in a certain coordinate system are known, v_j, then the components of the same vector in a different coordinate system, u_i, can be determined by transformation law as shown below:

$$u_i = a_{ij}v_j \qquad (i, j = 1, 2, 3) \qquad (7.1)$$

where a_{ij} = direction cosines

In matrix form it can be written as:

$$\begin{bmatrix} u_1 \\ u_2 \\ u_3 \end{bmatrix} = \begin{bmatrix} a_{11} & a_{12} & a_{13} \\ a_{21} & a_{22} & a_{23} \\ a_{31} & a_{32} & a_{33} \end{bmatrix} \begin{bmatrix} v_1 \\ v_2 \\ v_3 \end{bmatrix} \tag{7.2}$$

A vector is a first order tensor. A second order tensor has nine components which transform from one coordinate sytem to another according to the transformation law

$$v_{ij} = a_{ik}\, a_{jl}\, u_{kl} \qquad (i,j,k,l = 1, 2, 3) \tag{7.3}$$

The same equation can be written in a matrix form as

$$\begin{bmatrix} v_{11} & v_{12} & v_{13} \\ v_{21} & v_{22} & v_{23} \\ v_{31} & v_{32} & v_{33} \end{bmatrix} = \begin{bmatrix} a_{11} & a_{12} & a_{13} \\ a_{21} & a_{22} & a_{23} \\ a_{31} & a_{32} & a_{33} \end{bmatrix} \begin{bmatrix} u_{11} & u_{12} & u_{13} \\ u_{21} & u_{22} & u_{23} \\ u_{31} & u_{32} & u_{33} \end{bmatrix} \begin{bmatrix} a_{11} & a_{21} & a_{31} \\ a_{12} & a_{22} & a_{32} \\ a_{13} & a_{23} & a_{33} \end{bmatrix} \tag{7.4}$$

Equation (7.1) and (7.3) are the same equations as the matrix equations (7.2) and (7.4) respectively. Hence, tensor notation is a quite useful tool to express stress strain relationships in a compact form. Unless otherwise stated, second order tensors will be used in the project.

7.5.Stress

Given the stress vector F, with components F_j, which acts across a surface element A_i which is normal to the ith coordinate direction, the components of the stress tensor may be defined as (Baladi, 1984)

$$\sigma_{ij} = \lim_{A_i \to 0} \frac{F_j}{A_i} \tag{7.5}$$

where F_j is the component of the force in the coordinate direction j
A_i is the area normal to the ith axis on which F_j acts

The stress tensor can be written in terms of matrix notation in the form of

$$\sigma_{ij} = \begin{bmatrix} \sigma_x & \tau_{xy} & \tau_{xz} \\ \tau_{yx} & \sigma_y & \tau_{yz} \\ \tau_{zx} & \tau_{zy} & \sigma_z \end{bmatrix} \tag{7.6.}$$

The stress tensor is symmetrical i.e ($\tau_{xy} = \tau_{yx}$), ($\tau_{xz} = \tau_{zx}$),.($\tau_{yz} = \tau_{zy}$). Accordingly, the state of stress at a point can be described by six independent stress components. All compressive stresses are assumed to be positive since granular material cannot readily carry tensile stresses. Positive signs are shown in Figure 7.2.

7.6.Principal Stresses and Stress Invariants

Three mutually orthogonal planes exist at a point in a body where there are no shear stresses. These planes are the principal planes and the stresses on these planes are called principal stresses. Principal stresses σ_n can be determined as the roots of the determinental equation (Harr, 1977).

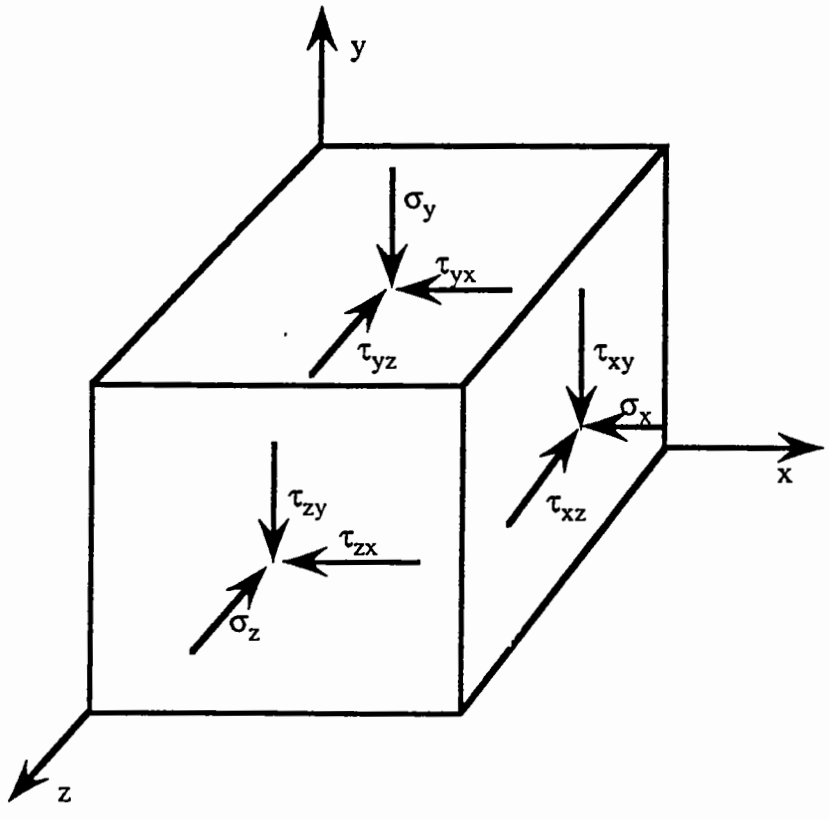

Figure 7.2. Positive stress directions

$$\begin{vmatrix} \sigma_x-\sigma_n & \tau_{xy} & \tau_{xz} \\ \tau_{xy} & \sigma_y-\sigma_n & \tau_{yz} \\ \tau_{xy} & \tau_{yz} & \sigma_z-\sigma_n \end{vmatrix} = 0 \qquad (7.7)$$

From equation (7.7), a characteristic equation ,shown below, can be obtained

$$\sigma_n^3 - I_1\sigma_n^2 + I_2\sigma_n - I_3 = 0 \qquad (7.8)$$

where $I_1 = \sigma_x + \sigma_y + \sigma_z$

$I_2 = \sigma_x\sigma_y + \sigma_x\sigma_z + \sigma_y\sigma_z - \tau_{xy}^2 - \tau_{xz}^2 - \tau_{yz}^2$

$I_3 = \sigma_x\sigma_y\sigma_z - \sigma_x\tau_{yz}^2 - \sigma_y\tau_{xz}^2 - \sigma_z\tau_{xy}^2 + 2\tau_{xy}\tau_{xz}\tau_{yz}$

I_1, I_2 and I_3 are independent of the orientation of the coordinate axes at a point. Consequently, they only depend on the stress state at the point and are called invariants of stress. Stress invariants can also be written in terms of principal stresses as below

$$I_1 = \sigma_1 + \sigma_2 + \sigma_3 \qquad (7.9)$$

$$I_2 = \sigma_1\sigma_2 + \sigma_1\sigma_3 + \sigma_2\sigma_3 \qquad (7.10)$$

$$I_3 = \sigma_1\sigma_2\sigma_3 \qquad (7.11)$$

The state of stress at a point with $\sigma_1>\sigma_2>\sigma_3$ is shown in Figure 7.3a. If $\sigma_1>\sigma_2=\sigma_3$ then the figure becomes a cylinder as shown in Figure 7.3b and if $\sigma_1=\sigma_2=\sigma_3$ then a hydrostatic or spherical stress system with any direction as a principal direction is obtained (Figure 7.3c)

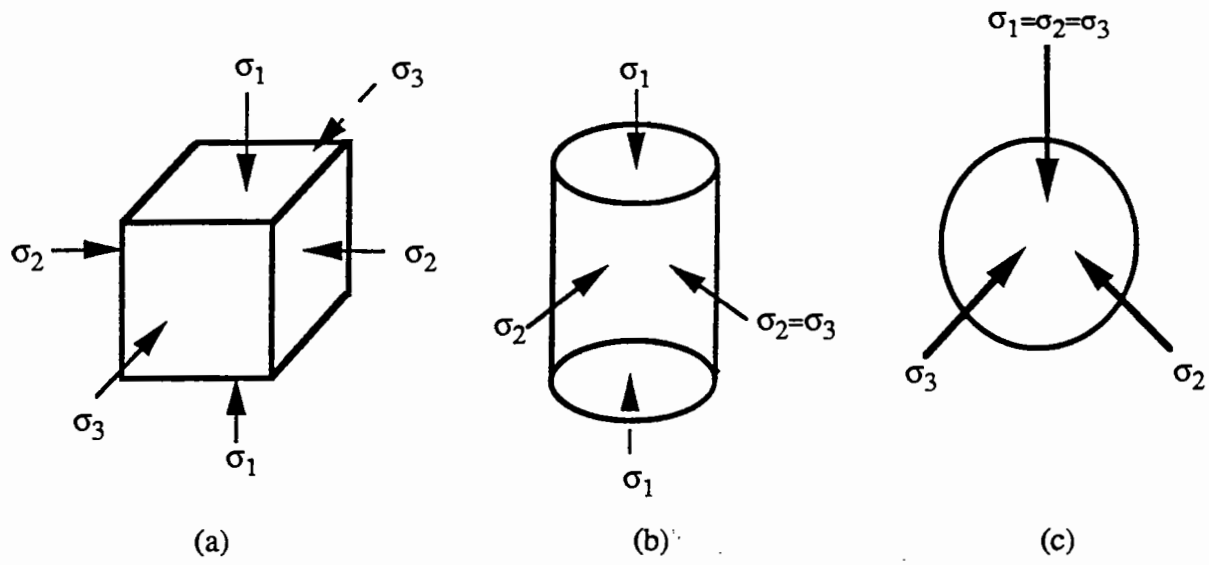

Figure 7.3. Pictural representation of relative magnitudes of principal stresses

The average normal stress is called the octahedral normal stress σ_{oct} and it is also an invariant:

$$\sigma_{oct} = \frac{\sigma_1 + \sigma_2 + \sigma_3}{3} = \frac{I_1}{3} \tag{7.12}$$

The resultant shearing stress acting on an octahedral plane, which is a plane whose normal makes equal angles with each other of the principal axes of stress, is the octahedral shearing stress τ_{oct} given by

$$\tau_{oct}^2 = \frac{1}{9}[(\sigma_1 - \sigma_2)^2 + (\sigma_1 - \sigma_3)^2 + (\sigma_2 - \sigma_3)^2] = \frac{2}{3} I_2 \tag{7.13}$$

7.7.Stress Invariants for Triaxial Test Condition

In the triaxal test axisymmetric conditions apply. There are two independent stress variables, the axial stress $\sigma_a = \sigma_1$ and the confining pressure $\sigma_r = \sigma_2 = \sigma_3$. For the triaxial test condition a different set of stress invariants p and q can be described as follows (Roscoe et al, 1958, Atkinson and Bransby, 1978, Wood, 1984)

$$p = \frac{1}{3}(\sigma_1 + 2\sigma_3) = \sigma_{oct} \tag{7.14}$$

$$q = \sigma_1 - \sigma_3 = \frac{3}{\sqrt{2}}\tau_{oct} \tag{7.15}$$

For a general three dimensional case p and q can be written in the form

$$p = \frac{1}{3}(\sigma_1 + \sigma_2 + \sigma_3) = \frac{I_1}{3} \tag{7.16}$$

$$q = \frac{1}{\sqrt{2}}[(\sigma_1 - \sigma_2)^2 + (\sigma_1 - \sigma_3)^2 + (\sigma_2 - \sigma_3)^2]^{1/2} \tag{7.17}$$

Equation (7.17) reveals that q always needs to be positive, therefore, equation (7.15) should be rewritten in an absolute form although it is often convenient to indicate the 90^o rotation of the vector q in the triaxial test when horizontal stress exceeds vertical stress (e.g. Figure 5.5) known as "extension condition".

$$q = |\sigma_1 - \sigma_3| \tag{7.18}$$

The parameter invariant p represents the average effective stress level in the material. The other stress invariant q indicates the departure of an actual collection of principal effective stresses from the average effective stress level (Wood, 1984). The

parameters p and q are enough to express the two degrees of freedom in the triaxial apparatus. For an ideal elastic material, increments of shear strain are dependent only on the increments of q whereas the increments of volumetric strain are dependent only on the increments of p (Atkinson and Bransby, 1978).

7.8.Strain

When a force is applied to a granular matrix it causes movements and deformation in the matrix. When two particles in a continuum move relative to each another, the matrix is said to be deformed or strained. Figure 7.4 shows a linear deformation of a continuum matrix.

Let A and B be two points in the matrix, a distance l_0 apart when the matrix is free from any external loading as shown in Figure 7.4. When the matrix is stressed, it will then be moved to another position A'B'. The distance between A and A' shows the displacement of particle A. If A'B' is parallel and equal to AB, the displacement is only due to only the sliding of particles. However, if l_0 is not equal to l after external loading, then a relative displacement of B with respect to A is observed. The ratio of the change in length to the original length is then defined as the direct or linear strain (Chen and Saleeb, 1982).

$$\text{linear strain} = \varepsilon = \frac{l_0 - l}{l_0} \tag{7.19}$$

Strain in a continuum body can also be expressed in terms of deformation. If the displacements are u, v and w in the negative x, y and z directions, the components of strain can be written as follows (Christian and Desai, 1977)

$$\varepsilon_x = \frac{\partial u}{\partial x} \quad , \quad \varepsilon_y = \frac{\partial v}{\partial y} \quad , \quad \varepsilon_z = \frac{\partial w}{\partial z} \tag{7.20}$$

$$\gamma_{xy} = \frac{\partial u}{\partial y} + \frac{\partial v}{\partial x}, \ \gamma_{xz} = \frac{\partial u}{\partial z} + \frac{\partial v}{\partial \gamma_{yz}}, \ \gamma_{yz} = \frac{\partial v}{\partial z} + \frac{\partial w}{\partial y} \tag{7.21}$$

Equation (7.20) shows normal strains in x, y and z directions respectively. Whereas Equation (7.21) shows shear strains in xy, xz and yz planes respectively. The normal and shear strain are shown diagramatically by Figure 7.4 and 7.5 respectively.

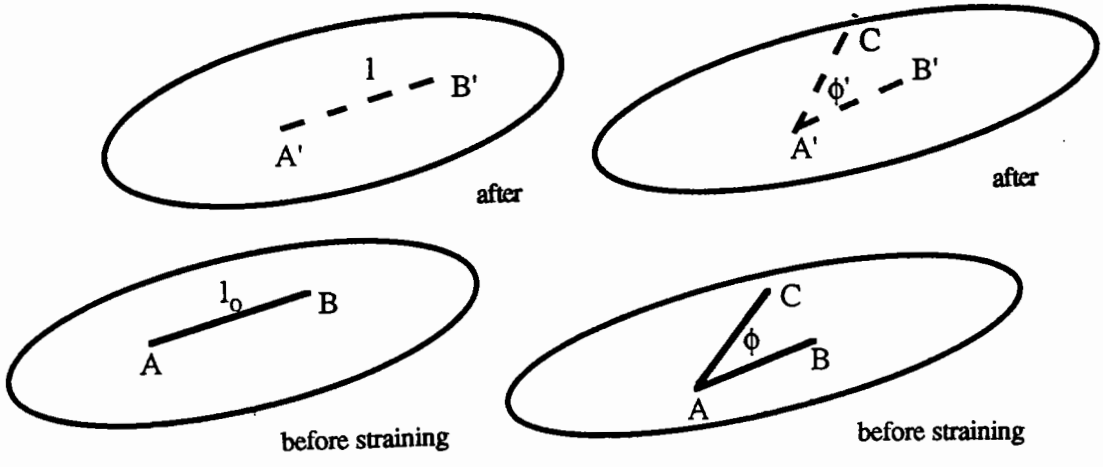

Figure 7.4.Normal strain
(Chen and Saleeb,1982)

Figure 7.5.Shear strain
(Chen and Saleeb, 1982)

Equation (7.20) and (7.21) can also be written in a short form by using a subscript notation in which u_1, u_2 and u_3 are displacements and x_1, x_2 and x_3 are directions (Timeshenko and Goodier, 1970).

$$\varepsilon_{ij} = \frac{1}{2}\left(\frac{\partial u_i}{\partial x_j} + \frac{\partial u_j}{\partial x_i}\right) \quad , \quad \gamma_{ij} = 2\varepsilon_{ij} \tag{7.22}$$

The latter are called engineering strains and they are most useful for experimental work as well as numerical applications. The former are called tensorial shear strains and they are useful tools for theoretical derivations. Unless otherwise stated engineering strains will be used.

7.9.Definition of strain from different sources

Although a linear strain definition is mostly used to analyse experimental results, it is possible to find other definitions of strain (Baladi, 1984). These are shown below:

Cauchy's strain $$\varepsilon^C = \frac{l_o - l}{l_o} \tag{7.23}$$

Green's strain $$\varepsilon^G = \frac{1}{2}\left(\frac{l_o^2 - l^2}{l_o^2}\right) \tag{7.24}$$

Henky's strain $$\varepsilon^H = \ln \frac{l_o}{l} \tag{7.25}$$

Almansi's strain $$\varepsilon^A = \frac{1}{2}\left(\frac{l_o^2 - l^2}{l}\right) \tag{7.26}$$

Swainger's strain $$\varepsilon^S = \frac{l_o - l}{l} \tag{7.27}$$

Although all measurements are different in form, when the ratio of l to l_o is close to one in other words for small deformation case ,which is the case in pavement engineering, all formulas yield the same results. In this project the Cauchy type of strain, i.e linear strain, was chosen.

7.10.Strain tensor

The strain tensor ε_{ij} is composed of a spherical part representing a change in volume and a deviatoric part representing a change in shape (distortion). That is

$$\varepsilon_{ij} = e_{ij} + \frac{1}{3}\varepsilon_{kk}\,\delta_{ij} \tag{7.28}$$

where e_{ij} = the deviatoric strain tensor

$\frac{1}{3}\varepsilon_{kk} = \frac{1}{3}(\varepsilon_x + \varepsilon_y + \varepsilon_z)$ the mean strain

The deviatoric strain tensor can be written in the matrix form

$$e_{ij} = \begin{bmatrix} \frac{2\varepsilon_x-\varepsilon_y-\varepsilon_z}{3} & \varepsilon_{xy} & \varepsilon_{xz} \\ \varepsilon_{yx} & \frac{2\varepsilon_y-\varepsilon_z-\varepsilon_x}{3} & \varepsilon_{yz} \\ \varepsilon_{zx} & \varepsilon_{zy} & \frac{2\varepsilon_z-\varepsilon_x-\varepsilon_y}{3} \end{bmatrix} \tag{7.29}$$

7.11.Principal strains and strain invariants

Principal strains can be derived in the same way as for principal stresses. The characteristic equation is given below

$$\varepsilon^3 - I'_1\varepsilon^2 + I'_2\varepsilon - I'_3 = 0 \tag{7.30}$$

where $I'_1 = \varepsilon_{11} + \varepsilon_{22} + \varepsilon_{33} = \varepsilon_x + \varepsilon_y + \varepsilon_z = \varepsilon_{ii}$

$I'_2 = \varepsilon_x\varepsilon_y + \varepsilon_x\varepsilon_z + \varepsilon_y\varepsilon_z - \varepsilon_{xy}^2 - \varepsilon_{xz}^2 - \varepsilon_{yz}^2$

$I'_3 = \varepsilon_x\varepsilon_y\varepsilon_z - \varepsilon_x\varepsilon_{xz}^2 - \varepsilon_y\varepsilon_{xz}^2 - \varepsilon_z\varepsilon_{xy}^2 + 2\varepsilon_{xy}\varepsilon_{xz}\varepsilon_{yz}$

In terms of principal strains

$$I'_1 = \varepsilon_1 + \varepsilon_2 + \varepsilon_3 \tag{7.31}$$

$$I'_2 = \varepsilon_1\varepsilon_2 + \varepsilon_1\varepsilon_3 + \varepsilon_2\varepsilon_3 \tag{7.32}$$

$$I'_3 = \varepsilon_1\varepsilon_2\varepsilon_3 \tag{7.33}$$

The octahedral normal strain ε_{oct} can be written in the form of

$$\varepsilon_{oct} = \frac{\varepsilon_1 + \varepsilon_2 + \varepsilon_3}{3} = \frac{I'_1}{3} = \frac{\varepsilon_{ii}}{3} \tag{7.34}$$

The octohedral shear strain γ_{oct} can be written as follows

$$\gamma_{oct} = \frac{1}{9}[(\varepsilon_1 - \varepsilon_2)^2 + (\varepsilon_1 - \varepsilon_3)^2 + (\varepsilon_2 - \varepsilon_3)^2] = \frac{2}{3} I'_2 \qquad (7.35)$$

Shear strain can be expressed in terms of octahedral strains and can also be written for triaxial test condition as below

$$\varepsilon_s = \frac{1}{\sqrt{2}} \gamma_{oct} = \frac{2}{3}(\varepsilon_1 - \varepsilon_3) \qquad (7.36)$$

7.12.Bulk modulus

If a hydrostatic pressure, i.e $\sigma_x = \sigma_y = \sigma_z = \sigma_o$, is applied to a cube that is an isotropic linearly elastic material (see Figure 7.6a), then the volumetric strain ε_v is

$$\frac{\Delta V}{V} = \varepsilon_v = \varepsilon_x + \varepsilon_y + \varepsilon_z = \Sigma \varepsilon_{ii} = 3\varepsilon_{oct} \qquad (7.37)$$

Bulk modulus K (see Figure 7.6c) is defined as the ratio of hydrostatic pressure to volumetric strain as shown in Equation (7.38).

$$K = \frac{\sigma_o}{\varepsilon_v} \qquad (7.38)$$

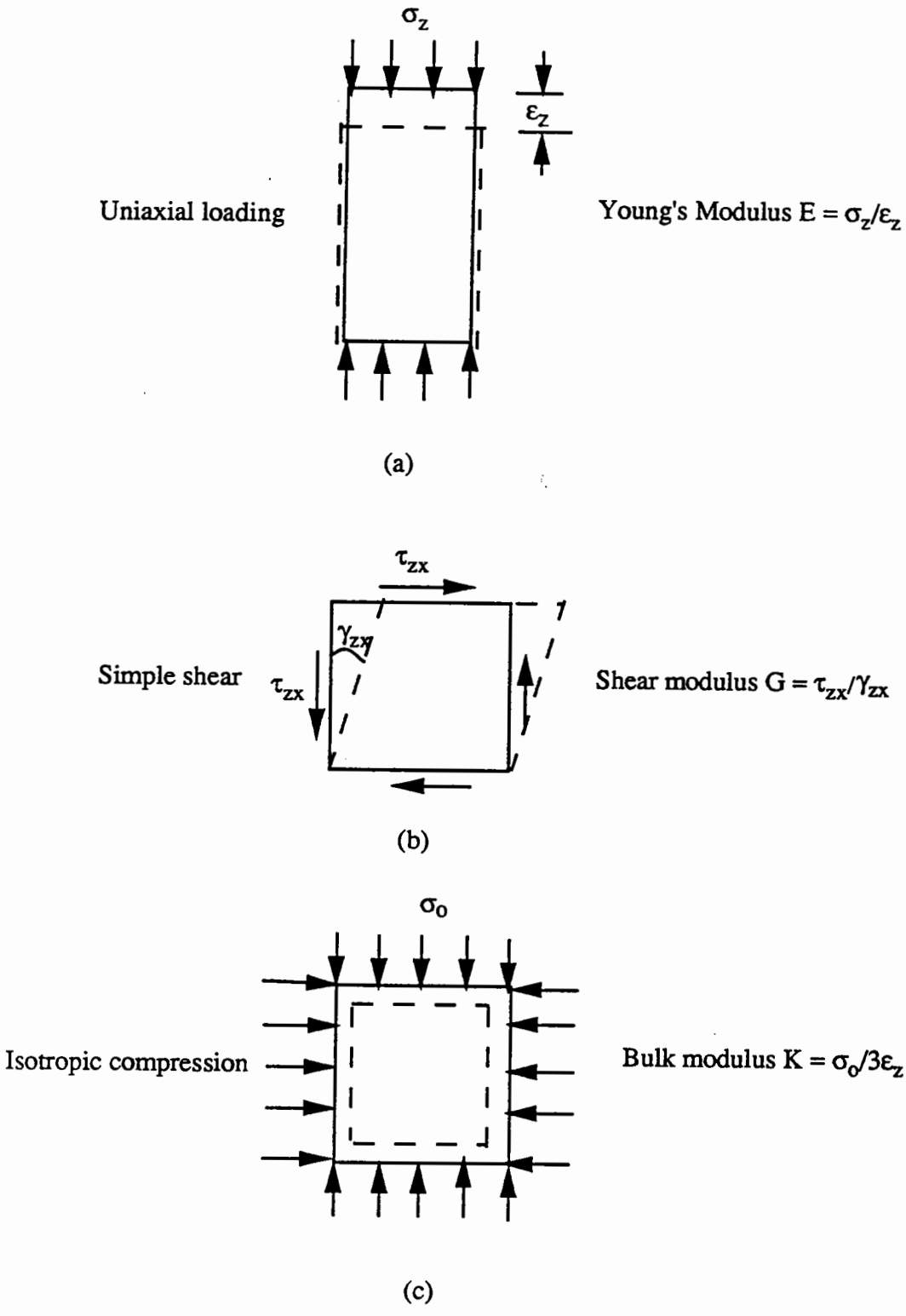

Figure 7.6. Definition of Young's, shear and bulk modulus

7.13.Shear modulus

If shear stresses τ_{zx} are applied to an elastic cube (see Figure 7.6b) there will be shear strain that can be calculated by equation (7.39).

$$\gamma_{zx} = \frac{\tau_{zx}}{G} \tag{7.39}$$

where G is the shear modulus

7.14.Young's modulus and Poisson's ratio

If a uniaxial stress σ_z is applied to a cylindrical sample (see Figure 7.6a), there will be vertical compression deformation and a lateral expansion deformation. Vertical strain ε_z caused by σ_z can be calculated as follows

$$\varepsilon_z = \frac{\sigma_z}{E} \tag{7.40}$$

where E is Young's modulus (elastic modulus)

Lateral strains can be calculated as

$$\varepsilon_x = \varepsilon_y = -\upsilon\varepsilon_z \tag{7.41}$$

where υ is Poisson's ratio $= -\frac{\varepsilon_x}{\varepsilon_z}$

Bulk modulus K and shear modulus G can be written in terms of E and υ such that

$$K = \frac{E}{3(1 - 2\upsilon)} \tag{7.42}$$

$$G = \frac{E}{2(1 + \upsilon)} \tag{7.43}$$

These transforms rely on the assumption of ideal elastic material behaviour.

7.15.The need for constitutive equations

For a material of volume V, three equations for equilibrium and six equations of compatibility between strains and displacements can be written. Therefore only nine equations for equilibrium and compatibility can be written for any material although fifteen unknown variables exist which are six stresses, six strains and three displacements. Hence, six additional equations or the stress-strain relationship are needed to to solve the indeterminate system. These six relationships are called constitutive equations or relations. These constitutive relations are material dependent and are determined from experimental results (Chen and Saleeb, 1982).

In the past very simple stress-strain relationships, such as linear elastic, were used in analytical pavement design programs because of the lack of computing power although it was well known that granular material behaviour was non-linear. More recently, the developments in the computer technology and the increase in computing speed have led to more widespread use of non-linear stress-strain relationships either for new design of pavements or for pavement evaluation. Finite element programs (FEP) are generally used for detailed pavement design although multilayer elastic theory is still used for routine pavement design. The accuracy of results mainly depends on the constitutive equation (stress-strain relation) employed in the FEP.

7.16.Elastic material

When a material is subjected to applied forces, it deforms. After removing the force, the body may completely recover to its original shape and size. This type of material is called perfectly elastic. However, there are also some materials which may show partly elastic behaviour, like soil. There may be two classification of elastic materials: linear elastic materials for which the change in deformation of a material is directly proportional to the change in applied stress, such as metals (Figure 7.7), and non-linear elastic material for which the change in deformation is not necessarily proportional to the change in applied stress (Figure 7.8).

Test results (chapter 6) have revealed that granular material behaves non-linearly and shows a hysteresis loop due to energy dissipation (Figure 7.9). It can be seen from

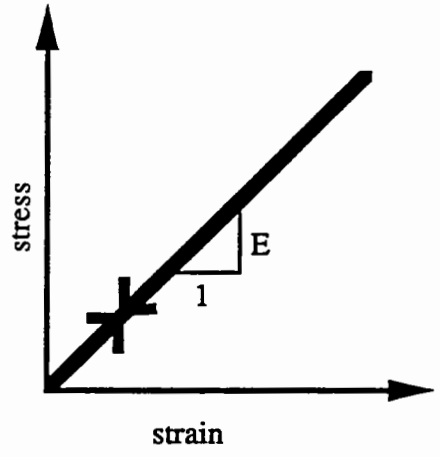

Figure 7.7. Linear elastic material

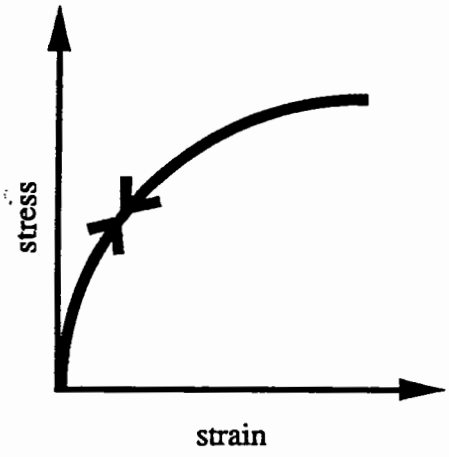

Figure 7.8. Non-linear elastic material

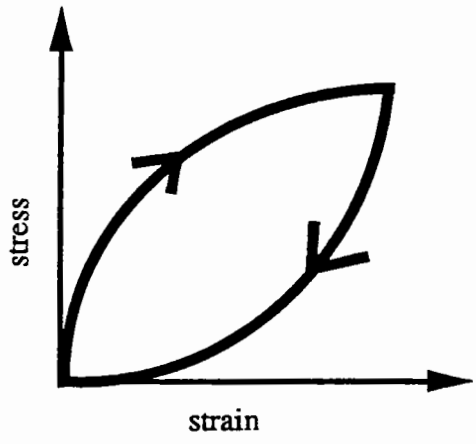

Figure 7.9. Rate-independent recoverable behaviour

Figure 7.9 that the behaviour is non-linear, but it does not follow the same path for loading and unloading stress conditions. It is interesting to note that no permanent deformation is developed after loading and unloading cycle although a hysteresis loop is observed. This behaviour may be called the rate-independent recoverable behaviour or anelastic behaviour (Lazan, 1968). In this dissertation, the behaviour of granular material is assumed to be non-linear elastic for consistency with other research (Boyce, 1980).

In numerical methods such as FEP for engineering purposes (Britto and Gunn (1990) and Brown and Almeida (1993)) the resulting strain due to loading is more important than hysteresis loops since loads are applied statically, therefore, only loading part of the cycle is taken into account. However, if a dynamic analysis is carried out for a certain number of cycles, then the hysteresis loop becomes an important parameter since long term performance of a pavement such as fatigue behaviour is controlled by the damping ratio due to the hysteresis loop.

7.17.Material symmetry properties

The reason for discussing the material symmetry is that the number of independent constants required by a constitutive equation can be reduced due to a materials symmetry since they will take the same value for particular symmetrical directions.

If the mechanical behaviour of the material is the same for certain directions, then the material is said to be symmetrical in these directions, if there is no symmetry the material is called anisotropic (Chen and Saleeb, 1982).

Three types of material symmetry, namely, orthotropic, cross-anisotropic and isotropic exist. An orthotropic material such as wood has three orthogonal planes of material symmetry (Fig 7.10a). If the material properties are the same in the x_1 and x_2 directions, which is the direction of rolling during manufacture, and different in the x_3 direction then the material is called cross-anisotropic (Fig 7.10b). This type of symmetry may represent the granular layer in a pavement. If the mechanical behaviour is the same in all directions, it is then said that the material is isotropic. For example polycrystalline metals, which are composed of randomly oriented grains, are considered isotropic (Chen and Saleeb, 1982).

7.18.Isotropic linear elastic constitutive equations

The general form of the linear elastic stress-strain relationship is given by (Chen and Saleeb, 1982)

$$\sigma_{ij} = B_{ij} + C_{ijkl}\,\varepsilon_{kl} \qquad (7.44)$$

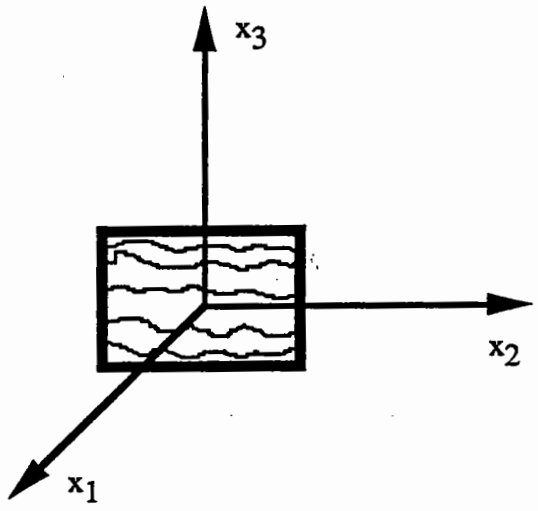

(a)

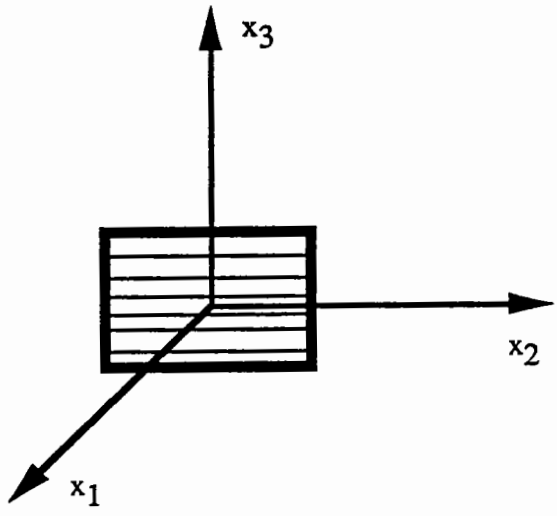

(b)

Figure 7.10. Material symmetry (a) orthotropic material (b) cross-anisotropic material (Chen and Saleeb, 1982)

where B_{ij} = components of initial stress tensor corresponding to the initial strain force state

C_{ijkl} = tensor of material elastic constants

σ_{ij} = stress tensor

ε_{kl} = strain tensor

If $B_{ij}= 0$, then Equation (7.44) becomes

$$\sigma_{ij} = C_{ijkl}\,\varepsilon_{kl} \tag{7.45}$$

Equation (7.45) is referred as the generalized Hooke's law. C_{ijkl} contains $(3)^4 = 81$ constants, however, due to the symmetry of σ_{ij} and ε_{kl}

$$C_{ijkl} = C_{jikl} = C_{ijlk} = C_{jilk} \tag{7.46}$$

The number of independent constants is reduced to 36. Another symmetry $C_{(ij)(kl)} = C_{(kl)(ij)}$ can also be introduced (Chen and Saleeb, 1982) which reduces constants to 21. That means that if 21 constants are known the 81 constants are also known.

For an isotropic material, C_{ijkl} takes the following form :

$$C_{ijkl} = \lambda\delta_{ij}\delta_{kl} + \mu(\delta_{ik}\delta_{jl} + \delta_{il}\delta_{jk}) \tag{7.47}$$

and hence

$$\sigma_{ij} = \lambda\delta_{ij}\delta_{kl}\varepsilon_{kl} + \mu(\delta_{ik}\delta_{jl} + \delta_{il}\delta_{jk})\varepsilon_{kl} \tag{7.48}$$

or

$$\sigma_{ij} = \lambda\varepsilon_{kk}\delta_{ij} + 2\mu\varepsilon_{ij} \tag{7.49}$$

Solving for ε_{ij} we get

$$\varepsilon_{ij} = \frac{\lambda\delta_{ij}}{2\mu(3\mu(3\lambda + 2\mu))}\sigma_{kk} + \frac{1}{2\mu}\sigma_{ij} \tag{7.50}$$

where λ and μ are Lame's constants.

Equation (7.50) is a general form of constitutive equation for an isotropic linear elastic material.

Equation (7.49) and (7.50) can also be expressed in different forms:

$$\sigma_{ij} = \frac{E}{(1 + \upsilon)}\varepsilon_{ij} + \frac{\upsilon E}{(1 + \upsilon)(1 - 2\upsilon)}\varepsilon_{kk}\delta_{ij} \tag{7.51}$$

$$\varepsilon_{ij} = \frac{1 + \upsilon}{E}\sigma_{ij} - \frac{\upsilon}{E}\sigma_{kk}\delta_{ij} \tag{7.52}$$

$$\sigma_{ij} = 2G\varepsilon_{ij} + \frac{3\upsilon K}{(1 + \upsilon)}\varepsilon_{kk}\delta_{ij} \tag{7.53}$$

$$\varepsilon_{ij} = \frac{1}{2G}\sigma_{ij} - \frac{\upsilon}{3K(1 - 2\upsilon)}\sigma_{kk}\delta_{ij} \qquad (7.54)$$

where E is Young's modulus
υ =Poisson's ratio
G = Shear modulus
K= Bulk modulus

For real elastic materials, experimental results have shown that

$$E>0 \quad G>0 \quad K>0 \qquad (7.55)$$

Using the inequalities given above, Poisson's ratio takes the value

$$-1 \leq \upsilon \leq 0.5 \qquad (7.56)$$

In pavement engineering, forces are generally applied to a pavement and critical strains in it are calculated. Therefore the open form of strain tensor is given in the matrix form for three dimensional (equation 7.57), plane strain (equation 7.58) and axisymmetric case (equation 7.59) cases.

$$\begin{Bmatrix} \varepsilon_x \\ \varepsilon_y \\ \varepsilon_z \\ \gamma_{xy} \\ \gamma_{yz} \\ \gamma_{zx} \end{Bmatrix} = \frac{1}{E}\begin{bmatrix} 1 & -\upsilon & -\upsilon & 0 & 0 & 0 \\ -\upsilon & 1 & -\upsilon & 0 & 0 & 0 \\ -\upsilon & -\upsilon & 1 & 0 & 0 & 0 \\ 0 & 0 & 0 & 2(1+\upsilon) & 0 & 0 \\ 0 & 0 & 0 & 0 & 2(1+\upsilon) & 0 \\ 0 & 0 & 0 & 0 & 0 & 2(1+\upsilon) \end{bmatrix}\begin{Bmatrix} \sigma_x \\ \sigma_y \\ \sigma_z \\ \tau_{xy} \\ \tau_{yz} \\ \tau_{zx} \end{Bmatrix} \quad (7.57)$$

$$\begin{Bmatrix} \varepsilon_x \\ \varepsilon_y \\ \varepsilon_z \end{Bmatrix} = \frac{1}{E}\begin{bmatrix} 1 & -\upsilon & 0 \\ -\upsilon & 1 & 0 \\ 0 & 0 & 2(1+\upsilon) \end{bmatrix}\begin{Bmatrix} \sigma_x \\ \sigma_y \\ \tau_{xy} \end{Bmatrix} \quad (7.58)$$

$$\begin{Bmatrix} \varepsilon_r \\ \varepsilon_z \\ \varepsilon_\theta \\ \gamma_{rz} \end{Bmatrix} = \frac{1}{E}\begin{bmatrix} 1 & -\upsilon & -\upsilon & 0 \\ -\upsilon & 1 & -\upsilon & 0 \\ -\upsilon & -\upsilon & 1 & 0 \\ 0 & 0 & 0 & 2(1+\upsilon) \end{bmatrix}\begin{Bmatrix} \sigma_r \\ \sigma_z \\ \sigma_\theta \\ \tau_{rz} \end{Bmatrix} \quad (7.59)$$

7.19.Cross-anisotropic elastic stress-strain relationship

The properties of granular material may differ in the vertical and horizontal directions. If the horizontal plane is assumed to be isotropic and the properties of the granular material are symmetrical about the vertical axis, then the material shows cross-anisotropic (transverse isotropy) behaviour, which is described using five elastic constants.

The strain-stress behaviour of a cross-anisotropic material is shown in matrix form below (Barden, 1963).

$$\begin{Bmatrix} \varepsilon_x \\ \varepsilon_y \\ \varepsilon_z \\ \gamma_{xy} \\ \gamma_{yz} \\ \gamma_{zx} \end{Bmatrix} = \frac{1}{E} \begin{bmatrix} \frac{1}{n} & -\frac{\upsilon_1}{n} & -\upsilon_3 & 0 & 0 & 0 \\ -\frac{\upsilon_1}{n} & \frac{1}{n} & -\upsilon_3 & 0 & 0 & 0 \\ -\frac{\upsilon_2}{n} & -\frac{\upsilon_2}{n} & 1 & 0 & 0 & 0 \\ 0 & 0 & 0 & \frac{2(1+\upsilon_1)}{n} & 0 & 0 \\ 0 & 0 & 0 & 0 & \frac{\upsilon_2+\upsilon_3+2\upsilon_2\upsilon_3}{\upsilon_2} & 0 \\ 0 & 0 & 0 & 0 & 0 & \frac{\upsilon_2+\upsilon_3+2\upsilon_2\upsilon_3}{\upsilon_2} \end{bmatrix} \begin{Bmatrix} \sigma_x \\ \sigma_y \\ \sigma_z \\ \tau_{xy} \\ \tau_{yz} \\ \tau_{zx} \end{Bmatrix} \quad (7.60)$$

where $\varepsilon_x, \varepsilon_y, \varepsilon_z$ are normal strains in x, y and z directions respectively
$\gamma_{xy}, \gamma_{yz}, \gamma_{zx}$ are shear strains in the plane of xy, yz and zx respectively
$\sigma_x, \sigma_y, \sigma_z$ are normal strains in the x,y and z directions respectively
$\tau_{xy}, \tau_{yz}, \tau_{zx}$ are shear stresses in the plane of xy, yz and zx respectively
E = the Young's modulus in the vertical direction
$n = E_h/E$ (the degree of anisotropy)
E_h = the Young's modulus in the horizontal direction
υ_1 = effect of horizontal strain in the horizontal strain
υ_2 = effect of horizontal strain on vertical strain
υ_3 = effect of vertical strain on horizontal strain

Barden (1963) showed that five elastic constants are not independent and they can be related to each other by

$$n = \frac{E_h}{E} = \frac{\upsilon_2}{\upsilon_3} \quad (7.61)$$

If a cubic triaxial sample is considered, for which only three independent principal stresses can be applied and there will not be any shear stresses, then equation (7.60) becomes

$$\begin{Bmatrix} \varepsilon_x \\ \varepsilon_y \\ \varepsilon_z \end{Bmatrix} = \frac{1}{E}\begin{bmatrix} \frac{1}{n} & -\frac{\upsilon_1}{n} & -\upsilon_3 \\ -\frac{\upsilon_1}{n} & \frac{1}{n} & -\upsilon_3 \\ -\frac{\upsilon_2}{n} & -\frac{\upsilon_2}{n} & 1 \end{bmatrix}\begin{Bmatrix} \sigma_x \\ \sigma_y \\ \sigma_z \end{Bmatrix} \qquad (7.62)$$

If a cylindrical sample is considered, the horizontal strains, ε_x and ε_y,in all directions are equal to each other as are the horizontal stresses ,σ_x and σ_y. Hence, the equation (7.62) becomes

$$\begin{Bmatrix} \varepsilon_x \\ \varepsilon_z \end{Bmatrix} = \frac{1}{E}\begin{bmatrix} \frac{1-\upsilon_1}{n} & -\upsilon_3 \\ -\frac{2\upsilon_2}{n} & 1 \end{bmatrix}\begin{Bmatrix} \sigma_x \\ \sigma_z \end{Bmatrix} \qquad (7.63)$$

7.20. Methods to develop a non-linear stress-strain relationship

Two methods are available to develop new non-linear elastic relations. The first method is to modify existing linear elastic relationships in a way that non-linearity can be introduced. For this purpose strains or stresses are generally expressed in terms of stress or strain invariants and mostly power laws. This approach has been taken so far by pavement engineers such as Hicks and Monismith (1971), Pappin (1979), Boyce

(1980), Pappin and Brown (1981, 1985). This approach is more practicable for the application of numerical analysis such as the finite element method and material constants in the model can be obtained from suitable test results. The second method is to use a general formulation of Cauchy elastic material, hyperelastic (Green) material or hypoelastic material. Although the second method is more theoretical (not practical) it is difficult, sometimes impossible, to find constants in a model because there is no methodology available to find them. In addition to this the number of constants in these type of models are generally more than in the modified elastic models and as the degree of equation increases in order to obtain more accurate results the number of constants in the model also increases. Both methods are introduced briefly.

7.20.1.Modification of elastic stress-strain relationships

Linear elasticity has been used for many years in soil mechanics and pavement engineering to design pavement structures. Although it is still in use for metals, it is not a valid approximation for soil and granular materials since the behaviour of granular material in the pavement is markedly non-linear especially where a thin layer of asphalt is used. This is also proven by laboratory experiments. However, for the sake of simplicity the behaviour has often been assumed to be linear elastic. Recent pavement design methods (AASHTO (1986) and ARRB (1991)) have introduced the routine use of non-linear characteristics of soil as well as of granular material for the design of new pavements.

The simplest types of non-linear elastic relationship for granular material in the pavement is the K-θ model (Section 2.4.1). Shackel (1973) and Uzan (1985,1992) modified the model in order to introduce the effect of deviatoric stress on the behaviour of the material. These types of models can be written in the from of

$$M_r = f(p,q) \tag{7.64}$$

More complicated models were developed by Pappin(1979), Brown and Pappin (1981, 1985) and Boyce (1980). These models express bulk modulus K and shear modulus G as functions of the mean normal stress p and deviatoric stress q so that no assumption of constant Poisson's ratio is made, such as a constant Poisson's ratio, to introduce non-linearity. These types of models can be written in the form:

$$\varepsilon_v = \frac{p}{K(p,q)} \tag{7.65}$$

$$\varepsilon_s = \frac{q}{3G(p,q)} \tag{7.66}$$

The advantages of using the models mentioned above is that they are mathematically and conceptually very simple in nature and non-linearity is taken into account. However, they generally show path independent behaviour (Chen and Saleeb, 1982) although Pappin (1979) considered the stress path length in the shear strain model.

Chen and Saleeb (1982) give a useful discussion on elastic stress-strain relationships. A review of their work is expressed below.

7.20.2.Cauchy elastic formulation

For a Cauchy elastic material the stress-strain relationship can be written in the form

$$\sigma_{ij} = F_{ij}(\varepsilon_{kl}) \tag{7.67}$$

where Fij = the elastic response function

ε_{kl} = the strain tensor

σ_{ij} = the stress tensor

This type of formulation is path independent, the current state of stress depends on the current state of deformation. This type of formulation is mostly used for the modification of the linear elastic idealization.

7.20.3.Hyperelastic (Green) formulation

Mathematical models based on hyperelastic material formulation benefit from the existence of a strain energy function ,ω, or complementary energy function, Ω. Strain

energy per unit volume or strain energy density, ω, which is the area under the σ-ε curve shown in Figure 7.11 can be expressed mathematically as

$$\omega(\varepsilon) = \int_0^{\varepsilon} \sigma d\varepsilon \tag{7.68}$$

In the multiaxial case it can be written as

$$\omega(\varepsilon_{ij}) = \int_0^{\varepsilon_{ij}} \sigma_{ij} d\varepsilon_{ij} \tag{7.69}$$

Similarly, the complementary energy function is the area above the σ-ε curve in Figure 7.11 and is expressed as

$$\Omega(\sigma) = \int_0^{\sigma} \varepsilon d\sigma \tag{7.70}$$

or, in the multiaxial case it can be written as

$$\Omega(\sigma_{ij}) = \int_0^{\sigma_{ij}} \varepsilon_{ij} d\sigma_{ij} \tag{7.71}$$

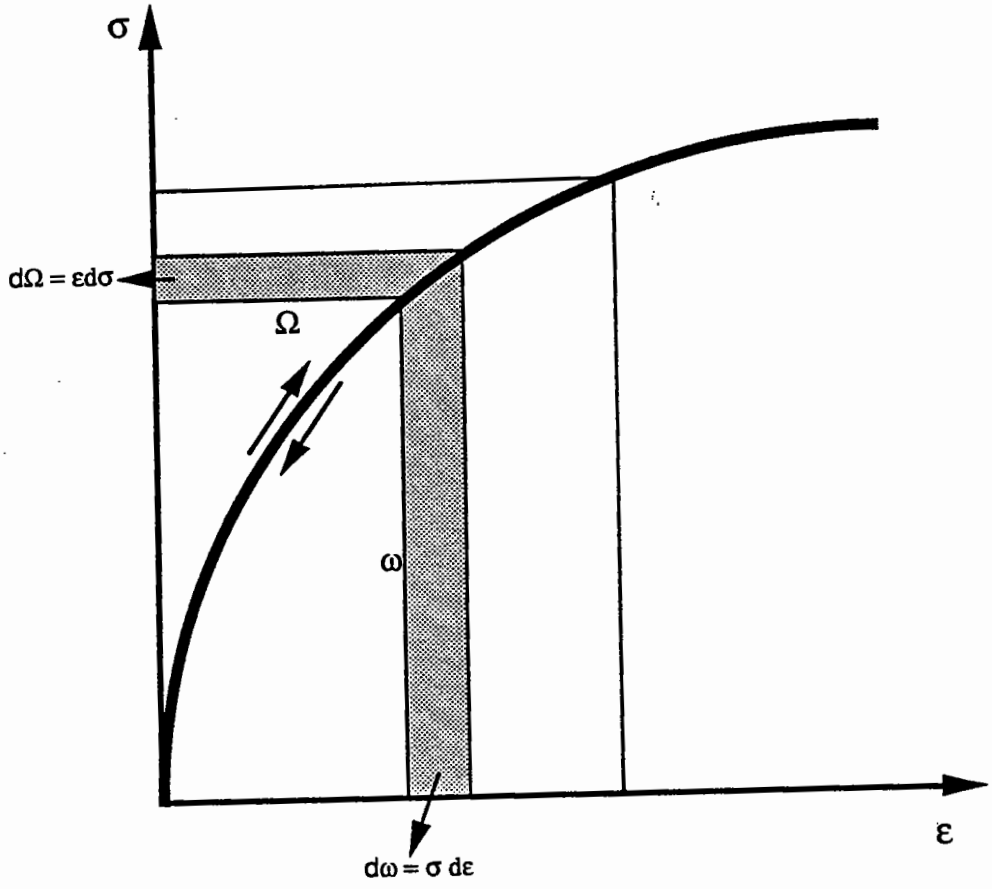

Figure 7.11. Strain energy density function ω and complementary energy density function Ω (Chen and Saleeb, 1982)

Several secant moduli constitutive relations can be obtained from the following

$$\sigma_{ij} = \frac{\partial \omega}{\partial \varepsilon_{ij}} \qquad \text{or} \qquad \varepsilon_{ij} = \frac{\partial \Omega}{\partial \sigma_{ij}} \tag{7.72}$$

The above relationships show that the current state of stress depends upon the current state of deformation (or vice versa), as for the Cauchy elastic formulation, and it is still path independent although the thermodynamics rules are satisfied (no energy can be generated or lost during load cycles).

The above formulae can also be written in terms of tangent moduli as shown below:

$$\dot{\sigma}_{ij} = \frac{\partial^2 \omega}{\partial \varepsilon_{ij} \partial \varepsilon_{kl}} \dot{\varepsilon}_{kl} = H_{ijkl} \dot{\varepsilon}_{kl} \tag{7.73}$$

$$\dot{\varepsilon}_{ij} = \frac{\partial^2 \Omega}{\partial \sigma_{ij} \partial \sigma_{kl}} \dot{\sigma}_{kl} = H'_{ijkl} \dot{\sigma}_{kl} \tag{7.74}$$

where H_{ijkl} and H'_{ijkl} is the Hessian matrix

Hyperelastic models exhibit strain or stress-induced anisotropy when formulated in terms of tangent moduli but a disadvantage of hyperelastic modelling is that it contains too many material constants and a large number of tests are required to determine these constants which may limit its use for practical purposes (Chen, 1984).

7.20.4.Hypoelastic formulation

The Cauchy and hyperelastic formulae have a major drawback in that they show path-independent behaviour. An improved version of these models is the hypoelastic formulation in which incremental stress and strain tensors are linearly related by variable material response moduli which are a function of the stress or strain state. The basic formula can be written thus:

$$\dot{\sigma}_{ij} = C_{ijkl}(\sigma_{mn})\dot{\varepsilon}_{kl} \tag{7.75}$$

$$\dot{\varepsilon}_{ij} = D_{ijkl}(\varepsilon_{mn})\dot{\sigma}_{kl} \tag{7.76}$$

where $\dot{\sigma}_{ij}$ and $\dot{\sigma}_{kl}$ are the stress tensor increments

$\dot{\varepsilon}_{ij}$ and $\dot{\varepsilon}_{kl}$ are the strain tensor increments

σ_{mn} and ε_{mn} are the current states of stress and strain respectively

C_{ijkl} and D_{ijkl} are the material response moduli

For an initially isotropic material, the first order hypoelastic model is shown below

$$\begin{aligned}\dot{\sigma}_{ij} = {} & a_1\dot{\varepsilon}_{kk}\,\delta_{ij} + a_2\dot{\varepsilon}_{ij} + a_{11}\sigma_{pp}\dot{\varepsilon}_{kk}\,\delta_{ij} \\ & + a_{12}\sigma_{mm}\dot{\varepsilon}_{ij} + a_{13}\,\sigma_{ij}\dot{\varepsilon}_{kk} + a_{14}\,(\sigma_{jk}\dot{\varepsilon}_{ik} + \sigma_{ik}\dot{\varepsilon}_{jk}) \\ & + a_{15}\sigma_{kl}\dot{\varepsilon}_{kl}\,\delta_{ij}\end{aligned} \tag{7.77}$$

where a_1 to a_{15} are material constants

"˙" shows the increment

The above equation shows initially isotropic behaviour, however, the last three terms show stress-induced anisotropic behaviour.

The degree of formulation can be increased, but, it will mean a large increase in the number of material constants. The advantage of this type of formulation is that it is path dependent and shows stress-induced anisotropy. However, it has some drawbacks. It is incrementally reversible and so will not model hysteresis, the tangent stiffness matrix is generally unsymmetrical therefore it causes an increase in storage and computation time when used in finite element analysis, it is difficult to determine the material constants (and more tests are needed to determine them) and energy generation in certain stress cycles is possible (Chen (1984) and Chen and Saleeb (1982)).

However, this type of formulation has been also used for the modification of linear elastic models by Gerstle (1981), Stankowski and Gerstle (1985) for concrete behaviour, Yin et al (1990) for soil behaviour and Allaart (1989) for granular material behaviour in the form:

$$\dot{\varepsilon}_v = \frac{\dot{p}}{K} + \frac{\dot{q}}{J} \tag{7.78}$$

$$\dot{\varepsilon}_s = \frac{\dot{p}}{J} + \frac{\dot{q}}{3G} \tag{7.79}$$

Gerstle (1981) did not include the coupling shear strain due to volumetric strain in his model and Stankowski and Gerstle (1985) used different coupling terms for shear and volumetric strain increments- in other words, J was different in Equations (7.78) and (7.79). The advantages of the type of models mentioned above are that they are mathematically simple, ideal for finite element implementation although it still gives unsymmetric stiffness matrix, relatively easy to fit and may be used for practical applications. Coupling between shear and volumetric strain is also considered.

7.21.Development of a new model

A new model was developed using repeated load triaxial test data obtained from six different granular materials. The primary aim was to simulate the triaxial test results as much as possible.

It was demonstrated by the triaxial test results (Chapter 6) that granular material is not isotropic. Rather it is anisotropic from the beginning of the test and the anisotropy is generally affected by the application of different stress paths and permanent strain because particles move around inside the sample and take a new structure under applied loads. However, some triaxial test equipment used for the investigation of granular material is not able to cycle cell pressure, therefore, it is impossible to obtain any information about anisotropy using these types of equipment. For this, more limited use, an isotropic model is also proposed.

Results have also revealed that, when only isotropic pressure is applied, it is normal to obtain some shear strain as well as volumetric strain or when only a deviatoric stress is applied, it is possible to obtain some volumetric strain as well as shear strain.Thus anisotropy and dilation have some importance

There is no magic method to develop a new non-linear relationship between stress and strain. However, Stackel (1973) suggested the use of either regression models or spline functions. In this dissertation the former was chosen since it is more flexible than the other method. Initially it was thought that the equation (7.65) and (7.66) were useful in developing a new relationship for volumetric and shear strain prediction, but results have revealed that volumetric strains sometimes change sign from positive to negative or vice versa when there is no corresponding change in applied stress. This prevents the use of a power law or many other continuous functions. In addition it was shown in the results that the change in repeated volumetric strain behaviour is not smooth when compared with axial, radial and shear strains (see Figures 6.15, 6.16 and 6.17). This may be the reason why many models, such as Boyce (1980), have failed to predict volumetric strain satisfactorily although they acceptably predict shear strain.

For this reason, it was thought sensible to develop a model to predict axial and radial strain since they do not change sign under the same stress regime. In addition, these strains are directly measured values available from the test. If required the volumetric and shear strain can then be predicted as long as the axial and the radial strains are predicted satisfactorily.

There are only two independent variables in a triaxial test, namely deviatoric and cell (confining) pressure, which affect the behaviour of granular material. Therefore, any stress-strain relationship resulting from the repeated load triaxial test apparatus must contain deviatoric stress and cell pressure. For convenience, the mean normal stress, p, and deviatoric stress, q, are used throughout the model development and four invariants are used in the formulae.

$$p = p_2 - p_1 \tag{7.80}$$

$$q = q_2 - q_1 \tag{7.81}$$

$$p_m = \frac{p_1 + p_2}{2} \tag{7.82}$$

$$q_m = \frac{q_1 + q_2}{2} \tag{7.83}$$

These four invariants are able to describe any stress path in p,q space (see Figure 7.12).

7.21.1.An isotropic model

For an isotropic material under constant cell pressure the axial and radial strain may be written in the form

$$\varepsilon_a = \frac{1}{M_r} q \tag{7.84}$$

$$\varepsilon_r = \frac{-\upsilon}{M_r} q \tag{7.85}$$

where ε_a, ε_r are axial and radial strain respectively

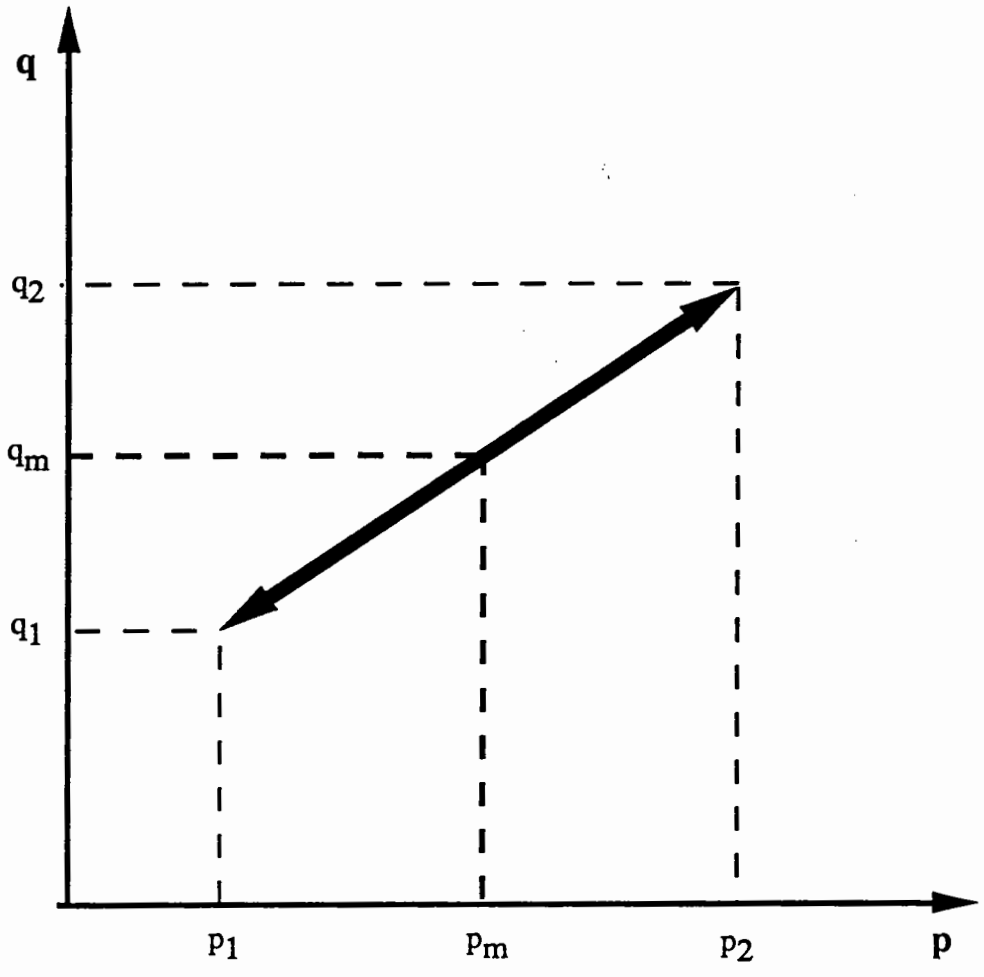

Figure 7.12. Stress path in p-q space

υ is Poisson's ratio

M_r is the resilient modulus (same as Young's modulus, E)

q is the deviatoric stress

From the experimental results it was observed that the resilient modulus, M_r, and Poisson's ratio, υ, are stress dependent and non-linear. In order to obtain a non-linear deformation law the regression method was used as suggested by Stackel (1973). Although Stackel recommended the use of a multiple linear regression method, the stepwise regression method was chosen. The reason for choosing a stepwise regression method is that there are four invariants that may probably control the behaviour of granular material, but it is difficult to see which invariant has more effect than others on certain parameters or which parameters have no effect on the behaviour for certain test conditions. The method is also able to choose an invariant which gives high regression coefficient as well as finding other invariants which increase the regression coefficient. To obtain a non-linear relationship, a regression model of the type shown below was chosen, however, it is always possible to put another invariant in, to use a combination, or to remove any unwanted invariant.

$$\ln(y) = \ln(a) + b\ln(p) + c\ln(q) + d\ln(p_m) + e\ln(q_m) \qquad (7.86)$$

where y = dependent variables (such as resilient modulus)

a = the intercept

b, c, d and e = the powers of p, q, p_m and q_m respectively

Regression coefficients R^2 for the resilient modulus from different combinations are shown in Table 7.1, 7.2, 7.3 and 7.4., (-) sign shows parameters which are not chosen

during the regression analysis; normal, italic and underlined characters show the regression coefficients of parameters chosen firstly, secondly and thirdly respectively. It should be noticed that the regression coefficients generally increase when another parameter is included in the regression model. Only constant cell pressure data has been processed to derive these.

Table 7.1.Regression coefficients for resilient modulus with p_m, q_m and q/p

	p_m	q_m	q/p
GWRS	0.09	-	*0.15*
SL	0.32	-	*0.32*
GS	0.15	-	*0.16*
SAG	0.19	-	*0.19*
FS	0.1	-	*0.18*
FBA	0.15	-	*0.22*

Table 7.2.Regression coefficients for resilient modulus with p,p_m and q

	p	p_m	q
GWRS	0.87	*0.97*	-
SL	-	*0.98*	0.82
GS	-	*0.97*	0.72
SAG	0.87	*0.99*	-
FS	-	*0.99*	0.88
FBA	0.91	*0.97*	-

Table 7.3.Regression coefficients for resilient modulus with p,p_m and q_m

	p	p_m	q_m
GWRS	0.45	*0.89*	0.89
SL	0.95	0.79	*0.89*
GS	*0.92*	0.83	0.94
SAG	*0.91*	0.79	0.92
FS	*0.97*	0.66	0.98
FBA	0.51	*0.86*	0.91

Table 7.4.Regression coefficients for resilient modulus with q, p_m and q_m

	q	p_m	q_m
GWRS	0.47	*0.89*	0.89
SL	*0.96*	0.78	0.99
GS	*0.92*	0.81	0.94
SAG	*0.92*	0.76	*0.92*
FS	*0.97*	0.63	0.98
FBA	*0.37*	0.2	0.43

In the first analysis, Table 7.1, modulus is assumed to be some function of p_m, q_m and q/p. Clearly using the ratio of q/p resulted in a very low regression coefficient, therefore the resilient modulus is not a function of it. From the results of Table 7.1 it can also be seen that the effect of q_m is negligible.

A second series of regression analyses were carried out with p, q and p_m, Table 7.2. It can be seen that the resilient modulus of GWRS, SAG and FBA is a function of p and

A second series of regression analyses were carried out with p, q and p_m, Table 7.2. It can be seen that the resilient modulus of GWRS, SAG and FBA is a function of p and p_m and the resilient modulus for SL, GS and FS is a function of q and p_m with a high regression coefficient. It was thus decided that two other regression analyses were necessary in order to see the effect of p and q on the other three materials. Results are shown in Table 7.3 and 7.4. From the results it was seen that the effect of q_m has a negligible effect on the resilient modulus, but either p and p_m or q and p_m can be used to model the resilient modulus. This may be a statistical problem, which is called multicollinearity by Schroeder et al (1986), but there is no analytical solution. They recommend the use of the variable that gives higher regression coefficients. On this bases the chosen relationship for the resilient modulus is shown below:

$$M_r = A\left(\frac{p_m}{p_u}\right)^B \left(\frac{p_u}{p}\right)^C \qquad (7.87)$$

where p_u is unit pressure (1 kPa)
A, B and C constants

The coefficients for the different materials are given in Table 7.5.

For the Poisson's ratio stepwise regression analyses were carried out using the variables p_m, q_m, p and q. The results have shown that the Poisson's ratio is a function of p_m, q_m and q for GWRS, SAG and FS, a function of p_m, q_m and q for SL, GS and FBA. The regression coeficients obtained are shown in Table 7.6. It was decided to do another regression to obtain a single best fit function for which one set of variables are p_m, q_m and q and another set consists of p_m, q_m and p. Results are shown in Tables 7.7 and 7.8. Two other regression analyses were also carried out to see any effect of stress ratio in the behaviour (Table 7.9 and 7.10). Results revealed that either p_m,q_m and q or p_m, q_m and q can be used to model Poisson's ratio. It is

again the problem of multicolinearity. Therefore one suitable set of variables could be chosen, in this case p_m, q_m and p were chosen. The Poisson's ratio can then be written as

$$\upsilon = D \left(\frac{q_m}{p_u}\right)^F \left(\frac{p_u}{p_m}\right)^H \left(\frac{p_u}{p}\right)^L \tag{7.88}$$

The material coefficients for the Poisson's ratio were shown in Table 7.11. It can be noticed that the regression coefficients obtained for the Poisson's ratio are not as great as for the resilient modulus. This may be due to low sensitivity of the measurement system in the horizontal direction. Hence, the prediction of Poisson's ratio is not good as the resilient modulus.

Table 7.5. Resilient modulus coefficients

	A	B	C
GWRS	115183	0.592	0.335
SL	56650	0.594	0.213
GS	42832	0.672	0.115
SAG	34392	0.642	0.110
FS	53929	0.567	0.197
FBA	37192	0.764	0.219

Table 7.6.Regression coefficients for Poisson's ratio with p_m, q_m, p, q

	p_m	q_m	p	q
GWRS	0.75	*0.6*	0.47	-
SL	0.29	*0.59*	-	0.61
GS	0.43	*0.43*	-	0.32
SAG	0.63	*0.63*	0.56	-
FS	0.87	*0.85*	0.54	-
FAB	0.34	*0.58*	-	0.58

Table 7.7.Regression coefficients for Poisson's ratio with p_m, q_m and q

	p_m	q_m	q
GWRS	0.74	*0.59*	0.46
SL	0.29	*0.59*	0.61
GS	0.43	*0.43*	0.32
SAG	0.63	*0.63*	0.55
FS	0.87	*0.85*	0.53
FBA	0.31	*0.56*	0.59

Table 7.8.Regression coefficients for Possion's ratio with p_m,q_m and p

	p_m	q_m	p
GWRS	0.75	*0.6*	0.47
SL	0.29	*0.59*	0.61
GS	0.43	*0.42*	0.32
SAG	0.63	*0.63*	0.56
FS	0.87	*0.85*	0.54
FBA	0.34	*0.58*	0.59

Table 7.9.Regression coefficients for Poisson's ratio with p/p_m and q/q_m

	p/p_m	q/q_m
GWRS	*0.35*	0.28
SL	0.28	*0.57*
GS	*0.33*	0.28
SAG	0.5	*0.52*
FS	*0.78*	0.76
FBA	0.43	*0.49*

Table 7.10.Regression coefficients for Poisson's ratio with p_m, q_m and q/p

	p_m	q_m	q/p
GWRS	0.11	*0.2*	0.34
SL	0.29	*0.59*	0.62
GS	0.03	*0.02*	0.003
SG	0.13	*0.12*	0.06
FS	0.23	*0.23*	0.2
FBA	0.34	*0.56*	0.6

Table 7.11.Material coefficients for Poisson's ratio

	D	F	H	L
GWRS	1.94	0.056	0.19	0.23
SL	0.876	0.27	0.36	0.07
GS	1.009	0.17	0.05	0.34
SAG	0.568	0.034	0.013	0.18
FS	0.79	0.253	0.102	0.386
FBA	3.73	0.112	0.52	0.064

7.21.2.A cross-anisotropic model

For a cubic triaxial sample a linear cross-anisotropic model is shown by equation (7.62) and for a cylindrical sample the same equation can be reduced to equation (7.63). Due to equation (7.61), the equation (7.63) can be rewritten in the form of

$$\begin{Bmatrix} \delta\varepsilon_r \\ \delta\varepsilon_a \end{Bmatrix} = \frac{1}{M_r}\begin{bmatrix} \frac{1-\upsilon_1}{n} & \frac{-\upsilon_2}{n} \\ \frac{-2\upsilon_2}{n} & 1 \end{bmatrix}\begin{Bmatrix} \delta\sigma_r \\ \delta\sigma_a \end{Bmatrix} \qquad (7.89)$$

It is impossible to measure directly υ_1 (effect of horizontal strain on the orthogonal horizontal strain) and υ_2 (the effect of horizontal stain on vertical strain) for the cylindrical triaxial sample.

n, the ratio of radial strain to axial strain (Biarez and Hicher, 1987), is the measure of inherent anisotropy which can be determined from isotropic test condition (cycling only the cell pressure). Once again a stepwise regression approach was used to deduce the possible relationship as

$$n = D\left(\frac{p}{p_u}\right)^F \qquad (7.90)$$

Regression coeffcients and material constants thus obtained for n from stepwise regression analysis are shown in Table 7.12.

Table 7.12.Regression coefficients for anisotropy and material constants

		Material constants	
	R^2	D	F
SL	0.91	0.039	0.586
GS	0.99	0.039	0.53
SAG	0.96	0.51	0.113
FS	0.98	0.05	0.54
FBA	0.92	0.037	0.437

Referring back to Equation 7.89, for the sake of simplicity let $\varphi = \frac{1-\upsilon_1}{nM_r}$. M_r from an isotropic model can also be used in a cross-anisotropic model. However, φ and υ_2 should be found from the results of cycling only cell pressure with constant deviatoric stress. From Equation (7.89) φ can be written as long as only the cell pressure is cycled and if $\delta\sigma_a = 0$. (The tests which showed a relative fixity of the load ram (see section 6.4.5) are believed to provide the stress paths closest to this condition which were performed in this research project)

$$\varphi = \frac{\varepsilon_r}{\sigma_3} \tag{7.92}$$

From (7.92) ($1-\upsilon_1$) may be written as

$$1-\upsilon_1 = \frac{n\varepsilon_r M_r}{\sigma_3} \tag{7.93}$$

$(1-\upsilon_1)$ is calibrated with results obtained from only repeated cell pressure test with constant deviatoric stress. In order to develop a non-linear relationship for $(1-\upsilon_1)$, a stepwise regression analysis was carried out including p, p_m, q_m and q. The resultant equation is shown below

$$1-\upsilon_1 = H\left(\frac{p}{p_u}\right)^L \left(\frac{q_m}{p_u}\right)^M \left(\frac{p_u}{p_m}\right)^N \tag{7.94}$$

Regression coefficients obtained from stepwise regression program and material constants are shown in Table 7.13 and 7.14. From this it can be seen that all three parameters must be modelled to obtain reasonably high regression values.

Table 7.13.Regression coefficients for $(1-\upsilon_1)$

	p	p_m	q_m
SL	0.29	*0.55*	0.83
GS	0.47	*0.69*	0.9
SAG	0.85	*0.84*	0.46
FS	*0.85*	0.44	0.88
FAB	*0.67*	0.47	0.78

It is also impossible to measure directly υ_2 (the effect of horizontal strain on the vertical strain) with a cylindrical sample. However, Equation (7.89) suggests that υ_2 can be calibrated againist axial strain measurements due to only cyclic cell pressure with constant deviatoric stress. The relationship from Equation (7.89) can be written as

Table 7.14. Material constants for $(1-\upsilon_1)$

	H	L	M	M
SL	0.442	0.44	0.1	0.44
GS	0.183	0.56	0.1	0.39
SAG	14.47	0.08	0.34	0.92
FS	0.114	0.39	0.07	0.1
FAB	0.226	0.32	0.1	0.27

$$\upsilon_2 = \frac{n\varepsilon_a M_r}{2\sigma_3} \tag{7.95}$$

M_r and n are known values from previous relatonships. The suggested relationship from stepwise regression analysis is in the form of

$$\upsilon_2 = R \left(\frac{p}{p_u}\right)^S \left(\frac{p_m}{p_u}\right)^T \left(\frac{p_u}{q_m}\right)^U \tag{7.96}$$

Regression coefficients and material constants obtained from stepwise regression analysis are shown in Table 7.15 and 7.16. Once again this analysis indicates the importance of correctly modelling all the parameters.

The Equation (7.89) can be written in the open form

$$\varepsilon_r = \frac{1-\upsilon_1}{nM_r}\sigma_3 - \frac{\upsilon_2}{nM_r}\sigma_1 \tag{7.95}$$

$$\varepsilon_a = -\frac{2\upsilon_2}{nM_r}\sigma_3 + \frac{1}{M_r}\sigma_1 \tag{7.96}$$

Table 7.15.Regression coefficients for υ_2

	p	q_m	p_m
SL	*0.81*	0.73	0.81
GS	*0.74*	0.66	0.8
SAG	0.89	*0.85*	0.73
FS	0.43	*0.8*	0.87
FBA	0.27	0.21	*0.26*

Table 7.16.Material constants for υ_2

	R	S	T	U
SL	0.021	0.584	0.084	0.28
GS	6.4*10-3	0.47	0.41	0.23
SAG	1.1*10-3	-0.22	1.4	0.325
FS	1.7*10-3	0.91	0.39	0.16
FBA	0.022	0.11	0.38	0.14

Equation (7.95) and (7.96) can also expressed in terms of p and q using Equation (7.97) and (7.98)

$$\sigma_1 = p + \frac{2}{3}q \tag{7.97}$$

$$\sigma_3 = p - \frac{q}{3} \tag{7.98}$$

$$\varepsilon_a = \frac{1}{M_r}\left[\left(1 - \frac{2\upsilon_2}{n}\right)p + \left(1 + \frac{\upsilon_2}{n}\right)\frac{2q}{3}\right] \tag{7.99}$$

$$\varepsilon_r = \frac{1}{nM_r}\left[\left(1 - \upsilon_1 - \upsilon_2\right)p - \left(1 - \upsilon_1 - 2\upsilon_2\right)\frac{q}{3}\right] \tag{7.100}$$

where:

$$n = D\left(\frac{p}{p_u}\right)^F$$

$$\upsilon_1 = 1 - H\left(\frac{p}{p_u}\right)^L\left(\frac{q_m}{p_u}\right)^M\left(\frac{p_u}{p_m}\right)^N$$

$$\upsilon_2 = R\left(\frac{p}{p_u}\right)^S\left(\frac{p_m}{p_u}\right)^T\left(\frac{p_u}{q_m}\right)^U$$

$$M_r = A\left(\frac{p_m}{p_u}\right)^B\left(\frac{p_u}{p}\right)^C$$

The volumetric and shear strain may be written using the Equation (7.36) and (7.39)

$$\varepsilon_v = \frac{1}{nM_r}\left[\left(2 + n - 2\upsilon_1 - 4\upsilon_2\right)p + \left(n - 1 + \upsilon_1 - 3\upsilon_2\right)\frac{2q}{3}\right] \tag{7.99}$$

$$\varepsilon_s = \frac{2}{3nM_r}\left[\left(n - 1 + \upsilon_1 - \upsilon_2\right)p - \left(1 + 2n - \upsilon_1\right)\frac{q}{3}\right] \tag{7.100}$$

The change of moduli with applied stress is generally referred to as stress-induced anisotropy (Chang et al, 1992). In order to introduce the stress-induced anisotropy into the model and to implement the model into a finite element program that uses tangential

stiffness approach, the equations (7.97), (7.98), (7.99) and (7.100) can be written in an incremental form of

$$\varepsilon_{at} = \frac{1}{M_t}\left[\left(1 - \frac{2\upsilon_{2t}}{n_t}\right) p + \left(1 + \frac{\upsilon_{2t}}{n_t}\right) \frac{2}{3} q \right] \tag{7.101}$$

$$\varepsilon_{rt} = \frac{1}{n_t M_t}\left[\left(1 - \upsilon_{1t} - \upsilon_{2t}\right) p - \left(1 - \upsilon_{1t} - 2\upsilon_{2t}\right) \frac{2}{3} q \right] \tag{7.102}$$

$$\varepsilon_{vt} = \frac{1}{n_t M_t}\left[\left(2 + n_t - 2\upsilon_{1t} - 4\upsilon_{2t}\right) p) + \left(n_t - 1 + \upsilon_{1t} + 3\upsilon_{2t}\right) \frac{2}{3} q) \right] \tag{7.103}$$

$$\varepsilon_{st} = \frac{2}{3 n_t M_t}\left[\left(n - 1 + \upsilon_{1t} - \upsilon_{2t}\right) p - \left(1 + 2n_t - \upsilon_{1t}\right) \frac{1}{3} q \right] \tag{7.104}$$

where p and q are the incremental mean normal and deviatoric stress respectively

' t ' means tangential

$$n_t = DF\left(\frac{p}{p_u}\right)^F \frac{\dot{p}}{p}$$

$$\upsilon_{1t} = H \left(\frac{p}{p_u}\right)^L \left(\frac{q_m}{p_u}\right)^M \left(\frac{p_u}{p_m}\right)^N \left(-\frac{L}{p} \dot{p} + \frac{N}{p_m} \dot{p}_m - \frac{M}{q_m} \dot{q}_m \right)$$

$$\upsilon_{2t} = R \left(\frac{p}{p_u}\right)^S \left(\frac{p_m}{p_u}\right)^T \left(\frac{p_u}{q_m}\right)^U \left(\frac{S}{p} \dot{p} + \frac{T}{p_m} \dot{p}_m - \frac{U}{q_m} \dot{q}_m \right)$$

$$M_t = A\left(\frac{p_m}{p_u}\right)^B \left(\frac{p_u}{p}\right)^C \left(\frac{B}{p_m} \dot{p}_m - \frac{C}{p} \dot{p} \right)$$

" . " means increment

The determination of constants of the new models and their advantages and disadvantages are discussed in Chapter 8. The best sequence of testing to obtain the necessary input data is listed in Appendix F. Use of secant and tangential stiffness approaches are illustrated in Figure 7.13.

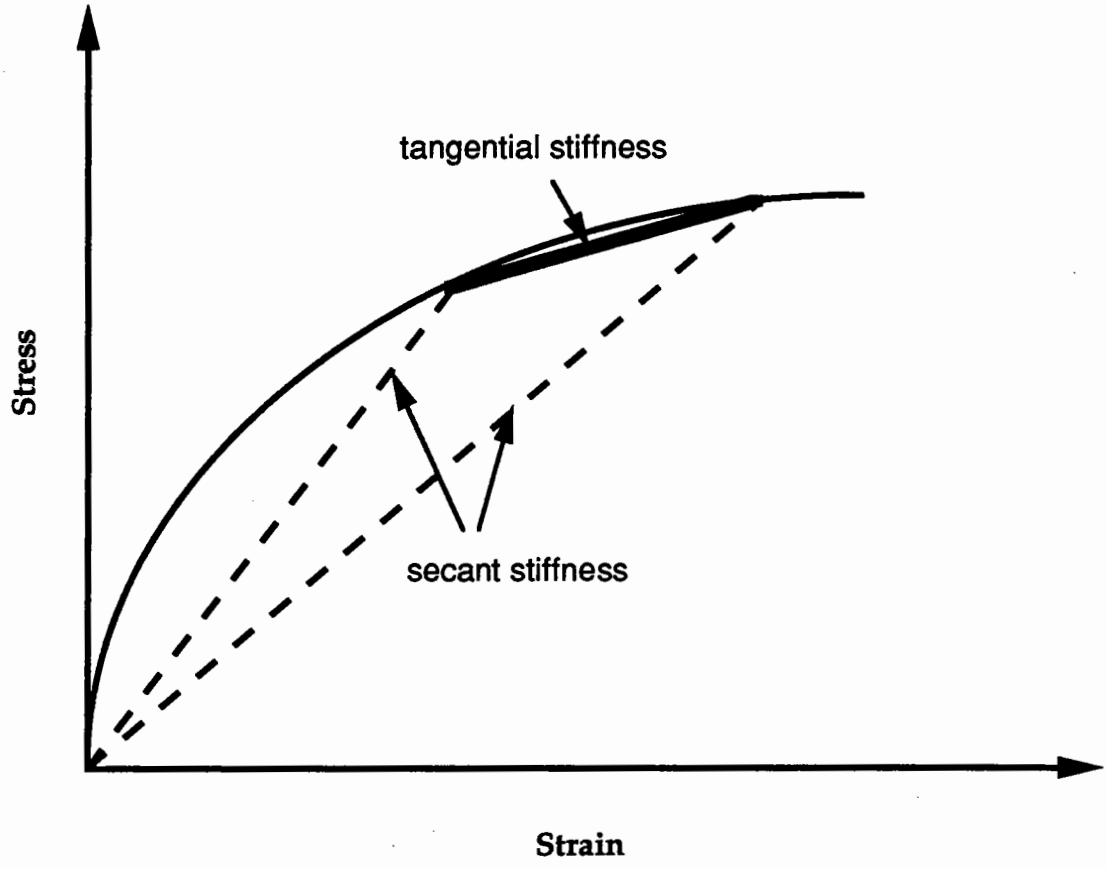

Figure 7.13. Definition of tangential and secant stiffness approach

CHAPTER 8

ASSESSING MODELS FOR GRANULAR MATERIAL BEHAVIOUR

8.1.Introduction

For this chapter, six different granular material models were investigated in order to fit the data from the repeated load triaxial tests. Five of these models were introduced in Chapter 2 and the sixth one was introduced in Chapter 7. These models are namely K-θ (Hicks and Monismith, 1971), Uzan (1985), Boyce (1980), Pappin and Brown (1980) and Elhannani (1991) and the new model. All models are expressed in terms of p (the mean normal stress) and q(the deviatoric stress). Model constants are shown in capital letters to standardize a model representation recommended by Scott (1987). In this chapter, determination of values for the model constants and prediction with different models will be presented.

8.2.Model constants

For each model, constants must be determined from experimental results. Ideally this determination should be simple, which is possible if the model can be rewritten in a linear form. The K-θ and Uzan models can be converted into a linear form by taking the logarithm of both sides of the equations. Hence, any linear regression program for

the former and a multivariable linear regression program for the latter model can be used to find constants. For the new model to predict strains due to repeated deviatoric stress with constant cell pressure a multivariable linear regression program can also be used by taking the logarithm of both sides.

8.2.1.Multiple non-linear regression analysis

Non-linear regression methods are used to estimate constants for models that are not linear in their parameters. The Boyce (1980), Pappin and Brown (1980) and Elhannani models are non-linear elastic models which cannot be converted in a linear form. Therefore, non-linear regression analysis have had to be used.

Allaart (1989) wrote a PC-based regression program particularly for the Boyce model (see section 2.4.2) assuming that B is initially known and A and C are to be calculated. A line which gives minimum error between calculated and experimental values was chosen and hence B determined by trial and error. Using the constants obtained from Allart's regression program the calculated and experimental results were compared for data from Chan (1990). It was seen that predicted values of volumetric and shear strain were many times larger than the experimental data. Therefore, other statistical packages, SPSS (1988) and BMDP (Dixon et al, 1988), which were available on the University of Nottingham mainframe computer, were used. For each of the software packages a program was written to obtain the model constants. The constants were

obtained in three ways using only the shear strain equation, using only the volumetric strain equation and using a combination of both equations

8.2.1.1.Testing packages

In order to check the packages a set of data were produced using the Boyce model assuming that A = 100, C = 150 and B =0.3 as shown in Table 8.1.

Both packages were then run using the data of Table 8.1 as input. As the solution is known, real constants are given as initial guess. The output from each regression program is given in Table 8.2.

Table 8.1. Set of data to check packages

p	q	ε_v	ε_s
30	10	0.0277	0.002055
20	20	0.0244	0.00546
10	30	0.0193	0.0133
50	40	0.0323	0.00579
20	40	0.0243	0.0109
50	50	0.0323	0.0078
30	50	0.0276	0.01027
40	50	0.0265	0.00840

Table 8.2. Results obtained from statistical packages

		A	B	C
shear	SPSS	+	0.299	150
strain	BMDP	+	0.301	150.47
volumetric	SPSS	99.99	0.337	150
strain	BMDP	105.9	0.315	*
shear+volumetric	SPSS	99.99	0.327	150
strain	BMDP	57.25	0.199	388.18
Perfect solution		**100**	**0.3**	**150**

+ A does not appear in the Boyce model for shear strain
* No convergence was obtained

The prediction of the two constants required to define the shear strain part of the Boyce model is successful with both programs. As can be seen from Table 8.2, BMDP failed to predict the three constants for the volumetric strain and for the combination of volumetric and shear strain. Therefore, the SPSS statistical package was initially chosen as the regression analysis program. Further tests were carried out using SPSS but scattering the original data firstly by 5% and secondly by 20% (Figure 8.1 and 8.2) as well as changing the initial guess for the constants. Results are shown in Tables 8.3 and 8.4 respectively. Regression coefficients outside the range +1 to -1 derive from the definition in a multi-variate situation see (SPSS (1988)). As can be seen in Table 8.3, with the 5% error in data the two shear strain constants are obtained satisfactorily when the regression coefficient is approximately unity. However, the volumetric and the combination of both strain constants cannot be obtained with high accuracy. Apart from this, many negative regression coefficients were obtained - suggesting a very poor fit even when constants were close to those sought - and many regression coefficients values close to unity were obtained - when the constant B was in error. With 20% error in data again the shear strain constants were predicted quite well. However,

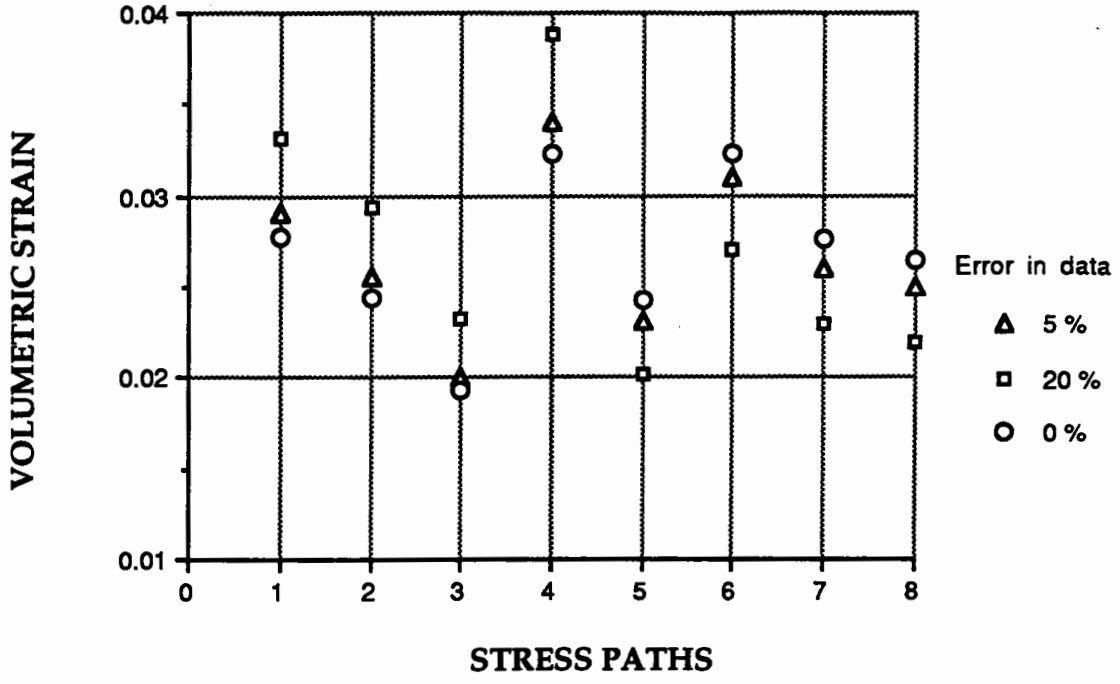

Figure 8.1 Data for testing SPSS software

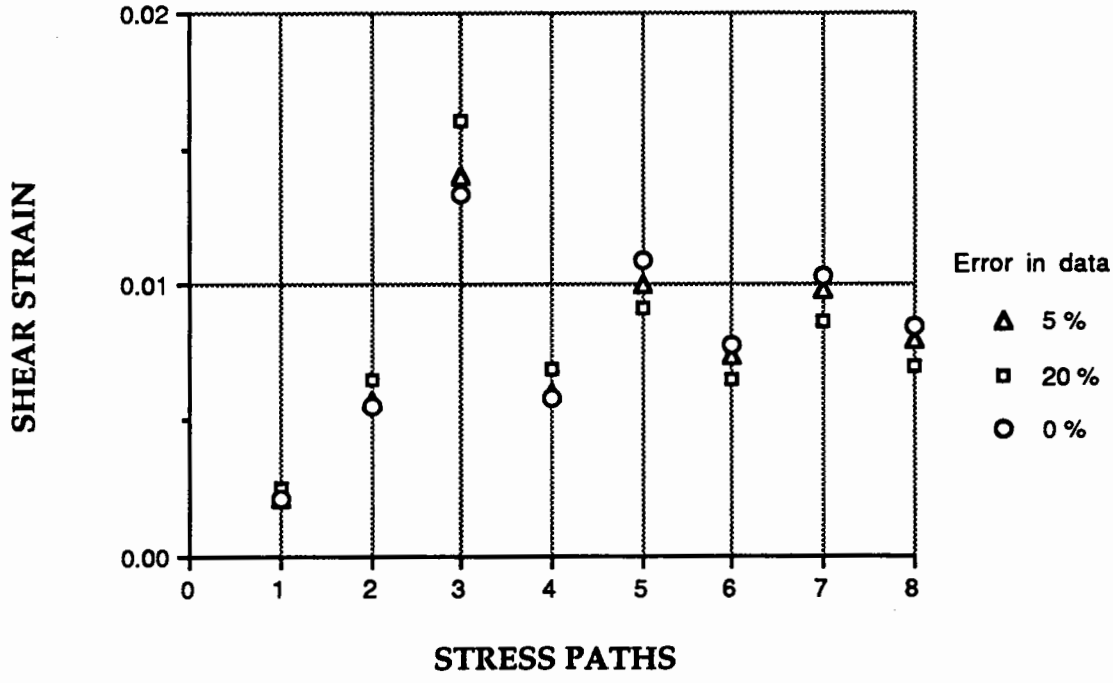

Figure 8.2 Data for testing SPSS software

Table 8.3.Prediction of Boyce(1980) model parameters using 5% error in original data

initial guess			shear strain parameters			volumetric strain parameters				volumetric+shear strain param.			
B	A	C	B	C	regression coef.	B	A	C	regression coef.	B	A	C	regression coef.
0.3	100	150	0.28	150	0.99	0.33	100	150	-0.58	0.32	100	150	-1.73
0.2	20	10	0.30	158	0.99	0.20	71	501	0.78	0.11	42	121251	0.42
0.2	50	70	0.03	70	0.83	0.15	50	70	-1.64	0.13	50	70	-1.41
0.5	70	50	0.30	158	0.99	0.03	37	136	0.65	0.20	70	50	-3.60
0.1	70	50	0.30	158	0.99	0.20	71	501	0.79	0.20	70	50	-3.60
0.5	20	30	0.30	158	0.99	0.20	71	501	0.79	0.11	43	101559	0.42
0.5	300	600	0.70	600	0.66	0.61	300	600	-0.56	0.62	300	600	-5.10
0.285	105	157.5	0.30	157.5	0.99	0.34	105	157	-0.56	0.34	105	157.5	-1.81

(Perfect solution is A=100, B= 0.3, C=150)

Table 8.4. Prediction of Boyce(1980) model parameters using 20% error in original data

initial guess			shear strain parameters			volumetric strain parameters				volumetric+shear strain parameters			
B	A	C	B	C	regression coef.	B	A	C	regression coef.	B	A	C	regression coef.
0.5	300	600	0.28	600	0.28	0.61	300	600	-0.61	0.62	300	600	-3.00
0.5	20	30	0.1	82	0.89	0.04	38	169	0.30	0.005	29	154732	0.00
0.1	70	50	0.0008	61	0.88	0.014	35	142	0.30	0.2	70	50	-2.39
0.5	70	50	0.0006	61	0.88	0.014	35	142	0.30	0.2	70	50	-2.39
0.2	70	50	0.0007	61	0.88	0.014	35	142	-0.44	0.2	70	50	-2.39
0.3	100	150	0.29	150	0.82	0.33	100	150	0.30	0.32	100	150	-1.58
0.2	20	10	0.1	82	0.89	0.04	39	169	0.30	0.006	29	102186	0.00
0.24	80	120	0.22	120	0.87	0.27	80	120	-0.47	0.26	80	120	-1.41
0.24	120	180	0.35	180	0.78	0.38	120	180	-0.45	0.37	120	180	-1.75

(Perfect solution is A=100, B=0.3, C=150)

misleading values of coefficients again occurred when fitting both the volumetric strain and the combination of both strains.

Another observation was that much of the time coefficients produced are similar to the initial guesses even when high regression values were obtained. In addition to this, different sets of constants could be obtained for the same data with almost the same regression coefficient because of the local maximum and minimum points. Furthermore, predicted values which, subjectively, are close to the ideal solution, yield poor regression coefficients.

8.2.1.2. Constants for experimental data

Experimental test results (Allaart, 1989) were also used to obtain the Boyce model constants. Using the same SPSS program as for the ideal data in Table 8.1, here, as can be seen from Table 8.5, often a zero divide error was obtained whilst attempting to fit the shear and volumetric strain together. Apart from this, no convergence and large negative regression were obtained for the single strain matching, whereas for the combination of both strains there was no clear convergence yet high regression coefficients were obtained-even though a variation in constant values of an order of magnitude was sometimes predicted. Therefore, it is hard to believe the regression coefficient value obtained from the SPSS package. It is evident that results obtained from SPSS cannot be directly used for the model prediction because of the above points.

Table 8.5.Prediction of Boyce(1980) model parameters using Allaart(1989) data-SPSS results

initial guess			shear strain parameters			volumetric strain parameters				volumetric+shear strain param.			
B	A	C	B	C	regression coef.	B	A	C	regression coef.	B	A	C	regression co.
0.4	10	20	zd*			zd*				zd*			
0.4	100	200	zd*			zd*				0.17	100	200	-39.98
0.4	200	300	zd*			zd*				0.2	200	300	-9.48
0.4	500	400	zd*			zd*				0.228	500	400	-0.99
0.4	1000	800	zd*			zd*				0.29	1000	800	0.28
0.4	2000	1800	zd*			zd*				0.39	2000	1800	0.296
0.4	4000	3600	zd*			zd*				0.456	4000	3600	0.967
0.4	40000	36000	1	40000	-3.3	1	40000	36000	-3.56	0.84	40000	36000	0.85
0.4	20000	18000	1	20000	-3.3	1	20000	18000	-3.56	0.71	20000	18000	0.92
0.4	10000	9000	1	10000	-3.3	1	10000	9000	-3.56	0.61	10000	9000	0.935
0.4	8150	6200	1	8150	-3.3	1	8150	6200	-3.56	0.51	8150	6200	0.737
0.4	7900	6200	zd*					zd*		0.536	7900	6200	0.966
0.1	79000	62000	1	79000	-3.3			zd*		0.95	79000	6200	0.78
0.536	7900	6200	1	7900	-3.3	1	7900	6200	-3.56	0.54	7900	6200	0.97

zd* zero divide error .

Because of the disadvantages of using SPSS, the BMDP software was used again. The advantage of using it is that it provides a direct comparison of individual measured and predicted values thus allowing the user to directly assess the quality of the fitting. The Allaart (1989) data were used and constants obtained from the model predictions were compared with the experimental results using a spreadsheet program. a linear regression analysis was carried out using Microsoft Excel software. Regression coefficient varied between 0.73 and 0.98 depending upon the model. Therefore, it was decided to use the BMDP package as a statistical tool.

8.3.Evaluation of models

Five types of models have been investigated which characterize the stress-strain behaviour of granular material. These models may have certain advantages and disadvantages, but it is difficult to quantify these.

In order to evaluate models, first model constants are determined for each model as explained in later sections using the same experimental data. Subsequently, all models are used to predict stress-strain behaviour. In order to measure a model's performance the regression coefficient between the measured and predicted behaviour was found to be insufficent. A good regression coefficient may be obtained although the measured values are much smaller or much higher than the predicted ones yet remain on a straight line. Therefore, the performance of each model must be measured using the slope of the linear regression line and the regression coefficient. For this purpose a simple regression analysis, forcing the intercept value to zero, was carried out assuming that

the x axis is the measured and the y axis the predicted value. If the slope is equal to 1 the best fit is obtained, if the slope is smaller than 1 then the model underestimates, if the slope is is larger than 1 then the model overestimates the measurements. Using these assessment methods LOTUS 123 was used to predict the results of the tests described. The results are shown in Table 8.6, 8.7, 8.8 and 8.9.

In the following sections the method to find the constants for each model and predictions with the models using these constants will be made. Advantages and disadvantages of each model will be discussed. In many cases, in the following sections it is clear that the fitting procedure is imperfect. No manual adjustment has, however been made to the regression derived results as this would introduce an undesirably subjective element to the analysis.

8.3.1. K-θ and Uzan Models

The K-θ model (Equation 2.1) has been widely used by pavement engineers to characterize the non-linear behaviour of granular material in which the resilient modulus is expressed in terms of the bulk stress (three times mean normal stress). However, the test results (Chapter 6) demonsrated that the deviatoric stress has also some effect although not as great as that due to the confining stress. Uzan (1985) modified the K-θ model in order to introduce the effect of deviatoric stress (Equation 2.2). The K-θ model was developed using simple deviatoric stress paths starting from zero with constant cell pressure. Matches between measured and predicted results for these stress paths are given in columns 1 and 3 of Table 8.10.

Table 8.6.Axial strain predictions due to cyclic deviatoric stress **

	K-Θ		Uzan		Boyce		Pappin		New	
	Slope	R squared	Slope	R squared	Slope	R squared	Slope	R squared	Slope	R squared
FBA	0.82	0.91	0.98	0.97	1.36	0.78	0.98	0.44	1.03	0.85
SL	0.89	0.95	0.98	0.99	1.11	0.93	0.94	0.74	1.01	1.00
GS	0.93	0.96	0.99	0.99	1.21	0.94	4.21	0.91	0.98	0.99
WRS	0.83	0.86	0.97	0.98	*	*	0.98	0.85	0.80	0.98
FS	0.94	0.96	1.00	1.00	1.10	0.95	0.82	0.96	1.08	1.00
SG	0.95	0.99	1.02	0.99	1.10	0.97	1.32	0.89	1.00	0.99

Table 8.7.Radial strain predictions due to cyclic deviatoric stress **

	Boyce		Pappin		New	
	Slope	R squared	Slope	R Squared	Slope	R squared
FBA	0.50	0.68	0.95	0.91	0.57	0.83
SL	0.65	0.79	0.88	0.85	0.91	0.98
GS	0.64	0.85	4.37	0.61	0.91	0.80
WRS	*	*	0.98	0.86	0.75	0.96
FS	0.62	0.93	0.72	0.86	1.05	0.96
SG	0.63	0.90	1.34	0.97	1.01	0.96

*Test data are not available from repeated cell pressure tests
"Slope" is the gradient of the measured strain:predicted strain regression line
**Only cyclic deviatoric stress results were used

Table 8.8.Axial strain predictions due to cyclic both stresses

	Boyce		Pappin		New	
	Slope	R squared	Slope	R squared	Slope	R squared
FBA	1.23	0.83	0.76	0.91	0.97	1.09
SL	1.30	0.94	1.36	0.88	0.99	0.94
GS	0.89	0.96	0.88	0.92	1.01	0.99
WRS	*	*	*	*	*	*
FS	0.93	0.64	1.25	0.73	0.95	0.90
SG	1.16	0.92	0.65	0.70	1.00	0.99

Table 8.9.Radial strain predictions due to cyclic both stresses

	Boyce		Pappin		New	
	Slope	R squared	Slope	R squared	Slope	R squared
FBA	0.84	0.48	0.51	-0.23	0.93	0.93
SL	0.58	0.63	0.65	-2.09	0.89	0.83
GS	0.63	-1.56	0.94	-1.83	0.71	-8.62
WRS	*	*	*	*	*	*
FS	0.09	-0.11	0.23	-0.99	0.85	0.56
SG	0.40	0.25	0.49	0.07	0.78	-0.97

*Test data are not available from repeated cell pressure tests
"Slope" is the gradient of the measured strain:predicted strain regression line
**Cyclic deviatoric, cell and both stresses results were used dependent on the model

The two models predict the axial strain (or resilient modulus) to be quite close to the experimental results under the condition of repeated deviatoric stress starting from zero with constant cell pressure. However, the Uzan model was superior when compared with K-θ model (Table 8.10). Thus the deviatoric stress also has some effect on the resilient behaviour of granular material.

However, when the general deviatoric stress paths, not necessarily starting from zero, were used, both models gave very poor predictions (columns 2 and 4 of Table 8.10). From this it can be concluded that the models can only be used to interpret the results of triaxial test in which the deviatoric stress is increased from essentially zero with constant cell pressure. A further disadvantage of this type of model is that, it assumes a constant Poisson's ratio although test results (Chapter 6) have revealed that the Poisson's ratio is not constant and is dependent on the applied stress. However, Poisson's ratio is a difficult parameter to determine from in-situ testing and generally 0.35 is accepted for all types of granular materials in the pavement, but it may have great influence on the critical strains in the pavement (ISAP, 1989). As a result the K-θ and Uzan models can reasonably be used to model repeated load triaxial test results where only vertical deformations are recorded. In pavements the methods may have applicability to, for example, non-destructive pavement test equipment such as the falling weight deflectometer (FWD) which is used to evaluate pavements by only applying vertical stress . The two models may be used to back-calculate resilient moduli of granular layers in these circumtances since the only information from the test is the vertical stress and deformation.

Table 8.10.Regression coefficients relating predicted to measured results for K-θ and Uzan models (BMDPresults)

	K-θ		Uzan	
	(0) stress paths	general	(0) stress paths	general
GWRS	0.26	0.23	0.82	0.23
FS	0.61	0.23	0.94	0.23
FBA	0.14	0.03	0.87	0.21
GS	0.87	0.4	0.96	0.4
SAG	0.85	0.42	0.95	0.43
SL	0.76	0.43	0.97	0.44

Another advantage of the models is that the model constants can be found by using a linear regression program for the K-θ model and a multiple linear regression program for the Uzan model (by taking the logarithm of both sides) in each case.

8.3.2. Boyce and Elhannani Models

The Boyce (1980) model (Equation 2.7 and 2.8) was developed using the theorem of reciprocity, that is the volumetric and shear strain are linked to each other by the theory of reciprocity

$$\frac{\partial \varepsilon_v}{\partial q} = \frac{\partial \varepsilon_s}{\partial p} \qquad (8.1)$$

where ε_v ,ε_s are the volumetric and shear strain respectively
p, q are the mean and deviatoric stresses respectively

The model (Equation 2.4 and 2.5) contains only 3 constants which is reasonably convenient for a non-linear elastic material since two constants are needed for a linear elastic material. Although the model was developed to predict the volumetric and shear strain, it can also be used to predict the axial and radial strain test results since the axial ε_a and radial strains ε_r can be expressed in terms of the volumetric and shear strain as shown below:

$$\varepsilon_a = \frac{\varepsilon_v}{3} + \varepsilon_s \qquad (8.2)$$

$$\varepsilon_r = \frac{\varepsilon_v}{3} - \frac{\varepsilon_s}{2} \qquad (8.3)$$

The volumetric strain equation contains three constants which may be determined from repeated load triaxial test results and two of them B and C are also used for the shear strain prediction. The problem is how to determine these three constants so that they will satisfy both equations at the same time.

Initially it was thought that constants might be found only from the volumetric strain equation since it also includes the constants for shear strain. In order to check this hypothesis a non-linear regression program was written for the BMDP software for both the volumetric and shear strain. If the hypothesis works, constants B and C in the model obtained from the volumetric and from shear strain data have to be the same. This would also show the applicability of the reciprocity theorem to granular material. However, results showed that B and C are different for both the volumetric and shear strain equation (Table 8.11). This tends to indicate that the reciprocity theorem is not

applicable to granular material behaviour. Clearly, the theorem is violated more by some materials than others.

Table 8.11. Boyce model constants from volumetric and shear strain data

	volumetric strain			shear strain	
	A	**B**	**C**	**B**	**C**
FS	774092	1.07	100000	0.16	8647
GS	285923	0.74	95248	0.14	10144
SAG	14642	0.47	69298	0.20	15179
GWRS	41936	0.67	14183	0.20	9765
FBA	11119	0.61	3664	0.27	7085
SL	11260	0.53	6465	0.10	5399

A second hypothesis was that, rather than using the volumetric and shear strain equations, either the axial or radial strain equation can be derived using equations (8.2) and (8.3). Using the constants obtained from the axial strain equation it was seen that the axial strain predictions were close to experimental results (see Figure 8.3 and Karasahin et al, 1993), but the radial strain predictions were similar in magnitude to axial strain since shear strain (Figure 8.4) obtained using the axial strain parameters was always close to zero in magnitude, hence the axial strain has to be equal to the radial strain (one third of volumetric strain) which was not according to the experimental data.

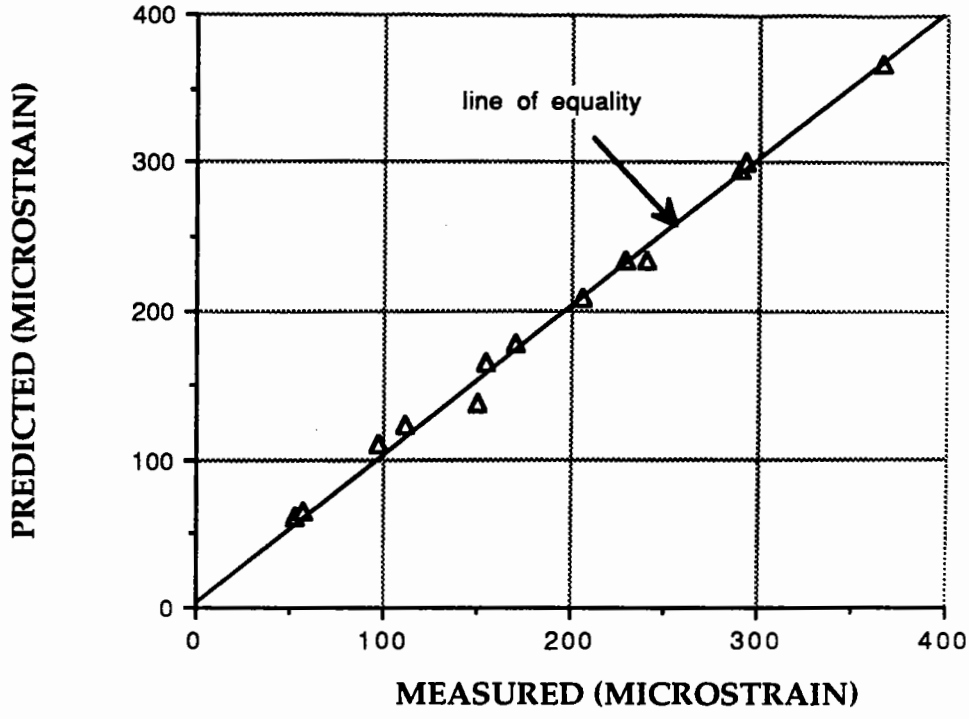

Figure 8.3 Boyce (1980) model prediction of axial strain with axial strain parameters (SAG)

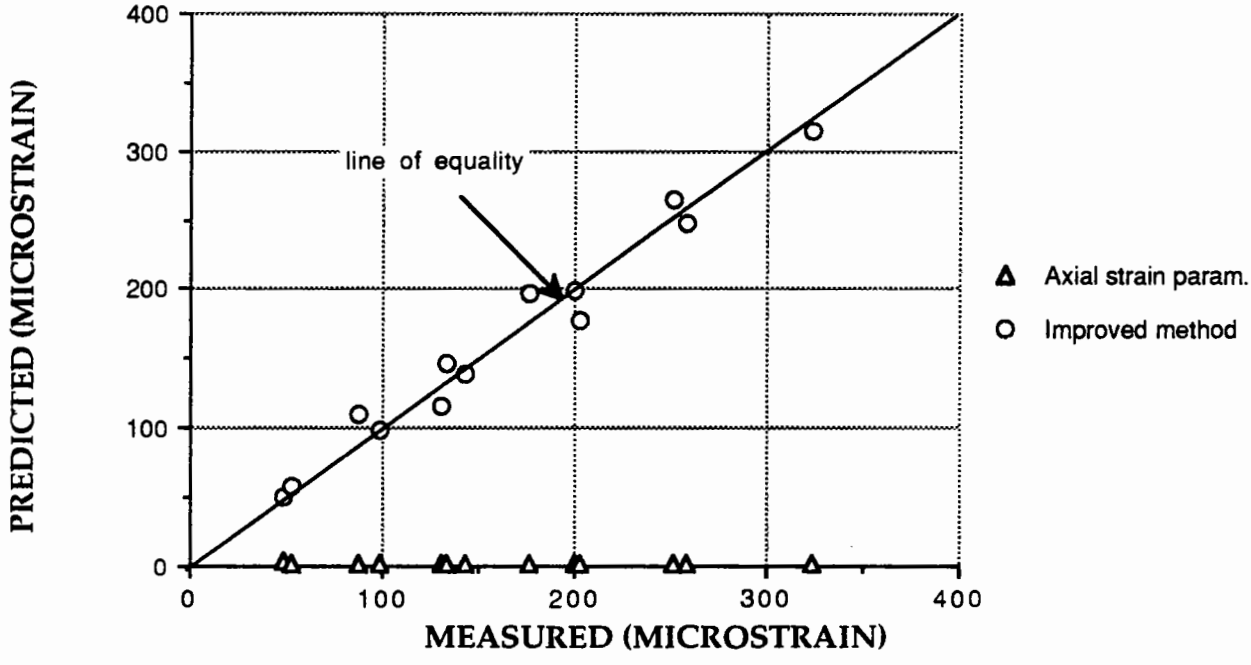

Figure 8.4 Comparison of methods to find shear strain constants for Boyce (1980) model (SAG)

In order to improve the model prediction, use can be made of the fact that the model is isotropic. Therefore the bulk modulus, which is due to A and B in Equation 2.7 can be determined from repeated cell pressure results. Therefore the only unknown in the model is C, due to shear modulus in the model. After having determined A and B, C can then be worked out from the shear strain equation using shear strain data from repeated deviatoric stress tests. This approach has worked and prediction with the model has improved (Figure 8.4 and 8.5).

In summary it is noted that the principal advantage of the model is that it only requires three constants which can be determined from repeated triaxial test results using a non-linear regression program. The model requires data from repeated cell pressure tests in order to improve prediction. The model still suffers from an inability to accurately predict volumetric strain (see Section 2.4.2).

Elhannani (1991) modified the model (Equation 2.9 and 2.10) in order to introduce anisotropy into the model. The modified model requires 4 constants, three as for the Boyce model and the fourth one to permit anisotropy. The model is able to predict shear due to repeated cell pressure test results where the deviatoric stress is zero whereas the Boyce model is not. A and B in the model can be determined from repeated cell pressure tests using the volumetric strain equation in the same way as for the Boyce model. D can also be obtained from the cyclic cell pressure results using the shear strain equation since other terms which include q will be zero in Equation 2.10. C can then be determined using the shear strain equation for deviatoric stress paths with constant cell pressure

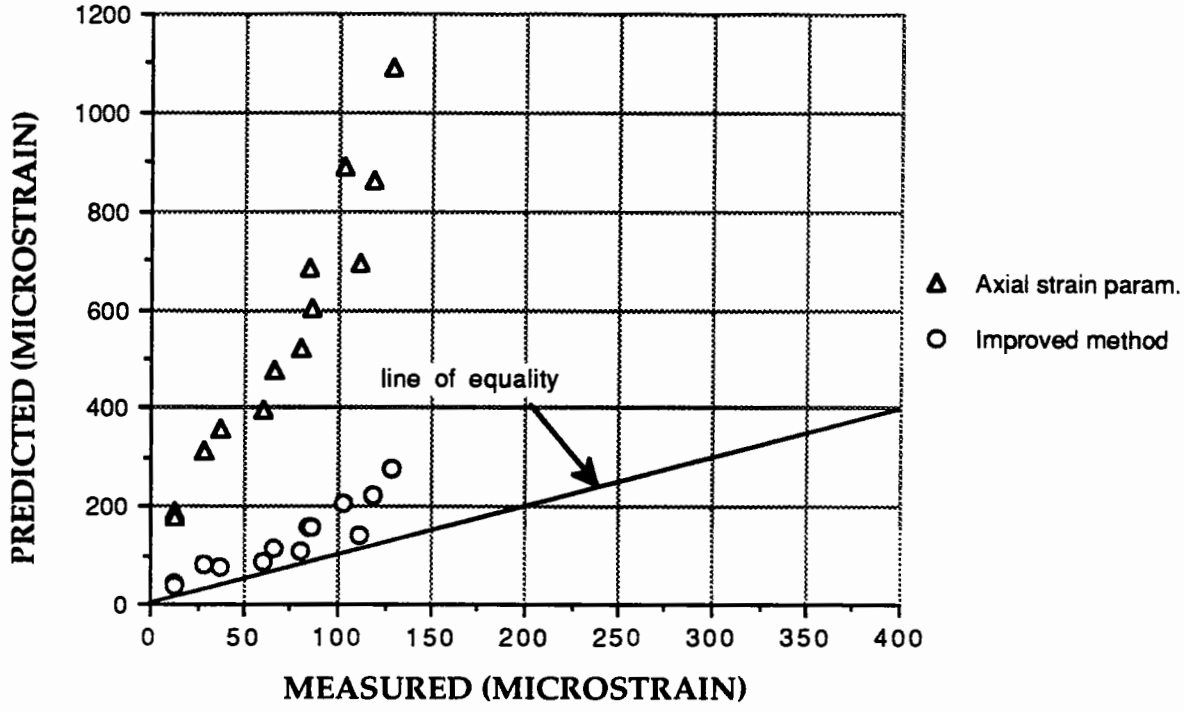

Figure 8.5. Comparison of methods to find volumetric strain constants for Boyce (1980) model (SAG)

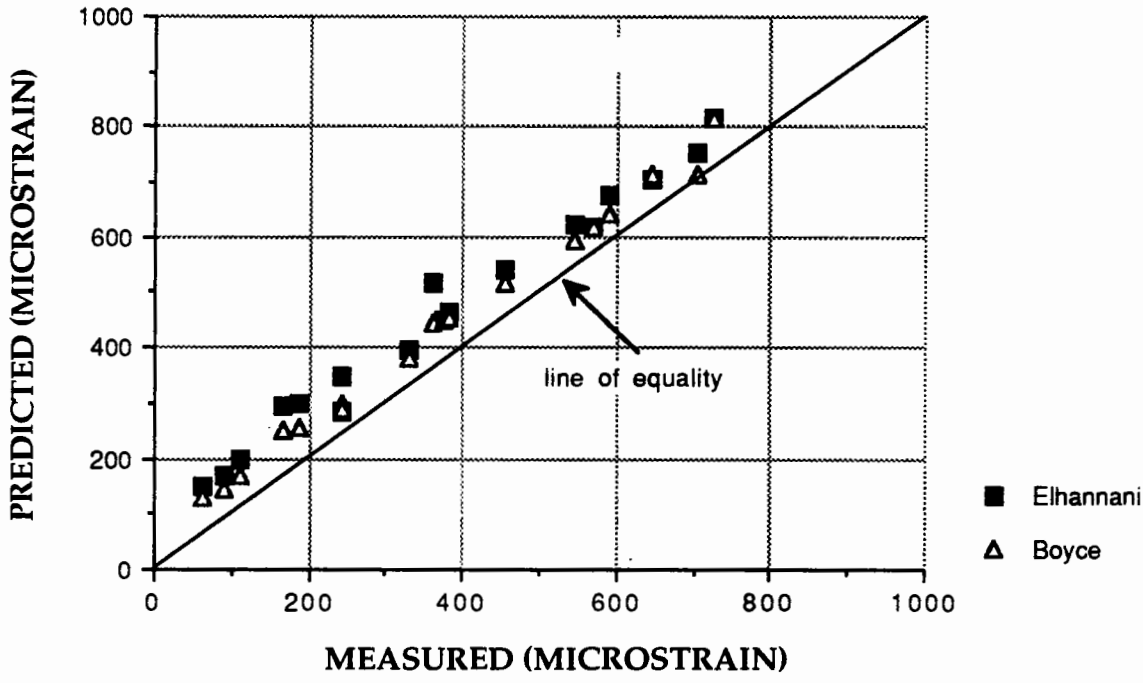

FIGURE 8.6. Axial strain due to cyclic both stresses (FS)

The model has the same drawbacks and advantages as the Boyce model. The only improvement is the introduction of anisotropy in the model. However, the effect of this improvement was not observed for the FS (Figure 8.6).

8.3.3. Pappin and Brown Model

The Pappin and Brown model was developed by separating the volumetric and shear strain so that the assumption of reciprocity was overcome. The model is better expressed in terms of contours (Pappin and Brown, 1985) and for this reason has come to be called a "contour model". The Boyce model can take a similar form when the reciprocity theorem is neglected. In this thesis, the model without stress path length dependency as written by Brown and Selig (1991) was used. As a result the model has 5 constants, 2 more constants than the Boyce model. Three of them are for the volumetric strain and 2 of them for the shear strain. A, B and C in the model, which are constants for the volumetric strain, can be determined from the volumetric strain results either from the repeated deviatoric stress with constant cell pressure or from the repeated cycling of both stresses using a non-linear regression program. D and E in the model which are constants for the shear strain are obtained in a similar way. The model can also be used to predict the axial and radial strain using Equation 8.2 and 8.3.

One of the advantages of the model is that, unlike the Boyce model, it does not need data from repeated cell pressure tests to predict the behaviour under repeated deviatoric stress results with constant cell pressure. Its ability to predict behaviour accurately is discussed in Section 8.4.

8.3.4.New model

The new model was developed using a stepwise regression analysis. In order to predict the results of repeated deviatoric stress results with constant cell pressure, requires 7 constants, 3 for the resilient modulus and 4 for the Poisson's ratio. Any multiple regression program can be used to determine the model constants. Although it contains more constants than the Pappin and Brown and the Boyce model, it is relatively easy to find them. This simplified 7-parameter version of the model is used in Figures 8.7, 8.8, 8.9, 8.10, 8.11 and 8.12 which follow.

In order to predict the observed test results when both stresses are repeated, inherent anisotropy is included in the model. The model is then expressed in a cross-anisotropic form in which 13 constants exist, 3 for the resilient modulus (which can be determined from the repeated deviatoric stress test), 2 for the inherent anisotropy which can be determined from the repeated cell pressure test , 4 for the Poisson's ratio due to the effect of horizontal strain on horizontal strain and 4 for the Poisson's ratio due to the effect of horizontal strain on vertical strain. These last 8 constants could also be determined from the results of the tests under repeated cell pressure tests in which constant deviatoric stress was intended. After determination of the resilient modulus coefficients from the repeated deviatoric stress results and the inherent anisotropy coefficients from the repeated cell pressure data using a multiple linear regression program , the Poisson's ratio due to effect of the horizontal strain on vertical strain.could be determined by a non-linear regression substituting the resilient modulus and inherent anisotropy constants into the axial strain equation. Poisson's ratio due to horizontal strain on horizontal strain could be then determined by a non-linear regression substituting the constants of Poisson's ratio due to horizontal strain on

vertical strain and inherent anisotropy into the radial strain equation. The 13-parameter model has been used in Figures 8.13, 8.14, 8.15 and 8.16.

The advantage of the model is the simplicity of the determination of constants to predict the repeated deviatoric stress results. When both stresses are cycled, which is similar to the case of traffic loading, inherent anisotropy is taken into account. However, non-linear regression analysis is required to determine the Poisson's ratio due to horizontal strain on horizontal strain and due to horizontal strain on vertical strain. One of the aims was to improve the volumetric strain prediction since the Boyce model suffers at this point. Figures 8.7 and 8.8 shows that Boyce and Elhannani models are far away from the prediction of volumetric strain, although the new and Pappin models make a good prediction. This may demonstrate that models developed using the idea of decoupled strains (no reciprocity) give better predictions of volumetric strain.

8.4.Prediction of strains

In this section predictions made by the different models are discussed in terms of axial and radial strain since they are the only direct measurements from the repeated load triaxial apparatus. The results shown in Tables 8.6, 8.7, 8.8 and 8.9 do not mean that a model is bad or good, but highlight some drawbacks of each model. The predictions are totally dependent on the model constants which have been derived using the BMDP statistical program and the experimental results, therefore some human factors

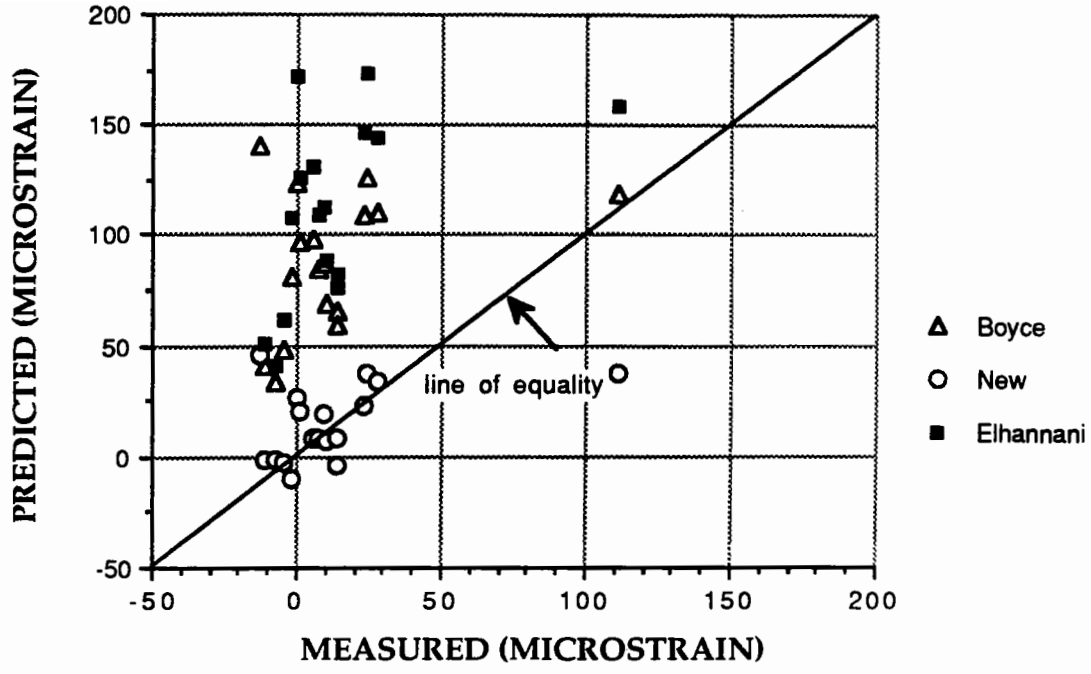

Figure 8.7. Volumetric strain due to repeated deviatoric stress (GS)

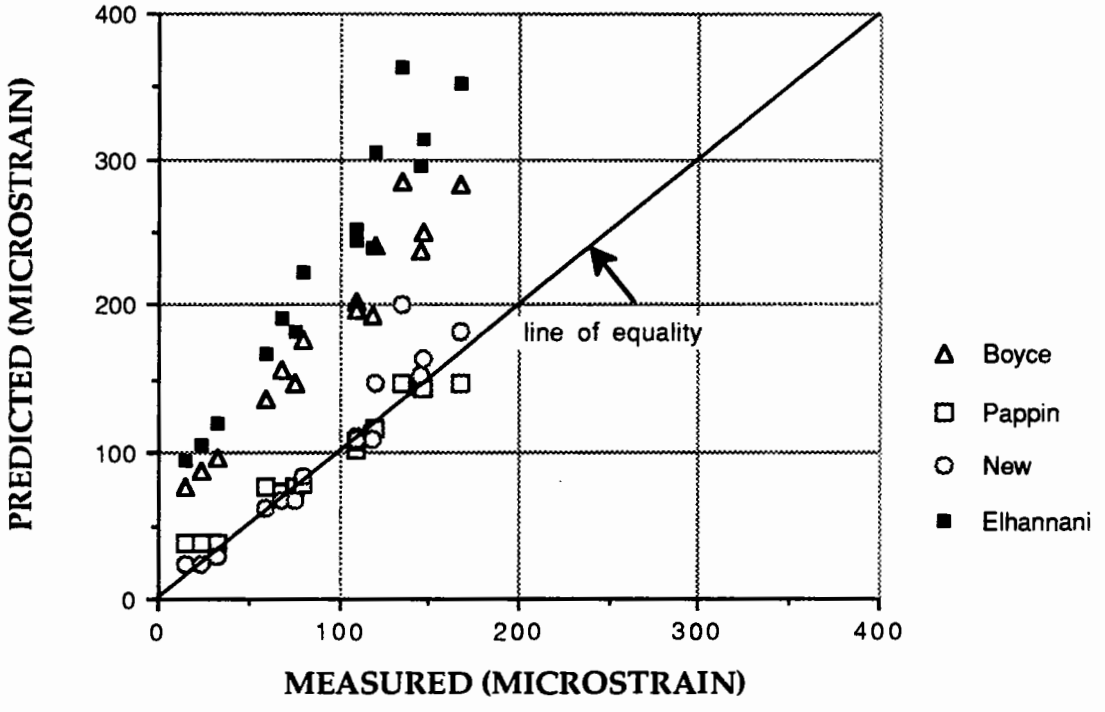

Figure 8.8. Volumetric strain due to repeated deviatoric stress (FS)

(particularly in making the estimate of regression procedure starting point) as well as computing factors have to be taken into account.

8.4.1.Axial strain predictions due to repeated deviatoric stress

All the models considered are able to predict the axial strain measurements due to the repeated deviatoric stress with constant cell pressure (see Figure 8.9 and 8.10 for examples). The Uzan model was superior overall for predictions when all materials were considered (Table 8.6). The Pappin and Brown model gave a low value of regression coefficient for FBA and substantially overpredicted the axial strain for GS. The Boyce model overestimated the axial strain for all materials whereas the K-θ model did the opposite.

If only axial strain predictions are important it is recommended that simple models such as K-θ, Uzan and the new model be used since it is relatively easy to find constants for them. However, where more complicated analysis such as a non-constant Poisson's ratio is considered, the Boyce, the Pappin and Brown and the new model are recommended.

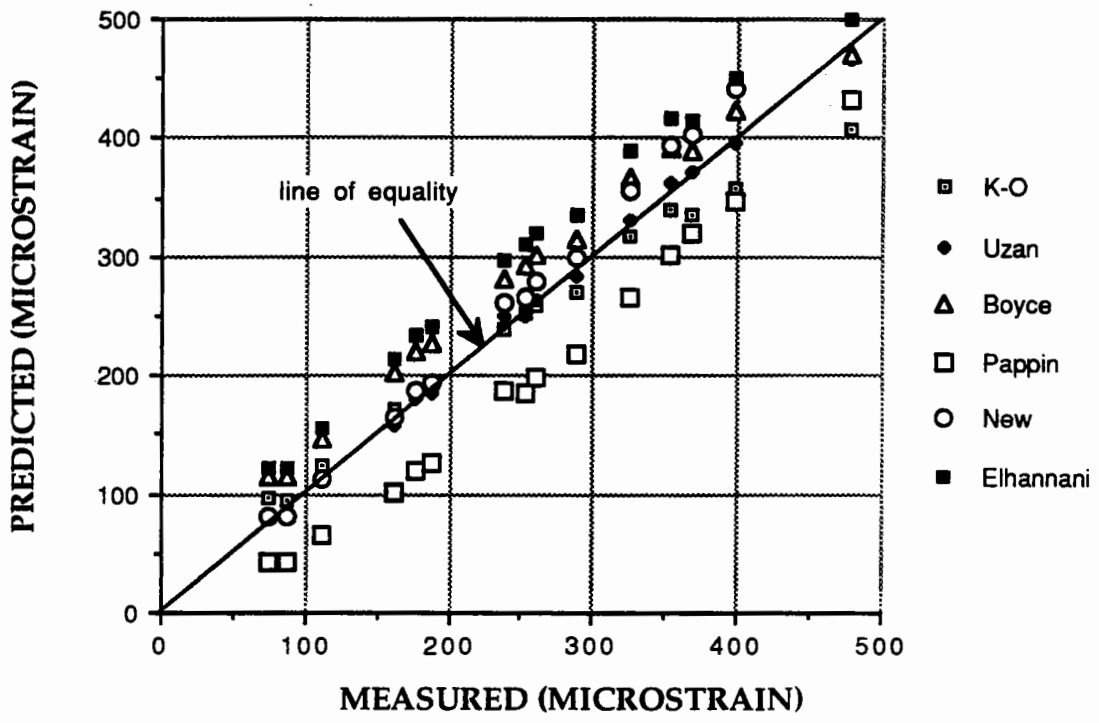

Figure 8.9. Axial strain due to repeated deviatoric stress (FS)

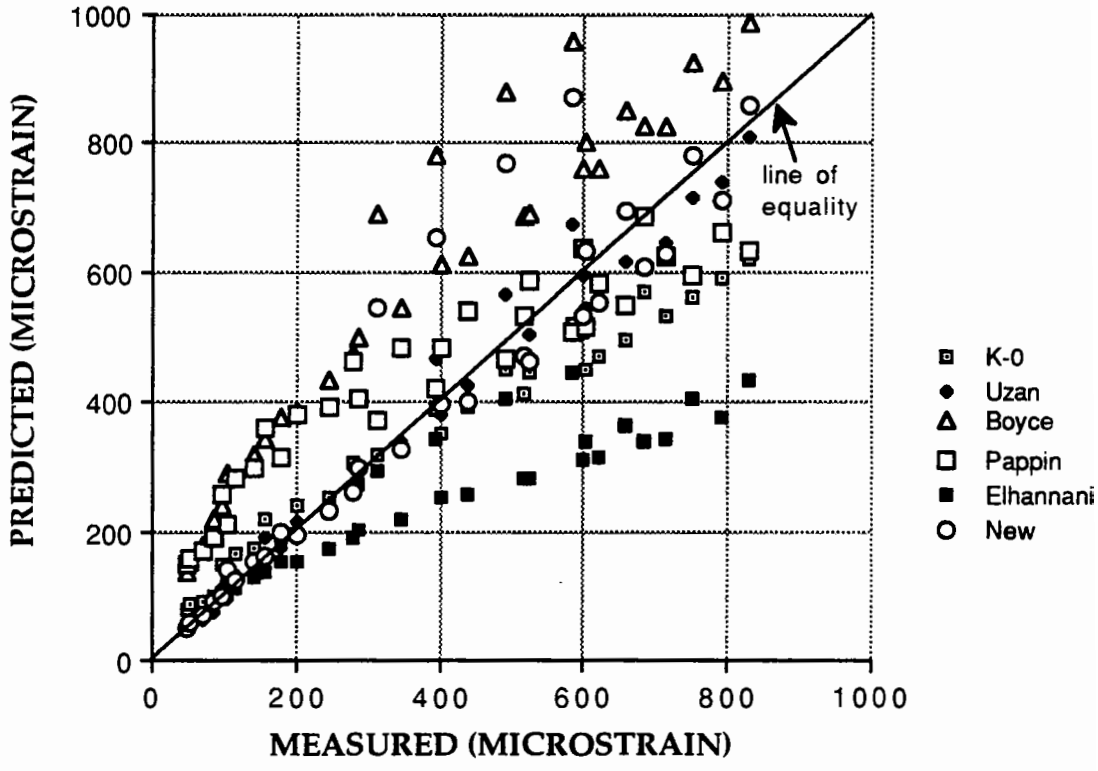

Figure 8.10. Axial strain due to repeated deviatoric stress (FBA)

8.4.2.Radial strain predictions due to repeated deviatoric stress

The K-θ and Uzan models assumes the constant Poisson's ratio. However, the test results (Chapter 6) revealed that this is not true for granular material. As a result these models were not used to predict the radial strain.

In the new model the Poisson's ratio is calculated by means of Equation (7.88) and the resultant radial strain is calculated by the Equation (7.85). The Boyce and the Pappin and Brown models are used to predict the radial strain using Equation 8.3.

The prediction of the radial strain is often not as good as that for the axial strain (Table 8.7) (see for example Figures 8.11 and 8.12). Some models showed a good performance for a particular material whereas a poor prediction for another material. The Pappin and Brown model again overpredicted the radial strain for gritstone. For the washed river sand there was no available data from the repeated cell pressure test, therefore no prediction was made by the Boyce model. The Boyce model underestimates the radial strain about as much as it did the axial strain. When overall performance is considered the new model was superior.

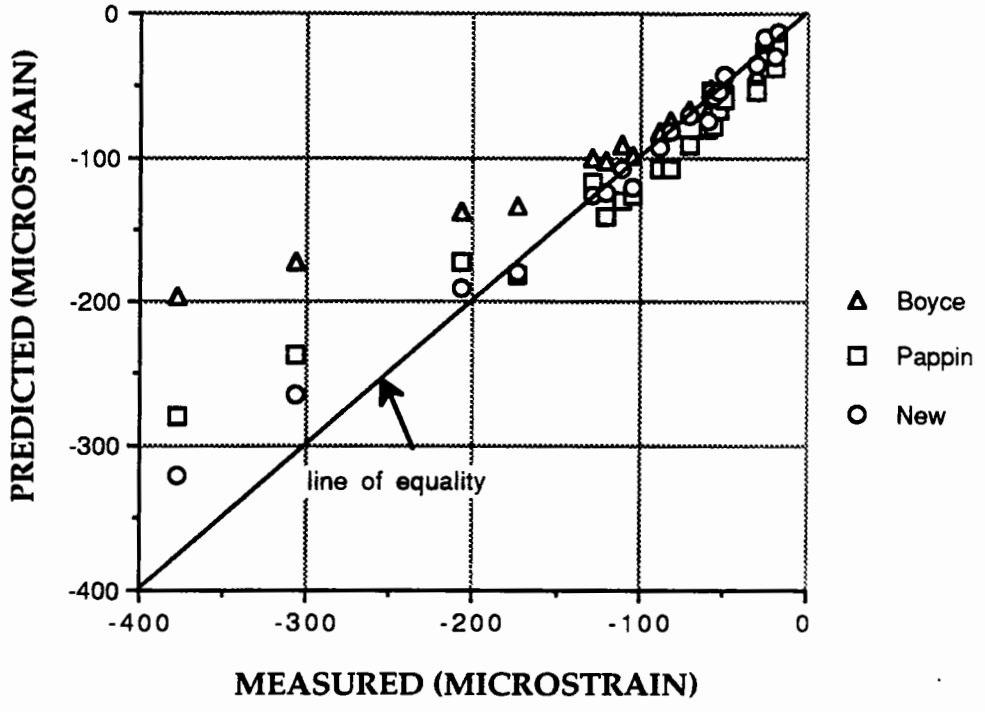

Figure 8.11. Radial strain due to repeated deviatoric stress (SL)

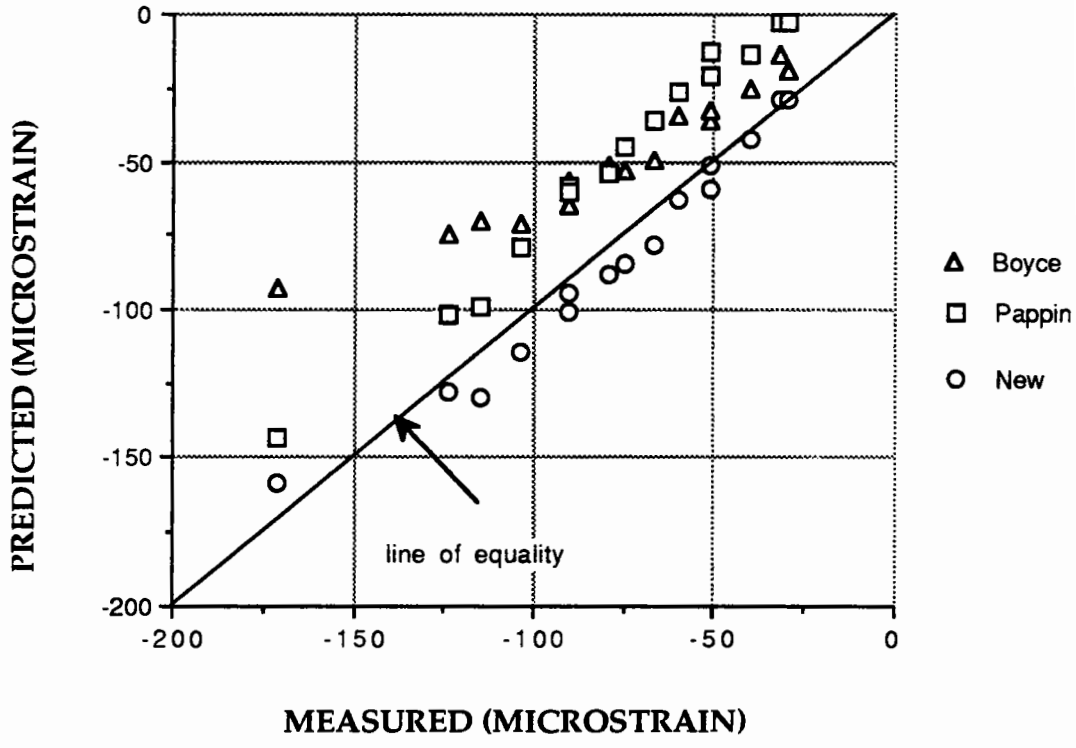

Figure 8.12. Radial strain due to repeated deviatoric stress (FS)

8.4.3.Axial strain predictions due to repeated axial and confining stresses

The Boyce, The Pappin and Brown and the new model (equation 7.99) were used to predict the axial strain due to repeatition of both stresses (Table 8.8). Generally all the models showed a good performance (see Figures 8.13 and 8.14). But the Boyce model for the Fontainebleu sand and the Pappin and Brown model for Fontainebleu sand and sand and gravel gave low regression coefficients. The new model performed better.

On this basis the new model should be used to predict the axial strain due to repeated both stresses, although it contains more constants than the other models which may be a disadvantage.

8.4.4.Radial strain predictions due to repeated axial and confining stresses

Unfortunately the prediction of the radial strain due to repetition of both stresses (Table 8.9) was not good when compared with other predictions (see for example Figures 8.5 and 8.6). Especially for GS the three models failed to predict radial strain satisfactorily. It is possible to see negative regression coefficients, clearly indicating the lack of fit. In particular the Pappin and Brown model largely failed to predict the

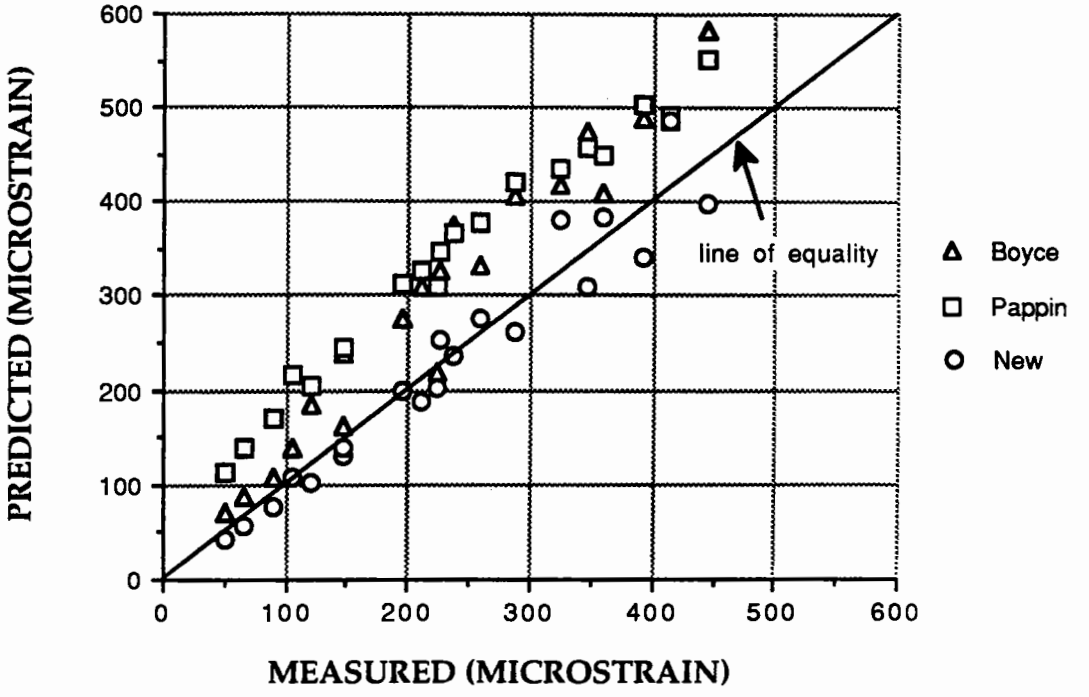

Figure 8.13. Axial strain due to repeated both stresses (FBA)

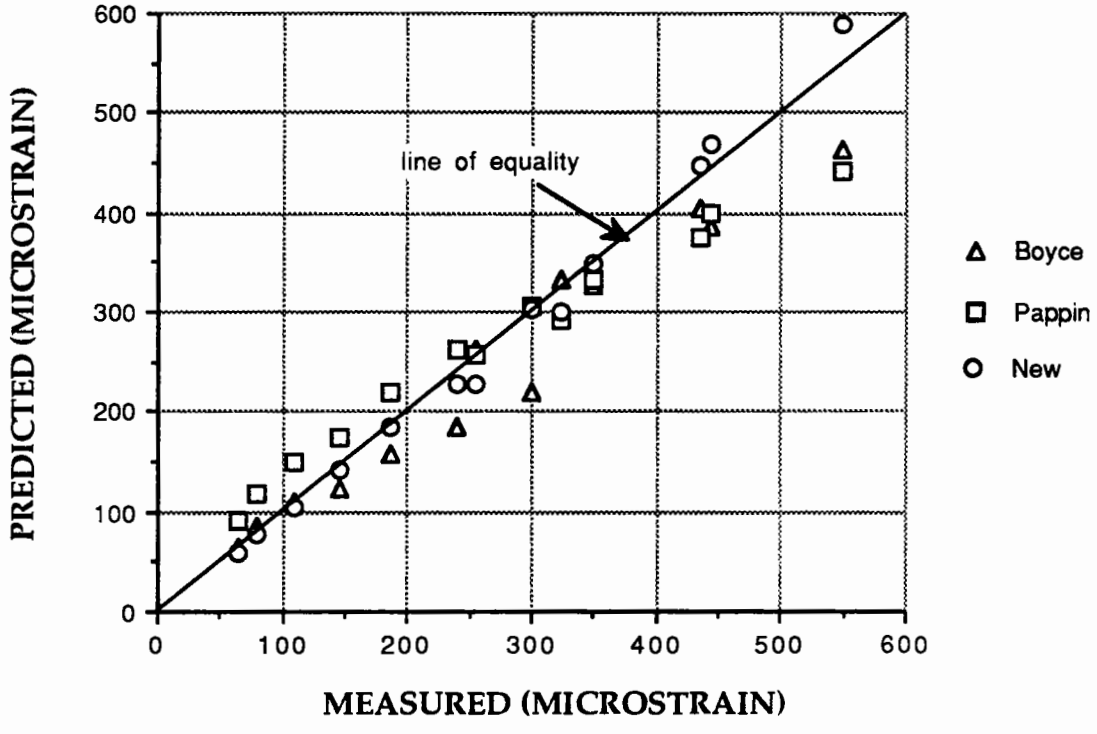

Figure 8.14. Axial strain due to repeated both stresses (SL)

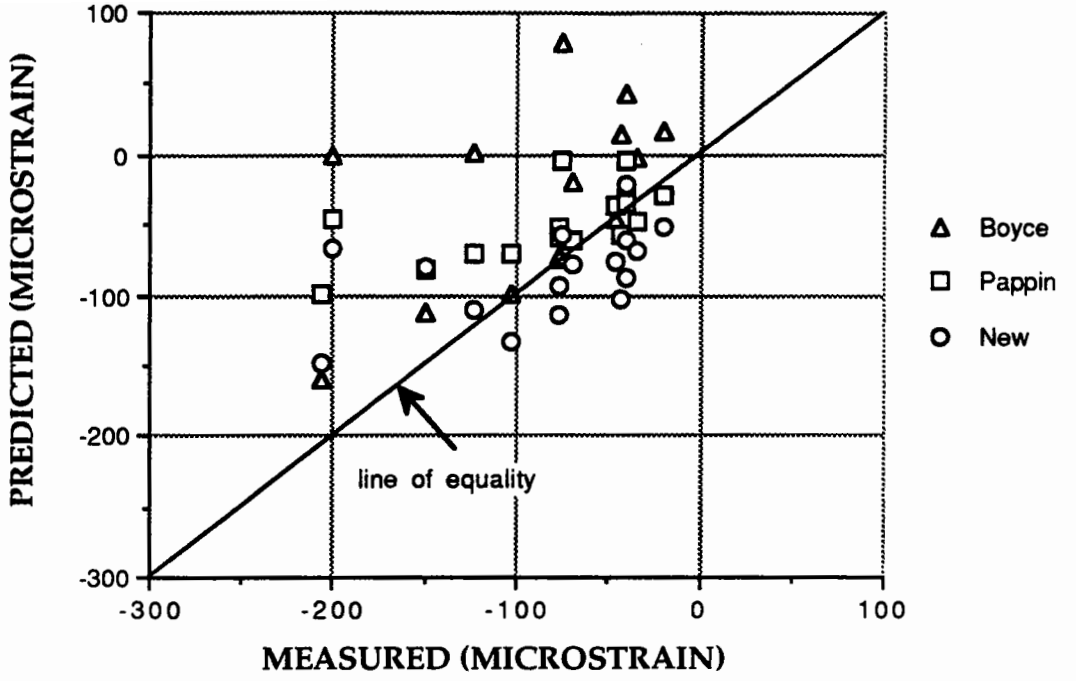

Figure 8.15. Radial strain due to repeated both stresses (SAG)

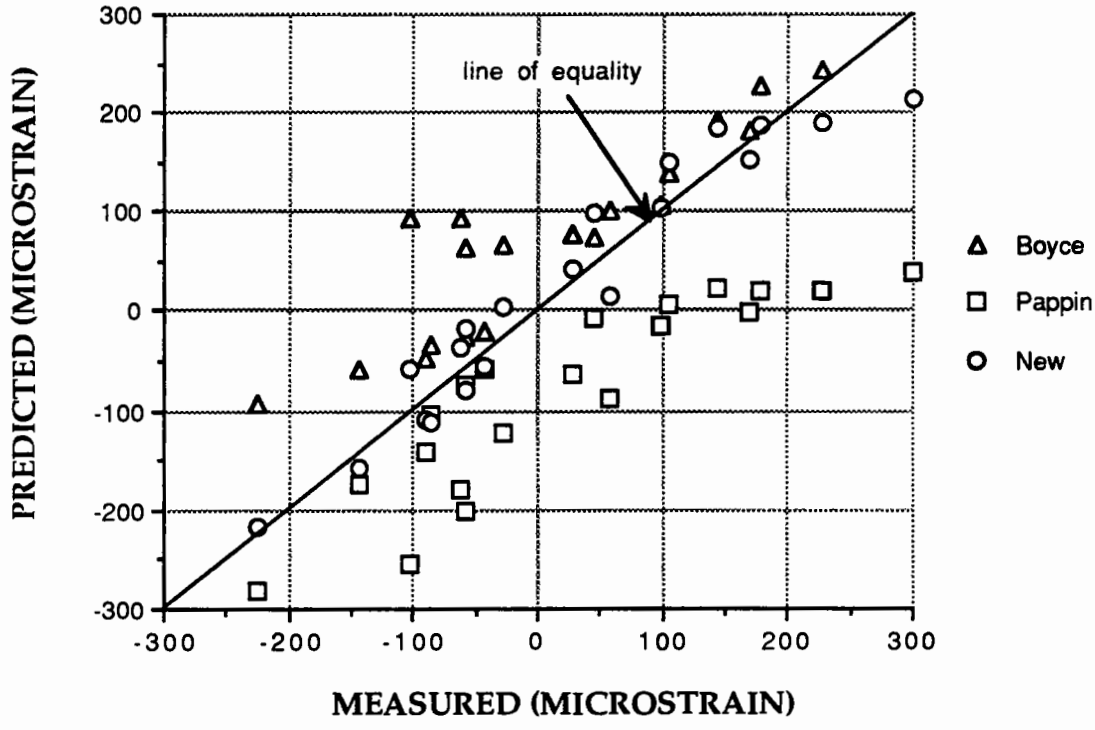

Figure 8.16. Radial strain due to repeated both stresses (FBA)

radial strain for all materials. The Boyce and the new model predictions were also not as good as previously discussed. This may show

• the difficulty of predicting the radial strain due to the repetition of both stresses,

• bad fitting of models to raw data,

• bad experimental measurements (radial strains measurements are often smaller under these combined-stress paths and thus more susceptible to noise),

• complicated behaviour of material under this stress condition.

8.4.5.Prediction of strains due to the repetition of both axial and confining stresses using the parameters obtained from repeated axial stress data

The aim of this section is to show whether repeated deviatoric stress test results (which are simple to perform) can be used to predict the complex stress-strain relationship when both stresses are cycled-which is closer to the situation in the pavement.

In Section 8.4.3 and 8.4.4 axial and radial strains due to the repetition of both axial and radial stresses were discussed using the Boyce, the Pappin and the new model. In this section other models (the K-θ, the Uzan and the Elhannani) are also included in order

to see their potential. The version of the new model considered here is to predict deviatoric stress results.

Materials discussed here are the same as in Section 8.4.3 and 8.4.4 (FBA, SL and SAG) so as to see the differences in predictions.

8.4.5.1.Axial strain predictions

FBA: The predictions are shown in Figure 8.17. The Boyce and the Pappin models gave higher predictions than before. The new model (which is developed for the prediction of repeated deviatoric stress results) gave a better fit. The Elhannani model made the largest over-predictions. Both the K-θ and the Uzan models made under-predictions. Table 8.11 shows comparison of different models using the regression coefficient and slope of the fitted line.

SL: Predictions are ahown in Figure 8.18. For this material the Boyce and the Pappin models make overpredictions when compared with the results obtained from the repetition of both stresses. But this time the predictions of the Pappin model is closer to the line of equality. The new model made overpredictions. The Elhannani model still made the most overpredictions. The K-θ and the Uzan models again made under-predictions.

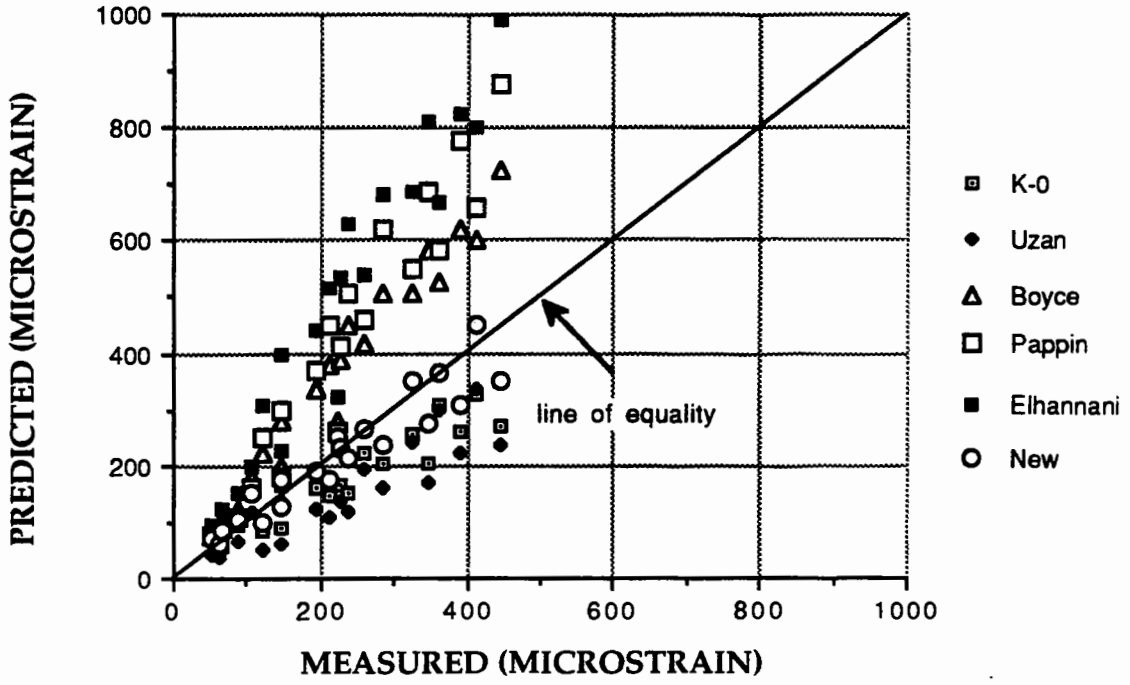

Figure 8.17 Axial strain due to repeated both stresses with deviatoric stress parameters (FBA)

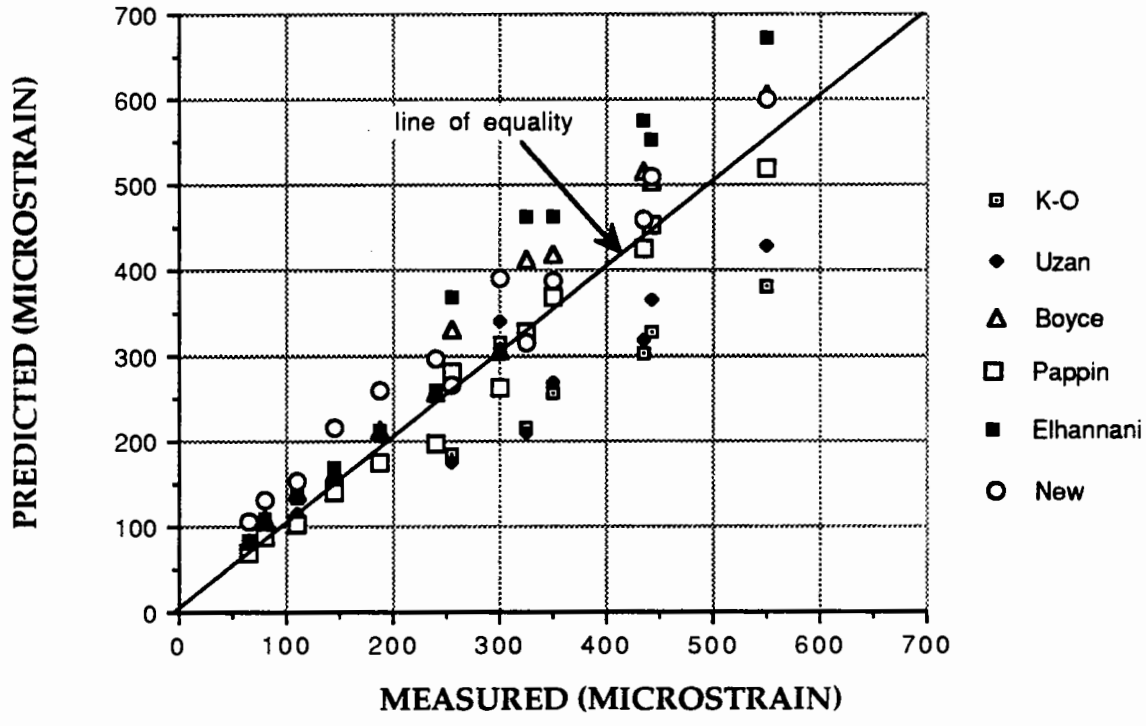

Figure 8.18 Axial strain due to repeated both stresses with deviatoric stress parameters (SL)

Conclusions can be drawn that

- The K-θ and the Uzan models probably make under-predictions,

- The Pappin and the Boyce models make over-predictions when they are compared with the predictions made with the parameters obtained from the repetition of both stresses,

- The Elhannani model probably over-predicts values,

- The new model makes over and under-predictions.

8.4.5.2.Radial strain predictions

In this section the K-θ and the Uzan models are exluded since they assume a constant Poisson's ratio.

FBA: Predictions are shown in Figure 8.19. It is interesting to note that the performance of the Boyce and the Pappin models increased considerably when compared with predictions made by parameters obtained from the repetition of both stresses. Both the Elhannani and the new model gave an under-prediction of radial strain.

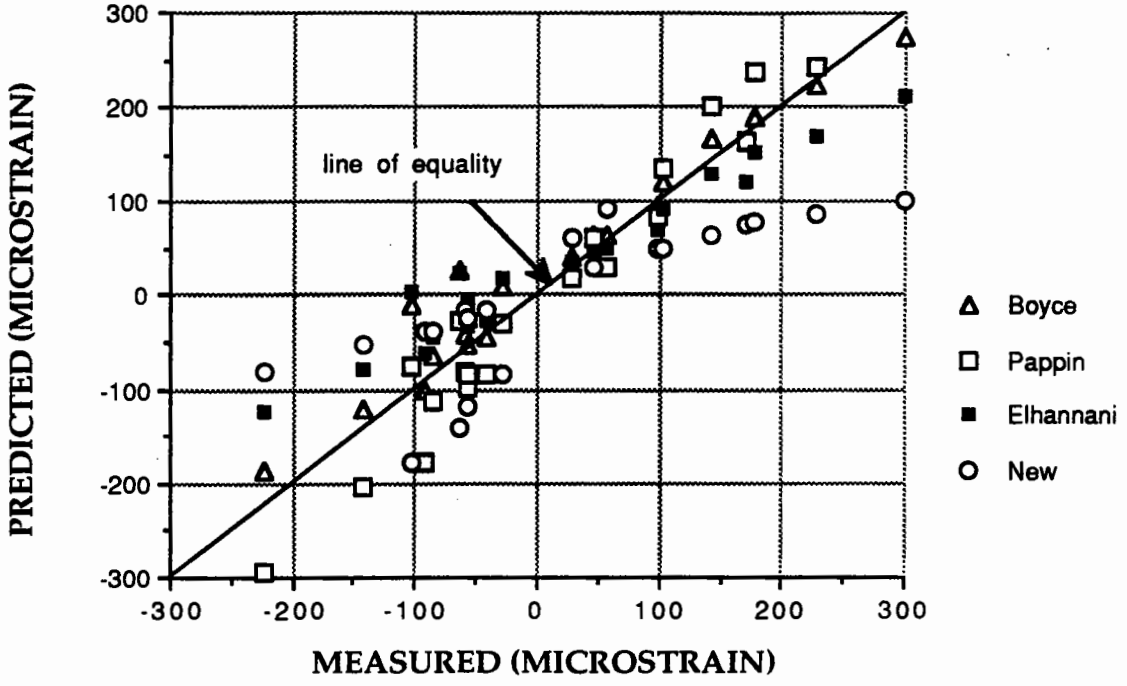

Figure 8.19 Radial strain due to repeated both stresses with deviatoric stress parameters (FBA)

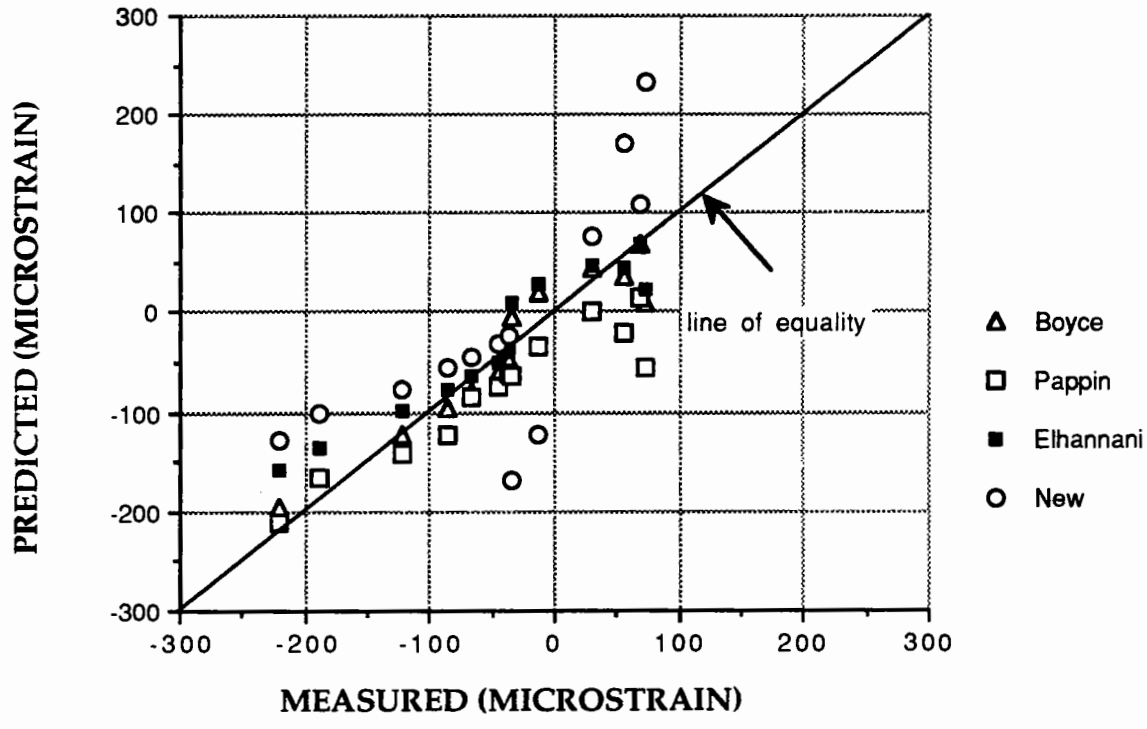

Figure 8.20 Radial strain due to repeated both stresses with deviatoric stress parameters (SL)

SAG: Predictions are shown in Figure 8.20. The Boyce model showed some improvement in the predictions. But performance of the Pappin model slightly decreased. The Elhannani model made similar predictions to the Boyce model. The prediction of the new model was the similar to other models.

Conclusions can be drawn from the above observations that:

- The performance of the Boyce model may improve when it is used with deviatoric stress parameters to predict repeated both stresses results,
- The Pappin model could make over or under predictions,
- The performance of the Elhannani and the new model are not good as the Boyce and the Pappin models.

8.4.5.3.Summary of results and conclusions

Summary of results are given in Tables 8.12 and 8.13 with regression coeffcients and slopes of the fitted linear lines.

The Boyce model made good predictions of radial strain at the price of over-predicting axial strain. However, it needs data from a repeated load traxial test apparatus which can cycle cell pressure even when only deviatoric stress cycling is to be modelled.

The Pappin model may also give better radial strain predictions at the price of over-predicting the axial strain. The benefit of the Pappin model is that it does not need data from repeated confining pressure tests. Therefore it might be good to use this model

Table 8.12 Prediction of axial strain due to repeated both stresses with deviatoric stress parameters

	FBA		SL	
Models	R^2	Slope	R^2	Slope
K-θ	0.76	0.75	0.69	0.78
Uzan	0.78	0.66	0.83	0.83
Boyce	0.96	1.60	0.98	1.15
Pappin	0.93	1.83	0.98	0.98
Elhannani	0.93	2.14	0.97	1.26
New	0.88	0.94	0.94	1.13

Table 8.13 Prediction of radial strain due to repeated both stresses with deviatoric stress parameters

	FBA		SAG	
Models	R^2	Slope	R^2	Slope
Boyce	0.93	0.91	0.31	0.47
Pappin	0.96	1.18	-0.10	0.43
Elhannani	0.89	0.67	0.31	0.45
New	0.63	0.49	-0.99	0.50

where only a repeated load triaxial apparatus which cannot cycle cell pressure is available.

The K-θ and the Uzan models always under-predict the axial strain at a maximum of about 34% (based on above observations).

The Elhannani model always over-predicts the axial strain when compared with other models and it also needs more parameters to determine. Therefore, the Boyce model is more preferable for this particular study.

The new model may be used to predict axial strain, but its performance is low for the prediction of radial strain.

8.4.6.Inherent anisotropy predictions

For this particular section two models are chosen which are the new and Elhannani (1991) models since they were developed to take anisotropy into account. The Elhannani model (Equation 2.9 and 2.10) can be rewritten in terms of the axial and the radial strain using the relationships of Equation 8.2 and 8.3. Then the ratio of axial strain to radial strain (anisotropy), assuming that q (deviatoric stress) is zero, takes the following form

$$n = \frac{2(D - 3A)}{2D + 3A} \qquad (8.4)$$

For the new model the equation (7.90) is used for prediction of inherent anisotropy.

The Elhannani model considers the anisotropy to be constant at all level of stress (see Equation 8.4). However, the new model considers the stress dependency of

anisotropy. The new model made a generally good prediction of inherent anisotropy except for SL and SAG (Figures 8.21, 8.22, 8.23, 8.24 and 8.25).

8.4.7.Comments on model predictions

The model constants used in the predictions are given in Appendix C. They could be readjusted according to the slope given in Table 8.6, 8.7, 8.8 and 8.9, then it might be possible to obtain better predictions. Here, no study was carried out in this way, the aim being to use the statistical package (which is BMDP) and to make predictions according to its results.

Thus the mismatch between measured and predicted readings could be a function of many things including the inefficiencies of the statistical program (such as the algorithm used). In addition to these user errors have also been considered such as the starting value for the non-linear regression program, lack of data or inconsistent test results.

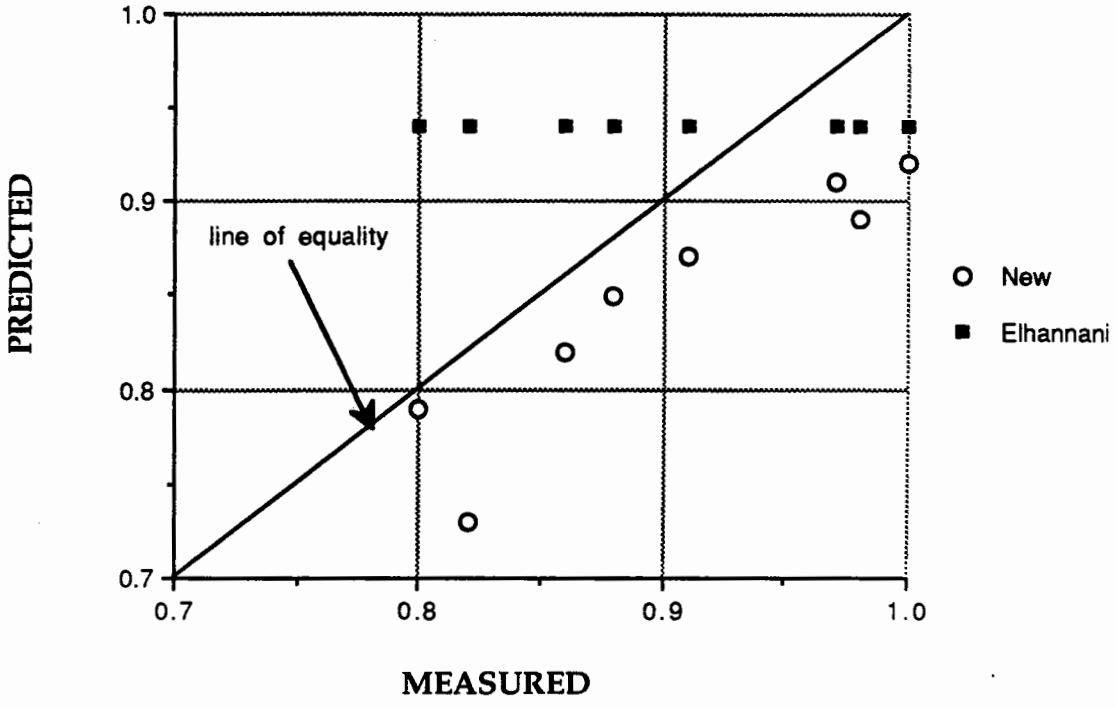

Figure 8.21. Inherent anisotropy predictions (SAG)

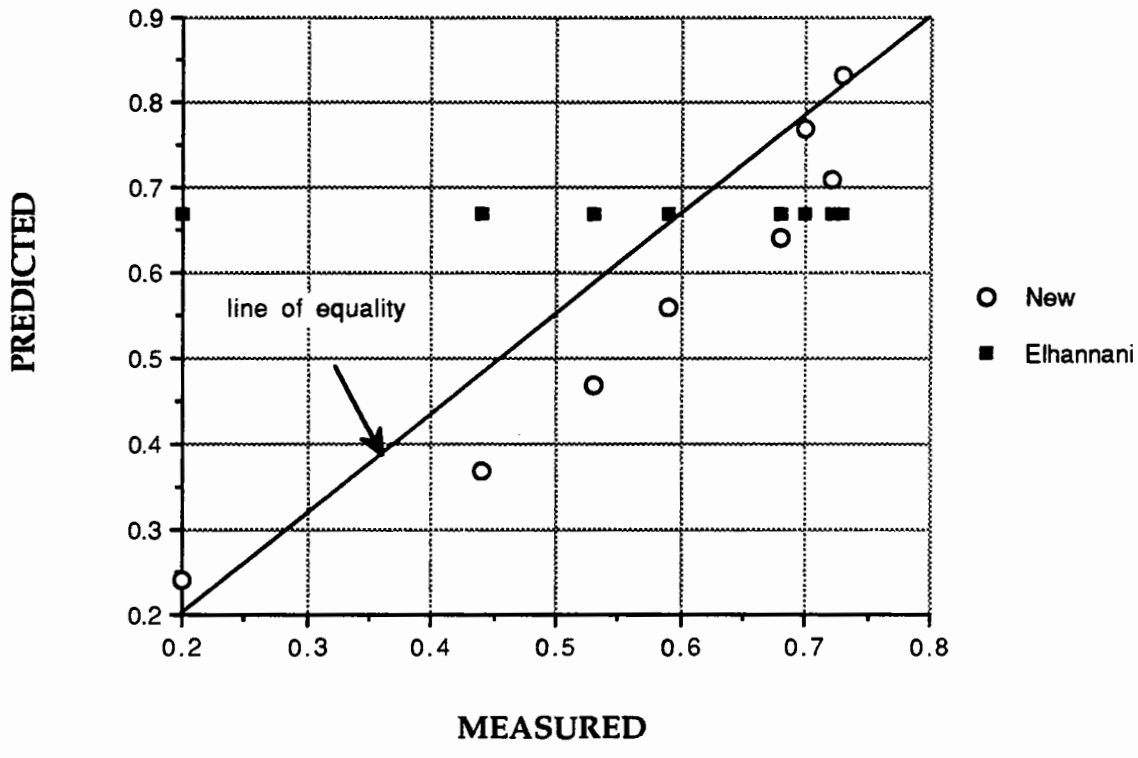

Figure 8.22. Inherent anisotropy predictions (SL)

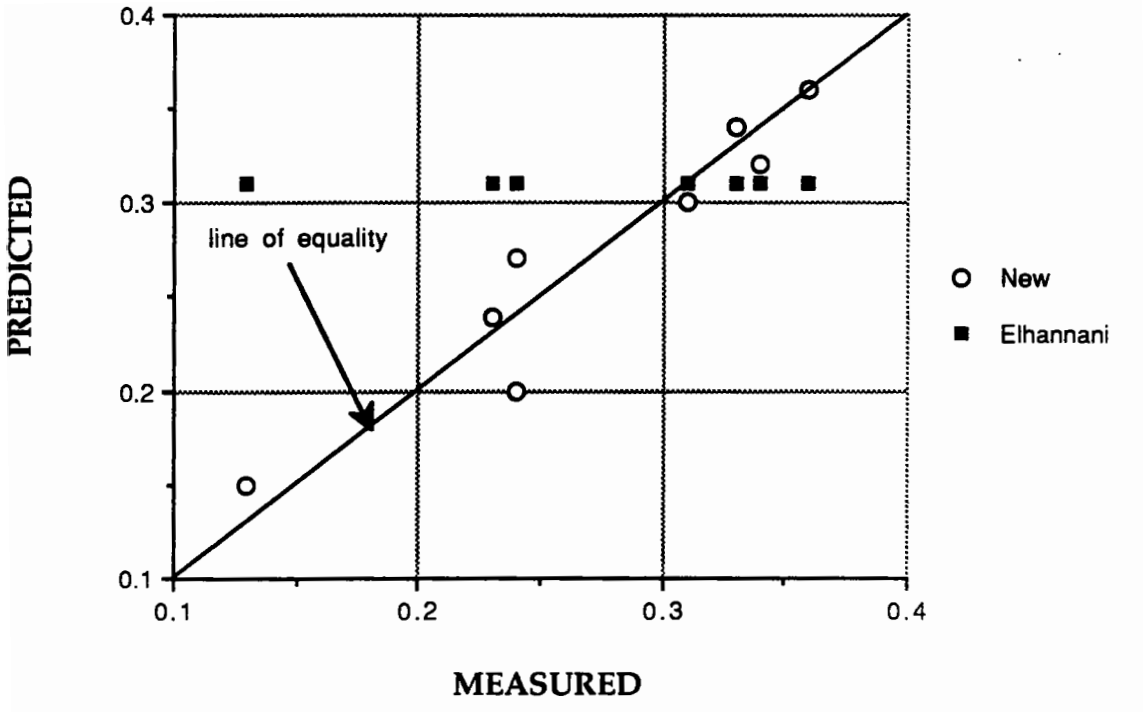

Figure 8.23. Inherent anisotropy predictions (FBA)

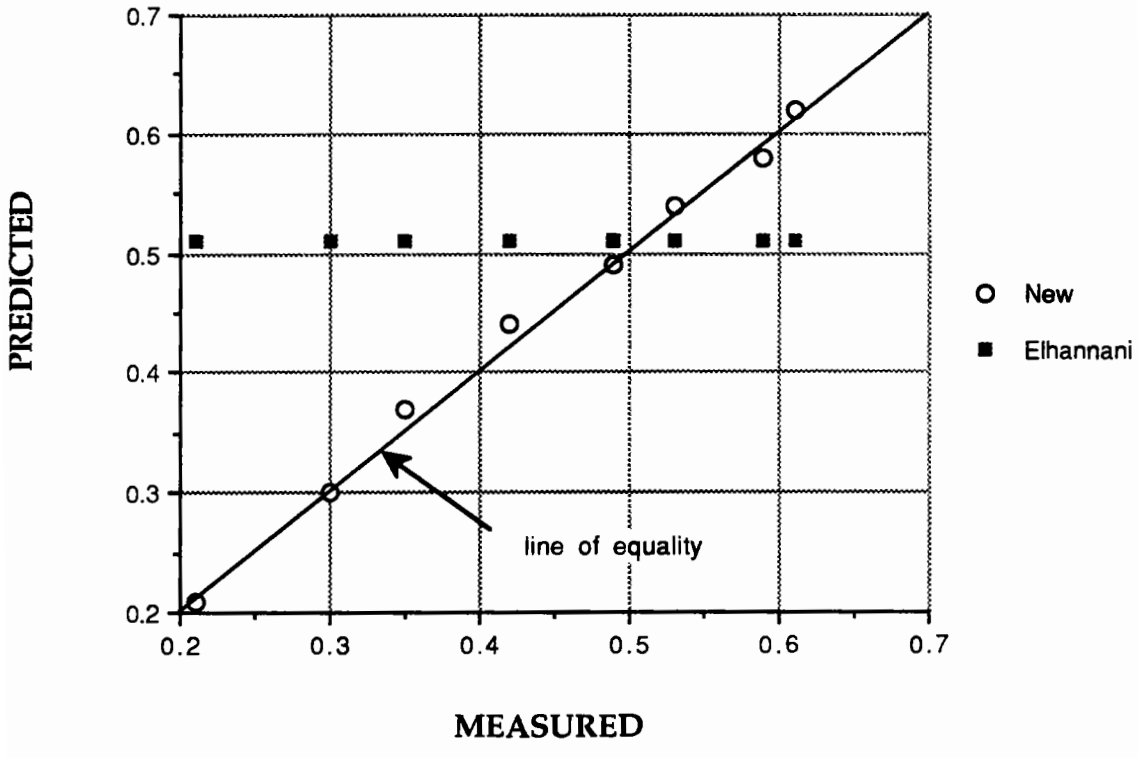

Figure 8.24. Inherent anisotropy predictions (GS)

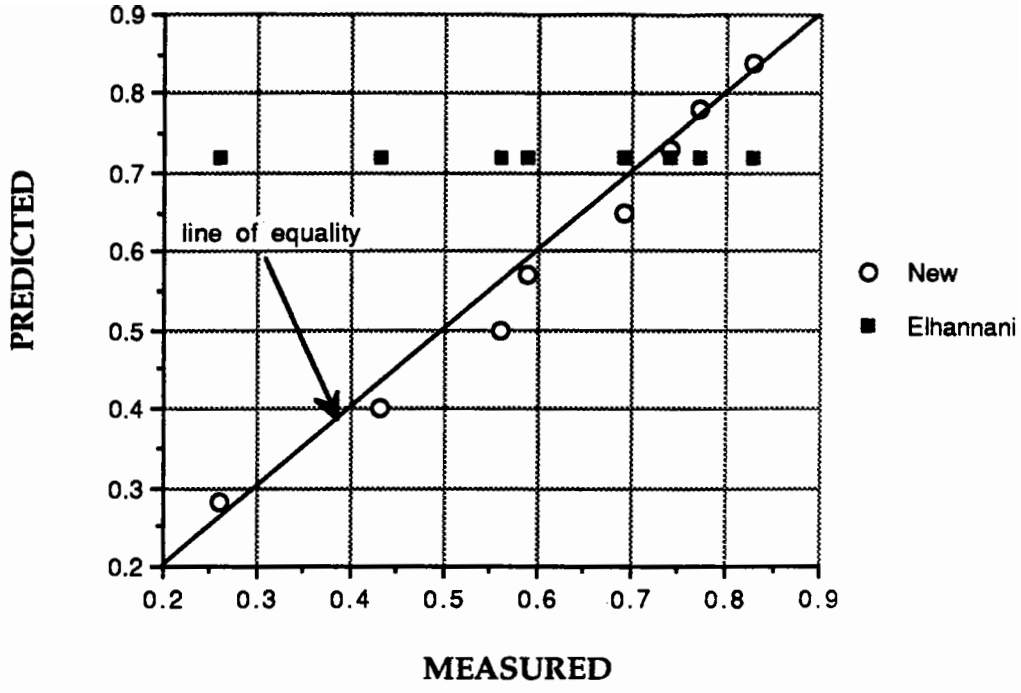

Figure 8.25. Inherent anisotropy predictions (FS)

CHAPTER 9

FINITE ELEMENT ANALYSIS OF GRANULAR MATERIAL IN PAVEMENTS

9.1.Introduction

Developing computer technology has made numerical techniques such as the finite difference method (FDM) and the finite element method (FEM) available for the analysis of engineering systems. The main difference between the two methods is that in the FDM the basic governing equation is discretized whereas in the FEM the physical body or continuum is discretized and, therefore, the FEM is more flexible than the FDM (Desai and Christian, 1977). The availability of many FEM packages and their use for different geometry conditions has made the method popular. In this study, the FEM was used.

The finite element method (FEM) has been used to determine the stresses and deformations in a given pavement structure. The increase in computing speed has made the FEM available for practical applications such as design of new roads (Thompson, 1992) or structural evaluation of pavements (Uzan et al, 1989) incorporating non-linearity in granular materials. However, when analysing a pavement with linear elastic properties, the FEM offers little or no advantage as compared with layered system analysis (Duncan et al, 1968). Therefore, in the context of this project, FEM will be most useful when non-linear properties of granular material are taken into account.

Non-linearity is introduced by means of successive iteration techniques (Desai and Christian (1980)) or incremental techniques (Britto and Gunn, 1987).

The FEM is an extension of the stiffness method used in structural engineering but in which there are no well-defined joints where equilibrium of forces can be established, unlike skeletal structures. Therefore, the continuum must be divided into a set of elements, which are called finite elements, connected at their imaginary nodal points.

These elements may be trianglular, quadrilateral, rod or brick-shaped or some combination of any, depending on the geometry and the problem type. Quadrilateral elements elements are generally used for the representation of pavements (Duncan and Monismith (1968), Pappin (1979), Paute and Martinez (1982), Sweere et al (1987)). Duncan et al (1968) found that the quadrilateral element stresses will be accurate as long as the ratio of length to width is smaller than five. The amount of time spent to solve a problem depends on the number of elements, therefore, if possible, less elements should be used. However, there is no unique way ,except by trial and error, to determine the optimum number of elements for a given problem.

The FEM method is explained in detail elsewhere (Zienkiewicz and Taylor (1989) and Cheung and Yeo (1979).

9.2.Stress-strain matrix

In order to implement a new model into the chosen FEM program (see Section 9.3) a tangential D matrix (stress-strain matrix) has to be constructed and some appopriate places has to be changed in the source code of the program. It was thought it may be useful to give a basic defination of the D matrix briefly.

The stresses are related to the strains by

$$\{\sigma\} = [D]\ \{\varepsilon\} \tag{9.1}$$

where [D] is the elasticity or stress-strain matrix.
$\{\varepsilon\}$ is the strain vector
$\{\sigma\}$ is the stress vector

For an axisymmetric element with isotropic properties, the [D] matrix is given by Zienkiewicz and Taylor (1989) as:

$$[D] = \frac{E(1-\upsilon)}{(1+\upsilon)\,(1-2\upsilon)} \begin{bmatrix} 1 & \frac{\upsilon}{1-\upsilon} & \frac{\upsilon}{1-\upsilon} & 0 \\ \frac{\upsilon}{1-\upsilon} & 1 & \frac{\upsilon}{1-\upsilon} & 0 \\ \frac{\upsilon}{1-\upsilon} & \frac{\upsilon}{1-\upsilon} & 1 & 0 \\ 0 & 0 & 0 & \frac{1-2\upsilon}{2(1-\upsilon)} \end{bmatrix} \tag{9.2}$$

where E is Young's modulus
υ is Poisson's ratio

Tangential model definitions are required for this formulation. Those for the Boyce model are given in section 7.21.2.

9.3.CRISP finite element package

The CRISP (**CRI**tical **S**tate **P**rograms) has been developed at Cambridge University, Soil Mechanics Group, since 1975 (Britto and Gunn, 1987). The package first introduced for the mainframe computers, was later also adopted for microcomputers. It was written in the FORTRAN 77 language code.

CRISP is mainly composed of geometry and main programs if post-processing programs (which are only available for microcomputers) are excluded. However, the geometry and the main programs are the same for both mainframe and microcomputers. In the early stages of this research the CRISP-84 (for mainframe) version was used. The Boyce(1980) model was implemented and a plotting program was written to see the initial mesh. After release of CRISP-90 for microcomputers, the new model developed in Chapter 7 was implemented in it. Since the geometry and main programs are more important than the post-processing programs, only these modules of the package will be explained.

9.3.1.Geometry program (GP)

The geometry program (GP) contains information describing the finite element mesh and creates a "link file" which is later needed by the main program. CRISP allows the use four different types of elements, namely, a linear strain triangle, a cubic strain triangle, a linear strain quadrilateral and a twenty noded brick element. It is also possible to use mixed types of elements in a mesh. The maximum number of nodes should be less than 751.

9.3.2.Main program (MP)

The advantage of dividing the programs into two parts is that if there is an error in the mesh, this error can be picked up before commencing the analysis (Gunn and Britto, 1984). Therefore, at the start of the main program, it may be assumed that there is no error resulting from the geometry program.

CRISP contains constitutive relations for anisotropic elastic, elastic model (linear variation with the depth), critical state (Cam Clay and Modified Cam Clay) and elastic-perfectly plastic (with Tresca, von Mises, Mohr Coulomb) models of geotechnical materials (Britto and Gunn, 1990).

The non-linear behaviour of soil with CRISP is considered in terms of a tangential stiffness approach in an incremental method in which the load is applied in many, sufficiently small, increments; and it being assumed that the difference between the piecewise linear assumption and the true (model) response is negligible (Britto and Gunn, 1990). Stiffness is calculated at the current stress state and no adjustment is made to the stress after each increment. Therefore, the stresses and strains may probably drift from the true (model) response of soil. In order to overcome this problem, two different numbers of increments can be chosen and results compared. If the results are totally different, then a larger increment number is chosen, however, at most 50 increments are enough to characterize non-linear behaviour of soil (Britto and Gunn, 1990).

9.3.3.Plotting program

The mainframe version of CRISP-84 has no plotting facility. From experience, it was seen that the initial shape of the finite element mesh is quite important. CRISP itself does not warn the user of errors in the mesh but it reports other errors, which are due to the mesh. Therefore, it was decided to write a plotting program called PLOT (Appendix D). The program reads the data from a link file which is obtained after running the geometry program. The program borrows some routines from the SIMPLE PLOT library (Cripps Computing Centre, 1989) which is available for mainframe computers at Nottingham University, CRIPPS Computer Centre. The program connects nodes to each other by a straight line and node numbers are shown in.

9.3.4.Implementing the Boyce model in CRISP

The Boyce (1980) model was implemented in the mainframe version of CRISP-84. CRISP has been written to handle Young's modulus (E) and Poisson's ratio (υ) whereas the model has a non-linear bulk modulus K and shear modulus G. Therefore, using an appropriate relation K and G need to be converted E and υ. In addition to this CRISP has been written for tangential stiffness, therefore, tangential formulations need to be used. Tangential bulk and shear modulus have been given by Boyce (1980) as shown below:

$$K_t = \frac{A\, p^{(1-B)/B}}{1 + (\beta\ (2 - B)\ q^2/Bp^2)} \tag{9.3}$$

$$G_t = Cp^{(1-B)} \tag{9.4}$$

where A, B and C are material constants

$$\beta = \frac{1 - B}{6C}$$

p and q are the mean and deviatoric stress respectively

Using the elasticity relation given below, tangential E_t and υ_t can be obtained

$$E_t = \frac{9K_t + G_t}{G_t + 3K_t} \tag{9.23}$$

$$\upsilon_t = \frac{3K_t - 2G_t}{6K_t + 2G_t} \tag{9.24}$$

Subsequently, a D matrix has been constructed for axisymmetric analysis and new matrix was incorporated in CRISP.

9.3.4.1.Testing the model in CRISP

In order to make sure whether the Boyce(1980) model had been implemented correctly, a check procedure was carried out. For this purpose, a Young's modulus, E, and Poisson's ratio, υ, have been chosen. The example is for a single, upright, element with four corner nodes subjected to vertical load only (Figure 9.1). E and υ were then converted into K and G using the relations shown below.

$$G = \frac{E}{2(1 + \upsilon)} \tag{9.5}$$

$$K = \frac{E}{3(1 - 2\upsilon)} \tag{9.6}$$

For the model, three constants B, A and C are needed. A and C can simply be obtained from the equations (9.5) and (9.6) with the assumption of linearity B=1, K_t = A and G_t = C. Using the the same stresses, both the model and linear elastic model were run. Results are shown in Table 9.1.

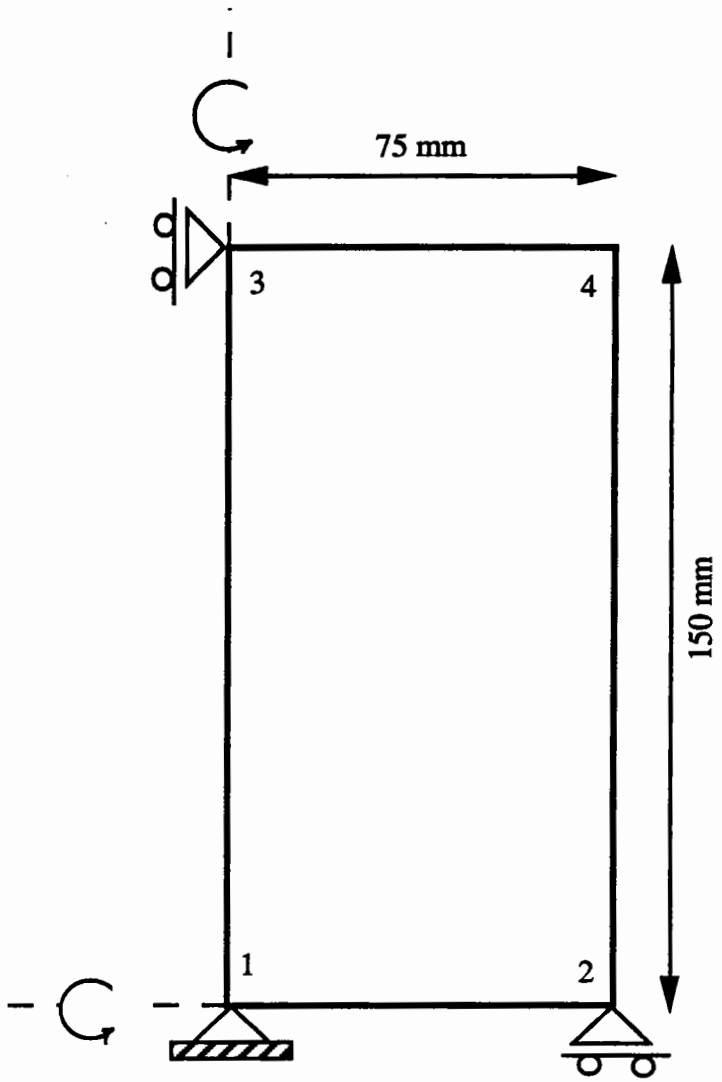

Figure 9.1. FE mesh for the simulation of triaxial apparatus

Table 9.1 shows that the Boyce model with B=1 gives comparable answers to the elastic model. This gives some confidence that the Boyce model has been implemented in CRISP correctly. A listing of the subroutine implementing the Boyce model, DSOILN is given in Appendix D.

Table 9.1.Comparison of the Boyce Model with linear parameters with the linear elastic model (displacements in milimeters)

	Elastic model E=785 N/mm^2 υ=0.154		**Boyce model** A= 379 N/mm^2 C= 340 N/mm2, B =1	
Nodes	x	y	x	y
1	0	0	0	0
2	7.3806	0	7.3777	0
3	0	-9.548	0	-9.5474
4	7.3806	-9.548	7.3777	-9.5474

9.3.4.2.Finite element modelling of triaxial test with Boyce Model

The CRISP program incorparating the Boyce model was used to investigate the performance of granular material in the triaxial test. Since the study was performed before carrying out triaxial tests, data were obtained from previous research tests at Nottingham University. Pappin (1979) tested crushed limestone under various stress paths using triaxial apparatus. Chan (1990) tested crushed dolomitic limestone under limited stress paths that begins with zero deviatoric stress using the triaxial apparatus.

A regression program that had been written by Allaart (1989) was used to obtain three constants for the Boyce model, but the program was slightly modified in order to consider the effects of cycling confining pressure (see Appendix D).

Because of symmetry only a quarter part of the triaxial sample was modelled by finite elements with an appropriate boundary condition (see Figure 9.1). The confining pressure was kept constant whereas the deviatoric stress changes. The volumetric strain prediction of the Boyce model yielded poor results whilst a good correlation between calculated and experimental results for the shear strain was found (see Figure 9.2, 9.3, 9.4,9.5).

9.3.5. Implementing new models into the CRISP

The new model developed in Chapter 7 was implemented in the CRISP package. In this section the means by which the model was implemented will be discussed.

9.3.5.1.Isotropic model

For the isotropic model a subroutine called DEVIATORIC was written in order to construct a tangential D matrix so that it can be implemented in CRISP. The model requires in-situ stresses as well as current stresses. The in-situ stresses were called from the subroutine INSTRS. The D matrix for anisotropic elastic material was then

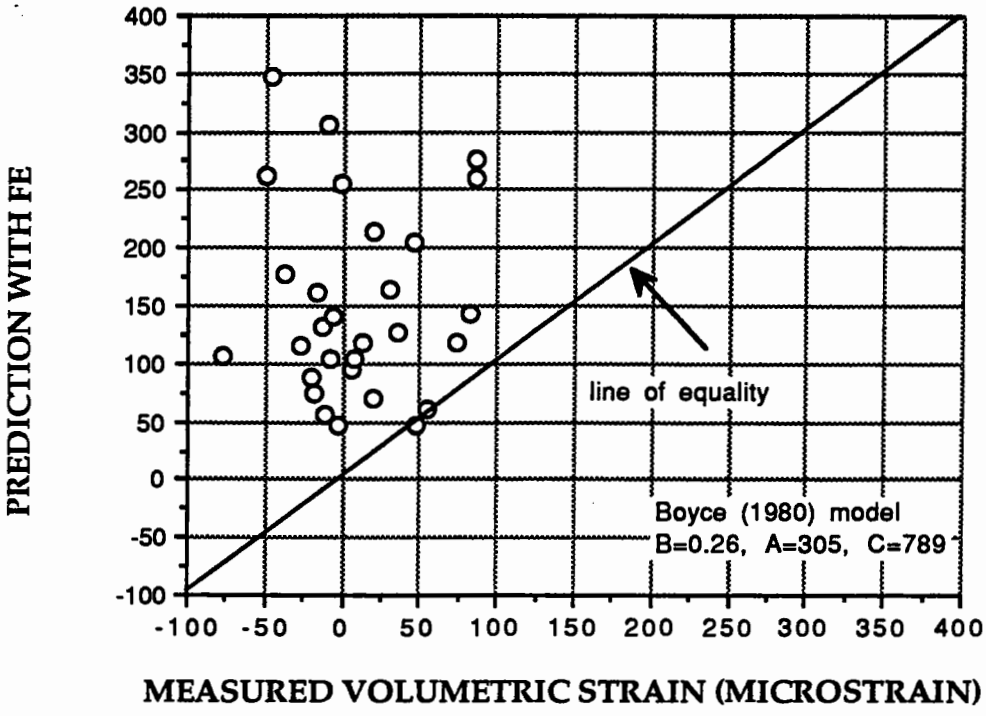

Figure 9.2. Prediction of volumetric strain with FE (Pappin (1979) data)

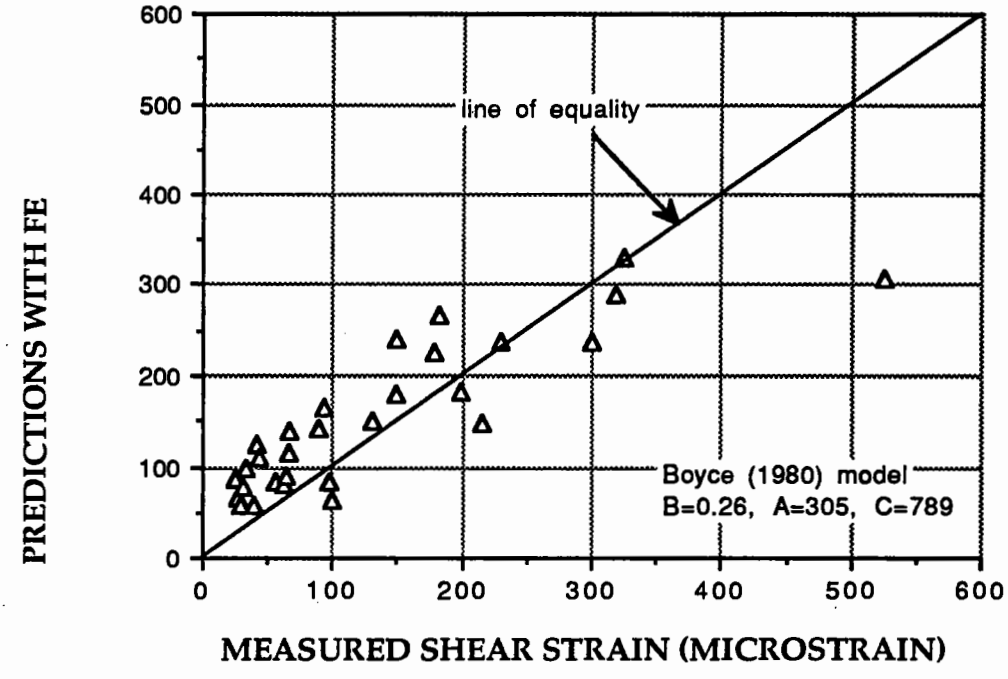

Figure 9.3. Prediction of shear strain with FE (Pappin (1979) data)

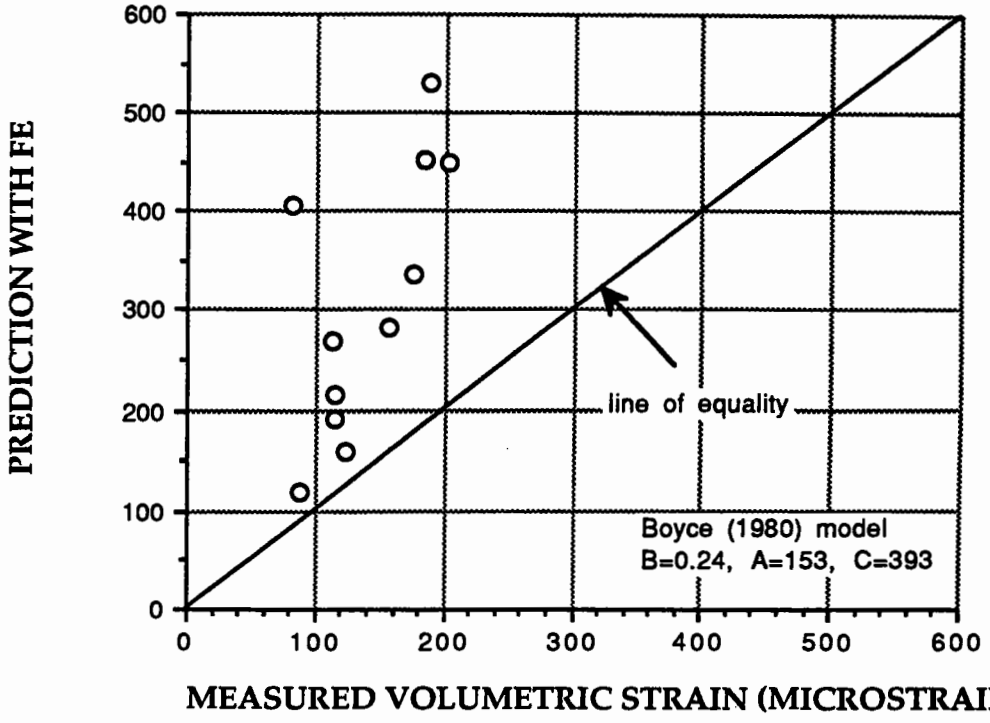

Figure 9.4. Prediction of volumetric strain with FE (Chan (1990) data)

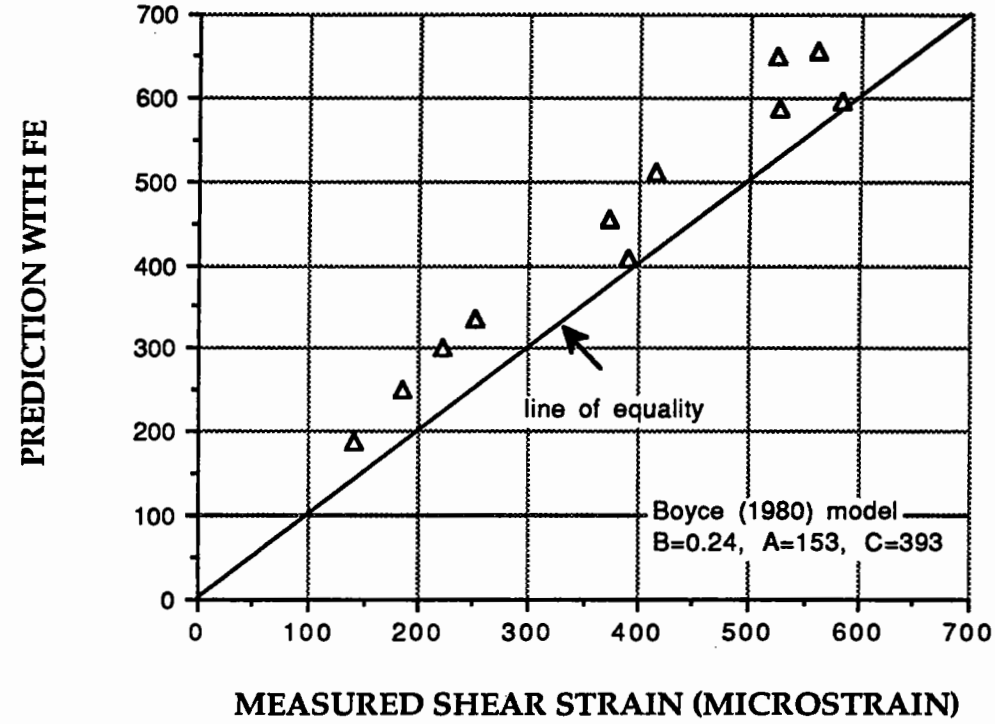

Figure 9.5. Prediction of shear strain with FE (Chan (1990) data)

modified to incorporate the non-linear elastic model but used with parameter values which would force isotropy. The model number was assigned to be 8. If the model needs to be used data line D in the main program input must have the form given in Appendix D.

9.3.5.2.Anisotropic model

For the anisotropic model a subroutine called GRAMM was written for implementation in CRISP-90. The model requires the in-situ stresses as for the isotropic model. The in-situ stresses were again called from the subroutine INSTRS. The tangential D matrix for anisotropic elastic material was modified in order to introduce the non-linear anisotropic elastic model, this time with parameter values which represent anisotropic behaviour.

9.5.3.3.An example with new models

In order to check whether the models are implemented correctly and to see the difference in results obtained from the isotropic and anisotropic model a mesh which has 120 elements and 143 nodes was chosen. 8 noded quadrilateral elements were chosen. Three layers of a pavement were modelled using linear elastic models for the asphalt and subgrade layers and non-linear elastic models for granular layers. Material properties and boundary conditions are shown in Figure 9.6. The finite element mesh is shown in Figure 9.7.

In order to compare the results of isotropic and anisotropic models, ten program runs were made as keeping the material properties of the asphalt and subgrade layers and the thickness of layers constant but only changing mineral types and models for granular layer (new isotropic and anisotropic).

Results show that (Table 9.2 and 9.3) the isotropic model produces more tensile strain underneath the asphalt layer than the anisotropic model. However, the anisotropic model produces more vertical strain in the subgrade layer than the isotropic model.

In order to interpret the FEM results in terms of permanent strain and fatigue design life, which are two important parameters in analytical pavement design, TRRL Laboratory Report 1132 (Powell et al, 1984) was used. The bituminous layer was assumed to be dense bitumen macadam at 20°C. Probability of survival was chosen to be 85% (Figure 4 in Page 19 in TRRL 1132).

Design results showed that the anisotropic model had a fatigue life 4.4 to 5.4 percent longer than the isotropic model (Figure 9.8 and Table 9.4). However, the isotropic model had a permanent deformation life 6 to 11 percent longer (Figure 9.9 and Table 9.4), which is the critical design parameter for this particular example.

Stress contours resulted from isotropic and anisotropic analysis are given in Appendix G. An example was given only for SL sonce other materials also show similar behaviour. Detailed discussion on stress contours obtained from isotropic and anisotropic models is presented in Appendix G.

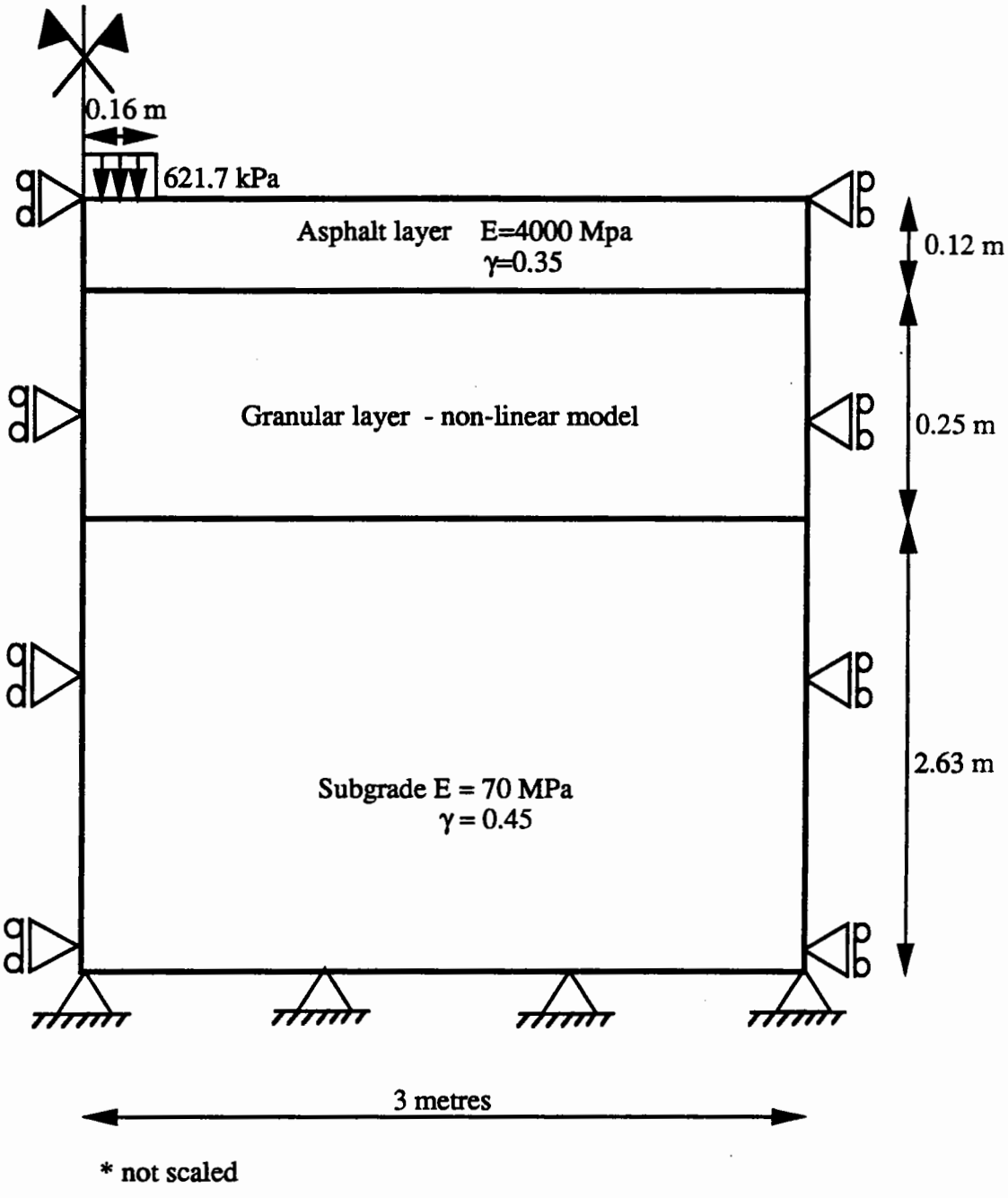

Figure 9.6. Material properties for FE analysis

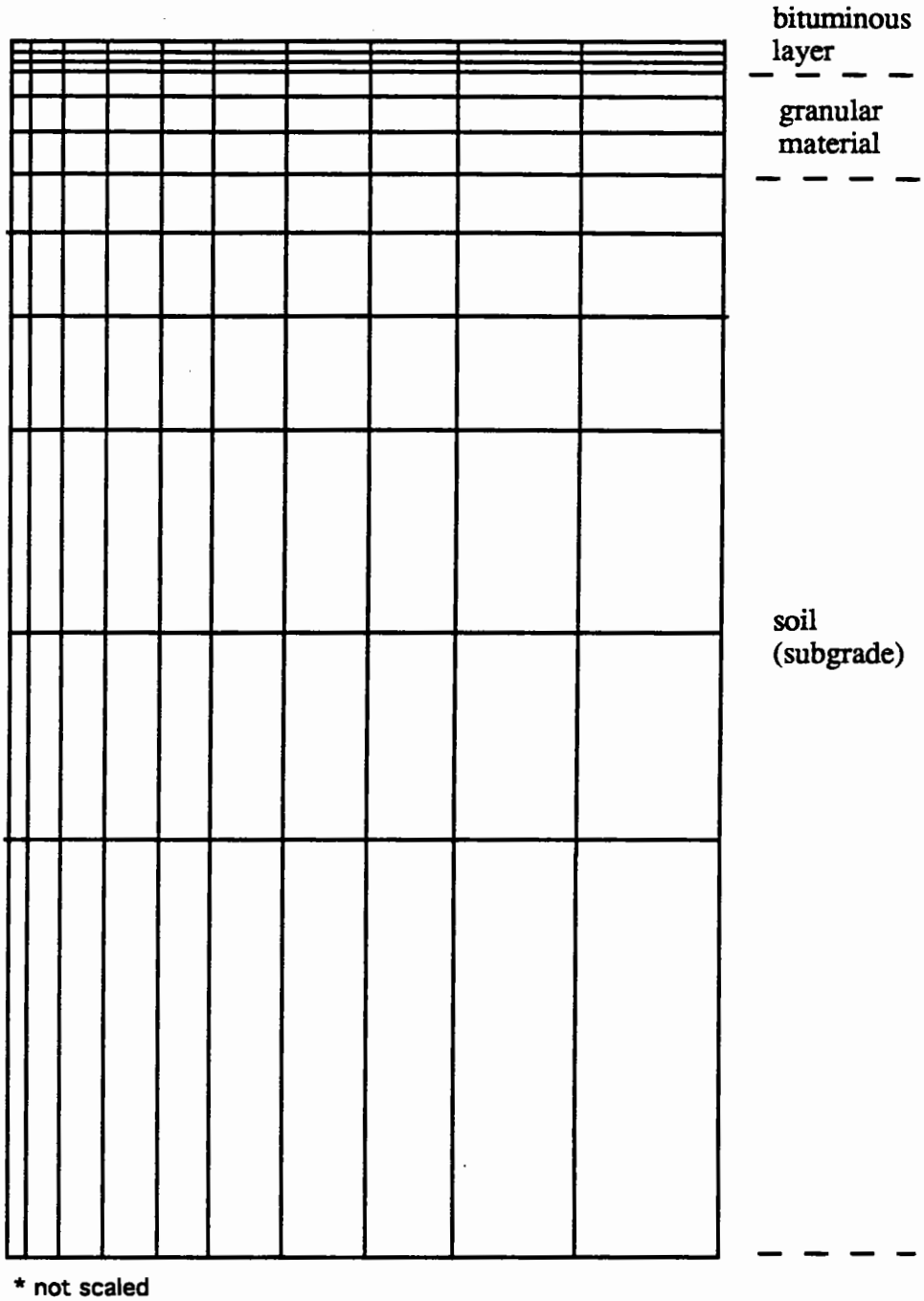

Figure 9.7. FE mesh

Table 9.2. Horizontal strains underneath asphalt layer (microstrain)

X(METRE)	SL		FS		SAG		GS		FBA	
	isotropic	anisotropic	isotropic	anisotropic	isotropic	anisotropic	isotropic	anisotropic	isotropic	anisotropic
0.04	-92	-73	-91	-76	-88	-70	-87	-71	-91	-76
0.12	-58	-50	-58	-52	-56	-49	-55	-49	-58	-52
0.23	30	22	30	23	30	24	29	24	29	23
0.4	15	13	15	13	14	12	14	12	15	13
0.5	7	7	7	7	7	6	7	6	8	7
0.8	4	4	4	4	4	3	4	3	4	4
1.125	2	2	2	2	2	2	2	2	2	2
1.575	1	1	1	1	1	1	1	1	1	1
2.1	1	1	0.8	0.7	0.8	1	0.7	1	1	1
2.7	1	1	0.6	0.5	0.6	0.5	0.6	0.6	1	0

Table 9.3. Vertical strain at formation level (microstrain)

X(METRE)	SL		FS		SAG		GS		FBA	
	isotropic	anisotropic	isotropic	anisotropic	isotropic	anisotropic	isotropic	anisotropic	isotropic	anisotropic
0.04	3762	4223	3822	4152	3803	4362	3706	4234	3820	4152
0.12	3060	3114	3099	3103	3120	3331	3162	3333	3091	3103
0.23	1595	1775	1584	1869	1626	1795	1612	1803	1572	1869
0.4	248	167	234	1704	210	100	197	1065	244	170
0.5	-16	-14	-14	-17	-22	-22	-22	-22	-13	-17
0.8	-22	-25	-22	-24	-20	-21	-20	-22	-22	-24
1.125	-23	-25	-22	-20	-21	-22	-21	-22	-23	-24
1.575	-20	-20	-19	-19	-19	-19	-18	-19	-20	-20
2.1	-19	-19	-9	-18	-18	-18	-18	-18	-18	-19
2.7	-19	-18	-2	-18	-18	-17	-18	-18	-18	-18

The effect of anisotropy (for this particular example) for fatigue design may be considered relatively unimportant, although the permanent deformation life is more affected by anisotropy in granular material. Thefore, using an isotropic model instead of an anisotropic model will result in prediction of a somewhat early failure of pavement due to permanent deformation. The following points should be noted in examining these results:

• From Table 9.4 it may be seen that FS and FBA have similar design lives for both fatigue and permanent deformation although they have very different anisotropic characteristics (compare Figures 6.41 and 6.43).

• Another important point is that for the isotropic model, repeated deviatoric stress test results were used (see Section 8.3.4) to determine material constants whereas for the anisotropic model data from repeated deviatoric, cell and both stresses were used. Hence the material behaviour may show different behaviour under different stress regimes,

• Unfortunately the number of stress paths was not the same for all materials (see Appendix B) because of the early failure of the sample, instrumentation problem and problems in control system during the testing. Therefore, material constants were probably affected by these factors. The effect of these difference on predicted pavement performance cannot be assessed.

Table 9.4. Comparison of design life of pavements

Material	Permanent deformation life (msa)			Fatigue design life (msa)		
	Isotropic	Anisotropic	Difference %	Isotropic	Anisotropic	Difference %
SL	2.37	2.17	9	7.41	7.82	5.5
FS	2.34	2.20	6	7.43	7.76	4.4
SAG	2.35	2.11	11	7.49	7.90	5.4
GS	2.39	2.16	11	7.51	7.88	4.9
FBA	2.34	2.20	6	7.43	7.76	4.4

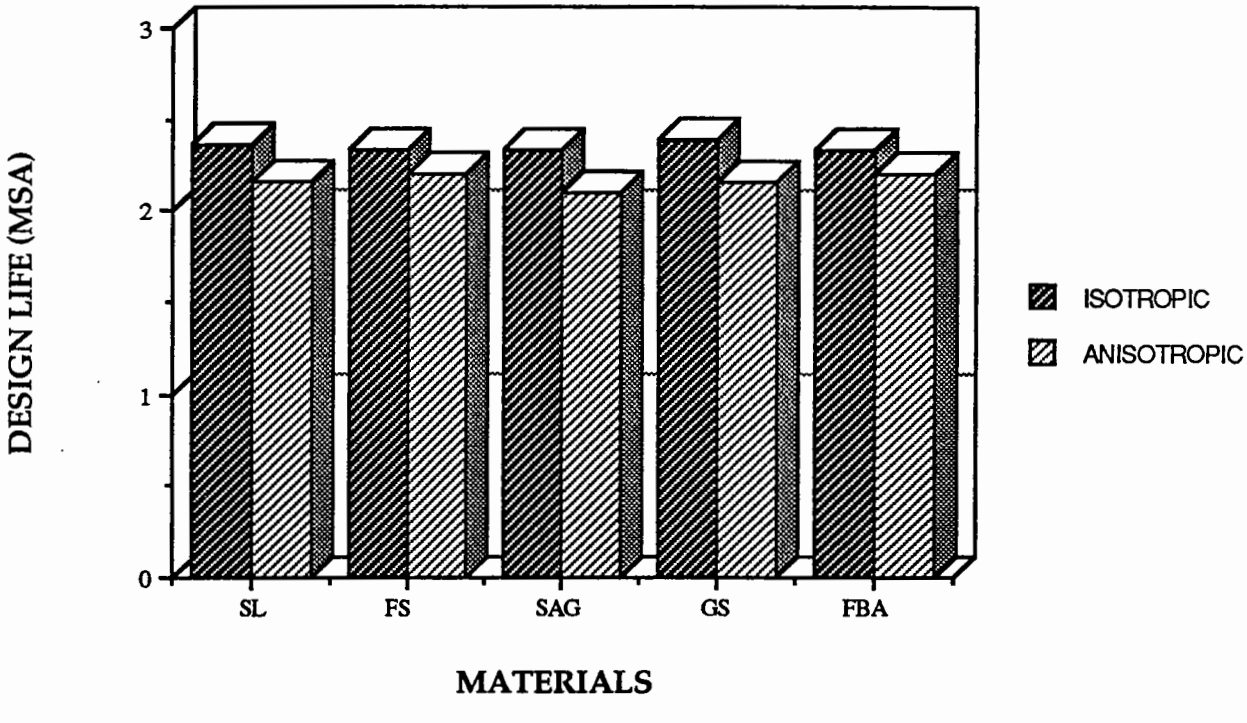

Figure 9.8. Comparison of permanent strain design life

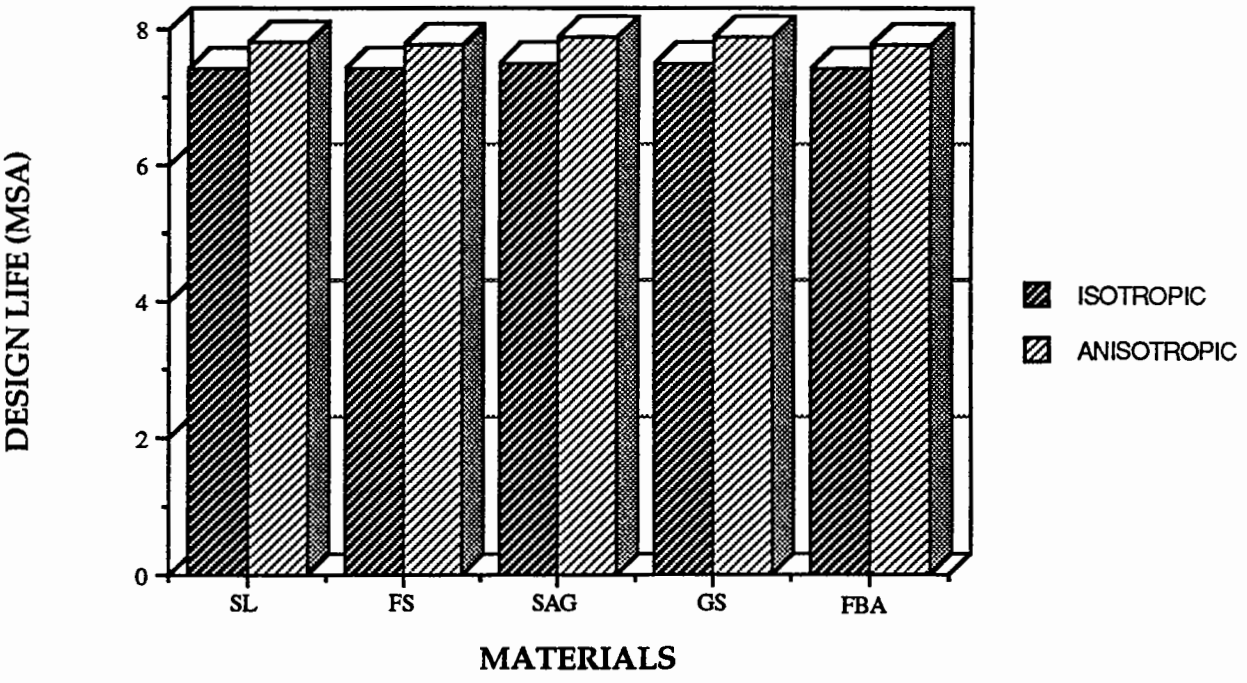

Figure 9.9. Comparison of fatigue design life

CHAPTER 10
CONCLUSIONS AND FUTURE WORK

10.1.Repeated load testing

Repeated load triaxial tests were carried out using six different materials from different origins. These are furnace bottom ash, Fontaineblau sand, washed graded river sand, sand and gravel, soft limestone and gritstone. Different stress paths, cycling only deviatoric stress with constant cell pressure, cycling cell pressure and cyclic both stresses, were chosen in order to approximately simulate the stresses on granular material in a pavement due to random traffic loading. Some conclusions which have been drawn from this testing work are as follows:

a) In order to improve the sample compaction a new stud system was developed. A good correlation was obtained between the old and the new stud system for axial and radial strain resulted from cyclic deviatoric stress. However, the new stud system gave larger radial strains when the cell pressure was cycled, although a good correlation was obtained for the axial strain. It probably shows that the new stud system also measures the penetration of membranes into the sample due to changes in cell pressure. Hence this system is only suitable for constant cell pressure tests.

b) As the deviatoric stress increases, the axial strain increases substantially. The relationship between the deviatoric stress and the axial strain is clearly non-linear and non-linearity increases as the confining pressure decreases.

c) At high levels of deviatoric stress, a disproportionate increase in radial strain was often observed. As the confining pressure increased, the radial strain due to the repeated deviatoric stress tended to decrease.

d) Under repeated cell pressure, it was seen that radial and axial strains increased as the cell pressure increased. Fontainebleu sand showed a linear response under repeated cell pressure.

e) Poisson's ratio is not constant during a cycle and takes different values during loading and unloading. As the confining stress increases its value decreases.

f) Anisotropy measurements were made using the repeated load triaxial apparatus cycling only cell pressure at different levels of stress. Three different types of anisotropy, namely inherent, stress-history-induced and stress-induced were investigated. Anisotropy is higher at lower levels of cell pressure. All materials showed inherent anisotropy. Stress-history due to plastic strain changes the structure of granular material and, hence, the inherent anisotropy is also changed. Furnace bottom ash showed similar responses as regards both inherent and stress-history induced anisotropy. Gritstone showed less stress-history-induced anisotropy than

inherent anisotropy. However, the other materials, sand and gravel, Fontaineblau sand and soft limestone, showed larger stress-history-induced anisotropy than inherent anisotropy. Results revealed that materials containing more fines are less sensitive to stress-history-induced anisotropy. In each individual cycle the granular material shows higher anisotropy during loading than during unloading . Anisotropic stresses (such as deviatoric stress) cause stress-induced anisotropy.

10.2.Constitutive models of resilient behaviour

Seven types of constitutive models were used to interpret repeated load triaxial test results. These are K-θ (Hicks and Monismith), Uzan (1985), Boyce (1980), Pappin and Brown (1985), Elhannani (1991) and new models. All models are written in the same format in order to see the similarities and differences. Some conclusions drawn from the investigation are as follows:

a) Determination of model constants for non-linear elastic models are very important since strain predictions will be based on these calculated model constants. Unfortunately, the model developers have not generally explained how to find the model constants eventhough this is crucial. For instance, different responses were found according to the method of determination of the model constants. Therefore, the method of model constant determination should be made very clear. Multivariate non-linear regression analyse of data often give unreliable, or even erroneous, values.

b) The axial strains predicted using the K-θ (Hicks and Monismith) and the Uzan (1985) models were quite close to the experimental results measured under repeated deviatoric stress starting from zero with constant cell pressure. However, under a general deviatoric stress path, not necessarily starting from zero, both models gave poor axial strain prediction. A disadvantage of these models is that they assume a constant Poisson's ratio which is not true for granular material. They may be used to interpret repeated load test results where only vertical deformations are recorded, such as the falling weight deflectometer (FWD).

c) The Boyce (1980) model needs only three constants which is reasonable for a non-linear elastic model. A method was proposed to find the model constants. The constants A (bulk modulus) and B can be determined from repeated cell pressure tests. Therefore the only unknown in the model after substituting B in the shear strain equation is C which can be determined from shear strain results. The model is able to predict shear strain results, accordingly axial strain, but poor predictions were observed for the volumetric strains. Elhannani (1991) modified the Boyce model to incorporate anisotropy, this did not affect the results significantly. The assumption of reciprocity, which both models use, thus appears to be unwarranted.

d) The Pappin and Brown (1985) model generally underestimates the strains. However it may be possible to adjust the model constants to improve the predictions. Volumetric strain predictions are superior when compared with the Boyce model. Finding the constants is relatively easy when compared with the Boyce model and data from repeated cell pressure tests are not needed.

e) Two new models were developed. One is for the prediction of test results due to deviatoric stress with constant cell pressure. This contains 7 constants which can be determined using a multiple regression program. The second model with 13 constants incorporates anisotropy and is particularly used to predict test results under repeated both stresses. The constants for the second model can be determined using both multiple regression and non-linear regression programs. Both models generally gave a better prediction of repeated load triaxial tests results than existing models.

10.3.Finite element analysis

The CRISP finite element package was used as an analytical tool. The two new models were incorporated into CRISP. In order to make a comparison between the new isotropic and the new anisotropic models a pavement consisting of 3 layers and defined as a series of quadrilateral elements was analysed by the program. Results showed that if the isotropic model is used larger tensile strains observed underneath the asphalt layer and smaller vertical strain is observed in the subgrade layer when compared with the anisotropic model. The effect of anisotropy (for a typical pavement) for fatigue design may be considered unimportant, but the permanent deformation life is considerably affected by anisotropy in granular material. Therefore, using an isotropic model instead of anisotropic model will result in prediction of an early failure of pavement due to permanent deformation.

10.4.Future study

It was found that anisotropy in granular material affected the whole pavement behaviour. It may be possible that other pavement layers such as the subgrade and even the asphalt layer have important anisotropic characteristics. Studies of anisotropic characteristics of clays are documented (Graham and Houlsby, 1983). However, it may also be important for asphalt layers. Crockford (1993) concluded that the rotation of principal stress direction due to traffic loading is one cause of permanent strain in the asphalt layer. This may be due to anisotropic characteristics of asphalt layers. Although in the paper only permanent strain is considered the resilient behaviour of asphalt layers may also be affected.

The study of anisotropy in all pavement layers, and particularly in the asphaltic layers should therefore be made. In particular a material study of bound materials similar to the one described in this thesis for granular material is suggested. The effect of anisotropic properties of pavement materials should then be included in detailed design procedures.

Granular material is a very complex material to model. In this thesis, only resilient behaviour is investigated. However, after each passage of wheel loading permanent deformation occurs even in very small amounts. This behaviour should be modelled with a dynamic finite element program using both a resilient and permanent model, or a combined model.

Fontainebleu sand showed a largely linear response under the repeated cell pressure test condition. This may be because it is a single size and fine material. This finding should be checked with other materials having similar characteristics.

In the project, resilient anisotropy measurements were made by the repeated load triaxial apparatus. However, it is also possible to use the hollow cylinder apparatus and true triaxial apparatus. If a correlation is found between these equipments using the same material, then any of these equipments may be used to accurately determine anisotropy .

The success and failure of a numerical method such as finite element method is dependent upon the model employed which has constants derived from test results. Hence the determination of model constants becomes an important factor. Before using any model with numerical methods it is essential that model constants are determined satisfactorily. For this purpose different statistical software may be employed. Improvements in the ability of such software are required and further study of means to obtain reliable constant determination is highly desirable. Alternatively it may suitable to write a special program to determine model constants for a particular model.

It is interesting to determine to what extent a repeated load triaxial test apparatus can simulate moving wheel load on the pavement. For this purpose an in-situ test may be carried out to measure real stresses and strains developed in the pavement. The same conditions (if possible) would then be applied to the sample using a repeated load triaxial apparatus.

Another important study is to see how anisotropy develops in-situ by roller-compaction during the construction and traffic loading thereafter. For this study again an in-situ test or pavement test facility is required. Horizontal stiffness may be measured by the pressuremeter and vertical stiffness may be measured by the plate bearing test or alternatively falling weight deflectometer. Ideally these measurements need to be made at the same time in order to relate this findings to the repeated load triaxial test results and this could give considerable practical difficulties.

REFERENCES

Allaart, A.P. (1989) "*GRAINS-A Non-linear Elastic Model*", Delft University of Technology, Faculty of Civil Engineering, The Netherlands.

Allen, J.T. and Thompson, M.R. (1974) " *Resilience Response of Granular Materials Subjected to Time-dependent Lateral Stresses*", Transportation Research Record 510, pp:1-13.

ASSHTO (1986) "*AASHTO Guide for Design of Pavement Sructures*", AASHTO publications, Washington D.C, USA.

Arthur, J.R.F. and Menzies, B.K. (1972) "*Inherent Anisotropy in a Sand*", Geotechnique, Volume 22, No:1, pp: 115-128.

Arthur, J.R.F. (1988) "*State of the art paper- cubical devices: versatility and constraints* " Advanced Triaxial Testing of Soil and Rock, Edited by Donache, Chaney and silver, ASTM, STP 977, Phidelphia, pp:743-766.

Arthur, J.R.F., Chua, K.S. and Dunstan, T. (1977) "*Induced anisotropy in a sand*", Geotechnique, Volume 27, No:1, pp:13-30.

Atkinson, J.H. and Bransby, P.L. (1978) "*The Mechanics of Soil :An Introduction to Critical State Soil Mechancis*", McGraw Hill Book Company (UK) Ltd, University Series in Civil Engineering.

Australian Road Reserach Board (ARRB) (1991) "*National Workshop on Elastic Characterisation of Unbound Materials and Subgrades*", Australian Road Resarch Borad, APRG Report, No:3.

Barden, L. (1963) "*Stresses and Displacements in a Cross-anisotropic Soil*", Geotechnique, Volume 13, pp:198-210.

Barksdale, R.D. and Itani, S.Y. (1989) " *Influence of Aggregate Shape on Base Behaviour* ", Transportation Research Record 1227, pp:173-181.

Biarez, J. and Wiendieck, K. (1963) "*La Comparaison Qualitative Entre L'anisotropie Mecanique et L'anisotropie de Structure des Milieux Pulverulents*", C.R. Hebd. Seance du Academie des Sciencs, Paris, 256, pp:1217-1220.

Biarez, J. and Hicher, P.Y. (1987) " *Simplified hypotheses on mechanical properties equally applicable to sands and clays*", Int. Workshop on Constitutive Equations for Granular Non-cohesive Soils, Cleveland, pp:19-32.

Bishop, A.W. and Henkel, D.J. (1962) "*The Measurement of Soil Properties in the Triaxial Test*", Second edition, Edward Arnold (Publishers) Ltd., London.

Boyce, J.R. (1976) " *The Behaviour of a Granular Material under Repeated Loading*" PhD thesis, University of Nottingham.

Boyce, J.R. and Brown, S.F. (1976) "*Measurement of Elastic Strain in Granular Materials*", Geotechnique, Volume 26, No:4, pp:637-640.

Boyce, J.R. (1980) "*A Non-linear Model for the Elastic Behaviour of Granular Materials under Repeated Loading*", Int. Conf. on Soils under Cyclic and Transient Loading, Swensea, pp:285-294.

Britto, A.M. and Gunn, M.J. (1987) "*Critical State Soil Mechanics Via Finite Elements*", Ellis Horwood Limited Publishers, John Wiley and Sons.

Britto, A.M. and Gunn, M.J. (1990) "*CRISP-90 User's and Programmer's Guide*", Cambridge University, Engineering Department.

Brown, S.F. and Hyde, A.F.L. (1975) "*Siginificance of Cycling Confining Stress in Repeated Load Triaxial Testing of Granular Material*", Transportation Research Record 537, pp:49-58.

Brown, S.F. (1981) "*The Structural Role of Granular Materials in Flexible Pavements*", Proc. Sym. on Unbound Aggregates in Roads, Edited by Jones, Dept. of Civil Eng., University of Nottingham.

Brown, S.F. and Pappin, J.W. (1981) "*Analysis of Pavements with Granular Bases*", Transportation Research Record 810, pp:17-22.

Brown, S.F. and Pappin, J.W. (1985) "*Modelling of Granular Materials in Pavements*", Transportation Research Record 1022, pp:45-51.

Brown, S.F. (1990) "*Introduction to Pavement Design*", Residential Course on Bituminous Pavements: Material, Design and Evaluation, University of Nottingham, Civil Engineering Department, pp:A1-A12.

Brown, S.F. and Selig, E.T. (1991) "*The Design of Pavement and Rail Track Foundations*", Cyclic Loading of Soils: From Theory to Design, Edited by O'Reilly and Brown, Blackie, pp:249-305.

Brown, S.F. and Almeida, J.R. (1993) "*Structural Evaluation of Pavements*", Report Submitted to SERC, University of Nottingham, Report no: PR93006.

Budiman J.S., Sture, S. and Ko, H-Y. (1992) "*Constitutive Behaviour of Stress-induced Anisotropic Cohesive Soil*", Journal of Geotechnical Engineering, ASCE, Volume 118, No:9, pp:1348-1359.

Casagrande, A. and Carillo, N. (1944) "*Shear Failure of Anisotropic Materials*", Proc. of Boston Society of Civil Engineers, Volume 31, pp:74-87.

Chan, F.W.K. (1990) "*Permanent Deformation Resistance of Granular Layers in Pavements*", PhD thesis, University of Nottingham.

Chan, C.K. and Sousa, J.B. (1991) "*State-of-the-art on Geotechnical Laboratory Testing*", Paper Presented at the Geotechnical Engineering Divison of ASCE, Geotechnical Engineering Congress, Boulder, Colorado.

Chang, C.S., Kabir, M.G. and Chang, Y. (1992) "*Micromechanics Modelling for Stress-strain Behaviour of Granular Soils II:Evaluation*", Journal of Geotechnial Engineering, ASCE, Volume 118, No:12, pp:1975-1993.

Chen, W.F. and Saleeb, A.F. (1982) "*Constitutive Equations for Engineering Materials*", Volume 1, Elasticity and Modelling, John Wiley and Sons.

Cheung, L.W. (1990) "*Research to Improve Road Foundatiion Design*", First Year Report, University of Nottingham, Report no: PR90043.

Cheung, Y.K. and Yeo, M.F. (1979) "*A Practical Introduction to Finite Element Analysis*", Pitman Publishing Limited, London.

Christian, J.T. and Desai, C.S. (1977) "*Constitutive Laws for Geologic Media* ", Numerical Methods in Geotechnical Engineering, Edited by Desai and Christian, McGraw Hill Book Company.

Collins, S.A. and Bachus, R.C. (1987) "*Use of Hypoelasticity to Model the Behaviour of Sands*", Proc. of Int. Workshop on Constitutive Equations for Granular Non- cohesive Soils, Cleveland, pp:201-236.

Coon, M.D. and Evans, R.G.(1971) "*Recoverable Deformation of Cohesionless Soils*", Journal of Soil Mechancis and Foundation, ASCE, Volume 97, No SM1, pp:375-391.

Coon, M.D. and Evans R.G (1972) "*Incremental Constitutive Laws and Their Associated Falure Criteria with Application to Plain Concrete*", Int. Journal of Solids and Structures, Volume 8, pp:1169-1183.

Cripps Compting Centre (1989) "*Using SIMPLE PLOT Library on VME System*", Crispps Computing Centre, University of Nottingham.

Crockford, W.W. (1993) "*Role of Principal-plane Rotation in Flexible Pavement Deformation*", Journal of Transportation Engineering, ASCE, Volume 119, No:1, pp:124-141.

Datong, Z. and Huichang, W. (1982) "*Non-linear Stress-strain Models of Soils under Cyclic Loading*", Proc. of Third Int. Earthquake Microzonation Conf., Seattle, USA, Volume 2, pp:1145-1156.

Dawson, A.R., Brown, S.F. and Thom, N.H. (1989) "*Use of Furnace Bottom Ash as a Subbase Material: Results of a Preliminary Study*", Submitted to CEGB, Report no: FBA/1, University of Nottingham.

Dawson, A.R. and Bullen, F. (1991) "*Furnace Bottom Ash: Its Engineering Properties and Its Use as a Subbase Material*", Proc, Inst. Civil Eng., Volume 90, part 1, pp:993-1009.

Department of the Environment (1970) "*A guide to the Structural Design of Pavements for new Roads*", Road Note 29, RRL.

Deresiewicz, H. (1958) "*Stress-strain Relations for a Simple Model of a Granular Medium*", Journal of Applied Mechanics, Volume 25, pp:402-406.

Dixon, W.J. Brown, M.B., Engelman, L., Hill, M.A. and Jennrich, R.I. (1988) "*BMDP Statistical Software Manual*", University of California Press, Berkeley, California.

Domaschuk, L. and Wade, N.H. (1969) "*A Study of Bulk and Shear Moduli for a Sand*", Journal of Soil Mechanics and Foundation Divison, ASCE, Volume 95, No: SM2, pp:561-581.

Duffy, J. and Mindlin, R.D. (1957) "*Stress-strain Relations and Vibrations of a Granular Medium*", Journal of Applied Mechanics, Volume 24, pp:585-593.

Duncan, J.M., Monismith, C.L. and Wilson, E.L. (1968) "*Finite Element Analyses of Pavements*", Highway Research Record 228, pp:18-33.

Duncan, J.M. (1980) "*Hyperbolic Stress-strain Relationships* ", Proc. of the Workshop on Limit Equilibrium, Plasticity and Generalized Stress-strain in Geotechnical Engineering, McGill University, pp:443-461.

Elhannani, M. (1991) "*Modelisation et Simulation Numerique des Chaussees Souples*", PhD thesis, University of Nantes, France.

El-Sohby, M.A. and Andrawes, K.Z. (1972) "*Discussion Paper on Inherent Anisotropy in a Sand*", Geotechnique, Volume 22, No:3, pp:538-541.

El-Sohby, M.A. and Andrawes, K.Z. (1973) "*Experimental Examination of Sand Anisotropy*" Int. Conf. on Soil Mechanics and Foundation. Engineering. Moscow, Vol.1, pp:103-109.

Evans, R.J. and Pister, K.S. (1972) "*Constitutive Equations for a Class of Non-linear Elastic Solids*", Int. Journal of Solid and Structures, Volume 2, pp:427-445.

Gazetas, G. (1982) "*Stresses and Displacements in Cross-anisotropic Soils*", Journal of Geotechnical Engineering, ASCE, Volume 108, No:GT4, pp:532-553.

Gerrard, C.M. and Mulholland, P. (1966) "*Stress Strain and Displacement Distributions in Cross-anisotropic and Two Layer Isotropic Elastic Systems*", ARRB Proceedings, Volume 3, Part 3, pp:1123-1158.

Gerrard, C.M. (1969) "*The Analysis of a Homogenous, Cross-anisotropic Elastic Half Space Undergoing Deformations that Possess a Vertical Plane of Symmetry*", Highway Research Record 282, pp:41-47.

Gerstle, K.H. (1981) "*Simple Formulation of Triaxial Concrete Behaviour*", Proceedings of American Concrete Institute, Journal, Volume 78, pp: 382-387.

Graham, J. and Houlsby, G.T. (1983) "*Anisotropic Elasticity of a Natural Clay*", Geotechnique, Volume 33, No:2, pp:165-180.

Harr, M.E. (1977) "*Mechanics of Particulate Media*", McGraw Hill International Book Company.

Haruyama, M.(1981) "*Anisotropic Deformation-strength Characteristics of an Assembly of Spherical Particles under Three Dimensional Stresses*", Soils and Foundations, Volume 21, No:4, pp:41-55.

Head, K.H. (1981) "*Manual of Soil Laboratory Testing*", Volume 2 and 3, Pentech Press, London.

Henkel, D.J. and Gilbert, C.D. (1952) "*The Effect of Rubber Membrane on the Measured Triaxial Compression Strength of Clay Samples*", Geotechnique, Volume 3, pp:20-29.

Hicher, P-Y. and Lade P.V. (1987) "*Rotation of Principal Directions in K_o Consolidated Soil*", Journal of Geotechnical Engineering, ASCE, Volume 113, No:7, pp:774-788.

Hicks, G.R. and Monismith C.L. (1971) "*Factors Influencing the Resilient Response of Granular Materials*", Highway Research Record 345, pp:15-31.

Hight, D.W., Gens, A. and Symes, M.J. (1983) "*The Development of New Hollow Cylinder Apparatus for Investigating the Effects of Principal Stress Rotation in Soils*", Geotechnique, Volume 33, No:4, pp:355-383.

Hveem, F.N. (1955) "*Pavement Deflections and Fatigue Failures*", Highway Research Board Bulletin 114, pp:43-73.

Iwan, W.D. (1966) "*A Distributed-element Model for Hysteresis and Its Steady-state Dynamic Response*", Journal of Applied Mechanics, Volume 33, pp:893-900.

Iwan, W.D. (1967) "*On a Class of Models for the Yielding Behaviour of Continuous and Composite Systems*", Journal of Applied Mechanics, Volume 34, pp:612-617.

Jouve, P., Martinez, J., Paute, J.L. and Ragneau, E. (1987) "*Rational Model for the Flexible Pavements Deformations*", Proc. of 6th Int. Conf. on the Structural Design of Asphalt Pavements, Volume 1, pp:50-64.

Kalcheft, J.V. and Hicks, G.R. (1973) "*A Test Procedure for Determining the Resilient Response Properties of Granular Materials*", Journal of Testing and Evaluation, Volume 1, pp:472-479.

Kamal, M.A., Dawson, A.R., Farouki, O.T., Hughes, D.A.B and Sha'at, A.A. (1993) "*Field and Laboratory Evaluation of the Mechanical Behaviour of Unbound Granular Materials in Pavements*", Presented at 72th Annual Meeting of Transportation Research Board, Washington D.C.

Kamal, M.A. (1993) "*Behaviour of Granular Materials Used in Flexible Pavements*", PhD thesis, The Quenns University of Belfast.

Karasahin, M., Dawson, A.R. and Holden, J.T. (1993) "*The Applicability of Resilient Constitutive Models of Granular Material for Unbound Base Layers*", Presented at 72th Annual Meeting of Transportation Research Board, Washington D.C., to be published in the Transportation Research Record.

Ko, H-Y. and Masson, K.M. (1976) "*Non-linear Characterization and Analysis of Sand*", Numerical Methods in Geomechanics, ASCE, pp:294-305.

Ko, H-Y, and Sture, S. (1980) "*State of the Art: Data Reduction and Application for Analytical Modelling*", Laboratory Shear Strength of Soil, ASTM, STP 740, Philadelphia, pp:329-387.

Kolymbos, D. (1987) "*Generalized Hypoelastic Constitutive Equation*", Int. Workshop on Constitutive Equations for Granular Non-cohesive Soils, Cleeveland, pp:349-367.

Kondner, R.L. (1963) "*Hyperbolic Stress-strain Response: Cohesive Soils*", Journal of Soil Mechanics and Foundation, ASCE, Volume 89, No: SM1, pp:115-143.

La Rochelle, P., Leroueil, S., Trak, B., Blais-Leroux, L and Tavenas, F. (1988) "*Observational Approach to Membrane and Area Corrections in Triaxial Tests*", Adanced Triaxial Testing of Soil and Rock, Edited by Donache, Chaney and Silver, ASTM, STP 977, Philadelphia, pp:715-731.

Lade, P.V. and Nelson, R.D. (1987) "*Modelling the Elastic Behaviour of Granular Materials*", Int. Journal for Numerical and Analytical Methods in Geomechanics, Volume 2, pp:521-542.

Lambe, T.W. and Whitman, R.V. (1979) "*Soil Mechanics, SI version*", John Wiley and Sons.

Lazan, B. (1968) "*Damping of Materials and Members in Structural Mechancis*", Pergamon Press, UK.

Little, P (1993) "*The Design of Unsurfaced Roads Using Geosynthetics*",PhD thesis, University of Nottingham.

Matsuoka, H. and Ishizaki, H. (1981) "*Deformation and Strength of Anisotropic Soil* ", Proc. 10th Int. Conf. on Soil Mechanics and Foundation Eng., Sweden, Volume 1, pp: 699-706.

May, R.W. And Witczak, W.W. (1981) "*Effective Granular Modulus to Model Pavement Responses*", Transportation Research Record 810, pp:1-9.

Mayhew, H.C. (1983) "*Resilient Properties of Unbound Roadbase under Repeated Triaxial Loading*", TRRL Laboratory Report 1088.

Mindlin, R.D. (1949) "*Compliance of Elastic Bodies in Contact*", Journal of Applied Mechanics, pp:259-268.

Nataatmadja, A. (1992) "*Resilient Modulus of Granular Materials under Repeated Loading*", 7th Int. Conf. on Asphalt Pavements, Nottingham, UK, Volume 1, pp:172-185.

Nataatmadja, A. and Parkin, A.K. (1989) "*Characterization of Granular Materials for Pavements*", Canadian Geotechnical Journal, Volume 26, pp:725-730.

Ochiai, H. and Lade, P.V. (1983) "*Three Dimensional Behaviour of Sand with Anisotropic Fabric*", Journal of Geotechnical Engineering, ASCE, Volume 109, No:10, pp:1313-1328.

Oda, M. and Sudoo, T. (1989) "*Fabric Tensor Showing Anisotropy of Granular Soils and Its Application to Soil Plasticity*", Powders and Grains, Edited by Biarez and Gourves, Balkema, Rotterdam.

O'Reilly, M.P. (1985) "*Mechanical Properties of Granular Materials for Use in Thermal Energy Stores*", PhD thesis, University of Nottingham.

O'Reilly, M.P. (1991) "*Cyclic Load Testing of Soils*", Cyclic Loading of Soils: From Theory to Design, Edited by O'Reilly and Brown, Blackie, Glasgow and London, pp:70-121.

O'Reilly, M.P. and Brown, S.F. (1992) "*Observations on the Resilient Shear Stiffness of Granular Materials*", Geotechnique, Volume 42, No:4, pp:631-634.

Pappin, J.W. (1979) "*Characteristics of a Granular Material for Pavement Analysis*", PhD thesis, University of Nottingham.

Pappin, J.W. and Brown, S.F. (1980) "*Resilient Stress-strain Behaviour of a Crushed Rock*", Proc. of Int. Symposium on Soils and Transient Loading", Volume 1, Swensea, pp:169-177.

Pappin, J.W., Brown, S.F. and O'Reilly, M.P. (1992) "*Effective Stress Behaviour of Saturated and Partially Saturated Granular Material Subjected to Repeated Loading*", Geotechnique, Volume 42, No:3, pp:485-497.

Paute, J.L. and Martinez, J. (1982) "*Structural Finite Element Design of Unbound Material Pavements from Cyclic Loading Triaxial Tests*", Proc. of 5th Int. Conf. on the Structural Design of Asphalt Pavements, Volume 1, pp:792-804.

Peattie, K.R. (1978) "*Flexible Pavement Design*", Developments in Highway Pavement Engineering, Volume 1, Edited by Pell, Applied Science Publishers Ltd, pp:1-40.

Pickering, D.J, (1970) "*Anisotropic Elastic Parameters for Soil*", Geotechnique, Volume 20, No: 3, pp:271-276.

Powell, W.D., Potter, J.F., Mayhew, H.C. and Nunn, M.E. (1984) "*The Structural Design of Bituminous Roads*", TRRL Laboratory Report 1132.

Roscoe, K.H., Schofield, A.N. and Wroth, C.P. (1958) "*On the Yielding of Soils*", Geotechnique, Volume 8, No:1, pp:22-52.

Rowe, P.W. (1971) "*Theoretical Meaning and Observed Values of Deformation Parameters for Soil*", Rescoe Memorial Symposium, Cambridge University, Session 2, pp:143-194.

RStO 86 (1986) "*Richtlinien fur die Standardisierung des Oberbaues von Verkehrsflachen*", Forschunggesellschaft Fur Strassen-und Verkehrswesen, Bonn, Germany.

Saada, A.S. and Townsend, F.C. (1980) "*State of the art: Laboratory Strength of Soils*", Laboratory Shear Strength of Soil, Edited by Yong and Townsend, ASTM, STP 740, pp:7-77.

Saada, A.S. (1988) "*State of art Paper-Hollow Cylinder Devices: Their Advantages and Limitations*", Advanced Triaxial Testing of Soil and Rock, Edited by Donaghe, Chaney and Silver, ASTM, STP 977, Philadelphia, pp:766-790.

Schroeder, L.D., Sjoquist, D.L. and Stepman, P.E. (1986) "*Understanding Regression Analysis an Introductory Guide*", Sage Publications Inc., USA.

Selig, E.T. and Roner, C.J. (1987) "*Effect of Particle Characterization on Behaviour of Granular Material* " Transporation Research Record 1131, pp:1-6.

Silveria, A and Souto Silveria, E.B. (1973) "*Elastic Parameters for Soils with Cross-anisotropy*", Proc. of 8th Int. Conf. on Soil Mechanics and Foundation Engineering, Volume1, Moscow, pp:361-365.

SPSS (1988) "*SPPS-X User's Guide*", Third edition, SPSS Inc. USA.

Stackel, B. (1973) "*The Derivation of Complex Stress-strain Relations*", Proc. of 8th Int. Conf. on Soil Mechanics and Foundation Engineering, Volume 1, Moscow, pp:353-359.

Stackel, B. (1991), "*Keynote Paper: Implications of Mechanistic Pavement Design on the Choice of Procedures for Testing Pavement Materials*", National Workshop on Elastic Characterisation of Pavement Materials and Subgrades, ARRB, ARPG Report No: 3.

Stankowski, T. and Gerstle, K.H. (1985) "*Simple Formulation of Concrete Behaviour under Multiaxial Load Histories*", Proceedings of the American Concrete Institute, Volume 82, pp:213-221.

Stojadinovic, S. (1989) "*The use of Uniform Sand for Road Construction*", Unbound Aggregates in Roads, Edited by Jones and Dawson, Butterworths, pp 380-387.

Sweere, G.T.H., Penning, A. and Vos, E. (1987) "*Development of a Structural Design Procedure for Asphalt Pavements with Crushed Rubble Base Courses*", Proc 6th Int. Conf. on the Structural Design of Asphalt Pavements", Volume 1, pp:34-49.

Sweere, G.T.H. (1990) "*Unbound Granular Bases for Roads*", PhD thesis, Delft University of Technology, The Netherlands.

Symes, M.J., Hight, D.W. and Gens, A. (1982) "*Investigating Anisotropy and the Effects of Principal Stress Rotation and of the Intermediate Principal Stress Using a Hollow Cylinder Apparatus*", IUTAM Conference on Deformation and Failure of Granular Materials, Delft, pp:441-449.

Tatsuoka, F., Iwasaki, T. and Takagi, Y. (1978) "*Hysteretic Damping of Sands under Cyclic Loading and Its Relation to Shear Modulus*", Soils and Founadation, Volume 18, No:2, pp:25-40.

Taylor, P.W. and Larkin T. (1978) "*Seismic Site Response of Non-linear Soil Media*", Journal of Geotechnical Engineering, ASCE, Volume 104, No:GT3, pp:369-383.

Terzaghi, K. (1943) "*Theoretical Soil Mechancis*", Wiley.

Thom, N.H. (1988) "*Design of Road Foundations*", PhD thesis, University of Nottingham.

Thom, N.H. and Brown, S.F. (1989) "*The Mechanical Properties of Unbound Aggregates from Different Sources*", Unbound Aggregates in Roads, Edited by Jones and Dawson, pp:130-142.

Thom, N.H. and Brown, S.F. (1988) "*The Effect of Grading and Density on the Mechanical Properties of a Crushed Dolomitic Limestone*", Proc. 14th ARRB Conf., part 7, pp:94-100.

Thompson, M.R. (1992) "*ILLI-PAVE Based Conventional Flexible Pavement Design Procedure*", 7th Int. Conf. on Asphalt Pavements,Nottingham, UK., Volume 1, pp:318-333.

Timoshenko, S.P. and Goodier, J.N. (1970) "*Theory of Elasticity*", McGraw-Hill International Editions, Engineering Mechanics Series, Third Edition.

Transportation Research Board (1975) "*Test Procedures for Characterising Dynamic Stress-strain Properties of Pavement Materials*", Special Report 162, Transporation Reserach Board, National Reserach Council, Washington D.C.

Truesdell, C. (1955) "*Hypo-elasticity*", Journal of Rational Mechanics Analysis, Volume 4, pp:83-133.

Uzan, J. (1985) "*Characterization of Granular Material*", Transportation Research Record 1022, pp:52-59.

Uzan, J., Lytton, R.L. and Germann, F.P. (1989) "*General Procedure for Backcalculating Layer Moduli*", Nondestructive Testing of Pavements and Backcalculation of Moduli, Edited by Bush and Baladi, ASTM, STP 1026, Philadelphia, pp:217-228.

Uzan, J. (1992) "*Resilient Characterization of Pavement Materials*", International Journal for Numerical and Analytical Methods in Geomechanics", Volume 16, pp:453-459.

Uzan, J.,Witczak, M.W, Scullion, T. and Lytton, R.L. (1992) "*Development and Validation of Realistic Pavement Response Models*", Proc. of 7th Int. Conf. on Asphalt Pavements Volume 1, pp:334-350.

Wesley, L.D. (1980) "*The Nature of Anisotropy in Soft Clays*", Third Australian-New Zealand Conf. on Geomechanics, Wellington, Volume 1, pp:219-224.

Wong, R.K.S and Arthur, J.R.F. (1985) "*Induced and Inherent Anisotropy in Sand*", Geotechnique, Volume 35, No:4, pp:471-481.

Wood, D.M.(1984) "*On stress parameters*", Geotechnique, Volume 34, pp:282-287.

Wood, D.M. (1991) "*Approaches to Modelling the Cyclic Stress-strain Response of Soils*", Cyclic Loading of Soils: From Theory to Design, Edited by O'Reilly and Brown, Blackie,Glasgow and London, pp:19069.

Yin, Y-H., Saadat, F. and Graham, J. (1990) "*Constitutive Modelling of a Compacted Sand-bentonite Mixture Using Three-modulus Hypoelasticty*", Canadian Geotechnical Journal, Volume 27, pp:365-372.

Zienkiewicz, O.C. and Taylor, R.L. (1989) "*The Finite Element Method*", Fourth edition, Volume 1, McGraw-Hill Book Company.

Zytynski, M., Randolph, M.F., Nova, R. and Wroth C.P. (1978) "*On Modelling the Unloading-reloading Behaviour of Soils*", International Journal for Numerical and Analytical Methods in Geomechanics, Volume 2, pp:87-94.

APPENDIX A

MATERIAL PROPERTIES

Table A.1.GS physical properties (Kamal, 1993)

Specific gravity	2.69
Water absorption	0.47%
Aggregate crushing value	16.6
Aggregate impact value	13.7
Aggregate abrasion value	5.1
Polished stone value	61

Table A.2.FBA physical characteristics (Dawson et al, 1989)

Specific gravity	2.24
10% fines value	24-33 kN
Optimum moisture content	8-12 %
Permeability index	0.0002 m/s

Table A.3. Soft limestone physical properties(Cheung, 1990)

Specific gravity	2.69
Water absorption	2.69%
10% fines value	130 kN
Aggregate impact value	31.30%
Aggregate abrasion value	16
Surface friction angle(degree)	31

Table A.4.Sand and gravel physical properties (Cheung, 1990)

Specific gravity	2.61
Water absorption	0.90%
10% fines value	305
Aggregate impact value	19.60%
Aggregate abrasion value	1.9
Surface friction angle(degree)	26

Table A.5.Specific gravity of other materials

FS	2.64
GWRS	2.64

APPENDIX B

REPEATED LOAD TRIAXIAL TEST RESULTS

Abbrevations used in this Appendix
c1 = initial cell pressure (kPa)
c2 = final cell pressure (kPa)
q1 = initial deviatoric stress (kPa)
q2 = final deviatoric stress (kPa)

TABLE B.1. FBA REPEATED LOAD TRIAXIAL TEST RESULTS

q1	q2	c1	c2	axial strain	radial strain
Repeated deviatoric stress with constant cell pressure					
0	50	199	199	52	-27
0	100	201	201	117	-56
0	149	202	202	202	-75
0	195	203	203	280	-107
1	-42	204	204	-63	31
0	-96	202	202	-186	65
-24	25	203	203	64	-38
-51	-99	205	205	-86	32
50	100	201	201	53	-26
0	50	252	252	48	-23
0	95	253	253	96	-51
0	144	252	252	157	-74
-9	182	250	250	227	-97
150	196	246	246	35	-25
97	141	247	247	39	-21
49	99	248	248	47	-30
-53	-100	253	253	-66	28
-50	48	253	253	120	-60
0	-50	251	251	-50	27
-46	54	152	152	182	-81
-50	-96	152	152	-111	39
-24	27	151	151	85	-46
0	-44	149	149	-85	39
0	50	151	151	71	-35
0	100	151	151	142	-69
0	148	151	151	247	-109
0	200	147	147	347	-160
0	50	101	101	85	-48
0	100	101	101	180	-101
0	149	102	102	287	-147
0	199	101	101	400	-221
100	200	100	100	114	-75
0	-46	101	101	-112	48
24	25	101	101	103	-50
-49	50	101	101	251	-108
0	50	51	51	104	-73
0	190	25	25	395	-503

q1	q2	c1	c2	axial strain	radial strain
0	149	25	25	312	-354
0	232	23	23	490	-650
0	279	23	23	585	-900
0	241	143	143	440	-299
0	281	143	143	526	-342
0	326	143	143	600	-408
0	374	143	143	685	-471
0	241	102	102	515	-388
0	284	101	101	619	-475
0	327	100	100	712	-560
0	372	98	98	793	-658
0	248	54	54	604	-617
0	281	56	56	658	-692
0	328	56	56	750	-809
0	373	56	56	830	-900
Repeated cell pressure					
217	217	102	149	6	116
217	217	149	196	7	77
200	200	200	246	20	53
200	200	150	242	27	138
50	50	49	97	23	162
51	51	108	155	26	95
50	50	107	200	58	150
50	50	200	245	27	47
150	150	101	149	20	97
149	149	148	195	18	75
148	148	100	195	40	184
145	145	197	243	10	57
100	100	101	147	23	90
97	97	148	195	27	68
100	100	197	243	18	52
100	100	150	241	42	124
0	0	50	97	47	138
0	0	98	145	30	74
0	0	50	145	86	216
0	0	146	193	30	56
0	0	147	239	51	109
0	0	195	241	24	48
0	0	99	192	60	134
194	194	102	195	8	210
148	148	150	242	33	134

q1	q2	c1	c2	axial strain	radial strain
0	0	100	147	35	85
Repeated both stresses					
0	47	198	184	50	-42
0	100	198	168	106	-91
0	49	149	134	66	-58
0	99	149	118	147	-143
0	144	148	103	223	-224
0	49	101	87	89	-86
0	51	100	146	120	46
0	99	99	148	194	28
0	141	100	147	259	-28
0	200	100	147	360	-57
0	50	53	100	147	99
0	94	53	100	225	58
0	149	53	100	324	-63
0	198	53	100	414	-102
0	95	53	145	236	170
0	138	52	190	345	227
0	97	100	194	210	104
0	143	100	240	286	143
0	193	50	238	445	299
0	196	100	277	391	178
0	51	244	181	28	-100
0	49	196	133	39	-130
50	99	134	72	56	-228
49	99	180	118	43	-146
-25	-41	58	85	-18	99

TABLE B.2. GWRS REPEATED LOAD TRIAXIAL TEST RESULTS

q1	q2	c1	c2	axial strain	radial strain
Repeated deviatoric stress with constant cell pressure					
0	141	200	200	227	-86
0	190	198	198	348	-115
0	100	195	195	106	-42
0	46	253	253	47	-22
0	92	255	255	113	-41
0	183	256	256	268	-94
149	196	250	250	47	-22
100	149	251	251	43	-24
-50	50	259	259	133	-45
0	50	152	152	74	-31
0	185	151	151	382	-156
1	50	100	100	81	-46
0	99	101	101	215	-93
0	149	103	103	317	-149
Repeated cell pressure					
200	200	100	147	11	129
201	201	147	193	12	92
200	200	195	241	11	69
199	199	147	240	35	160
50	50	53	100	10	193
49	49	52	146	22	335
49	49	100	146	10	115
50	50	100	193	35	209
160	160	100	145	12	121
160	160	146	192	12	90
160	160	99	192	28	227
159	159	195	241	16	76
112	112	100	147	10	112
113	113	148	194	14	80
111	111	196	242	14	68
111	111	147	241	39	150
0	0	47	94	103	300
0	0	49	144	242	460
0	0	98	144	80	152
0	0	150	197	79	118
0	0	150	244	144	250
0	0	199	245	63	98

TABLE B.2. GWRS REPEATED LOAD TRIAXIAL TEST RESULTS

q1	q2	c1	c2	axial strain	radial strain
Repeated deviatoric stress with constant cell pressure					
0	141	200	200	227	-86
0	190	198	198	348	-115
0	100	195	195	106	-42
0	46	253	253	47	-22
0	92	255	255	113	-41
0	183	256	256	268	-94
149	196	250	250	47	-22
100	149	251	251	43	-24
-50	50	259	259	133	-45
0	50	152	152	74	-31
0	185	151	151	382	-156
1	50	100	100	81	-46
0	99	101	101	215	-93
0	149	103	103	317	-149
Repeated cell pressure					
200	200	100	147	11	129
201	201	147	193	12	92
200	200	195	241	11	69
199	199	147	240	35	160
50	50	53	100	10	193
49	49	52	146	22	335
49	49	100	146	10	115
50	50	100	193	35	209
160	160	100	145	12	121
160	160	146	192	12	90
160	160	99	192	28	227
159	159	195	241	16	76
112	112	100	147	10	112
113	113	148	194	14	80
111	111	196	242	14	68
111	111	147	241	39	150
0	0	47	94	103	300
0	0	49	144	242	460
0	0	98	144	80	152
0	0	150	197	79	118
0	0	150	244	144	250
0	0	199	245	63	98

TABLE B.3. FS REPEATED LOAD TRIAXIAL TEST RESULTS

q1	q2	c1	c2	axial strain	radial strain
Repeated deviatoric stress with constant deviatoric stress					
0	49	198	198	75	-30
0	98	198	198	177	-51
0	139	198	198	260	-75
0	187	198	198	354	-104
0	-49	200	200	-34	84
0	-93	200	200	-190	53
-25	25	199	199	83	-31
-49	-95	200	200	-91	32
0	98	250	250	162	-51
0	147	247	247	253	-67
0	190	250	250	325	-90
125	174	251	251	58	-35
99	148	251	251	65	-33
49	100	252	252	65	-28
-48	-93	253	253	-73	28
-49	49	253	253	165	-53
0	-49	250	250	-79	35
-49	47	156	156	203	-62
-50	-99	157	157	-110	36
-23	21	153	153	87	-38
0	-50	144	144	-101	43
-5	42	149	149	87	-32
-5	88	148	148	188	-60
0	130	147	147	289	-90
-11	178	145	145	398	-115
0	49	106	106	112	-40
0	100	106	106	238	-79
0	148	108	108	368	-124
0	187	110	110	477	-171
98	191	104	104	181	-83
0	-49	109	109	-126	43
-24	25	107	107	119	-46
-49	45	107	107	255	-78
49	148	109	109	220	-83
49	98	109	109	98	-41

q1	q2	c1	c2	axial strain	radial strain
Cycling cell pressure					
207	207	102	149	15	114
206	206	151	196	18	90
207	207	200	244	18	73
208	208	150	242	61	174
64	64	56	103	25	153
60	60	57	149	80	263
59	59	102	150	36	102
62	62	102	195	94	196
64	64	202	248	25	78
160	160	102	149	26	110
155	155	150	196	25	94
160	160	103	193	72	203
150	150	198	244	25	80
100	100	101	149	25	107
110	110	149	196	25	84
115	115	200	244	29	73
112	112	149	242	76	158
0	0	54	100	76	136
0	0	100	146	54	83
0	0	53	146	173	228
0	0	148	194	54	71
0	0	150	235	108	140
0	0	196	240	43	64
0	0	100	191	138	152
Repeated both pressures					
-7	41	196	181	62	-60
-11	86	195	165	166	-107
0	49	148	133	90	-64
-2	89	148	118	188	-130
0	92	149	102	166	-188
0	49	101	86	112	-86
0	93	101	72	242	-172
0	90	103	148	329	-56
-2	136	103	149	456	-60
-2	186	102	149	589	-22
0	91	55	103	383	-86
-2	139	56	101	546	-60
-2	185	55	101	705	-30
0	190	194	133	362	-251

q1	q2	c1	c2	axial strain	radial strain
-5	-25	56	103	29	178
2	45	54	101	242	129
0	149	54	196	647	-301
-7	82	102	192	376	-148
-7	131	102	234	571	-196
-16	180	100	275	726	-370

TABLE B.4. GS REPEATED LOAD TRIAXIAL TEST RESULTS

q1	q2	c1	c2	axial strain	radial strain
Repeated deviatoric stress with constant cell pressure					
0	50	202	202	45	-28
0	93	201	201	88	-39
0	146	201	201	143	-71
0	198	200	200	197	-43
99	187	197	197	71	-43
0	-50	203	203	-52	18
0	-97	205	205	-147	52
-25	25	202	202	52	-32
-50	-98	205	205	-71	26
50	99	199	199	38	-24
0	46	250	250	35	-21
0	100	250	250	82	-34
0	145	250	250	119	-55
0	199	248	248	168	-70
100	145	249	249	30	-21
50	100	249	249	41	-21
-50	-98	259	259	-48	25
-50	49	256	256	97	-33
-49	0	256	256	-45	25
-50	45	145	145	160	-56
-50	-98	148	148	-97	30
-25	24	147	147	70	-26
0	-46	147	147	-67	26
0	50	150	150	55	-30
0	100	148	148	119	-56
0	147	148	148	175	-76
0	188	147	147	220	-98
0	49	100	100	82	-34
0	100	100	100	144	-69
0	149	100	100	212	-106
0	195	101	101	283	-148
100	196	98	98	89	-55
0	-46	102	102	-93	37
-25	25	101	101	86	-34
-50	49	101	101	207	-97
0	49	49	49	96	-49

q1	q2	c1	c2	axial strain	radial strain
Repeated cell pressure					
203	203	99	146	10	61
203	203	147	194	11	47
195	195	195	242	11	41
201	201	146	240	14	90
50	50	50	98	11	101
49	49	50	144	26	215
33	33	98	145	11	73
51	51	99	192	20	130
31	31	196	242	11	42
150	150	99	145	6	60
137	137	147	193	6	47
150	150	93	193	18	127
132	132	195	242	7	37
99	99	99	145	11	63
120	120	146	193	11	40
122	122	195	242	11	32
97	97	146	240	19	83
0	0	51	98	45	90
0	0	50	144	104	151
0	0	99	146	33	52
0	0	147	194	22	37
0	0	145	241	56	75
0	0	195	241	22	30
Repeated both pressures					
0	49	193	177	26	-34
0	95	192	158	60	-61
0	49	148	130	34	-33
0	100	145	115	75	-81
0	146	144	100	123	-139
0	94	97	82	103	-82
0	45	97	82	41	-48
0	98	97	66.7	100	-122
0	48	145	97	78	-33
0	103	144	97	130	-25
0	137	144	98	171	-20
0	189	145	98	216	-30
0	49	97	49	119	-69
0	100	99	50	179	-41
0	198	98	50	231	-21

q1	q2	c1	c2	axial strain	radial strain
0	198	97	50	280	-38
0	196	190	129	130	-142
-39	-50	96	50	41	-83
0	147	97	26	189	-623

TABLE B.5. SAG REPEATED LOAD TRIAXIAL TEST RESULTS

q1	q2	c1	c2	axial strain	radial strain
Repeated deviatoric stress with constant cell pressure					
0	45	197	197	57	-22
0	95	194	194	150	-45
-3	143	190	190	238	-69
-5	181	192	192	302	-96
92	185	187	187	120	-44
50	95	189	189	60	-22
0	48	247	247	53	-20
0	99	247	247	111	-37
0	147	247	247	170	-45
0	199	248	248	240	-64
150	190	247	247	40	-16
50	99	247	247	47	-17
-25	25	150	150	83	-27
0	99	150	150	155	-45
0	145	150	150	228	-72
0	193	149	149	293	-95
0	50	101	101	97	-34
0	100	101	101	205	-60
0	149	101	101	290	-86
0	195	101	101	366	-119
Repeated cell pressure					
209	209	100	147	6	103
207	207	143	190	7	58
195	195	190	237	7	48
217	217	145	240	13	110
50	50	54	100	6	161
49	49	54	147	10	263
63	63	100	147	6	76
47	47	100	194	16	138
48	48	196	242	10	42
153	153	100	147	6	85
150	150	148	194	7	66
152	152	100	194	10	165
149	149	195	241	10	41
100	100	101	147	7	90

q1	q2	c1	c2	axial strain	radial strain
100	100	147	194	6	57
99	99	196	241	10	46
99	99	147	241	16	102
Repeated both stresses					
0	47	195	180	41	-40
0	86	195	164	72	-77
0	45	148	132	55	-46
0	86	148	116	100	-103
0	139	100	146	212	-201
0	96	100	83	183	-149
0	47	100	83	69	-77
0	98	100	68	186	-207
0	100	100	147	180	-20
0	145	100	147	273	-35
0	184	100	147	345	-69
0	99	53	101	269	-40
0	149	53	100	378	-43
0	186	53	100	457	-124

TABLE B.6. SL REPEATED LOAD TRIAXIAL TEST RESULTS

q1	q2	c1	c2	axial strain	radial strain
Repeated deviatoric stress with constant cell pressure					
0	50	199	199	74	-25
0	99	198	198	164	-49
0	144	198	198	236	-71
0	199	199	199	342	-111
0	-42	200	200	-80	16
0	-100	200	200	-247	60
-50	-97	200	200	-108	28
50	99	198	198	65	-21
0	46	248	248	62	-17
0	100	248	248	141	-31
0	141	248	248	207	-56
0	186	247	247	280	-82
150	198	246	246	43	-16
100	144	248	248	43	-18
51	101	247	247	55	-14
-50	49	247	247	157	-42
0	-50	247	247	-76	21
-50	45	153	153	233	-59
-50	-93	153	153	136	-30
-25	25	153	153	94	-29
0	-48	152	152	-105	27
0	49	151	151	80	-26
0	97	151	151	189	-53
0	148	151	151	287	-88
0	188	151	151	370	-121
0	49	102	102	92	-20
0	97	103	103	197	-59
0	143	103	103	313	-104
0	199	102	102	470	-174
98	197	103	103	157	-61
0	-49	104	104	-127	35
-25	24	105	105	108	-30
-50	51	104	104	325	-91
0	50	53	53	148	-58
0	100	54	54	302	-128
0	146	56	56	431	-207
0	199	57	57	559	-307

q1	q2	c1	c2	axial strain	radial strain
0	232	54	54	692	-378
Repeated cell pressure					
201	201	100	147	10	112
201	201	150	197	6	80
200	200	201	247	7	65
200	200	150	243	18	135
54	54	50	96	10	165
52	52	49	142	19	302
59	59	102	148	10	95
57	57	102	195	30	165
50	50	201	248	10	63
157	157	100	147	7	102
158	158	150	197	7	74
159	159	100	193	18	194
154	154	201	247	10	66
100	100	100	146	10	100
101	101	150	197	10	69
101	101	201	248	11	58
99	99	150	244	26	131
0	0	50	96	73	126
0	0	102	148	40	72
0	0	49	103	153	219
0	0	150	197	29	61
0	0	150	242	73	112
0	0	198	244	18	47
0	0	101	195	95	148
202	202	100	193	15	200
156	156	150	244	18	144
Repeated both pressures					
0	46	205	188	65	-37
0	93	205	173	145	-85
0	50	150	133	80	-44
0	99	149	118	187	-122
0	149	149	103	301	-220
0	50	99	83	109	-66
0	97	100	69	241	-188
0	94	100	147	254	30
0	138	100	147	349	-13
0	184	100	147	443	-35
0	92	51	98	324	69

q1	q2	c1	c2	axial strain	radial strain
0	137	51	98	436	55
0	183	51	98	549	72

TABLE B.7. INHERENT ANISOTROPY TEST RESULTS (SAG)

initial cell pressure (kPa)	final cell pressure (kPa)	ANISOTROPY
27	50	0.82
27	74	0.80
27	97	0.86
27	121	0.88
27	145	0.91
27	168	0.98
28	192	0.97
27	215	1.01

TABLE B.8. STRESS-HISTORY INDUCED ANISOTROPY TEST RESULTS (SAG)

initial cell pressure (kPa)	final cell pressure (kPa)	ANISOTROPY
26	50	0.15
25	73	0.24
25	95	0.29
25	119	0.35
25	141	0.40
24	164	0.43
23	187	0.47
22	210	0.48

TABLE B.9. INHERENT ANISOTROPY TEST RESULTS (GS)

initial cell pressure (kPa)	final cell pressure (kPa)	ANISOTROPY
26	49	0.21
26	73	0.30
26	96	0.35
26	121	0.42
26	144	0.49
27	167	0.53
27	190	0.59
27	214	0.61

TABLE B.10. STRESS-HISTORY INDUCED ANISOTROPY TEST RESULTS (GS)

initial cell pressure (kPa)	final cell pressure (kPa)	ANISOTROPY
27	50	0.29
27	74	0.39
26	96	0.5
26	121	0.57
26	144	0.66
26	167	0.72
26	191	0.75
26	213	0.78

TABLE B.11. INHERENT ANISOTROPY TEST RESULTS (SL)

initial cell pressure (kPa)	final cell pressure (kPa)	ANISOTROPY
25	48	0.20
25	71	0.44
25	95	0.53
25	119	0.59
25	143	0.68
25	165	0.72
26	190	0.70
26	212	0.73

TABLE B.12. STRESS-HISTORY INDUCED ANISOTROPY TEST RESULTS (SL)

initial cell pressure (kPa)	final cell pressure (kPa)	ANISOTROPY
26	49	0.11
25	72	0.12
26	96	0.23
26	119	0.31
26	143	0.34
26	166	0.39
26	190	0.43
26	213	0.46

TABLE B.13. INHERENT ANISOTROPY TEST RESULTS (FS)

initial cell pressure (kPa)	final cell pressure (kPa)	ANISOTROPY
28	52	0.26
30	77	0.43
30	100	0.56
30	122	0.59
30	147	0.69
27	169	0.74
27	190	0.77
26	213	0.83

TABLE B.14. STRESS-HISTORY INDUCED ANISOTROPY TEST RESULTS (FS)

initial cell pressure (kPa)	final cell pressure (kPa)	ANISOTROPY
25	49	0.26
25	72	0.42
25	96	0.47
25	118	0.54
24	142	0.61
24	165	0.66
24	187	0.72
24	211	0.78

TABLE B.15. INHERENT ANISOTROPY TEST RESULTS (FBA)

initial cell pressure (kPa)	final cell pressure (kPa)	ANISOTROPY
25	48	0.13
25	71	0.24
23	93	0.23
22	116	0.24
25	142	0.31
26	166	0.34
26	189	0.33
26	213	0.36

TABLE B.16. STRESS-HISTORY INDUCED ANISOTROPY (FBA)

initial cell pressure (kPa)	final cell pressure (kPa)	ANISOTROPY
24	47	0.16
26	72	0.25
26	96	0.25
23	118	0.27
26	143	0.31
27	167	0.32
27	190	0.34
26	214	0.35

APPENDIX C

MODEL CONSTANTS

TABLE C.1. NEW MODEL CONSTANTS (ANISOTROPIC) *

	M_r			N		υ_1				υ_2			
	A	B	C	D	F	H	L	M	N	R	S	T	U
SL	56650	0.594	0.213	0.039	0.586	2.020	0.590	-0.390	0.320	-0.233	-0.420	-0.100	-0.140
FS	53929	0.567	0.197	0.050	0.540	33.160	0.244	-0.175	0.829	-0.006	0.375	0.510	0.260
SAG	34392	0.642	0.110	0.510	0.113	0.650	0.330	-0.300	0.004	1.0E-06	-0.950	2.170	-1.160
GS	42832	0.672	0.115	0.039	0.530	1.740	-0.100	0.450	0.540	0.016	1.290	0.850	1.550
FBA	37192	0.764	0.217	0.037	0.437	0.910	-0.040	0.330	0.285	-1.2E-04	-0.215	1.310	-0.100

TABLE C.2. NEW MODEL CONSTANTS(ISOTROPIC) **

	M_r			υ			
	A	B	C	D	F	H	L
GWRS	115183	0.592	0.335	1.940	0.056	0.190	0.230
SL	56650	0.594	0.213	0.876	0.270	0.360	0.070
GS	42832	0.672	0.115	1.009	0.170	0.050	0.340
SAG	34392	0.642	0.110	0.568	0.034	0.013	0.180
FS	53929	0.567	0.197	0.790	0.253	0.102	0.386
FBA	37192	0.764	0.219	3.730	0.112	0.520	0.064

* Based on data from all stress paths

** Based on constant cell pressure stress paths

TABLE C.3. K-θ MODEL CONSTANTS *

	A	B
FBA	103107	0.285
GS	15550	0.637
SAG	8628	0.678
SL	14842	0.564
GWRS	46284	0.410
FS	29450	0.440

TABLE C.4. UZAN (1985) MODEL CONSTANTS *

	A	B	C
FBA	149832	0.536	-0.370
GS	17741	0.738	-0.166
SAG	12429	0.723	-0.140
SL	31351	0.622	-0.235
GWRS	60297	0.649	-0.390
FS	25643	0.610	-0.203

TABLE C.5. BOYCE (1980) MODEL CONSTANTS **
(REPEATED DEVIATORIC STRESS)

	A	B	C
FBA	2936	0.367	5521
SL	2914	0.370	6266
GS	2165	0.280	6651
FS	8846	0.536	15126
SAG	183	0.072	1795
GWRS	-	-	-

TABLE C.6. BOYCE (1980) MODEL CONSTANTS
(REPEATED BOTH STRESSES)***

	A	B	C
FBA	2936	0.367	11360
SL	2914	0.370	8460
GS	2165	0.280	11311
FS	8846	0.536	11786
SAG	183	0.072	2134

* Based on constant cell pressure stress paths

** Based on data for repeated cell pressure with zero deviatoric stress and repeated deviatoric stress with constant cell pressure

*** Based on data for repeated cell pressure with zero deviatoric stress and repeated both stresses

TABLE C.7. ELHANNANI (1991) MODEL CONSTANTS (REPEATED DEVIATORIC STRESS)

	A	B	C	D
SAG	13180	0.072	130119	-1015778
GS	58900	0.283	206725	-454275
FS	74848	0.536	137486	-1087854
SL	52860	0.370	123175	-631690
FBA	54219	0.367	125193	-273120
GWRS	-	-	-	-

TABLE C.8. ELHANNANI (1991) MODEL CONSTANTS (REPEATED BOTH STRESSES)

	A	B	C	D
FS	74848	0.536	129532	-1087854
SAG	13180	0.072	253752	-1015778
GS	58900	0.283	383583	-454275
SL	52860	0.370	223078	-631690
FBA	54219	0.367	676070	-273120

TABLE C.9. PAPPIN AND BROWN (1980) MODEL CONSTANTS (REPEATED DEVIATORIC STRESS)

	A	B	C	D	E
FBA	4615352	0.610	0.200	1.0E+08	0.586
SL	39634688	0.530	0.135	1.0E+08	0.600
SAG	107426300	0.560	1.0E-08	1.0E+08	0.624
GS	819502	1.7E-04	5.9E-05	1.0E+07	0.640
GWRS	23743	1.900	1.0E-08	1.0E+08	0.608
FS	546873	0.964	1.0E-08	1.0E+07	0.730

TABLE C.10. PAPPIN AND BROWN (1980) MODEL CONSTANTS (REPEATED BOTH STRESSES)*

	A	B	C	D	E
FBA	3.9E-03	0.650	0.270	3.0E-06	0.33
FS	0.110	0.840	0.035	7.0E-06	0.33
GS	3.000	1.190	0.230	2.7E-05	0.33
SAG	2.9E-03	0.570	0.030	1.5E-05	0.33
SL	0.140	0.920	0.160	6.0E-06	0.33

* Based on data for repeated cell pressure with zero deviatoric stress and repeated deviatoric stress with constant cell pressure

** Based on data for repeated cell pressure with zero deviatoric stress and repeated both stresses

*** Based on data from constant cell pressure stress paths

**** Based on data from repeated both stresses, microstrain

APPENDIX D

SUBROUTINES AND CRISP DATA FILES

D.1. Main program data file for CRISP for the new anisotropic model*

RECORD D

P(1)	P(2)	P(3)	P(4)	P(5)	P(6)**	P(7)	P(8)***	P(9)
A	B	C	D	F		H		L

P(10)	P(11)	(P12)	P(13)****	P(14)****	P(15)****
M	N	R	S	T	U

* See model constants in Appendix B
** It is the indicator of anisotropy or isotropy
1= anisotropic
0= isotropic
*** Density
**** Second line

D.2. Main program data file for CRISP for the isotropic model

RECORD D

P(1)	P(2)	P(3)	P(4)	P(5)	P(6)*	P(7)	P(8)**	P(9)	P(10)	P(11)
A	B	C	D	F		H		L	0	0

P(12)
0

* The indicator of anisotropy or isotropy
1= anisotropic
0= isotropic
** Density

SUBROUTINE DEVIATORIC

```
      SUBROUTINE DEVIATORIC(IP,I,MUS,IET,NEL,NIP,NVRS,NDIM,NS,
     +                NPR,NMT,VARINT,MAT,D,PR,IPLSTK)
C=======================================================================
C   ISOTROPIC MODEL
C=======================================================================
      IMPLICIT DOUBLE PRECISION (A-H,O-Z)
      DIMENSION VARINT(NVRS,NIP,NEL),D(NS,NS),MAT(NEL),PR(NPR,NMT)
      COMMON/DIN/DEL(3),DEP(21)
      COMMON/INSITU/PE,QE
      COMMON/INCREMENT/JC
      REAL SX,SY,SZ,PM,Q2,Q,QM,P,EV1,EV,VV1,VV,A,TXY,NI
      INTEGER IPLSTK,AN,JC
      KM=MAT(I)
      SX=VARINT(1,IP,I)
      SY=VARINT(2,IP,I)
      SZ=VARINT(3,IP,I)
      TXY=VARINT(4,IP,I)
      P=ABS((SX+SY+SZ)/3.0)
      Q2=ABS((SX*(SX-SY))+(SY*(SY-SZ))+(SZ*(SZ-SX))+3*TXY*TXY)
      IF(Q2.LE.0.0) THEN
      Q2=1.0E-4
      ENDIF
      Q=ABS(SQRT(Q2))
      QM=ABS((QE+Q)/2.0)
      PM=ABS((PE+P)/2.0)
      AN=1
      EV1=PR(1,KM)*(PM**PR(2,KM))/(P**(PR(3,KM)))
      EV=EV1*(((PR(2,KM)/PM)*(PM/JC))-((PR(3,KM)/P)*(P/JC)))
      VV1=PR(4,KM)*(QM**PR(5,KM))/((P**PR(7,KM))*(PM**(PR(9,KM))))
      VV=VV1*(((PR(5,KM)/QM)*(QM/JC))-((PR(7,KM)/P)*(P/JC))-
     + ((PR(9,KM)/PM)*(PM/JC)))
      A=EV/((1.0+VV)*(1.0-VV-2.0*VV*VV))
C
      CALL ZEROR2(D,NS,NS)
      D(1,1)=A*(1.0-VV*VV)
      D(1,2)=A*VV*(1.0+VV)
      D(1,3)=A*VV+(VV*VV)
      D(2,1)=D(1,2)
      D(2,2)=A*(1.0-VV*VV)
      D(2,3)=D(1,2)
      D(3,1)=D(1,3)
      D(3,2)=D(2,3)
      D(3,3)=D(1,1)
      D(4,4)=EV/(2.0*(1-VV))
C
      DEL(1)=D(1,1)
      DEL(2)=D(1,2)
      DEL(3)=D(4,4)
C
      IS=0
      DO 40 J1=1,NS
      DO 40 I1=1,J1
      IS=IS+1
   40 DEP(IS)=D(I1,J1)
      RETURN
      END
```

SUBROUTINE GRAMM

```
      SUBROUTINE GRAMM(IP,I,MUS,IET,NEL,NIP,NVRS,NDIM,NS,
     +            NPR,NMT,VARINT,MAT,D,PR,IPLSTK)
C ================================================================
C   NON-LINEAR ANISOTROPIC MODEL
C================================================================
      IMPLICIT DOUBLE PRECISION (A-H,O-Z)
      DIMENSION VARINT(NVRS,NIP,NEL),D(NS,NS),MAT(NEL),PR(NPR,NMT)
      COMMON/DIN /DEL(3),DEP(21)
      COMMON/INSITU/PE,QE
      COMMON/INCREMENT/JC
      REAL SX,SY,SZ,PM,Q2,Q,QM,P,EV,EH,VH,VV,AN,A,TXY,EV1,VV1,VH1
      INTEGER IPLSTK,JC
      KM=MAT(I)
C
      SX=VARINT(1,IP,I)
C     PRINT *,SX
      SY=VARINT(2,IP,I)
C     PRINT *,SY
      SZ=VARINT(3,IP,I)
C     PRINT *,SZ
      TXY=VARINT(4,IP,I)
C     PRINT *,PE
C     PRINT *,QE
      P=ABS((SX+SY+SZ)/3.)
      PM=ABS((PE+P)/2.0)
      Q2=ABS((SX*(SX-SY))+(SY*(SY-SZ))+(SZ*(SZ-SX))+(3*TXY*TXY))
      IF(Q2.LE.0.0) THEN
      Q2=1.0E-4
      ENDIF
      Q=ABS(SQRT(Q2))
      QM=ABS((QE+Q)/2.0)
C
      AN=PR(1,KM)*PR(2,KM)*(ABS(P-(Q/3))**(PR(2,KM)-1))*
     + ((ABS(P-Q/3))/JC)
      EV1=(PR(3,KM)*(PM**(PR(4,KM))))/(P**(PR(5,KM)))
      EV=EV1*(((PR(4,KM)/PM)*(PM/JC))-((PR(5,KM)/P)*(P/JC)))
      EH=EV*AN
      VH1=PR(7,KM)*(P**PR(9,KM))*(QM**PR(10,KM))/(PM**PR(11,KM))
      VH=VH1*(-((PR(9,KM)/P)*(P/JC))+((PR(11,KM)/PM)*(PM/JC))-
     + ((PR(10,KM)/QM)*(QM/JC)))
      VV1=PR(12,KM)*(PM**PR(13,KM))*((P**PR(14,KM)))/(QM**PR(15,KM))
      VV=VV1*(((PR(13,KM)/PM)*(PM/JC))+((PR(14,KM)/P)*(P/JC))-
     + ((PR(15,KM)/QM)*(QM/JC)))
      A=EV/((1.0+VH)*(1.0-VH-2.0*AN*VV*VV))
C
      CALL ZEROR2(D,NS,NS)
      D(2,2)=A*(1.0-VH*VH)
      D(1,2)=A*AN*VV*(1.0+VH)
      D(1,3)=A*AN*VH+AN*VV*VV
      D(2,1)=D(1,2)
      D(1,1)=A*AN*(1.0-AN*VV*VV)
      D(2,3)=D(1,2)
      D(3,1)=D(1,3)
      D(3,2)=D(2,3)
      D(3,3)=D(1,1)
      D(4,4)=EV/(2.0*(1-VV))
C
      IPLSTK=1
```

```
      DEL(1)=D(1,1)
      DEL(2)=D(1,2)
      DEL(3)=D(4,4)
C
      IS=0
      DO 40 J1=1,NS
      DO 40 I1=1,J1
      IS=IS+1
   40 DEP(IS)=D(I1,J1)
      RETURN
      END
```

SUBROUTINE DSOILN

```
      SUBROUTINE DSOILN(I7,I,IET,NEL,NIP,NVRS,NDIM,NS,
     1 NPR,NMT,VARINT,MAT,D,PR,IPLSTK)
C-----------------------------------------------------------------------
C     THIS SUBROUTINE IS WRITTEN TO PUT BOYCE(1980) MODEL
C-----------------------------------------------------------------------
C     PRINT*, 'ENTER DSOILN'
      DIMENSION MAT(NEL),VARINT(NVRS,NIP,NEL),D(NS,NS),PR(NPR,NMT)
      COMMON/ DIN/ DEL(3),DEP(21)
      REAL N,K1,G1,B,AL,DL,E,V,GT,KT,A,P,Q2,Q
      KM=MAT(I)
      N=PR(1,KM)
      G1=PR(2,KM)
      K1=PR(3,KM)
      IW3=3
      IW6=6
C     WRITE(IW6,900)N,G1,K1
C 900 FORMAT(1X,'N =',G12.4,2X,'G1 =',G12.4,2X,'K1=',G12.4)
      SX= VARINT(1,I7,I)
      SY= VARINT(2,I7,I)
      SZ= VARINT(3,I7,I)
      TXY=VARINT(4,I7,I)
      P=(SX+SY+SZ)/3.
      Q2=SX*(SX-SY)+SY*(SY-SZ)+SZ*(SZ-SX)+3.*TXY*TXY
      Q=SQRT(Q2)
      B=(1.-N)*K1/(6.*G1)
      IF (P.EQ.0.0) THEN
      P=0.1E-18
      GOTO 3
      ENDIF
      IF (P.LT.0.0) THEN
      GOTO 5
      ENDIF
    3 KT=((K1/N)*(P**(1.-N)))/(1.+(B*(((2.-N)/N)*((Q*Q)/(P*P)))))
      GT=G1*(P**(1.-N))
      GOTO 6
    5 KT=((-K1/N)*((-1.*P)**(1.-N)))/(1.+(B*(((2.-N)/N)*((Q*Q)/(P*P)))))
      GT=-G1*((-1.*P)**(1.-N))
    6 WRITE(IW3,901)SX,SY,SZ,P,Q
  901 FORMAT(1X,'SX =',G12.4,2X,'SY=',G12.4,2X,'SZ=',G12.4
     1,2X,'P =',G12.4,2X,'Q =',G12.4)
   15 E=(9.*GT*KT)/(3.*KT+GT)
      V=(3.*KT-2.*GT)/(6.*KT+2.*GT)
      WRITE(IW3,902)E,V
  902 FORMAT(1X,'E=',G12.4,'V=',G12.4)
      IF (V.EQ.-1) THEN
      V=-.9999999999
      ENDIF
      A=(E/((1.-2.*V)*(1.+V)))
```

```
      AL=A*(1.-V)
      DL=A*V
      G=A*(0.5-V)
      CALL ZEROR2(D,NS,NS)
      D(1,1)=AL
      D(2,1)=DL
      D(3,1)=DL
      D(1,2)=DL
      D(2,2)=AL
      D(3,2)=DL
      D(1,3)=DL
      D(2,3)=DL
      D(3,3)=AL
      D(4,4)=G
C     DO 200 I=1,NS
C     WRITE(IW3,903)(D(I,J),J=1,NS)
C 200 CONTINUE
  903 FORMAT(1X,4G12.4)
C
      DEL(1)=D(1,1)
      DEL(2)=D(1,2)
      DEL(3)=D(4,4)
C
      IS=0
      DO 90 J1=1,NS
      DO 90 I1=1,J1
      IS=IS+1
   90 DEP(IS)=D(I1,J1)
C     STOP
      RETURN
      END
```

```
      PROGRAM MESH
      DIMENSION KLT(50),NCORR(300,30),MAT(120),NREL(1012),MREL(300),
     +NRELVV(405),MRELVV(120),LTYP(120),NW(406),XYZ(500,500)
      REAL SA,TA,XMAX,YMAX,XMIN,YMIN,YTT,YT,YM,YA,XTT,XT,XM,XA
      CHARACTER CAP*50
      PRINT*,'ENTER YOUR TITLE PLEASE'
      READ(*,500) CAP
500   FORMAT(A50)
      CALL DIG
      CALL SIMBEG
      CALL NEWPIC
      IR4=4
      IW6=6
C-----------------------------------------------------------------------
      REWIND IR4
      REWIND IW6
      READ(IR4,700)LINK1
      READ(IR4,700)NN,NVTX,ND,NNOD1,NNZ,NDZ,MDZ,NEDZ
      READ(IR4,700)NEL,MUMAX
      READ(IR4,700)NDF,NDIM,NTPE,NPL,LTZ,INXL
      READ(IR4,700)IFRZ,MAXNFZ,MCORE,NCORET
      READ(IR4,700)(KLT(IK),IK=1,LTZ)
      SA=0
      TA=0
      XM=0
      YM=0
      XT=0
      YT=0
C-----------------------------------------------------------------------
      DO 10 IN=1,NN
      READ(IR4,710) (XYZ(ID,IN),ID=1,NDIM)
C     WRITE(IW6,720)XYZ(ID,IN)
C 720 2G12.4
CCC   SA=MAX(200.,XYZ(1,IN))
CCC   TA=MAX(200.,XYZ(2,IN))
CCC   WRITE(6,*) XYZ(1,IN),XYZ(2,IN)
      IF (SA.LE.XYZ(1,IN)) THEN
      SA=XYZ(1,IN)
      ENDIF
      IF (TA.LE.XYZ(2,IN)) THEN
      TA=XYZ(2,IN)
      ENDIF
      IF (XM.GE.XYZ(1,IN)) THEN
      XM=XYZ(1,IN)
      ENDIF
      IF (YM.GE.XYZ(2,IN)) THEN
      YM=XYZ(2,IN)
      ENDIF
  10  CONTINUE
      WRITE(IW6,900) SA,TA,XM,YM
  900 FORMAT(1X,'SA=',G12.4,'TA=',G12.4,'XM=',G12.4,'YM=',G12.4)
      DO 20 J=1,NEL
C     XT=XT+XYZ(1,I)
C     YT=YT+XYZ(2,I)
  20  READ(IR4,720) (NCORR(J,I),I=1,NEDZ)
      READ(IR4,700) (MAT(J),J=1,NEL)
      READ(IR4,700) (NREL(I),I=1,NNZ)
      READ(IR4,700) (MREL(I),I=1,MUMAX)
      READ(IR4,700) (NRELVV(I),I=1,NN)
      READ(IR4,700) (MRELVV(I),I=1,NEL)
      READ(IR4,700) (LTYP(J),J=1,NEL)
```

```
      READ(IR4,700) (NW(I),I=1,NNOD1)
  700 FORMAT(20I5)
  710 FORMAT(3F16.3)
  720 FORMAT(20I5)
C     SA=MAX(400.,XYZ(1,IN))
C     TA=MAX(400.,XYZ(2,IN))
C     -------------------------------
C     SCALE ,PAGE AND GRAPHIC SIZES
C     -------------------------------
      XMAX=SA*1.1
      YMAX=TA*1.1
      XMIN=XM
      YMIN=YM
      WRITE(IW6,901) XMAX,YMAX,XMIN,YMIN
  901 FORMAT(1X,'XMAX=',G12.4,'YMAX=',G12.4,'XMIN=',G12.4,'YMIN=',G12.4)
C     CALL SCALES(XMIN,XMAX,1,YMIN,YMAX,1)
      CALL PAGE(85.0,85.0)
      CALL PICSIZ(80.0,80.0)
      CALL SCALES(XMIN,XMAX,1,YMIN,YMAX,1)
C     ---------------------------------------
C     READING ELEMENT COORDINATES IN TURN
C     ---------------------------------------
      CALL PEN(1)
      DO 40 I=1,NEL
      DO 30 J=1,NEDZ
      K=NCORR(I,J)
      XA=XYZ(1,K)
      YA=XYZ(2,K)
      XT=XT+XYZ(1,K)
      YT=YT+XYZ(2,K)
C     ---------------------------------------
C     PLOTTING STRAIGHT LINE FOR EACH SIDE
C     ---------------------------------------
C     CALL JOINPT(XA,YA)
C     CALL NUMBPT(XA,YA,4,K)
   30 CALL JOINPT(XA,YA)
      XTT=XT/NEDZ
      YTT=YT/NEDZ
C     CALL NUMBPT(XTT,YTT,16,I)
      K=NCORR(I,1)
C     CALL NUMBPT(XTT,YTT,16,I)
      XA=XYZ(1,K)
      YA=XYZ(2,K)
      CALL JOINPT(XA,YA)
C     CALL NUMBPT(XTT,YTT,16,I)
      WRITE(IW6,903)XA,YA,XT,YT
  903 FORMAT(1X,'XA=',G12.4,'YA=',G12.4,'XT=',G12.4,'YT=',G12.4)
      WRITE(IW6,904) XTT,YTT,K
  904 FORMAT(1X,'XTT=',G12.4,'YTT=',G12.4,'K=',20I5)
   40 CALL BREAK
C     CALL NUMBPT(XTT,YTT,16,I)
      CALL PEN(2)
C     ----------------
C     NODE NUMBERING
C     ----------------
      DO 100 I=1,NVTX
      XA=XYZ(1,I)
      YA=XYZ(2,I)

  100 CALL NUMBPT(XA,YA,2,I)
C     ----------------
C     TITLE
```

```
C      ----------------
       CALL PEN(4)
       CALL TITLE7('T','C',CAP)
       CALL ENDPLT
       STOP
       END
```

REGRESSION PROGRAM

```
      PROGRAM REGRN
C
C     REGRESSION ANALYSIS
C
C
      INTEGER I,M
      REAL H1,H2,H3,H4,H5,H6,H7,H8,H9,H10,H11,H12,A1,B1,A2,B2,
     1 SA,KSA,SA1,SA2,N,NH,K1,KH1,G1,GH1,BETA
      REAL SCON(1:100),SSTAT(1:100),SCYCL(1:100),EAX(1:100),
     1 ERAD(1:100),EV(1:100),ES(1:100),P(1:100),P1(1:100),
     1 P2(1:100),Q(1:100),Q1(1:100),Q2(1:100),X1(1:100),
     1 X2(1:100),Y1(1:100),Y2(1:100),S1(1:100),S2(1:100),
     1 EPSV(1:100),EPSS(1:100),AFW1(1:100),AFW2(1:100),
     1 TSCON(1:100),CON(1:100)
C       THE NUMBER OF MEASUREMENT****
C
      OPEN (UNIT=10,FILE='TNICKS.DAT',STATUS='OLD')
C
      READ (10,*) M
      DO 100,I=1,M
      READ (10,*) SCON(I),TSCON(I),SSTAT(I),SCYCL(I),EAX(I),ERAD(I)
      SCON(I)=1.E-3*SCON(I)
      TSCON(I)=1.E-3*TSCON(I)
      SSTAT(I)=1.E-3*SSTAT(I)
      SCYCL(I)=1.E-3*SCYCL(I)
      P1(I)=SCON(I)+SSTAT(I)/3
      IF (SCON(I).EQ.TSCON(I)) GOTO 5
      CON(I)=TSCON(I)-SCON(I)
      P2(I)=SCON(I)+CON(I)+(SSTAT(I)+SCYCL(I))/3
      GOTO 6
    5 P2(I)=SCON(I)+(SSTAT(I)+SCYCL(I))/3
    6 Q1(I)=SSTAT(I)
      Q2(I)=SSTAT(I)+SCYCL(I)
      EAX(I)=1.E-6*EAX(I)
      ERAD(I)=1.E-6*ERAD(I)
      EV(I)=EAX(I)+2*ERAD(I)
      ES(I)=2*(EAX(I)-ERAD(I))/3
      P(I)=P2(I)-P1(I)
      Q(I)=Q2(I)-Q1(I)
  100 CONTINUE
      PRINT *,'-------------------------------------------
     1  ----------------------------'
      PRINT *,'STEUN    STAT    CYCL    PMIN    PMAX    QMIN     QMAX
     1 EPSV    EP   EPSAX    EPSRAD'
C
      PRINT  *,'-------------------------------------------------
     1 -------------------------'
      DO 200,I=1,M
      H1=10**3
      H2=H1*SCON(I)
      H13=H1*TSCON(I)
      H3=H1*SSTAT(I)
      H4=H1*SCYCL(I)
      H5=H1*P1(I)
      H6=H1*P2(I)
```

```
      H7=H1*Q1(I)
      H8=H1*Q2(I)
      H9=H1*H1*EV(I)
      H10=H1*H1*ES(I)
      H11=H1*H1*EAX(I)
      H12=H1*H1*ERAD(I)
      PRINT 150,H2,H3,H4,H5,H6,H7,H8,H9,H10,H11,H12
  150 FORMAT(F6.1,1X,F6.1,1X,F6.1,1X,F6.1,1X,F6.1,1X,F6.1,1X,F6.1,
     1 1X,F6.0,1X,F6.0,1X,F6.0,1X,F6.0)
  200 CONTINUE
      PRINT 210,'-----------------------------------------------
     1 ---------------'
  210 FORMAT (///// 2X,A)
      PRINT 220, 'N','K1','SA1','G1','SA2','SA'
  220 FORMAT (3X,A,7X,A,10X,A,9X,A,10X,A,9X,A)
      PRINT *,'-----------------------------------------------
     1 ---------------'
      KSA=10000000
      DO 350,N=0.01,1.005,0.01
      A1=0
      B1=0
      A2=0
      B2=0
      DO 250,I=1,M
      S1(I)=P2(I)**(N-1)*Q2(I)-P1(I)**(N-1)*Q1(I)
      S2(I)=P2(I)**(N-2)*Q2(I)*Q2(I)-P1(I)**(N-2)*Q1(I)*Q1(I)
      IF (S1(I).EQ.0) THEN
      S1(I)=0.000000000000001
      ENDIF
C     PRINT *,S1(I)
      X1(I)=EV(I)+((1-N)/2)*ES(I)*S2(I)/S1(I)
      Y1(I)=P2(I)**N-P1(I)**N
      A1=A1+X1(I)*Y1(I)
      B1=B1+X1(I)*X1(I)
C     PRINT *,B1
  250 CONTINUE
      K1=A1/B1
      DO 300,I=1,M
      X2(I)=ES(I)
      Y2(I)=S1(I)/3
      A2=A2+X2(I)*Y2(I)
      B2=B2+X2(I)*X2(I)
  300 CONTINUE
      G1=A2/B2
      IF (K1.LT.0) THEN
      SA=100
      ELSE IF(K1.LT.(0.66667*G1/(2-N))) THEN
      SA=1000
      ELSE
      SA1=0
      SA2=0
      BETA=K1*(1-N)/(6*G1)
      DO 330,I=1,M
      EPSV(I)=(1/K1)*((P2(I)**N)-(P1(I)**N)-BETA*S2(I))
      EPSS(I)=(1/(3*G1))*S1(I)
```

```
      AFW1(I)=ABS(EPSV(I)-EV(I))
      SA1=SA1+(AFW1(I)*AFW1(I))/9
      AFW2(I)=ABS(EPSS(I)-ES(I))
      SA2=SA2+AFW2(I)*AFW2(I)
  330 CONTINUE
      SA=SA1+SA2
      ENDIF
      IF(SA.LT.KSA) THEN
      KSA=SA
      NH=N
      KH1=K1
      GH1=G1
      ENDIF
      PRINT 340,N,K1,SA1,G1,SA2,SA
  340 FORMAT (3X,F4.2,1X,F10.2,5X,E10.2,3X,F10.2,5X,E10.2,4X,E10.2
  350 CONTINUE
      PRINT 360,'I','EPSV','AFW1','EPSS','AFW2'
  360 FORMAT(3X,A,6X,A,9X,A,9X,A,9X,A)
      N=NH
      K1=KH1
      G1=GH1
      BETA=K1*(1-N)/(6*G1)
      DO 400,I=1,M
      S1(I)=P2(I)**(N-1)*Q2(I)-P1(I)**(N-1)*Q1(I)
      S2(I)=P2(I)**(N-2)*Q2(I)*Q2(I)-P1(I)**(N-2)*Q1(I)*Q1(I)
      EPSV(I)=(1/K1)*((P2(I)**N)-(P1(I)**N)-BETA*S2(I))
      EPSS(I)=(1/(3*G1))*S1(I)
      AFW1(I)=(EPSV(I)-EV(I))
      AFW2(I)=(EPSS(I)-ES(I))
      PRINT 390,I,EPSV(I),AFW1(I),EPSS(I),AFW2(I)
  390 FORMAT (3X,I2,3X,E10.2,4X,E10.2,4X,E10.2,4X,E10.2)
  400 CONTINUE
      PRINT 420,'N','K1','G1'
  420 FORMAT (3X,A,7X,A,9X,A)
      PRINT 430,N,KH1,GH1
  430 FORMAT (3X,F4.2,1X,F10.2,3X,F10.2)
      PRINT 435,'I','EV','EPSV'
  435 FORMAT (3X,A,7X,A,8X,A)
      DO 440,I=1,M
      PRINT 450,I,EV(I),EPSV(I)
  440 CONTINUE
  450 FORMAT (3X,I2,3X,E10.2,4X,E10.2)
      PRINT 210,'-----------------------------------------'
      PRINT 435,'I','ES','EPSS'
      DO 460,I=1,M
      PRINT 450,I,ES(I),EPSS(I)
  460 CONTINUE
      END
```

SPSS program to find Boyce (1980) model constants

```
data list free file ='file name'/ p1 p2 q1 q2 ev es
compute es=es/1000000.
model program n=0.28 g1=1000.
compute pn1=p1**n.
compute pn2=p2**n.
compute pred=(pn2*q2/3/g1/p2)-(pn1*q1/3/g1/p1.
cnlr es with p1,q1,p2,q2 / bounds 0<n<1 ; 0<g1.

compute ev=ev/1000000.
model program n=0.28 g1=1000 k1=1000.
compute pn1=p1**n.
compute pn2=p2**n.
compute beta=k1*(1-n)/6*g1
compute pred=((pn2*(1-beta*(q2/p2)**2)/k1)-(pn1*(1-
beta*(q1/p1)**2)/k1).
cnlr ev with p1,q1,p2,q2 / bounds 0<n<1 ; 0<g1 ; 0<k1.

compute ev=ev/1000000.
compute es=es/1000000.
compute etot =ev + es.
model program n=0.28 g1=1000 k1=1000.
compute pn1 =p1**n.
compute pn2=p2**n.
compute pred1=(pn2*q2/3/g1/p2) - (pn1*q1/3/g1/p1).
compute pred2 =(pn2*(1-beta*(q2/p2)**2)/k1)-((pn1*(1-
beta*(q1/p1)**2)/k1).
compute pred = pred1+pred2
cnlr etot with p1,q1,p2,q2 / bounds 0<n<1 ; 0<g1 ; 0<k1.
```

BMDP program to find Boyce (1980) model constants

```
/input variables are 4. file=' file name'. format=free.
/variables names are p,q,ev,es.
/regress param=2. depend es.
/parameter names are n, g1.
        initial   = 0.2, 200.
        max       = 1, 1000000.
        min       = 0, 0.
/function pn=p**n.
        f=pn*q/3/g1/p.
/end.
/regress param = 3. depend = emu.
/parameter names are n, g1, k1.
        initial   = 0.2, 1800, 1000.
        max       = 1, 1000000, 1000000.
        min       = 0, 0.
/function pn=p**n. beta = k1*(1-n)/g1.
        f = pn*(1 - beta*(q/p)**2)/k1.
/end.
/regress param=3. depend =etot.
/parameter names are n, g1, k1.
        initial   = 0.3, 200, 100.
        max       = 1, 1000000, 1000000.
        min       = 0, 0, 0.
/function pn= p**n. beta =k1*(1-n)/g1.
        f1 = pn*q/3/g1/p.
        f2 = pn*(1 - beta*(p/q)**2)/k1.
        f = f1 + f2.
/end.
```

Example BMDP programs to find new model constants

υ_2

```
/input variables are 9. file='file name'. format free.
/variables names are q,c1,c2,p1,p2,pm,dp,ea,er.
        use = q, c1, c2, pm, dp, ea, er.
/transform p1= c2-c1. c1=(0.05*(p1**0.54). c2=53929*(pm**0.567/(dp**0.197).
        ea=er/10**6. er=ln(c1*c2*2*ea/p1).
        pm=ln(pm). dp=ln(dp). q=ln(q).
/regress depend=ea.
        indep=pm,dp,q.
        enter=0.001,0.001.
/print data.
/end.
```

variables names:
c1 and c2=initial and final cell pressure values
q=constant axial load
p1 and p2=initial and final mean normal stresses
pm=mean value of mean normal stresses
dp=difference between the mean normal stresses
ea=axial strain
er=radial strain
Noe: Variable c1, c2 and er are reutilized within the proram and become anisotropy, resilient modulus and υ_2 respectively.

Example BMDP programs to find new model constants

$1-\upsilon_1$

```
/input variables are 9. file='file name'. format free.
/variables names are q, c1, c2, pm, dp, ea, er.
        use= q, c1, c2, pm, dp, ea, er.
/transform p1= c2-c1. c1= (0.05*(p1**0.54). c2= 53929*(pm**0.567/(dp**0.197).
        er= er/10**6. ea= ln(c1*c2*er/p1).
        pm= ln(pm). dp=ln(dp). q= ln(q).
/regress depend= ea.
        indep= pm, dp, q.
```

```
        enter= 0.001, 0.001.
/print data.
/end.
```

Example BMDP programs to radial strain due to cyclic both stresses (non-linear regression)

```
/input variables are 13. file='file name'. format free.
/variables names are q1,q2,p1,p2,pm,ea,er,n,es,dp,c2,pm,qm,mr.
        use=q1,q2,p1,p2,pm,ea,er,dp,c2,qm,mr,n.
/transform      qm=(q1+q2)/2. pm=(p1+p2)/2.
                n=0.037*(abs(((3*p2-q2)/2)-(1.5*p1)))**0.437.
                mr=37192*(pm**0.764/dp**0.217).
                c2=abs(((3*p2-q2)/2)-1.5*p1).
/regress param=4. depend=ea. iter=300.
/parameter names are a, b, c, d.
                initial = 1,0.51,0.5,0.54.
                max = 10, 2, 3, 2.
                min = -10, -2, -2, -2.
/function
f= (-2*a*(dp**b)*(pm**c)/(qm**d)*(c2/(n*mr))*10**6+(q2/mr)*10**6.
/end.
```

Example BMDP programs to axial strain due to cyclic both stresses (non-linear regression)

```
/input variables are 13. file='file name'. format free.
/variables names are q1,q2,p1,p2,pm,ea,er,n,es,dp,c2,pm,qm,mr.
        use=q1,q2,p1,p2,pm,ea,er,dp,c2,qm,mr,n.
/transform      qm=(q1+q2)/2. pm=(p1+p2)/2.
                n=0.037*(abs(((3*p2-q2)/2)-(1.5*p1)))**0.437.
                mr=37192*(pm**0.764/dp**0.217).
                c2=abs(((3*p2-q2)/2)-1.5*p1).
/regress param=4. depend=ea. iter=300.
/parameter names are a, b, c, d.
                initial = 1,0.51,0.5,0.54.
```

```
                max = 10, 2, 3, 2.
                min = -10, -2, -2, -2.
/function
f= (-2*a*(dp**b)*(pm**c)/(qm**d))*(c2/(n*mr))*10**6+(q2/mr)*10**6.
/end.
```

APPENDIX E

PLATES

Plate 1.
Apparatus to measure membrane extension modulus

Plate 2.
Repeated load triaxial apparatus

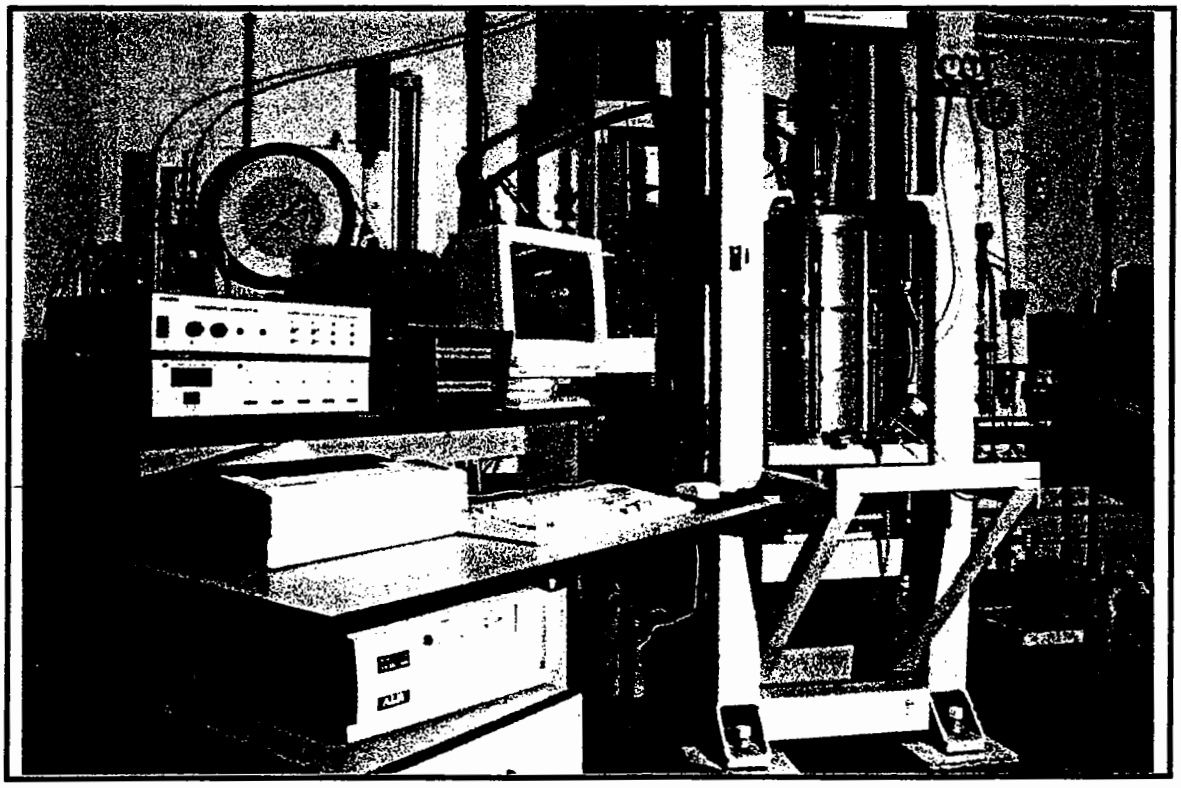

Plate 3.
A triaxial sample with instrumentation

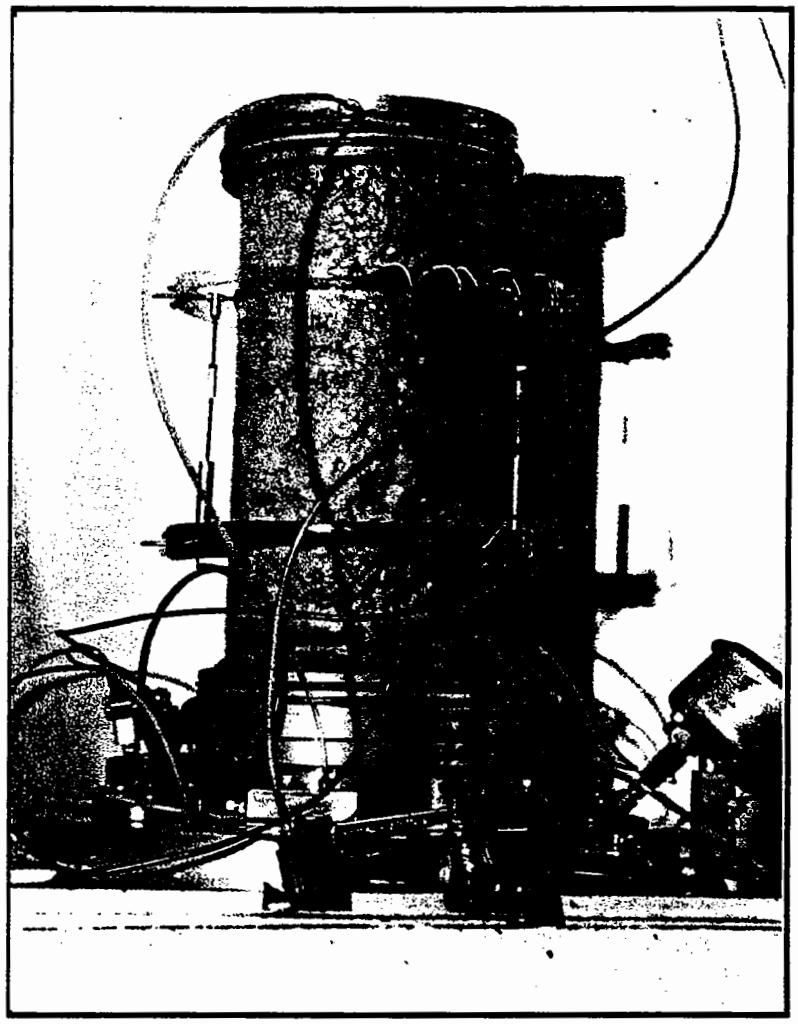

Plate 4.
Details of sample instrumentation

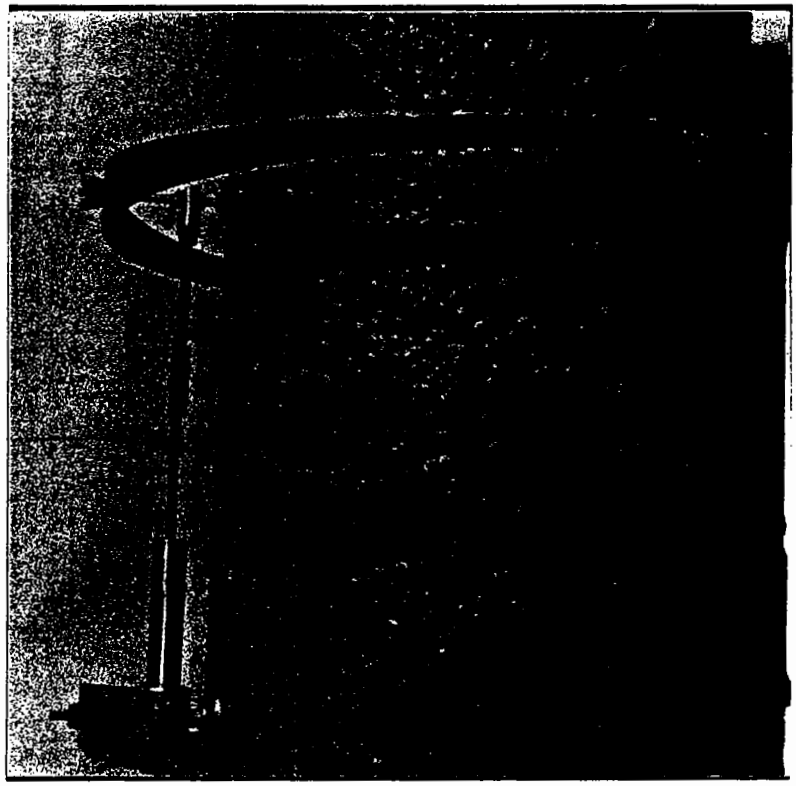

APPENDIX F

SEQUENCE OF TESTING

SEQUENCE OF TESTING

1. Inherent anisotropy measurements : A sample was first subjected to a repeated cell pressure with half sine waveform from a low stress of 25 kPa to an upper stress, increased in 25 kPa increments, ranging from 50 kPa to 225 kPa. During the test, the load ram was not connected.

2. Resilient repeated cell pressure tests with constant, non-zero, deviatoric stress: For these tests the load ram was connected. Initially an axial load was applied (intended to be constant) and the cell pressure was cycled. Cell pressure levels were dependent on the level of deviatoric stress. Cell pressures were changed in increments typically of 50 and 100 kPa. See Appendix B for details.

3. Resilient deviatoric stress tests with constant cell pressure: For this type of test, the initial cell pressure was set to 250 kPa and subsequently repeated deviatoric stress was applied at 0-50, 0-100, 0-150 and 0-200 kPa. The cell pressure was then reduced progressively in 50 kPa increments to 50 kPa and the sequence of deviatoric stress cycling repeated (unless large permanent strain resulted. Fully compression-space tests were followed by q= +25 to -25 kPa tests and then q=0 to -50 kPa paths at levels of cell pressure which prevented large permanent strains.

4. Both stresses repeated: For this type of tests the cell pressure and axial load were set to their initial values. After that both stresses were cycled either both in phase or 180° out of phase. In Figure 5.5, the vertical (parallel to the q axis) stress paths are in the opposite phase, whereas stress paths shown as inclined dashed lines are applied in phase. The sequence is as follows:

a) p_o = 67 kPa ; q_o = 0 ; Δq = 200, 150, 100, 50 kPa (at q/p = 1.5)

These stress paths are then repeated with identical deviaotor stresses but with p_o = 33 kPa.

b) p_o = 250 kPa ; q_o = 0 kPa ; Δq = 50, 100, 150, 200 kPa (vertical paths)

Paths as b) are then repeated for p_o = 200, 150, 100 but with one less Δq path each time.

5. Stress-history induced anisotropy measurements: Firstly a sample is subjected to about 1% axial permanent deformation with the deviatoric stress level of 250 kPa with 50 kPa cell pressure. The load ram was again disconnected and the stress paths for stage 1 above were repeated.

APPENDIX G

STRESS CONTOURS FROM FE ANALYSIS

STRESS-CONTOURS FROM FE ANALYSIS

Ten CRISP analyses were performed for a typical pavement arrangement (see Figure 9.6) using a range of granular material types. All the results showed similar tendencies. In this appendix, one case- using SL- is studied by way of example.

Figures G.1 to G.8 show contours obtained from FE analysis. The vertical axis shows the full thickness of granular layer (the numbers represent the height in metres from the base of the FE mesh). Horizontal axis shows the radius along the pavement width. Figures G.1 to G.4 show the stress contours in the whole granular layer in the pavement. However, it is difficult to differentiate isotropic and anisotropic model results. Therefore, Figures G.5 to G.8 were constructed in order to show stresses caused by the wheel loading on elements just underneath wheel. The radius of the wheel is 0.16 m. Therefore the last element towards the right is free of direct wheel loading. Contours of stresses are given in kPa.

The pavement which used anisotropic material properties experienced higher mean normal stresses but similar deviatoric stresses in the granular layer (compare Figure G.1 with G.2 and G.3 with G.4). This means that the granular material becomes stiffer when anisotropic properties are used. The change in stress magnitudes is steeper with isotropic properties, hence the load is distributed over a smaller area.

Sometimes it is possible to obtain negative horizontal stresses (tension) in granular layer. In theory it is generally accepted that the granular material cannot withstand

tension. From FE results some negative horizontal stresses, as large as 45 kPa, were obtained at the bottom of the granular layer beneath the loaded area for both isotropic and anisotropic models. However, in a real pavement, the suction may overcome this small negative horizontal stress. Furthermore the tensions were almost identical for isotropic and anisotropic analyses indicating that sensible comparisons of results may still be made.

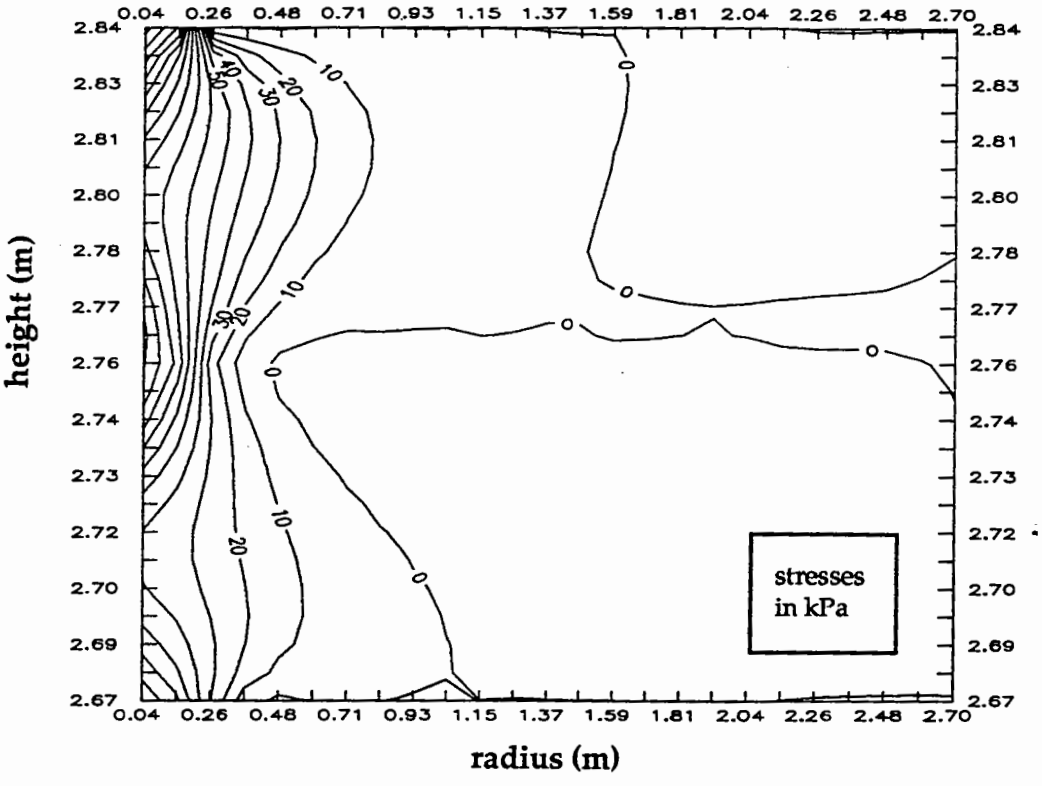

Figure G.1. Mean normal stress contours in granular layer- isotropic properties (SL)

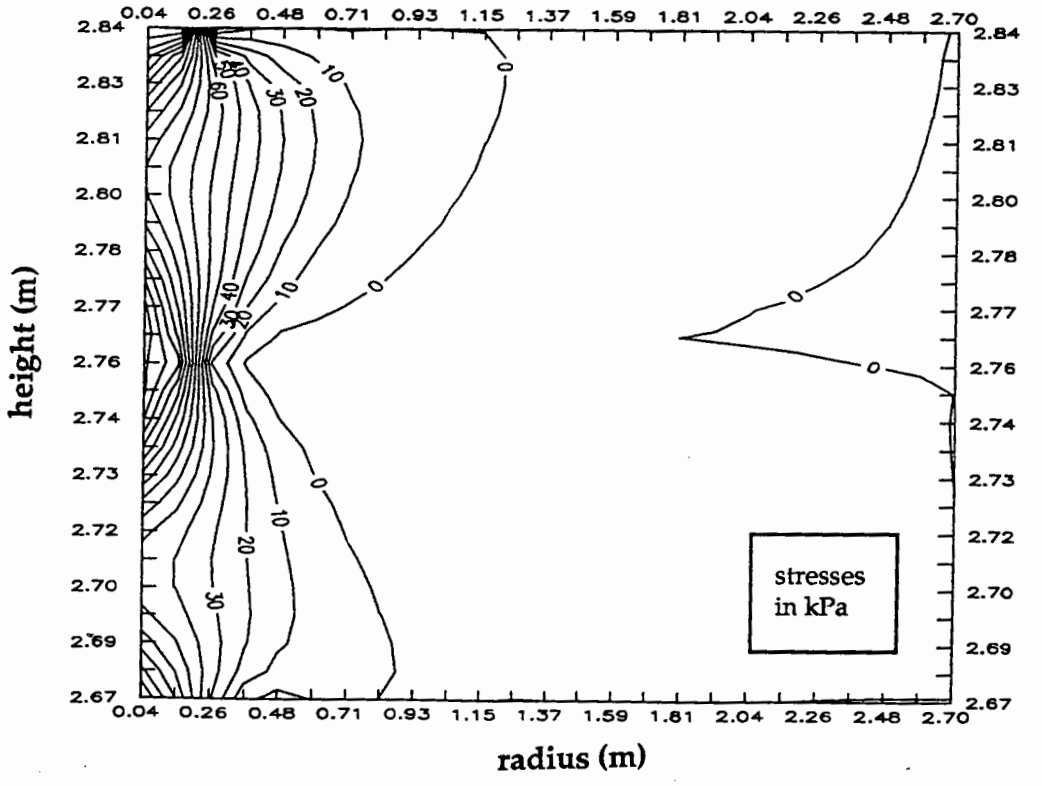

Figure G.2. Mean normal stress contours in granular layer- anisotropic properties (SL)

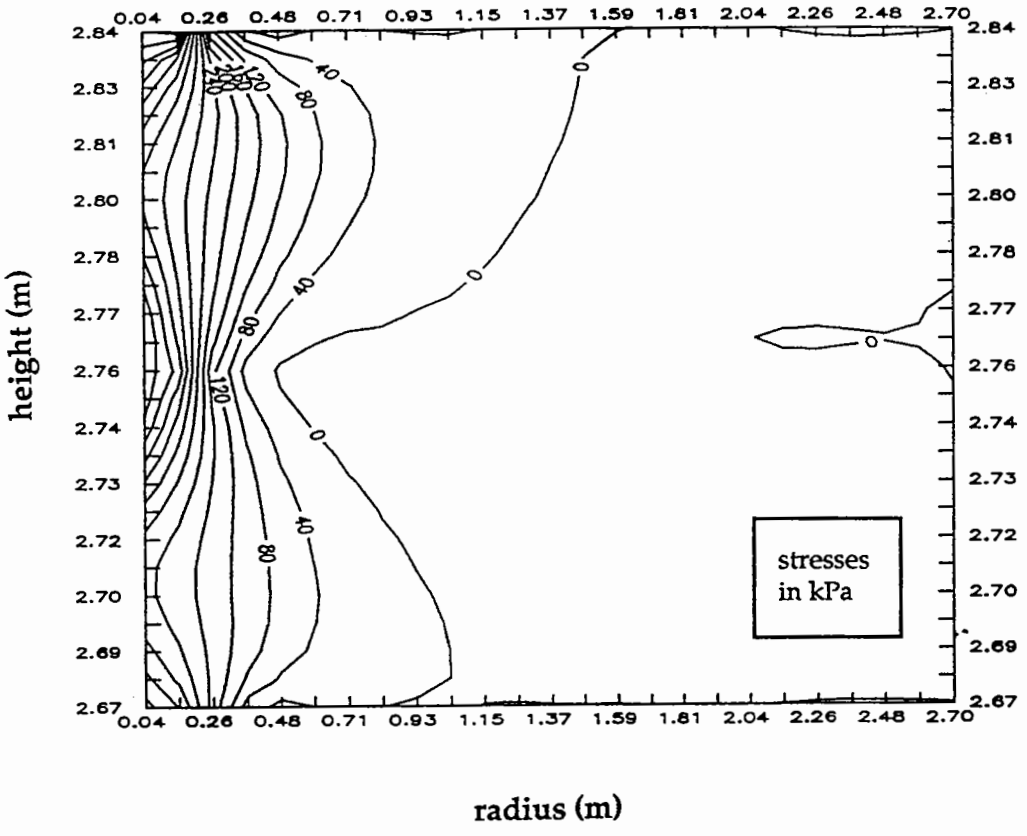

Figure G.3. Deviatoric stress contours in granular layer- isotropic properties (SL)

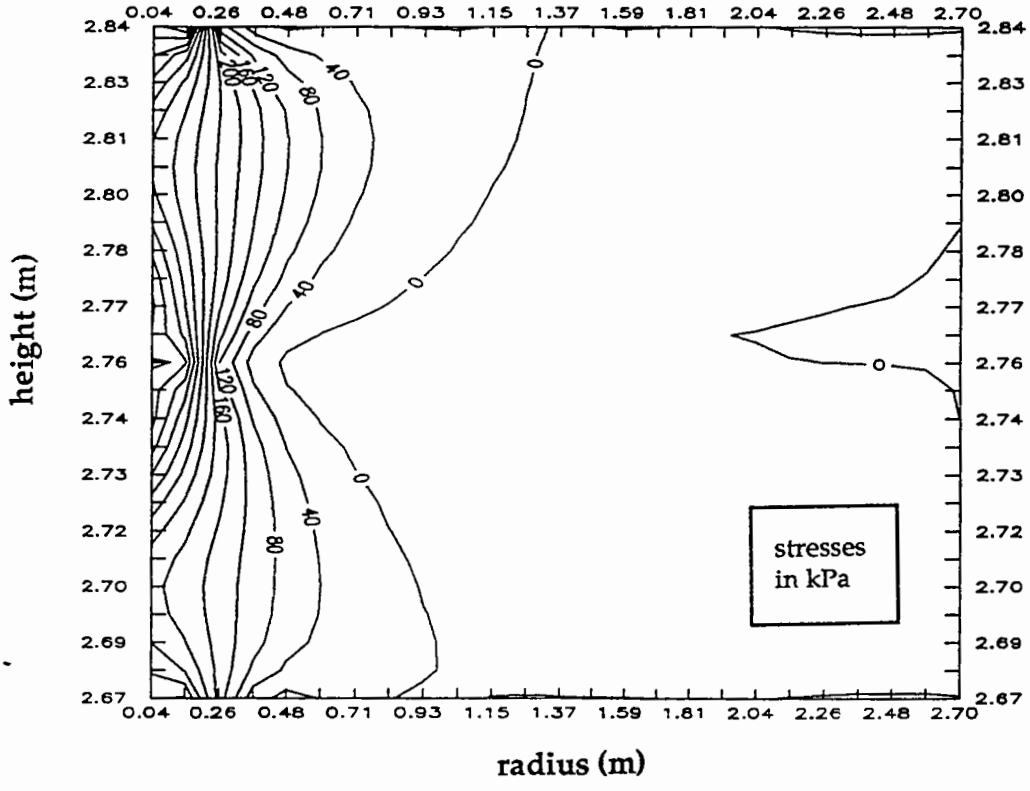

Figure G.4. Deviatoric stress contours in granular layer- anisotropic properties (SL)

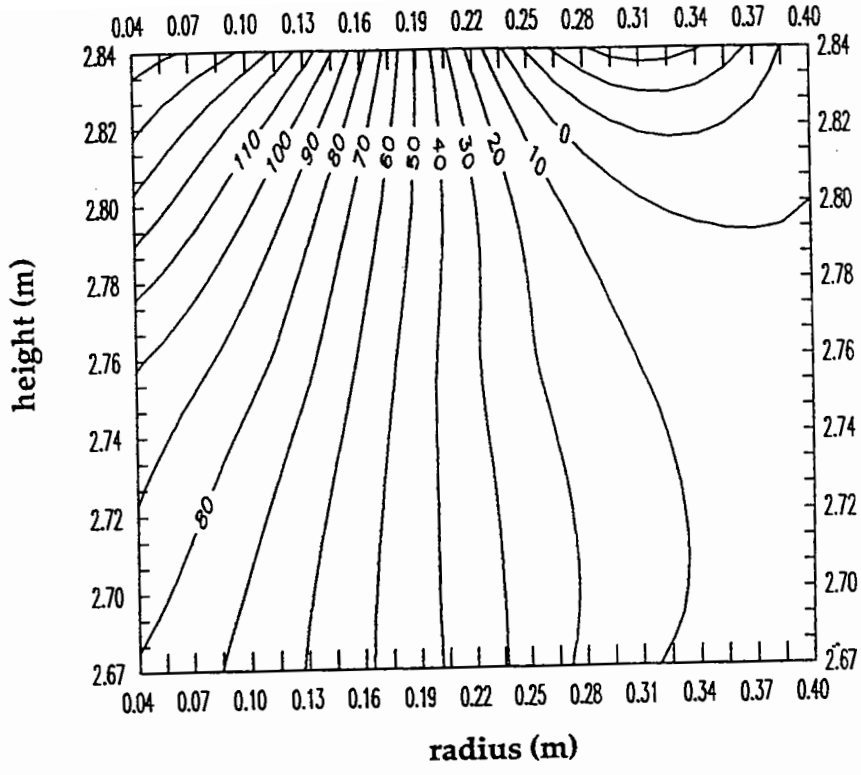

Figure G.5. Mean normal stress contours underneath wheel loading-isotropic material properties (SL)

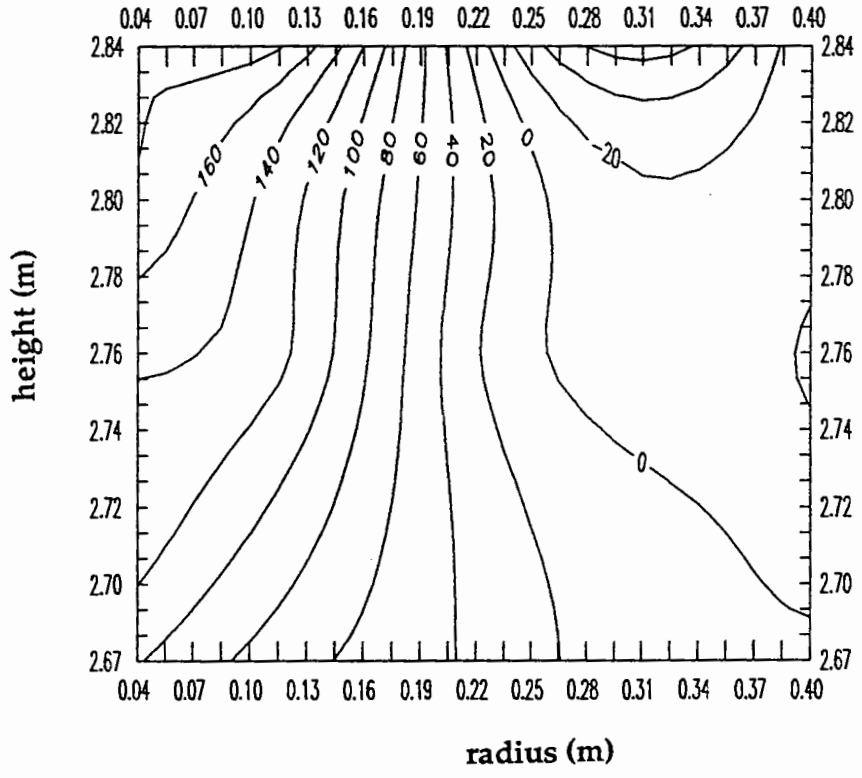

Figure G.6. Mean normal stress contours underneath wheel loading-anisotropic material properties (SL)

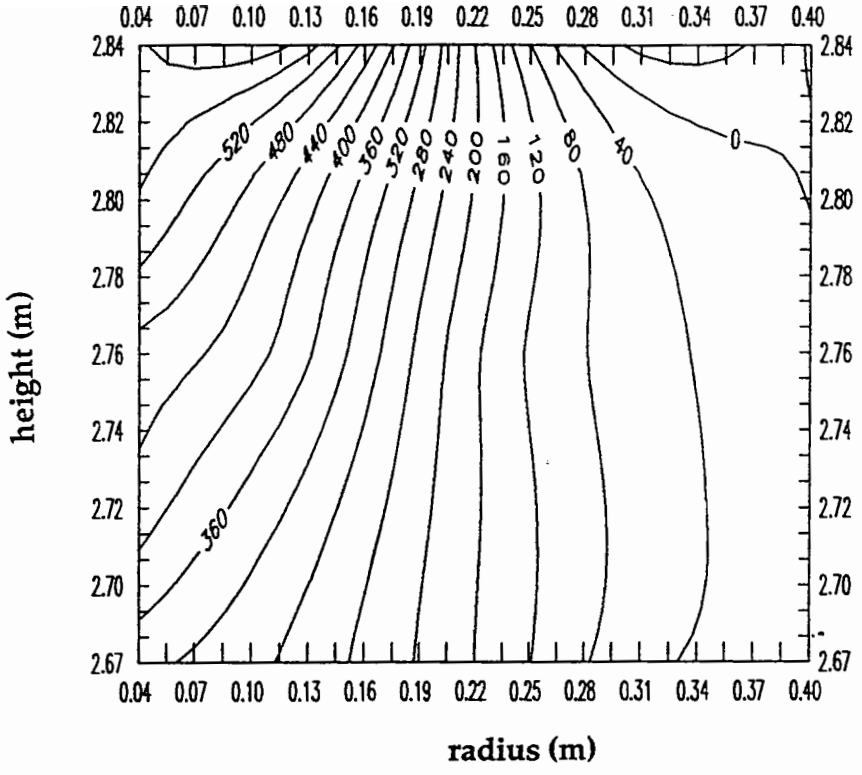

Figure G.7. Deviatoric stress contours underneath wheel loading- isotropic material properties (SL)

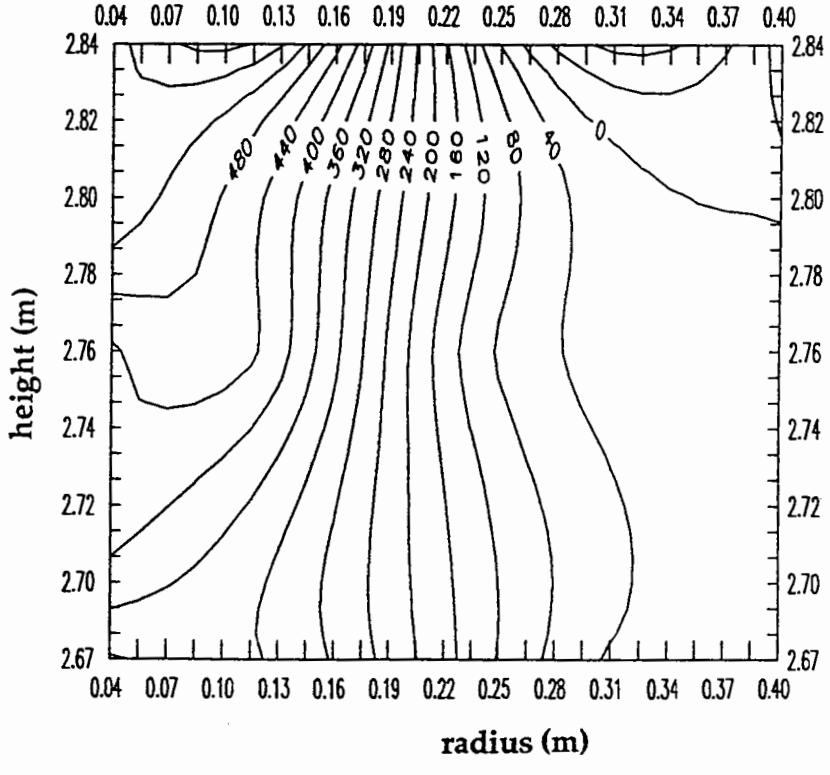

Figure G.8. Deviatoric stress contours underneath wheel loading- anisotropic material properties (SL)